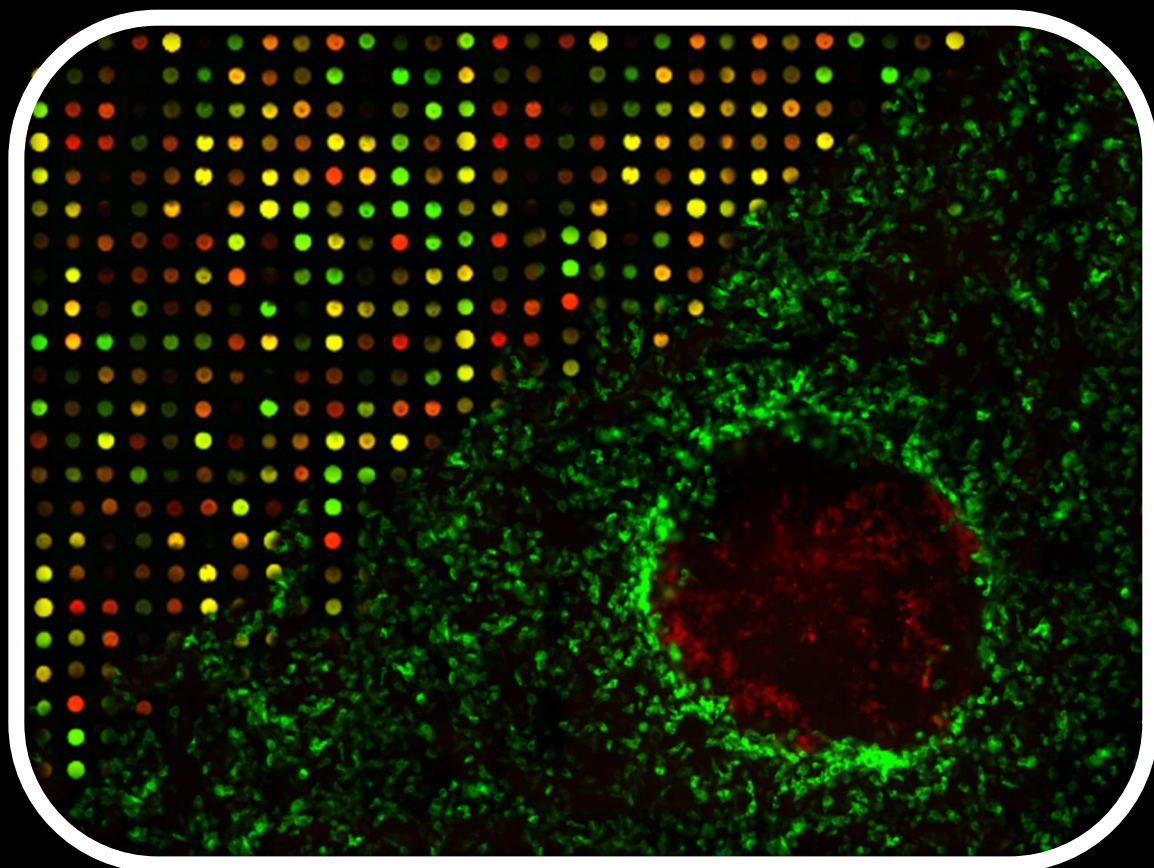


Integrated functional genomics for improved manufacture of recombinant enveloped virus

Transcriptional profiling and metabolic engineering of retrovirus producer cells

Ana Filipa Rodrigues



Dissertation presented to obtain the Ph.D degree in Engineering and Technology Sciences – Biotechnology

Instituto de Tecnologia Química e Biológica | Universidade Nova de Lisboa

Oeiras,
November, 2013



INSTITUTO
DE TECNOLOGIA
QUÍMICA E BIOLÓGICA
/UNL

Knowledge Creation



Integrated functional genomics for improved manufacture of recombinant enveloped virus

Transcriptional profiling and metabolic engineering of retrovirus producer cells

Ana Filipa Albuquerque Ferreira Rodrigues

Dissertation presented to obtain the Ph.D degree in
Engineering and Technology Sciences, Biotechnology
Instituto de Tecnologia Química e Biológica | Universidade Nova de Lisboa

Oeiras, November, 2013



INSTITUTO
DE TECNOLOGIA
QUÍMICA E BIOLÓGICA
/UNL

Knowledge Creation



INTEGRATED FUNCTIONAL GENOMICS FOR IMPROVED MANUFACTURE OF RECOMBINANT ENVELOPED VIRUS

Transcriptional profiling and metabolic engineering of retrovirus producer cells

Ana Filipa A. F. Rodrigues

Dissertation presented to obtain a Ph.D degree in Engineering and Technology Sciences, Biotechnology, at the Instituto de Tecnologia Química e Biológica, Universidade Nova de Lisboa

Supervisor: **Ana Sofia S. V. Coroadinha**

Co-Supervisor: **Wei-Shou Hu**



Oeiras, November 2013

With the financial support from FCT, under contract SFRH/BD/48393/2008

FCT

Fundação para a Ciência e a Tecnologia
MINISTÉRIO DA CIÊNCIA, TECNOLOGIA E ENSINO SUPERIOR

Integrated functional genomics for improved manufacture of recombinant enveloped virus
Transcriptional profiling and metabolic engineering of retrovirus producer cells

By Ana Filipa A.F. Rodrigues

Second Edition: January 2014

Front cover: composite image of (i) a two-channel microarray and (ii) a colony of retrovirus producer cells surrounded by a layer of target cells infected by the produced viruses.

Back cover: retrovirus particle (iii).

i) Adapted from <http://www.people.vcu.edu/~mreimers/OGMDA/image.html>.

ii) High-titer clone isolated with the single step cloning-titration method (Chapter VII).

iii) by Ana Filipa A.F. Rodrigues.

ITQB-UNL/IBET Animal Cell Technology Unit

Instituto de Tecnologia Química e Biológica/

Instituto de Biologia Experimental e Tecnológica

Av. Da República EAN, 2780-157 Oeiras, Portugal

Phone: 00351 214469520; Fax: 00351 214421161

<http://tca.itqb.unl.pt>

<http://www.itqb.unl.pt>

<http://www.ibet.pt>

Copyright © 2014 by Ana Filipa A.F. Rodrigues

All Rights Reserved

Printed in Portugal



From left to right: Prof. Manuel Carrondo, Dr. Pedro Cruz, Dr. Otto Merten, Prof. Wei-Shou Hu, Ana Filipa Rodrigues, Dr. Ana Sofia Coroadinha, Dr. Dagmar Wirth and Prof. Maria Arménia Carrondo

Supervisors

Dr. Ana Sofia Coroadinha, Head of the Cell Line Development and Molecular Biotechnology Laboratory, Animal Cell Technology Unit, IBET/ITQB-UNL, Oeiras, Portugal (supervisor).

Prof. Wei-Shou Hu, Biotechnology Institute, Distinguished McKnight University Professor, Department of Chemical Engineering and Materials Science, University of Minnesota, Minneapolis, MN, USA (co-supervisor).

Jury

Dr. Otto-Wilhelm Merten, Head of the Applied Vectorology and Innovation group of Genethon, Genethon, Evry, France

Dr. Dagmar Wirth, Head of the Model Systems for Infection Research Group, Helmholtz Centre for Infection Research, Braunschweig, Germany.

Prof. Manuel J. T. Carrondo, Cathedratric Professor of Chemical and Biochemical Engineering at Faculdade de Ciências e Tecnologia, UNL, Caparica, Portugal, and Director of Instituto de Biologia Experimental e Tecnológica, Oeiras, Portugal.

Dr. Pedro Estilita P. M. Cruz, Investigator and CSO of ECBio, Portugal

Foreword

The present thesis dissertation is the result of four years of research at the Animal Cell Technology Unit of Instituto de Tecnologia Química e Biológica – Universidade Nova de Lisboa and Instituto de Biologia Experimental e Tecnológica (Oeiras, Portugal) and at the Biotechnology Institute, Department of Chemical Engineering and Materials Science, University of Minnesota (Minneapolis, MN, USA) under the supervision of Dr. Ana Sofia Coroadinha and Prof. Wei-Shou Hu.

This PhD thesis aimed at contributing with knowledge on the physiological constraints modulating retroviral vector production in human cell lines by using functional genomics tools and to improve their productivity performance by means of reverse metabolic engineering.

Acknowledgements

I would like to express my gratitude to all of those whom, directly or indirectly have helped me during these years and contribute to the present thesis. Also to the hosting institutions, IBET and ITQB, for the excellent working conditions.

To my supervisor, Dr. Ana Sofia Coroadinha. For taking me with you on this incredible journey which shaped me both as a scientist and as person. Your endless support and friendship are far beyond the highest expectations I could ever conceive. For pushing my best strengths and prompting my natural enthusiasm with science: there was not a single day during these years that I woke up not feeling like coming to work. Also for skirting my faults and helping me to mitigate them while still accepting me as I am. For all that you taught me and keep teaching every day: discussing science with you is a pleasure that enthuses me for more and more ambitious challenges. For letting me step on quicksand always trusting my capabilities to escape stronger. For making me feel a peer. Most of all, for the example: your integrity is a role model, your creativity an inspiration.

To Prof. Wei-Shou Hu, for the amazing time spent at the University of Minnesota. I'm thankful for your scientific enthusiasm, for letting me know that "it's fair if you want to *do it* just because you want to *know better*". For opening me the world of microarray analysis. But also for your rough skepticism, which taught me to always have a second look on the obvious and the non-obvious. More importantly, for having received me with open arms making me feel welcome.

To Dr. Paula Alves for the scientific support and excellent conditions provided during all these years. For all the opportunities and for granting me all the means I could need even when not totally sharing my vision. For the example in leadership and personal dedication. For giving your best and fighting hard for this team taking the change of, many times, being misunderstood: driving the ship always seems easier from the ballroom than from the helm.

To Prof. Manuel Carrondo, for founding and enlarging a research institute of excellence in which I have the privilege to work. Against the odds, the endless bureaucratic burden, the asphyxiating lack of means that always haunted our country... now, more than never, Portugal needs more spirits like yours.

To the financial support provided by Fundação para a Ciência e a Tecnologia (PTDC/EBB-BIO/100491/2008 and SFRH/BD/48393/2008).

To my former colleagues from the Hu Lab, at the University of Minnesota. For contributing to the great experience that those months were. In particular to Siguang

Sui, Huong Le, Bhanu Mulukutla, Shikha Sharma, Nitya Jacobs and Nandita Vishwanathan. For all the help, from bench work, to data analysis, to scientific and philosophic discussions. Also for the companion and support outside the lab.

To all my colleagues from the Animal Cell Technology team, in particular to those of the Cell Line Development and Molecular Biotechnology Lab: Hugo, Paulo, Rute, Hélio, Vanessa, Ana Isabel, Miguel and Ana Oliveira. For the great moods in the virus lab. For always trying to row in the same direction and keep the enthusiasm, particularly during these challenging times.

To Miguel and Ana Oliveira, I would like to emphasize my very special “thank you”. Teaching you was a pleasure and seeing you, now, growing as persons and scientists, a truth reward. Believe me or not, it has also taught me a lot. I’m grateful for your dedication, for your (very!) hard work, for embracing the challenges with the conviction that it will always be worth it. Your commitment to this project strength my every day enthusiasm.

To my Minnesotan (international) partners, Terk and David. Some people pass through our life leaving nothing, others leave something, and others never leave. You will never leave. Minnesota would not have been the same without our endless laughs, blind weekend trips, scientific (and non-scientific...) night outs sponsored by Starbucks (and many others...).

À minha grande amiga de faculdade e de laboratório, Francisca. Agradeço todos os bons momentos que proporcionas, e os maus que tornas melhores. Por me puxares para a tona da água nos pequenos (e grandes) naufrágios. Pelas conversas intelectuais que nos inspiram a uma existência melhor, as pseudointelectuais que começam no metafísico e resvalam para a tolice, ou as simplesmente idiotas que nos fazem rir, rir muito. Estes anos de doutoramento teriam sido mais pobres sem ti.

Ao Ricardo e à Ana Teresa, os meus amigos de ontem, de hoje e de sempre. De há tanto e tanta coisa que já nem contamos. Porque não é possível contar o tanto que nos deram estes quinze anos de aventuras, confidências, cumplicidade, entreaajuda, algumas tristezas e muitas alegrias. Também ao André, que fortaleceu este círculo nos últimos anos.

A toda a minha família e em especial aos meus queridos pais e irmão. Devo-vos tudo, e quaisquer palavras que intencionassem verbalizar a minha infinita gratidão e amor seriam tentativas vãs.

Aos meus pais

Ao meu irmão

Porque o carácter vem do exemplo, a força da estrutura, a confiança do amor incondicional.

Abstract

Biopharmaceuticals derived from recombinant viruses comprise a plethora of prophylactic and therapeutic products from vaccines to gene therapy vectors. Retroviruses occupy an important segment of this market. Replication-defective vectors have extensively been used as delivery vehicles in gene therapy protocols. Retrovirus-like-particles have shown promising results in vaccinology as immunogen display platforms. Replication-competent particles have efficiently been used as oncolytic agents.

The manufacture of retroviral vectors faces many challenges. The titers obtained from cell culture bulk range 10^6 to 10^7 infectious particles *per* mL, demanding 10 to 100 L of culture volume to treat a single patient. Also, viral preparations are characterized by low ratios of infectious to total particles further reducing the therapeutic efficiency of the infectious ones. Moreover, long-term vector production is dependent on animal blood serum, an ill-defined culture supplement and potential source of pathogen contamination, hindering the safety and standardization required in clinical-grade manufacture processes. Thus, the productivity performance of retroviral vector manufacture systems is below the therapeutic needs and far from meeting the biopharmaceutical industry demands for the transition clinical-to-market.

This PhD thesis aimed at using functional genomics to understand the physiological constraints of retroviral vector production in human cell lines to improve their productivity performance by means of reverse metabolic engineering.

In the first part of this work (**Chapter II**), the transcriptional and central carbon metabolite profiling of the transition 'parental-to-producer' of two retroviral vector producer cell lines – 293 FLEX and Te Fly – was evaluated. Eight pathways were identified to be recruited in the virus production state: amino acid catabolism, carbohydrate catabolism and integration of the energy metabolism, nucleotide metabolism, glutathione metabolism, pentose phosphate pathway, polyamines

biosynthesis and lipid metabolism. Their ability to modulate viral titers was validated by media manipulation, leading to improved productivities up to 6-fold. Within recruited pathways a mining strategy was devised to identify potential targets for gene manipulation in the view of enhanced viral titers. More than 30 genes were identified.

In **Chapter III** the physiological determinants behind serum heterotrophy in retroviral vector production were investigated. A thorough study of viral production kinetics, vector characterization and cell growth and metabolic behavior was conducted, for 293 FLEX and Te Fly producer cells using different serum concentrations. The absence of the serum lipid fraction was identified to be a major cause for serum heterotrophy. Following these findings, in **Chapter IV** an adaptation to serum deprivation of the two cell lines was conducted, and analyzed the effects on lipid biosynthetic pathways and infectious vector production. Total lipid content as well as cellular cholesterol were quantified and lipid biosynthesis was assessed by ¹³C-NMR spectroscopy. The effects of adaptation to serum deprivation in lipid biosynthesis were found to be cell line specific and directly correlated with infectious virus titers: 293 FLEX cells faced severe lipid starvation and a 68-fold reduction in infectious vector titers. Te Fly cells were able to maintain total lipid content by rising *de novo* lipid biosynthesis, particularly cholesterol, with the consequent recovery of infectious vector productivities. Yet, for 293 FLEX no evident blockage in cholesterol biosynthesis was found. Therefore, in **Chapter V.a**, a whole-transcriptome microarray analysis of both cell lines under serum deprivation was conducted. Two potential blockage points in cholesterol biosynthesis were identified, exclusive of 293 FLEX cells: mevalonate kinase (MVK) and lanosterol synthase (LSS).

In the first part of this thesis, several metabolic pathways and the corresponding genes were identified as potential targets to improve vector titers and viral preparation quality (e.g.: removal of serum from the culture medium).

In the second part of this work (**Chapters V.b to VIII**), gathered knowledge was used for the rational design of metabolic manipulation strategies by means of gene over-expression or down-regulation.

In **Chapter V.b**, lipid metabolism of 293 FLEX cells was manipulated by the over-expression of mevalonate kinase (MVK), lanosterol synthase (LSS), and sterol regulatory element binding transcription factors 1 and 2 (SREBF1 and SREBF2). When individually over-expressing MVK and LSS serum heterotrophy was mildly alleviated but, when combined, it was totally reverted. The over-expression SREBF2 alone not only promoted the complete reversion of serum heterotrophy but resulted in higher infectious titers than those of standard serum supplementation conditions. This action was cholesterolgenesis-specific since the over-expression of sterol regulatory binding factor 1 (SBRF1), more related to fatty-acid biosynthesis, had no effect neither on viral productivity nor in the capability of reverting serum heterotrophy.

In **Chapter VI**, the energy metabolism of 293 FLEX cells was targeted, namely by the down-regulation of the Warburg effect (WE) lactogenic phenotype. A proof-of-concept metabolic engineering study was conducted based on the down-regulation of two key molecular effectors of the WE: hypoxia inducible factor 1 (HIF1) and pyruvate dehydrogenase kinase (PDK), simultaneously tackling reduced lactate accumulation and enhanced channeling of glycolytic intermediates into the tricarboxylic acid cycle (TCA). For single gene manipulation, (HIF1 or PDK), clones producing up to 30-fold higher titers of infectious particles were isolated. Without substantial differences in glucose consumption, lactate production was diminished up to 4-fold, indicating the channeling of the consumed glucose into non-lactogenic routes. The physiological fingerprints associated to high-titer HIF1 down-regulated clones also showed significant recruitment of (non-lactogenesis) metabolic pathways previously related to virus production.

For the isolation of high-producing phenotypes in WE down-regulated clones, hundreds of other low-producing clones were individually analyzed. Clone screening required over one year, making it impracticable to use the same strategy for the more than 30 gene candidates identified in the first part of the work. To overcome this bottleneck, a novel method for fast screening of the individual clone's productivity was implemented: the single step cloning-titration method (**Chapter VII**). This method

makes use of split-GFP, a green fluorescent protein separated into 2 fragments – S10 and S11 – which fluoresce only upon transcomplementation. Retrovirus producer cells secreting S11-viruses are cloned and co-cultured with S10-expressing cells and during the period of clone expansion S11 viruses infect S10 target cells reconstituting the GFP signal. Only the clones yielding high signal are isolated, avoiding cell expansion, cell banking and posterior growth/titration studies, of the low titer clones. Moreover, as each well contains a clone-derived colony, transcomplemented fluorescence data can be treated as an estimation of clone's productivity and analyzed in terms of density distribution. The method combines the power of single-cell resolution with the dynamics of cell population analysis.

The traditional approaches for cell engineering involve labor-intensive steps, turning multiple manipulations extremely difficult. Current state-of-the-art in multi-gene mammalian cell engineering has been restricted to 2-3 genes. The development and implementation of the single step cloning-titration method unlocked the manipulation of multiple genes by reducing the one year process of clone screening to two weeks (**Chapter VIII**). Herein more than 30 gene candidates for vector productivity improvement were identified, and 17 have been tested: lanosterol synthase (LSS), mevalonate kinase (MVK), sterol regulatory element binding factors 1 and 2 (SREBF1 and SREBF2), isocitrate dehydrogenase 1 and 2 (IDH1 and IDH2), glutathione synthase (GSS), cystathionine β -synthase (CBS), cystathionase (CTH), heat shock 70kDa protein 5 (HSPA5), ornithine decarboxylase 1 (ODC1) and its anti-enzyme inhibitor 1 (AZIN1), arginase 1 (ARG1), argininosuccinate synthase 1 (ASS1), the inhibitor of the α -subunit of hypoxia inducible factor 1 (HIF1AN), B-cell CLL/lymphoma 2 (BCL2) and X-box binding protein 1 (XBP1). Individually, these manipulations delivered clones producing up to 15-fold higher infectious particles titers (e.g: CBS). Future follow-up work will profit from the already validated genes showing to improve vector productivity, which will be combined in search of novel metabolic dynamics steering enhanced retroviral vector production.

Apart from the therapeutic potential, retrovirus based vectors represent a class of highly complex biopharmaceuticals – RNA enveloped viruses – thereby, an attractive study model for metabolic optimization. Thus, the manipulations herein conducted are likely to be of interest to other enveloped virus replicating in mammalian cells (e.g. lentivirus). Additionally, the knowledge on the metabolic determinants of virus replication is still scarce and the use of integrated strategies to improve hosts productivity and upstream bioprocess an under-explored territory. This thesis contributed to change that landscape: deepening the understanding on the metabolic traits modulating virus production; identifying engineerable targets; leveraging the analytical tools to support gene manipulation and clone screening. All were combined in a pioneer multi-gene manipulation approach, the most extensive metabolic engineering study so far performed in mammalian cells, further enlightening virus-host interaction dynamics.

Resumo

Os biofármacos derivados de vírus recombinantes abrangem inúmeros produtos profiláticos e terapêuticos desde vacinas a vectores de terapia génica. Os retrovírus ocupam um segmento importante deste mercado. Vectores sem capacidade replicativa tem sido extensivamente usados para entrega de material genético em protocolos de terapia génica. Partículas semelhantes a vírus tem demonstrado resultados promissores em vaccinologia como plataformas de apresentação de imunogénios. Partículas com capacidade replicativa tem sido eficientemente usadas como agentes oncolíticos.

A manufactura de vectores retrovirais enfrenta vários desafios. Os títulos obtidos em cultura de células animais encontram-se na ordem das 10^6 às 10^7 partículas infecciosas por mL, requerendo 10 a 100 litros de volume de cultura para tratar um único paciente. Adicionalmente, as preparações virais são caracterizadas por baixas razões de conteúdo de partículas infecciosas por partículas totais. Mais ainda, a produção destes vectores durante períodos longos de cultura depende de soro de sangue animal, limitando a segurança, standardização e qualidade necessárias aos processos de manufactura para uso clínico. Assim, a performance produtiva dos sistemas de manufactura de vectores retrovirais encontra-se abaixo das necessidades terapêuticas e longe de ir ao encontro das exigências da indústria biofarmacêutica para efectuar a transição do clínico para o mercado.

Esta tese de doutoramento usou genómica funcional para compreender as limitações fisiológicas associados à produção de vectores retrovirais em linhas celulares humanas, para aperfeiçoar a sua performance produtiva usando engenharia metabólica reversa.

Na primeira parte deste trabalho (**Capítulo II**), o perfil transcricional e de metabolitos das reacções de carbono central associados à transição 'parental-para-produtora' de duas linhas celulares produtoras de vectores retrovirais – 293 FLEX e Te Fly – foi efectuado. Oito vias foram identificadas como sendo recrutadas na produção

viral: catabolismo de amino ácidos, catabolismo de carboidratos e integração do metabolismo energético, metabolismo nucleotídico, metabolismo do glutatióno, via dos fosfatos de pentose, biossíntese de poli aminas e metabolismo lipídico. A sua capacidade como modeladoras dos títulos virais foi validada por manipulação do meio de cultura, levando a aumentos de produtividade até 6 vezes. Dentro das vias recrutadas, uma nova estratégia exploratória foi usada para identificar potenciais alvos para manipulação génica tendo em vista o aumento de produtividade. Mais de 30 genes foram identificados.

No **Capítulo III**, as limitações fisiológicas subjacentes à heterofia de soro na produção de vectores retrovirais foram investigados. Um estudo aprofundado de cinética de produção viral, caracterização dos vectores e metabolismo de carbono central foi efectuado para as linhas celulares produtoras 293 FLEX e Te Fly usando diferentes concentrações de soro. A ausência da fracção lipídica do soro foi identificada como uma das principais causas da heterotrofia do soro. No seguimento destes resultados, no **Capítulo IV** foi realizada uma adaptação das duas linhas celulares à deprivação de soro, e foram analisados os efeitos nas vias de biossíntese lipídica e produção de vectores infecciosos. O conteúdo celular lipídico total bem como o de colesterol foram quantificados e a biossíntese lipídica avaliada por espectroscopia de ressonância magnética nuclear de Carbono 13. Os efeitos da adaptação à deprivação do soro apresentaram-se como sendo específicos de cada linha celular e directamente correlacionados com os títulos de vectores infecciosos: a linha celular 293 FLEX apresentou uma deprivação lipídica severa e uma redução em 68 vezes do seu título de vírus infecciosos. A linha celular Te Fly foi capaz de manter o conteúdo lipídico total através do aumento da biossíntese lipídica *de novo*, em particular de colesterol, com a consequente recuperação da produtividade de vectores infecciosos. Porém, para a linha celular 293 FLEX, não havia sido encontrado um bloqueio evidente na biossíntese de colesterol. Assim, no **Capítulo V.a**, foi efectuado uma análise por *microarrays* em ambas as linhas celulares em condições de deprivação de soro. Dois pontos de

bloqueio na biossíntese de colesterol foram identificados, exclusivos da linha celular 293 FLEX: os enzimas mevalonato cinase (MVK) e lanosterol sintase (LSS).

Na primeira parte desta tese, várias vias metabólicas e correspondentes genes foram identificados como alvos potenciais para o melhoramento dos títulos e qualidade das preparações retrovirais (por exemplo, para remoção do soro).

Na segunda parte deste trabalho, (**Capítulos V.b a VIII**), o conhecimento reunido foi usado para o delineamento de estratégias racionais de manipulação metabólica através de sobre-expressão ou redução da expressão génica.

No **Capítulo V.b**, o metabolismo lipídico da linha celular 293 FLEX foi manipulado através da sobre-expressão dos enzimas mevalonato cinase (MVK), lanosterol sintase (LSS) e dos factores de transcrição que se ligam a elementos de regulação em esteróis (SREBF1 e 2). Quando sobre-expressados individualmente o MVK e o LSS, a heterotrofia do soro foi ligeiramente aliviada mas, quando em combinação, foi totalmente revertida. A sobre-expressão do SREBF2, não só promoveu a completa reversão da heterotrofia do soro como ainda resultou em títulos infecciosos superiores aos obtidos nas condições *standard* de suplementação. Esta acção foi específica da colesterolgêneses uma vez que a sobre-expressão do SREBF1, mais relacionado com a biossíntese de ácidos gordos, não teve qualquer efeito na produtividade viral nem na capacidade de reverter a heterotrofia do soro.

No **Capítulo VI**, foi manipulado o metabolismo energético da linha celular 293 FLEX, nomeadamente pela redução do fenótipo lactogénico mediado pelo efeito de Warburg (WE). Um estudo de engenharia metabólica para prova de conceito foi efectuado baseado no abaixamento da expressão de dois efectores moleculares chave do efeito de Warburg: o factor indutível por hipóxia 1 (HIF1) e o enzima cinase do complexo piruvato desidrogenase (PDK), simultaneamente visando a redução da acumulação de lactato e um aumento da canalização dos intermediários glicolíticos para o ciclo dos ácidos tricarboxílicos (TCA). Para manipulações génicas únicas (HIF1 ou PDK), foram isolados clones a produzir até 30 vezes mais. Sem diferenças substanciais no consumo de glucose, a produção de lactato diminuiu até 4 vezes, indicando uma maior

canalização da glucose consumida para vias não lactogénicas. As especificidades fisiológicas associadas aos clones de elevados títulos na manipulação do HIF1 demonstraram adicionalmente uma activação de vias metabólicas previamente identificadas com sendo recrutadas na produção de vírus.

Para o isolamento de fenótipos de elevada produtividade dos clones manipulados no efeito de Warburg, centenas de outros clones de baixa produtividade foram individualmente analisados. A análise de clones exigiu mais de um ano, tornando impraticável o uso da mesma estratégia para os mais de 30 genes candidatos identificados na primeira parte do trabalho. Para ultrapassar esta limitação, um novo método foi implementado para a análise rápida da produtividade clonal individual: o método de clonagem e titulação num único passo (**Capítulo VII**). Este método faz uso da GFP fragmentada, uma proteína fluorescente verde separada em dois fragmentos – S10 e S11 – que apenas fluorescem após transcomplementação. Células produtoras que secretam retrovírus para a expressão de S11 são clonadas e co-cultivadas com células que expressam S10 e durante o período de expansão clonal os vírus S11 infectam as células S10 reconstituindo o sinal da GFP. Apenas os clones que originam sinais elevados são isolados, evitando a expansão celular, constituição de banco celular, e estudos posteriores de crescimento e titulação de clones de baixo título. Mais ainda, como cada poço contém uma colónia derivada de uma única célula, os dados de fluorescência transcomplementada podem ser tratados como uma estimativa da produtividade clonal e analisados em termos de distribuição de densidade. Este método combina o poder resolucional da análise célula-a-célula com a dinâmica da análise da população de células.

As abordagens tradicionais para engenharia celular requerem vários passos trabalhosos, tornando manipulações multi-génicas extremamente difíceis. O estado-da-arte em engenharia de células de mamífero tem estado restrito a 2-3 genes. O desenvolvimento e implementação do método de clonagem e titulação num único passo abriu as portas à manipulação de múltiplos genes reduzindo o processo de análise clonal de um ano para duas semanas (**Capítulo VIII**). Nesta tese, mais de 30

genes foram identificados como candidatos para aumentos de produtividade e 17 foram avaliados: lanosterol sintase (LSS), mevalonato cinase (MVK), factores de ligação a elementos regulatórios de esteróis 1 e 2 (SREBF1 and SREBF2), isocitrato desidrogenase 1 e 2 (IDH1 and 2), glutationo sintase (GSS), cistationina β -sintase (CBS), cistationase (CTH), proteína de choque térmico 5 de 70 KDa (HSPA5), descarboxilase de ornitina 1 (ODC1) e o inibidor do seu anti-enzima (AZIN1), arginase (ARG1), argininosuccinato sintase (ASS1), o inibidor da subunidade α do factor indutível por hipóxia (HIF1AN), o factor 2 do linfoma das células B (BCL2), e a proteína de ligação à *box X* (XBP1). Individualmente, estas manipulações originaram clones a produzir até 15 vezes mais partículas infecciosas (por exemplo, CBS). A continuação deste trabalho beneficiará da análise dos genes já validados que demonstraram aumentar a produtividade viral, e que serão combinados em busca de novas dinâmicas metabólicas conducentes a elevados títulos virais.

À parte do seu potencial terapêutico, os retrovírus representam uma classe de biofármacos de elevada complexidade – vírus envelopados de RNA – portanto um modelo de estudo atractivo para optimização metabólica. Assim, as manipulações genéticas conduzidas nesta tese terão provavelmente interesse para outros vírus envelopados que repliquem em células de mamífero (por exemplo, lentivírus). Adicionalmente, o conhecimento sobre as limitações metabólicas da replicação viral é ainda escasso, e o uso de estratégias integradas para melhorar a produtividade dos substratos celulares e parâmetros de bioprocesso um território sub-explorado. Esta tese contribuiu para alterar esse cenário: aprofundado o entendimento sobre os atributos metabólicos que modulam a produção viral; identificando alvos genéticos engenháveis, alavancando as ferramentas analíticas para suportar a manipulação génica e a análise clonal. Tudo isto foi combinado numa abordagem pioneira de manipulação multigénica, o estudo de engenharia metabólica mais extensivo até hoje conduzido em células de mamífero, contribuindo ainda para a elucidação da dinâmica de interacção vírus-hospedeiro.

Thesis publications

Published:

1. Rodrigues AF, Formas-Oliveira AS, Bandeira VS, Alves PM, Hu WS, Coroadinha AS, Metabolic pathways recruited in the production of a recombinant enveloped virus: mining targets for process and cell engineering. 2013 *Metab. Eng.* Nov; 20: 131-145
2. Rodrigues AF, Amaral AI, Veríssimo V, Alves PM, Coroadinha AS, Adaptation of retrovirus producer cells to serum deprivation: implications in lipid biosynthesis and vector production, *Biotechnol Bioeng.* 2012 May;109(5):1269-79
3. Rodrigues AF, Alves PM, Coroadinha AS, 2011. Production of retroviral and lentiviral gene therapy vectors: challenges in the manufacturing of lipid enveloped virus. In: Ke Xu (Ed.), *Viral Gene Therapy*, ISBN: 9780080885049, *InTech Publisher*.
4. Rodrigues AF, Carmo M, Alves PM, Coroadinha AS, Retroviral vector production under serum deprivation: the role of lipids. *Biotechnol Bioeng.* 2009 Dec 15;104(6):1171-81

Submitted:

5. Rodrigues AF, Formas-Oliveira AS, Guerreiro MR, Tomas HA, Alves, Coroadinha AS, Single step cloning-titration method: fast cell line development and dynamic study of the physiological traits in high-titer retrovirus producer cells, (*submitted*)
6. Rodrigues AF, Alves PM, Carrondo MJT, Coroadinha AS, Metabolic hallmarks in the replication of animal viruses: supporting rational manufacture of virus based biopharmaceuticals, (*submitted*)

In preparation:

7. Rodrigues AF, Guerreiro MR, Formas-Oliveira AS, Fernandes P, Blechert A-, Genzel Y, Alves PM, Hu WS, Coroadinha AS, On the down-regulation of the Warburg effect in retrovirus replicating cells: beyond the lactogenic phenotype, (*in preparation*)
8. Rodrigues AF, Formas-Oliveira AS, Alves PM, Hu WS, Coroadinha AS, Reversion of serum heterotrophy in retrovirus replicating cells: reactivation of cholesterol biosynthesis (*in preparation*)
9. Rodrigues AF, Formas-Oliveira AS, Guerreiro MR, Alves PM, Hu WS, Coroadinha AS, Multi-gene engineering retroviral vector producer cells: walking the road to hyperproductivity, (*in preparation*)

Other first-author publications in the scope of 'engineering retrovirus producer cells':

10. Rodrigues AF, Guerreiro MR, Santiago VM, Dalba C, Klatzmann D, Alves PM, Carrondo MJ, Coroadinha AS., Down-regulation of CD81 tetraspanin in human cells producing retroviral-based particles: tailoring vector composition. *Biotechnol Bioeng.* 2011 Nov;108(11):2623-33
11. Rodrigues AF, Guerreiro MR, Castro R, Tomas HA, Dalba C, Klatzmann D, Alves PM, Carrondo MJ, Coroadinha AS, Down-regulation of CD81 in human cells producing HCV-E1/E2 retroVLPs. *BMC Proc.* 2011 Nov 22;5 Suppl 8:P72

Abbreviation list

AAV	Adeno-associated virus
AdV	Adenovirus
AMPK	Adenosine 5' monophosphate-activated protein kinase
BHK	Baby hamster kidney
BSR	Blasticidin resistance gene
CHO	Chinese hamster ovary
CMV	Citomegalovirus
EMCV	Encephalomyocarditis virus
ER	Endoplasmic reticulum
FBS	Foetal bovine serum
FC	Fold-change
FDR	False discovery rate
FLP	Flippase
FRT	Flippase recombination target
GaLV	Gibbon ape leukemia virus
GMP	Good manufacturing practices
HBV	Hepatitis B virus
HCV	Hepatitis C virus
HEK293	Human embryonic kidney 293 cell line
HIF1	Hypoxia inducible factor 1
HIV	Human immunodeficiency virus
HRSV	Human respiratory syncytial virus
HRV	Human rhinovirus
HSV	Herpes simplex virus
HygTK	hygromycin B phosphotransferase/thymidine kinase
IRES	Internal ribosome entry site
KSHV	Kaposi sarcoma-associated herpesvirus
LacZ	Beta galactosidase
LTR	Long-terminal repeat
LV	Lentivirus
MCS	Multiple cloning site
MLV	Murine leukemia virus
MOI	Multiplicity of infection
MSCV	Murine stem cell virus
PBS	Phosphate buffered saline
PDH	Pyruvate dehydrogenase
PDK	Pyruvate dehydrogenase kinase

PEI	Polyethylenimine
PGK	phosphoglycerate kinase
RCME	Recombinase mediated cassette exchange
RNAi	RNA interference
RNS	Reactive nitrogen species
ROS	Reactive oxygen species
RSV	Rous sarcoma virus
RV	Retrovirus
SARS	Severe acute respiratory syndrome virus
SCID	Severe combined immunodeficiency
SFV	Semliki Forest virus
shRNA	Short-hairpin RNA
SSCT	Single step cloning-titration method
SV40	Simian vacuolating virus 40
TCA	Tricarboxylic acids
TK	Thymidine kinase
VACV	Vaccinia virus
VBB	Virus based biopharmaceutical
VLP	Virus like particle
VSV-G	Vesicular stomatitis virus G protein
VZV	Varicella zoster virus
WAD	Weighted average difference

List of contents

Chapter I – Introduction 1

The physiological constraints modulating retroviral vector production

Chapter II – Metabolic pathways recruited in the production of recombinant retrovirus 41

Chapter III – Retroviral vector production under serum deprivation: the role of lipids 71

Chapter IV – Adaptation of retrovirus producer cells to serum deprivation: implications in lipid biosynthesis and vector production 93

Chapter V.a – Identification of lipid biosynthesis bottlenecks underlying serum heterotrophy 115

Metabolic engineering of retrovirus producer cells

Chapter V.b – Reactivation of cholesterol biosynthesis reverts serum heterotrophy 131

Chapter VI – On the down-regulation of the Warburg effect in retrovirus replicating cells: beyond the lactogenic phenotype 141

Chapter VII – Single-step cloning titration method: a high-throughput screening tool for multi-gene engineering 177

Chapter VIII – Multi-gene engineering retroviral vector producer cells 205

Chapter IX - Discussion and perspectives 241

Chapter I

INTRODUCTION

Part of this chapter is adapted from the book chapter:

Rodrigues AF, Alves PM, Coroadinha AS, 2011. Production of retroviral and lentiviral gene therapy vectors: challenges in the manufacturing of lipid enveloped virus. Ke Xu (Ed.), *Viral Gene Therapy*, ISBN: 9780080885049, InTech Publisher.

And from the manuscript:

Rodrigues AF, Alves PM, Carrondo MJT, Coroadinha AS, Metabolic hallmarks in the replication of animal viruses: supporting rational manufacture of virus based biopharmaceuticals, (*submitted*)

Contents

1.	The market of biopharmaceuticals based on recombinant virus.....	3
1.1	Pipeline and strategic trends in biopharmaceuticals based on recombinant virus	3
1.1.1.	Gene delivering particles – gene therapy and oncolytic virotherapy	4
1.1.2.	Antigen delivery and display – virus like particles and DNA vaccines.....	7
2.	Retroviral vectors: valuable therapeutic particles and dynamic study models	8
2.1.	Therapeutic and research applications of retroviral derived particles	8
2.2.	Retrovirus biology and life cycle.....	11
2.3.	State-of-the-art of manufacturing retroviral vectors.....	13
2.3.1.	Retroviral vector producer cell lines	13
2.3.2.	Retroviral vector production systems and process optimization.....	15
3.	Metabolic changes induced by animal viruses: a virus-host interaction perspective	18
3.1.	Lipid metabolism	18
3.2.	Energy metabolism.....	19
3.3.	Nucleic acid metabolism and pentose phosphate pathway	21
3.4.	Oxidative stress metabolism	22
3.5.	Protein processing and post-translational modifications	23
3.6.	Polyamines metabolism	24
4.	Integrated functional genomics in cell engineering: understand to intervene....	25
5.	Metabolic optimization of cell-culture process in virus production	27
5.1.	Media design	28
5.2.	Gene engineering	29
6.	Scope of this thesis.....	31
7.	Author contribution.....	32
8.	References.....	32

1. The market of biopharmaceuticals based on recombinant virus

Virus based biopharmaceuticals (VBBs) constitute an important segment of pharma industry being the vaccine field the most expressive, with an estimate market of US \$40 Billion by 2015 and predictable sustained growth over the next 15 years (Renub Research 2011). More than expanding, this market is moving towards high-margin products based on recombinant viral particles such as the recently licensed human papillomavirus vaccine, Cervarix® (GSK) (Kresse and Shah 2010). Additionally, as these particles offer safer and more flexible platforms for antigen delivery, an increasing interest in non-prophylactic applications including cancer treatment (Cawood et al. 2012) and self-antigen related diseases (Shimada et al. 2013) is emerging. More modest, but witnessing significant investments, is the market of gene therapy expected to generate a US\$ 484 Million market by 2015 (Global Industry Analysts Inc 2012). In November 2012, the European Commission has granted marketing authorization for the first gene therapy medicine, Glybera® (uniQure), anticipating active research and investment in the field over the next decade. Overall, the market of recombinant VBBs is not only experiencing comfortable growth as it holds the promise of novel prophylactic and therapeutic goods for the 21st century.

1.1 Pipeline and strategic trends in biopharmaceuticals based on recombinant virus

Virus based biopharmaceuticals (VBBs) can be defined as any virus derived component or virus-based particle which is able to be used with a therapeutic benefit. This definition includes i) free viral proteins, alone or conjugated; ii) virus-like particles (VLPs), viral genome-free particles assembled to mimic the viral structure; iii) recombinant viruses, in which the viral genome has been modified for a therapeutic purpose and iv) the wild type viruses, inactivated or attenuated, as in the case of many traditional vaccines. The large majority of VBBs of categories ii) and iii), is still in the early phases of clinical development, placing their market potential in the beginning of

next decade. Some of them are, however, in latter stages, with market potential within this decade. A few have already reached the market (Table I).

1.1.1. Gene delivering particles – gene therapy and oncolytic virotherapy

Gene therapy is defined as the transfer of genetic material into an individual's cells or tissues, to treat or prevent a disease. Oncolytic virotherapy appears as sub-field of gene therapy, specifically aiming at eliminating cancer cells, typically – but not exclusively – by delivering suicide genes. The first gene therapy clinical trial was initiated in 1989, for the treatment of patients with advanced melanoma (Rosenberg et al. 1990). But the best well-known are those started right after to treat patients suffering from severe combined immunodeficiencies (SCIDs) which, despite relevant clinical successes, were also associated to serious adverse events (for a review see Fischer et al. (2013)). In both cases, genes were delivered by recombinant Murine Leukemia Virus (MLV) making MLV-based vectors the first ever used and probably the best well studied gene therapy viral vector until today. Since then, the number of viral vectors and treatable conditions by viral gene therapy has been growing.

From the almost 1300 currently ongoing trials, viral vectors account for more than 70% of gene delivery vehicles (Edelstine 2013). Among these, the top most used are based on: i) adenovirus, ii) retrovirus, iii) vaccinia virus, iv) poxvirus, v) adeno-associated virus and vi) herpes simplex virus (Ginn et al. 2013).

Adenoviruses (AdV) have been the blockbuster vector for cancer therapy due to the transient nature of their transgene expression and very high transduction efficiency. Although they represent the most widely used gene therapy viral vector in total clinical trials, the growth rate of their use is dropping. The major drawback associated to these viruses is the strong – and potentially lethal – immune response induced to the patients (Raper et al. 2003). In 2004, Gendicine[®], an adenoviral based vector, was the first human gene therapy product gaining market approval by the Chinese FDA (Pearson et al. 2004) (Table I).

Table I – Pipeline of biopharmaceuticals based on recombinant virus

Indication	Tradename	Company / Institution	VBB	Clinical phase				Cell host
				I	II	III	Market	
Lipoprotein lipase deficiency	Glybera	uniQure	AAV	[Orange]				Insect cells
Hemophilia B	AMT-060	uniQure	AAV	[Orange]				Insect cells
Alpha-1 antitrypsin deficiency	AGTC-0106	Applied Genetic Technologies	AAV	[Orange]				Insect cells
Cardiomyopathy	Mydicar	Celladon	AAV	[Orange]				Insect cells
Parkinson's disease	AAV-hAADC-2	Genzyme	AAV	[Orange]				Insect cells
Anemia	Ad-MG/EPO-1	Medgenics	AdV	[Orange]				Human cells (HEK 293)
Parkinson's disease	ProSavin	Oxford BioMedica	EIAV	[Orange]				Human cells (HEK 293)
Age related macular degeneration	RetinoStat	Oxford BioMedica / Sanofi	EIAV	[Orange]				Human cells (HEK 293)
Stargardt disease	StarGen	Oxford BioMedica / Sanofi	EIAV	[Orange]				Human cells (HEK 293)
Usher Syndrome	UshStat	Oxford BioMedica / Sanofi	EIAV	[Orange]				Human cells (HEK 293)
ADA-SCID	GSK 2696273	GSK	RV	[Orange]				Human cells (HEK 293)
Beta thalassemia	Lentiglobin	Bluebird Bio	LV	[Orange]				Human cells (HEK 293)
Primary and metastatic disease	GMCI	Advantagene	AdV	[Red]				Human cells (HEK 293/ PER.C6)
Prostatic cancer	ProstAtak	Advantagene	AdV	[Red]				Human cells (HEK 293/ PER.C6)
Malignant gliomas	GliAtak	Advantagene	AdV	[Red]				Human cells (HEK 293/ PER.C6)
Pancreatic cancer	PancAtak	Advantagene	AdV	[Red]				Human cells (HEK 293/ PER.C6)
Head/neck cancer	Gendicine	Shenzhen SiBiono GeneTech	AdV	[Red]				Human cells (HEK 293)
Lung cancer	Gendicine	Shenzhen SiBiono GeneTech	AdV	[Red]				Human cells (HEK 293)
Several cancers	Oncorine H101	Shanghai Sunway Biotech	AdV	[Red]				Human cells (HEK 293)
Several cancers	Oncorine H103	Shanghai Sunway Biotech	AdV	[Red]				Human cells (HEK 293)
Prostate / malignant gliomas	Ad.hulFN-β	Biogen	AdV	[Red]				Human cells (HEK 293)
Solid tumors	Rexin G	Epeius Biotechnologies	RV	[Red]				Human cells (HEK 293)
Melanoma and head/neck cancer	Talimogene laherparepvec	Amgen	HSV	[Red]				Green monkey cells (Vero)
Respiratory Syncytial Virus	N/A	Novavax	RSV	[Blue]				Insect cells
Seasonal flu	N/A	Novavax	(H5N1) (H7N9) (H7N3)	[Blue]				Insect cells
Pandemic flu	N/A	Novavax	(H1N1)	[Blue]				Insect cells
HIV-AIDS	ALVAC-HIV	Sanofi	Canarypox / HIV	[Blue]				N/A
Tuberculosis	AERAS-402/ Crucell Ad35	Crucell /Aeras	AdV	[Blue]				Human cells (PER.C6)
Malaria	Ad35-CS malaria	Crucell/GSK	AdV	[Blue]				Human cells (PER.C6)
HIV-AIDS	Ad26.ENVA.01	Crucell / Harvard	AdV	[Blue]				Human cells (PER.C6)
Ebola and Marburg	N/A	Crucell/GSK	AdV	[Blue]				Human cells (PER.C6)
Human Papillomavirus	Cervarix	GSK	HPV	[Blue]				Insect cells
Dengue	N/A	Sanofi-Pasteur	YFV / Dengue	[Blue]				Green monkey cells (Vero)
HCMV infection	N/A	AlphaVax, Inc	VEE	[Blue]				Green monkey cells (Vero)
HIV infection	N/A	AlphaVax, Inc	VEE	[Blue]				Green monkey cells (Vero)

Orange: gene therapy; red: oncolytic virotherapy; blue: vaccines; N/A: not available; AAV: adeno-associated virus; AdV: adenovirus; EIAV: equine infectious anemia (lenti)virus; HIV: human immunodeficiency (lenti)virus; HPV: human papillomavirus; HSV: herpes simplex virus; LV: lentivirus; RSV: respiratory syncytial virus; RV: retrovirus; VEE: Venezuelan equine encephalitis virus; YFV: yellow fever virus.

Simple *retroviruses* (RVs) were the most widely used viral vector until 2004. This top position was displaced by adenovirus afterwards (Edelstein et al. 2004). Together with their complex counterparts, *lentiviruses* (LVs), retroviruses are the blockbuster vectors for the treatment of monogenic and infectious diseases (Edelstine 2013). The use of lentiviruses has been experiencing notable growth rates, from only 12 clinical trials between 2004-2007 to the 67 currently ongoing protocols, an impressive 500% increase. No other vector has grown as much and lentiviruses are likely to place over retrovirus in gene therapy in the years to come. Retro and lentiviral vectors most attractive features as gene transfer tools include minimal immune response, high transduction efficiency *in vivo* and *in vitro*, the ability to permanently modify the genetic content of the target cell and, in the case of lentiviruses, the ability to transduce non-dividing cells. In 2007, the Philippine FDA has granted market authorization for Rexin-G[®], an MLV-based vector bearing cyclin G1 for the treatment of solid tumors (Gordon and Hall 2010) (Table I).

Vaccinia virus (VACV) has over 200 years of experience since, in 1798, Edward Jenner demonstrated protection from smallpox by vaccination (Niemiłowski et al. 1996). It was first used as a gene deliver vector in 1995 as immunotherapy for cervical cancer (Borysiewicz et al. 1996). Vaccinia is a cytoplasmic virus with no evidence of latent infection, turning it particularly interesting for cancer therapy. Indeed, vaccinia based vectors have mainly been used for the treatment of cancer and, to a small extent, infectious diseases (HIV and HCV) (Edelstine 2013). However, due to the WHO campaign to eradicate smallpox, finished in the late 70's, many patients over 30 years presents vigorous immune response to vaccinia vectors decreasing the levels of transgene expression and overall therapy efficacy.

Herpes simplex virus (HSV) offers an interesting platform for gene deliver due to broad host range, high infectivity, ability to transduce non-dividing cells and latent but lifelong infection. They are specially suited for neurological disorders due to the natural neurotropism although the majority of clinical trials have targeted cancer (Edelstine 2013). In fact, their capacity to express the autologous *tk* gene, encoding the

thymidine kinase enzyme, a well characterized suicide gene, makes them particularly interesting for oncolytic virotherapy (Chen et al. 1995). Yet, 70-80% of population from low and 40-60% from improved socio-economic status carries latent HSV infection (Chayavichitsilp et al. 2009), raising safety concerns on reversion of replication deficiency by homologous recombination.

Adeno-associated (AAVs) viral vectors were firstly used in cystic fibrosis gene therapy in 1994. Since then, the applications extended to hemophilia, ocular diseases, Alzheimer's and Parkinson's disease, muscular dystrophies, cardiac failure, dyslipidemia and cancer (Carter 2005; Mueller and Flotte 2008). AAVs are non-pathogenic, readily transducing dividing or non-dividing cells and can persist essentially for the whole cell life-time. Additionally, they accommodate a myriad of modifications from serotype cross-species and serotype variations for versatile capsid engineering to achieve very specific tropism (Asokan et al. 2012). Glybera®, the first human gene therapy product approved in the European market, is a recombinant AAV vector for dyslipidemia treatment (Moran 2012). Adeno-associated viruses are, together with lentivirus, the gene therapy viral vector experiencing the highest growth rate, 96% in the period of 2007-2012 (Ginn et al. 2012) and, likely to take over a significant segment of the gene therapy viral vector market in the future years (Table I). Their main drawback is the small genetic payload they can accommodate.

1.1.2. Antigen delivery and display – virus like particles and DNA vaccines

While for gene therapy vectors, the viral biology dictates the application and, thereby, the trends for future usage, in antigen delivery/display one looks for the development of VBBs targeting diseases for which the prophylactic treatment is insufficient or inexistent. Thus, these are either i) virus-like particles displaying the antigenic proteins of the pathogen to be treated but lacking the nucleic acid content or ii) chimeric particles delivering the pathogen antigens genes.

A good example of i) is the virus like particle (VLP) based vaccine from GSK for preventing human papillomavirus (HPV), Cervarix® (Table I). This vaccine contains

the HPV L1 viral protein from HPV16 and HPV18 assembled into a HPV-like proteic architecture but no nucleic acid is delivered (Monie et al. 2008).

In the category ii) fall, for instance the ALVAC-HIV or the dengue vaccine, both from Sanofi, under clinical testing (Table I). ALVAC-HIV is a chimeric particle comprised by a harmless canary poxvirus structure delivering the *gag* and the *env* genes of HIV-1. ALVAC-HIV was the first vaccine showing significant improvement in preventing HIV infection in human subjects although the results were considered modest (Rerks-Ngarm et al. 2009). The dengue vaccine is also a chimera consisting of ENV glycoproteins of 4 DENV serotypes delivered by a yellow fever virus (YFV) backbone (and also displayed on its surface). Chimeric particles are considered a safer approach for antigen delivery pursued to treat life-threatening pathogens. Their safer profile is achieved by reducing the pathogen antigens to the minimum essential for eliciting a good immune response, delivered by vector backbones derived from less pathogenic viruses. Manufacturing issues may also be a consideration for the development of chimeras for viruses difficult to replicate in cell culture as hepatitis C virus (HCV). Only a few HCV genotypes are capable of cell culture replication and do so by accumulating several mutations poorly resembling those occurring in a clinical context (Bukh et al. 2002). Thus, chimeric particles consisting of an MLV backbone delivering and displaying HCV E1 and E2 antigens are being tested in animal models for the development of a vaccine against HCV (Huret et al. 2013).

2. Retroviral vectors: valuable therapeutic particles and dynamic study models

2.1. Therapeutic and research applications of retroviral derived particles

Gamma-retroviral vectors, commonly designated retroviral vectors, and their derived particles have found a myriad of applications (Fig. 1).

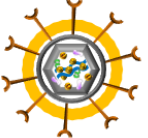
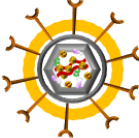


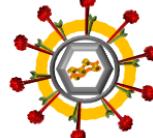
Retroviral genome content	Viral genome containing particles		Viral genome free-particles		
Nucleic acid content	Modified MLV genome		Empty-particles		Heterologous nucleic-acid
Retroviral particles					
	<i>Replication deficient particles</i>	<i>Replication competent particles</i>	<i>Virus-like particles for antigen display</i>	<i>Lipoparticles for probing membrane protein interactions</i>	<i>Virus-like particles for DNA/RNA vaccines</i>
Applications	Gene and Cell Therapy	Oncolytic Therapy	Vaccines	Research	Vaccines

Figure 1 – Therapeutic and research applications of retroviral based particles.

Replication-defective vectors have extensively been used as gene transfer tools in gene therapy protocols. According to the most recent updates, retroviral (together with lentiviral) vectors represent 23% of all the vector types and 33% of the viral vectors used in gene therapy clinical trials (Edelstine 2013). Approved protocols target haemophilia, severe combined immunodeficiency (SCID), HIV infection, Gaucher's disease, β -thalassaemia, muscular dystrophy, Parkinson's disease and cancer (Edelstine 2013).

Virus-like-particles (VLPs) have demonstrated promising results in the vaccinology field as immunogen display platforms, with the additional potential for nucleic-acid delivery (DNA/RNA vaccines). Indeed, retrovirus, retroVLPs included, can easily be pseudotyped with glycoproteins of several virus families, such as lymphocytic choriomeningitis virus, spleen necrosis virus, vesicular stomatitis virus, hepatitis C virus, human immunodeficiency virus, yellow fever virus, West Nile virus and influenza virus (Dalba et al. 2007).

Replication-competent particles (RCP) were developed and efficiently used as oncolytic agents (Dalba et al. 2007). In fact, replicative competent RV vectors are particularly suited for this proposes since they can only integrate and replicate in dividing cells, providing an inherent means for targeting malignant cells that divide actively, while surrounding normal cells are generally quiescent. Furthermore, after transduction, each tumor cell acquires the capability to produce more vectors that will improve the transduction efficiency of the surrounding malignant cells. Hence, they

have been investigated for the treatment of a wide range of cancers including ovarian cancer, breast cancer, brain tumors and lung cancer.

In research, retrovirus based particles have been used as carriers of conformationally-complex membrane proteins to study protein interactions (Willis et al. 2008) and as transduction vehicles of difficult-to-transfect cells (Lindemann and Schnittler 2009) including germ-line cells for research and transgenic mice generation (Kanatsu-Shinohara et al. 2004). Moreover, the major breakthrough in stem cell biology – reprogramming adult somatic cells to a primitive embryonic state establishing the induced pluripotent stem cells (iPSCs) – was firstly achieved, and is still one of the most used means, by retroviral transduction of the Oct-3/4, SOX2, c-Myc, and Klf4 transcription factors (Takahashi and Yamanaka 2006).

More recently, the interest in lentiviral (LV) vectors, derived from complex retroviruses such as the human immunodeficiency virus (HIV), has been growing. LVs embrace the majority of the advantages of simple retrovirus with the additional plus of transducing non-dividing cells (Lewis and Emerman 1994). For human gene therapy they are, in fact, considered as a safer alternative since MLV shows a strong bias to integrate near transcription start sites, potentially activating the expression of oncogenes (Mitchell et al. 2004). However, lentiviral vectors present manufacture challenges identical to those of simple retrovirus, with the additional drawback of high cytotoxicity of some of the vector components hampering stable cell line development (Schweizer and Merten 2010). Commonly, LVs are produced by co-transfecting HEK 293 derived cells with three or four different plasmid constructs. However transient transfection systems are difficult to scale-up, irreproducible, cost-ineffective, and time consuming unlikely to be a valuable approach for large-scale production after the transition clinical-to-market. Still, stable and continuous lentiviral vector production has been achieved by codon-optimization of the viral constructions and their delivery through viral infection (Ikeda et al. 2003; Stornaiuolo et al. 2013). Although these approaches pose safety considerations, they should pave the way towards stable lentiviral vector production in a close future. Until then, and due to their similarity,

strategies for improved manufacture of simple retroviral vectors are a valuable study model, in principle, readily transferable for their complex counterparts. In fact, retroviral vector manufacture is, in general, a very attractive model for process optimization and metabolic engineering studies: i) current producer cells and upstream process are sub-productive offering plenty of room for improvement; ii) they are non-cytotoxic, allowing for metabolic manipulation without the constraints of cell growth arrestment and iii) they represent a complex biopharmaceutical, composed by nucleic acids, lipids and (glycosylated) proteins. Thus, strategies for improved retrovirus production are likely to be of interest to other enveloped virus produced in mammalian cells.

2.2. Retrovirus biology and life cycle

Retroviruses are enveloped viruses characterized by the ability to “reverse-transcribe” their genome from RNA to DNA. Virions measure 100-120 nm and contain a dimeric genome of identical (+)RNA strands complexed with the nucleocapsid (NC) proteins. The genome is enclosed into a proteic capsid (CA) that also contains enzymatic proteins, namely the reverse transcriptase (RT), the integrase (IN) and proteases (PR), required for infection. The matrix proteins (MA) form a layer outside the capsid core that interacts with the envelope, a lipid bilayer derived from the host cellular membrane (Coffin et al. 1997). Anchored on this bilayer are the viral envelope glycoproteins (ENV) responsible for recognizing specific receptors on the host cell and initiating the infection process. Envelope proteins are formed by two subunits, the transmembrane (TM) that anchors the protein into the lipid membrane and the surface (SU) which binds to the cellular receptors (Fig. 2A).

Based on the genome structure, retroviruses are classified into simple (e.g. MLV) or complex retroviruses (e.g. HIV) (Coffin et al. 1997). Both encode four genes: *gag* (group specific antigen), *pro* (protease), *pol* (polymerase) and *env* (envelope) (Fig. 2B). The *gag* sequence encodes the three main structural proteins: MA, CA, NC. The *pro* sequence, encodes proteases (PR) responsible for cleaving Gag and Gag-Pol during

particles assembly, budding and maturation. The *pol* sequence encodes the enzymes RT and IN, the former catalyzing the reverse transcription of the viral genome from RNA to DNA during the infection process and the latter responsible for integrating the proviral DNA into the host cell genome. The *env* sequence encodes for both SU and TM subunits of the envelope glycoprotein.

Retroviral genome also presents non-coding *cis*-acting sequences such as two long terminal repeats (LTRs), containing elements to drive gene expression, reverse transcription and integration into the host cell chromosome, a sequence named packaging signal (ψ) required for specific packaging of the viral RNA into newly forming virions, and a polypurine tract (PPT) that functions as the site for initiating the positive strand DNA synthesis during reverse transcription (Coffin et al. 1997).

Retroviruses enter the cell by receptor mediated endocytosis. The viral envelope glycoproteins bind to specific receptors on the cell surface triggering the fusion of viral and cellular membranes and subsequent release of the viral core into the cytoplasm. Here, it is partially degraded to form a large nucleoprotein – termed pre-integration complex – that is transported to the nucleus. During this process, the viral RNA genome is reverse transcribed into double stranded proviral DNA by the viral reverse transcriptase enzyme (RT). Simple retroviruses are not able to pass through the nuclear membrane, thereby, accessing the nucleus only during mitosis when the nuclear membrane is disassembled. In the nucleus, the proviral DNA is stably integrated into the host chromosomes by the viral integrase enzymes (IN). By using the cellular machinery, the integrated provirus is transcribed to new viral genomic RNA and the viral proteins are translated. Finally, the virions assemble in cholesterol and sphingolipid-rich domains of the plasma membrane – the lipid rafts – being released out of the host cell by budding. At this stage, the virions are still immature particles, becoming mature infectious virus by proteolytic processing carried by the viral protease (PR) (Coffin et al. 1997).

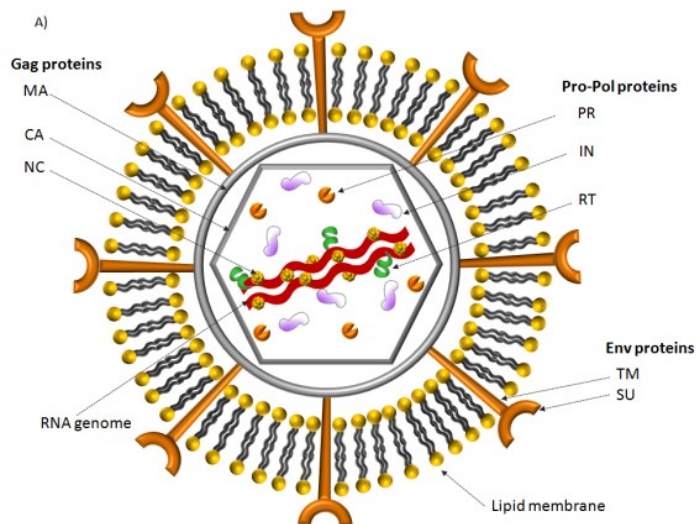


Figure 2 – Retrovirus structure and genome. Schematic representation of a retroviral particle (A) and the retroviral genome (B). CA: capsid; MA: matrix; IN: integrase; NC: nucleocapsid; PR: protease; RT: reverse transcriptase; SU: surface subunit; TM: transmembranar subunit.

2.3. State-of-the-art of manufacturing retroviral vectors

2.3.1. Retroviral vector producer cell lines

Retroviral based vectors are essentially produced in mammalian cells, typically murine or human derived cell lines. This can be based on a short-term transfer of the viral constructs, known as transient production, into exponentially growing cells followed by 24-72 hours vector production and harvesting, or by their stable integration and constitutive expression into the host cell genome, named packaging cell lines, for continuous production (for a review see Coroadinha et al. (2010)).

The establishment of retroviral packaging cell lines is based on the physical separation of the viral genome into different transcriptional units, reducing the risk of generating replicative competent retrovirus (RCRs). Several packaging systems, named generations, have been developed. Each generation aimed at reducing the risk of RCRs

formation face to the previous one. Currently, 3rd generation is applied for the production of retroviral vectors, requiring the transfection of three independent expression cassettes encoding gag-pol, env and transgene functions (Fig. 3A).

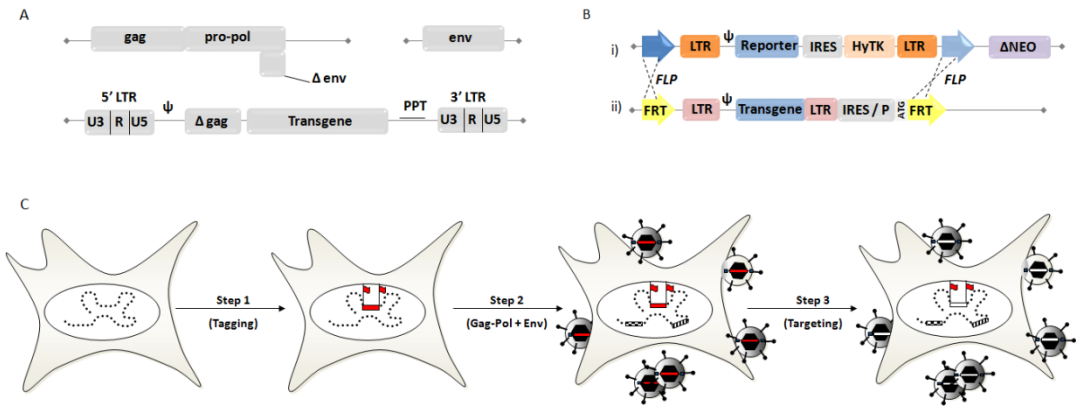


Figure 3 – Retroviral vector construction for 3rd generation retroviral vector producer cell lines. Third generation split genome for replicative deficient RV production including the packaging functions (*gag-pro-pol*) retroviral backbone transgene and envelope (A). Schematic representation of the modular cell lines transgene based on recombinate mediated cassette exchange technology (B): (i) integrated retroviral transgene cassette harboring a marker gene and (ii) targeting therapeutic transgene plasmid allowing for fast exchange and establishment of a new retroviral producer cell. Strategy for the generation of the retroviral vector producer cell line with exchangeable transgene (Coroadinha et al. 2006b) (C).

Since the 3rd generation of MLV vectors requires the expression of three genetic cassettes it is necessary to perform three steps of transfection and clonal selection for stable cell line development. This process takes an average time-frame of one year. To alleviate this burden, a new generation of retrovirus packaging cells (modular cell lines) was developed based on recombinate mediated cassette exchange (RCME) systems allowing for flexible switch of the transgene and/or envelope (Fig. 3B and C) (Coroadinha et al. 2006b; Schucht et al. 2006). A favorable chromosomal site for stable and high retroviral vector production is first identified and tagged. Due to the presence of two heterologous non-compatible flippase recombinase target (FRT) sites flanking the tagged retroviral genome, the subsequent re-use of this defined chromosomal site by means of recombinate-mediated cassette exchange (RMCE) is then performed to express, for instance, a therapeutic gene (Fig. 3B). To select cell clones that underwent

correct targeted integration reaction, the targeting viral vector contains a start codon that complements a transcriptionally inactive ATG-deficient selection marker (Fig. 3B). An example of a modular producing cell line is the 293 FLEX (Coroadinha et al. 2006b) one of the cell lines used in this PhD work. This cell line contains a LacZ transgene tagging a chromosomal locus of high expression that can be exchanged through RMCE technology, MLV gag-pol packaging functions and Gibbon Ape Leukemia Virus (GaLV) ecotropic envelope. The modular producer cell lines present several advantages: they are safer since integration of the vector within the packaging cell line is identified, the duration of the entire development process is reduced as there is no need for screening and, in addition, production conditions are favorable due to the possibility of pre-adaptation of the master cell line to culture conditions and media. Thus, therapeutic virus production from bench to bedside becomes safer, faster, and cheaper (Coroadinha et al. 2006b).

The development of stable retroviral vector producer cell lines is a laborious and time consuming process. However, it is compensated by obtaining continuously producing and highly consistent cell systems, prone to single-effort bioprocess and product characterization, a critical consideration for market approval. Retroviral vector manufacture, including those used in clinical trials, has used stable cell lines for more than 10 years (Coroadinha et al. 2010).

3.3.2. Retroviral vector production systems and process optimization

Despite the advances in the development of suspension cultures for stirred tank bioreactors and its clear advantage from the bioprocess view-point, retroviral vector manufacture for clinical batches has mainly been based on static and, preferably, disposable systems, including large T-flasks, cell factories and roller bottles (Eckert et al. 2000; Merten et al. 2011; Przybylowski et al. 2006; Wikstrom et al. 2004). A good example is retroviral vector production at the National Gene Vector Laboratory, Indiana University, (Indianapolis, IN), a US National Institutes of Health initiative that has as main to mission provide clinical grade vectors for gene therapy trials (Cornetta

et al. 2005). These systems allow for 10 to 100 L vector production under good manufacturing practices (GMP) conditions, meeting the needs for initial clinical trials, where usually a reduced number of patients is involved.

The first bioreaction cell culture system using cells in suspension reported for high-titer retroviral vector production was based on a T-lymphoblastoid cell line using a 3rd generation packaging construct, producing MLV derived retroviral vectors pseudotyped with amphotropic envelope: CEMFLYA cell (Pizzato et al. 2001). These cells were able to produce in the range of 10^7 infectious units *per* mL and, the potential for scale-up production was demonstrated by continuous culture during 14 days in a 250 mL spinner flask. After CEMFLYA, other high-titer suspension cells were reported, namely suspension-adapted 293GPG cells producing MLV retrovirus vector pseudotyped with the vesicular stomatitis virus G (VSV-G) envelope protein and expressing a TK-GFP fusion protein in a 3L acoustic filter-based perfusion bioreactor (Ghani et al. 2006). Another landmark was achieved when the same group published for the first time retroviral vector production in suspension and under serum-free conditions (Ghani et al. 2007).

The cell culture parameters used in retrovirus manufacture may impact the virus titer by affecting the cellular productivities and/or vector stability. The optimal cell culture parameters have been shown to be cell line and viral vector dependent. Optimal pH range for retroviral vector production was found to be between 6.8 and 7.2 for FLY RD18 and Te FLY A7; outside this range the cell specific productivities were considerable lower (McTaggart and Al-Rubeai 2000; Merten 2004) while the retroviral vector was observed to be stable between pH of 5.5 and 8.0 in ecotropic pseudotyped vectors (Ye et al. 2003). Both retroviral (MLV derived) and lentiviral vectors (HIV-1 derived), VSV-G pseudotyped, were stable at pH 7, while decreasing rapidly for $\text{pH} \leq 6.0$ and $\text{pH} \geq 8.0$ (Higashikawa and Chang 2001). The viral half-life is also dependent on the temperature: at lower temperatures the vector decay kinetics are slower (Le Doux et al. 1999). Therefore one strategy explored in the production of retroviral vectors has been the reduction of the culture temperatures (28-32°C). It was also shown that

lower culture temperature reduced the cholesterol content of the viral membrane, increasing the stability (Beer et al. 2003; Coroadinha et al. 2006c). CO₂ gas concentration in the cultures was shown not to affect virus production in packaging cell lines (Kotani et al. 1994; McTaggart and Al-Rubeai 2000). The dissolved oxygen levels used are between 20-80% and, within this range, do not affect viral production unless they became limiting to cell growth (Merten 2004).

Retroviral and lentiviral vector titers obtained in the production prior to purification are in the range of 10⁶ to 10⁷ infectious particles *per* mL of culture medium. Considering the average amount needed to treat a patient in a clinical trial, in the order of 10¹⁰ -10¹² infectious vector (Stacey and Merten 2011), around 10-100 L of culture volume can be estimated for each patient. Also, viral preparations are typically characterized by low ratios of infectious to total particles (around 1:100-1000) which further reduces the therapeutic efficiency of the infectious ones (Carrondo et al. 2008). Additionally, these vectors are extremely sensitive losing their infectivity relatively fast: reported half-lives are between 8-12 hours in cell culture supernatant at 37°C (Carmo et al. 2008; Higashikawa and Chang 2001; Le Doux et al. 1999). On the top, long-term retroviral vector production is dependent on animal blood serum, an ill-defined culture supplement and potential source of pathogen contaminations, hindering the safety and standardization standards required in clinical-grade manufacturing processes.

The problems of low titers, short half-life and low ratios of infectious particles reports to the (wild type) viral biology: the infection is typically chronic and characterized by persistent but low titers in the blood stream, with high amounts of non-infectious particles contaminants and with equivalently low half-lives (Perelson et al. 1996; Rusert et al. 2004). Several strategies have been attempted to circumvent these “natural” drawbacks in packaging cell lines, including engineering mutant vectors with improved resistance features (Vu et al. 2008) optimizing the transcriptional cassettes driving retroviral vector components expression (Schambach et al. 2007) and understanding and optimizing the metabolic pathways leading to improved productivities. Studying the metabolic features supporting high titer retroviral vector

production is the pillar for the work developed during this PhD work and is further discussed in section 5.

3. Metabolic changes induced by animal viruses: a virus-host interaction perspective

Viruses depend upon cellular metabolism for the production of macromolecular substrates and energy. Thus, viral replication comes with marked metabolic changes representing the cellular response to the viral intrusion and, often, the virus usurping the cellular machinery. This section provides an overview on some of the most well described metabolic changes resulting from viral infection in animal cells.

3.1. Lipid metabolism

The role of cellular lipids in viral replication has long been acknowledged. In fact, the hijack of cellular lipid metabolism is a hallmark of many viruses, especially those enveloped, but also for the non-enveloped ones. All viruses rely on lipid scaffolds – whether it is the nucleus, the endoplasmic reticulum (ER), the golgi or the plasma membranes – to provide a physical support for the concentration of viral and cellular factors/proteins required for replication and assembly. For example, (+)RNA viruses rely on membrane structures derived from the secretory pathway including ER invaginations (e.g.: dengue virus) (Welsch et al. 2009), ER derived densely packed double membrane vesicles (e.g.: SARS coronavirus) (Knoops et al. 2008), vesicles derived from Golgi fragmentation (e.g.: HRV1A) (Quiner and Jackson 2010) and autophagosomes (e.g.: HBV) (Li et al. 2011). Other viruses assemble at nuclear membrane such HSV and HCMV (Mettenleiter et al. 2006) or adenovirus (Wodrich et al. 2003). And others, like retrovirus (Ono 2010) or influenza (Nayak et al. 2004) assemble at the plasma membrane.

This reliance on membrane structures often dictates significant changes in host lipid metabolism in benefit of maximum progeny generation. Increased biosynthetic rate of

fatty acids and phospholipids has been shown to occur after infection of HCMV (Munger et al. 2008), dengue (Heaton et al. 2010), poliovirus (Nchoutmboube et al. 2013) and HCV (Fukasawa et al. 2006; Lambert et al. 2013). Moreover, the inhibition of these biosynthetic pathways often results in the impairment of viral replication or defective particles formation in both enveloped (Spencer et al. 2011) and non-enveloped virus (Gaunt et al. 2013). For example, blocking sphingomyelin biosynthesis leads to intracellular trafficking defects of influenza glycoproteins hemagglutinin (HA) and neuraminidase (NA) and substantial reduction in viral production (Tafesse et al. 2013). Increased fatty acid and phospholipid metabolism in viral replication occurs through the expression and activation of lipid biosynthetic enzymes (Spencer et al. 2011), lipid biosynthesis transcriptional machinery (Waris et al. 2007) or reduced lipid oxidation (Seo and Cresswell 2013).

3.2. Energy metabolism

From the entrance into the cellular environment to progeny release, the entire viral cycle occurs at substantial energy expenses for the host. As an example, T. Ando and co-workers estimated ATP concentrations within HCV replicating cells to be about 5 mM at replicating sites (and 1 mM at peripheral sites that did not appear to be involved in HCV replication) in contrast with the 2 mM cytoplasmic ATP levels in non-replicating cells (Ando et al. 2012). These findings suggest that cellular energy resources may be diverted to support viral replication. Three main mechanisms – not necessarily exclusive or independent – by which viruses usurp the cellular energy generation machinery have been described: i) AMPK interaction, ii) Warburg effect-like metabolic reprogramming and iii) mobilization of lipid storages.

Adenosine 5' monophosphate-activated protein kinase (AMPK) functions as a key regulator of the cellular energy status. AMPK activation occurs in response to ATP depletion leading to the inhibition of anabolic processes – including synthesis of protein, lipids and nucleic acid – while stimulating catabolic routes such as lipid oxidation and glucose uptake. AMPK activation has been demonstrated following the

infection of many viruses including HCMV (McArdle et al. 2012), avian reovirus (Ji et al. 2009) and SV40 (Kumar and Rangarajan 2009). Interestingly, not all viruses report to AMPK activation. For instance, HCV and HIV infection has been shown to lead to AMPK inhibition (Mankouri et al. 2010; Zhang and Wu 2009). The mechanisms by which viruses interact with AMPK were suggested to depend on the type of established infection – acute or chronic/latent – the former predominantly associated to AMPK activation and the latter to AMPK inhibition (Mankouri and Harris 2011). Indeed, maintaining cell metabolism in a continuously anabolic status better fits the needs of chronic viruses. This generalization should, however, be taken carefully.

Metabolic reprogramming with enhanced flux through glycolysis and, in some cases, TCA cycle, has been demonstrated for a vast majority of viruses: RSV (Singh et al. 1974), FLV (Bardell and Essex 1974), poliovirus (Levy and Baron 1957), KSHV (Delgado et al. 2010), HCMV (Munger et al. 2006), HSV-1 (Abrantes et al. 2012) and HIV (Hollenbaugh et al. 2011). For the later, the authors report different glycolytic activation behavior depending on if the infected cells were CD4⁺ T cells or macrophages demonstrating that, even the same virus can usurp the metabolic machinery by different means. Enhanced glycolytic flux occurs based on increased expression or activity of the glycolytic enzymes, namely phosphofructokinase (PFK), and is usually associated to an increase in cellular ATP content (Abrantes et al. 2012; Munger et al. 2006; Munger et al. 2008). Even in the cases cellular ATP content remains unchanged, increased ATP is believed to occur but used for viral replication (Silva da Costa et al. 2012). In other cases, such as rubella or adenovirus, ATP rapidly diminishes, seeping out in viral benefit (Bardeletti 1977). The lipid storages may also be used as an energy supply source in viral infections. For example, dengue virus was shown to accumulate on lipid droplets (Samsa et al. 2009) and mobilize their triacylglycerol content enhancing β -oxidation to ensure sufficient ATP levels for replication (Heaton and Randall 2010). Both metabolic reprogramming as well as lipid mobilization processes might be the downstream result of virus-induced AMPK activation.

3.3. Nucleic acid metabolism and pentose phosphate pathway

Any virus carries the biological aim of, by using the cellular resources, to produce as many self-copies as possible, thus, strongly affecting nucleic acid metabolism of host cells. The *modus operandi*, diverges from increasing total RNA/DNA synthesis and substantial *de novo* nucleotide biosynthesis (Maassab et al. 1957; Munger et al. 2006; Tanaka et al. 1975), to arresting nucleic acid synthesis and hijacking nucleic acid content for viral replication (LaColla and Weissbach 1975; Lucas and Ginsberg 1971; Wagner and Roizman 1969). The former seems to be more predominant in latent/chronic viruses while the latter is typical of lytic and acute infections. Mechanisms of cellular nucleic acid content mobilization have also been described: poliomyelitis virus infection was shown to increase the rate of cellular RNA breakdown thereby, expanding the available nucleotide pool, by the possible release of a ribonuclease (Salzman et al. 1959). In the cases of increased *de novo* nucleotide biosynthesis, a set of metabolic rearrangements were shown to occur: increased consumption of nucleic acid precursor amino acids (glutamine, glycine and aspartate) and nucleoside backbones (Munger et al. 2006; Munger et al. 2008). These changes have also been associated with increased enzyme activity and/or expression of nucleotide biosynthesis preceding routes such as pentose phosphate pathway (PPP). For HCV infection increased abundance of PPP enzymes, transketolase (TKT) and transaldolase (TALDO1), were observed (Diamond et al. 2010) while increased activity of glucose 6-phosphate dehydrogenase, catalyzing the first step in PPP has been reported for chicken cells infected with SFV (Cassells and Burke 1973). Changes in PPP metabolites have also been reported in KSHV infection, including significantly elevated levels of ribose 5-phosphate and the ribulose 5-phosphate (and/or xylulose 5-phosphate) (Delgado et al. 2012).

3.4. Oxidative stress metabolism

Viral infections have long been recognized to induce significant oxidative stress to the host, mediated by reactive oxygen and nitrogen species (ROS and RNS). More recently, it began to be understood that this burden plays a role in viral pathogenesis and, what was initially conceived as an inflammation response against a foreign invasion, may well serve as nursing environment for virus replication (Akaike 2001).

HCV is probably the most exhaustively described virus inducing oxidative damage. Several HCV proteins, including the core and NS5A appear to contribute to ROS generation both at mitochondria and ER level by increasing Ca^{2+} uptake, superoxide production, oxidation of the mitochondrial glutathione pool and inhibiting the electron transport complex I activity. The mechanisms on how HCV induces oxidative stress were recently reviewed in (Paracha et al. 2013). Some aspects on how it relates to viral pathogenesis have also been highlighted. For instance, ROS can induce viral genome heterogeneity, which facilitates viral escape during treatment (Serone et al. 2011) and from the immune system (Forns et al. 1999). Anti-oxidants interfere with viral replication and are actually prescribed as part of anti-HCV therapy (Berkson 1999). For other viruses, e.g. influenza A, a decrease in the total concentration of anti-oxidant metabolites as glutathione and vitamins C and E was observed in mice after infection (Hennet et al. 1992). The authors also simulated a ROS-mediated inactivation of α 1-antiprotease – a cellular protein limiting viral maturation – with an impressive 10.000-fold increase in viral infectivity resulting from proteolytic cleavage of haemagglutinin, thereby, showing a beneficial role of ROS in influenza infection. Also HIV has been reported to lead to significant anti-oxidant defenses impairment including reduced levels of ascorbic acid, tocopherols, carotenoids, selenium, superoxide dismutase, and glutathione. Even asymptomatic HIV-infected patients at early stages of the disease exhibit oxidative stress indicators (Pace and Leaf 1995). In cell culture systems, oxidizing agents, such as H_2O_2 , promote replication of HIV and antioxidants, as N-acetyl-cysteine, have the opposite effect (Staal et al. 1990).

A body of evidences suggests oxidative environment as nursing milieu for viral replication. This conclusion may, however, not be straightforward. For example, HCMV was shown to induce intracellular ROS generation within minutes after infection to facilitate its own gene expression and replication through the activation of factor nuclear kappa B (NFkB). Conversely, antioxidants inhibited HCMV immediate-early gene expression and viral replication (Speir et al. 1996). But it has also been recently shown that HCMV activates cellular anti-oxidant defenses by increasing glutathione and glutathione synthesizing enzymes as well as detoxification enzymes such as superoxide dismutase (SOD) and glutathione peroxidase (GPX1). More importantly, this up-regulation appeared to be critical to viral replication as short-interfering RNA experiments for these genes significantly impaired viral titer. These results were postulated to show a virally-driven mechanism to maintain redox homeostasis and control ROS induced stress responses to favor efficient replication (Tilton et al. 2011). However, they might simply be the mirror of the anti-oxidant cellular defenses responding to the redox unbalance caused by viral infection. In fact, other viruses reported to generate high ROS upon infection – as influenza A and HCV – were shown to up-regulate the expression of anti-oxidant enzymes including MnSOD, but not Cu/ZnSOD, in both cases (Jacoby and Choi 1994; Qadri et al. 2004).

3.5. Protein processing and post-translational modifications

The large majority of viruses carries cellular entry through receptor-mediated endocytosis, following the attachment of the viral spikes to the cell surface receptors. For the vast majority, these receptors are glycosylated proteins. It is thus not surprising that viral replication significantly impacts protein processing in the ER and post-translational modifications (PTMs) pathways. Glycosylation is one of the most relevant PTMs in viral replication. Several viruses have been shown to take advantage of the cellular glycosylation machinery to modify viral proteins and, in most viruses, glycosylation has a role in viral biogenesis, stability, antigenicity and infectivity. The importance of glycosylation to viral virulence and immune evasion has been reviewed

in Vigerust and Shepherd (2007). Highly glycosylated proteins include the surface proteins of influenza A, hemagglutinin (HA) and neuraminidase (NA), HCV E1, lassa virus glycoprotein (GP), Newcastle virus hemagglutinin-neuraminidase (HN), ebola virus glycoprotein (GP), and the envelope protein (gp120) of HIV-1 which is one of the most heavily glycosylated proteins in nature. More than using the available resources, viruses can hijack and modulate glycosylation machinery. For example, K. Nyström and colleagues studied the transcriptional activation mediated by HSV, HCMV and varicella zoster virus (VZV) and demonstrated activated expression of several fucosyltransferases (FUT3, FUT5 and FUT6) that were either dormant or expressed at low levels in uninfected cells. They also found CMV, but not VZV, to induced transcription of FUT1, FUT7, and FUT9 (Nystrom et al. 2004; Nystrom et al. 2007).

Another well described PTM targeted by viral infection is ubiquitination. Several viral factors target or mimic components of the SUMOylation (Small Ubiquitin-like Modifier) machinery. For example, KSHV encodes an enzyme, K-bZip, which displays E3 SUMO ligase activity catalyzing SUMO conjugation to host targets – as p53 and Retinoblastoma (Rb) protein – potentially modulating host genes expression in the early stage of viral infection (Chang et al. 2010). Ebola virus encodes VP35, a protein that binds to the enzyme PIAS1 (protein inhibitor of activated STAT 1) and increases the SUMOylation level of IRF7 (interferon regulatory factor 7) potentially contribution to the dampening of the anti-viral response upon infection (Chang et al. 2009).

3.6. Polyamines metabolism

The role of polyamines in viral replication was most prominently studied in the late 70's and early 80's. A. Raina and colleagues investigated the role of polyamines in the replication of HSV and SFV and observed marked inhibition of virus production in BHK21 cells depleted of polyamines by treatment with alpha-difluoromethylornithine, a specific inhibitor of polyamines synthesis. This inhibition was reversed by supplementation with polyamines (putrescine, spermidine and spermine) and at least

partially reversed by several other diamines and polyamine analogs. They also found the activity of viral RNA polymerase to be significantly decreased in polyamine-depleted cells but rapidly increased after addition of spermidine to the culture medium (Raina et al. 1981). W. Gibson and co-workers reached similar conclusions for HCMV (Gibson et al. 1984). Increased activity (greater than 10-fold) of mammalian type C retroviral DNA polymerases was also reported (Marcus et al. 1981). The authors described two possible mechanisms by which polyamines could enhance polymerase activity: i) interaction with the enzyme-DNA complex in order to stimulate their synthesis or ii) interaction with the activated DNA template limiting of the formation of "dead-end" enzyme-DNA complexes. Although the studies were carried *in vitro*, the same mechanisms are likely to occur *in vivo*. Polyamines can bind to nucleic acids participating in their stabilization, modulate gene transcription events, play a role in membrane rigidity and present anti-oxidant properties (Wallace et al. 2003). These properties may have a beneficial effect on viral replication, particularly by stabilizing viral genome leading to improved encapsidation, changing viral membrane rigidity and preventing its lipid peroxidation.

More recently, D.Kim reported an inhibitory effect of polyamines in the initiation process of SV40 DNA replication *in vitro* (Kim et al. 2008). Interestingly, this inhibition seemed to be mediated by high polyamines concentration, while at low levels the stimulatory effect was confirmed. It is thus difficult to state whether polyamines are beneficial for just a set of viruses and inhibitory for others. In fact, large quantities of polyamines may leverage the effects of another phenomenon – oxidation – as oxidized polyamines are known to exhibit potent anti-viral activity (Bachrach 2007).

4. Integrated functional genomics in cell engineering: understand to intervene

Engineering animal cells metabolism is far from trivial. The classical 'target' approach to cell engineering using single gene manipulation, albeit using rational

strategies, has yielded mixed and often disappointing results (Bro and Nielsen 2004; Lim et al. 2010; O'Callaghan and James 2008). The ultimate wish of cell culturists will be the understanding and the control of the biomolecular and physiological attributes of high producing cell lines for a more directed design of therapeutic producing hosts (Seth et al. 2006). In this context, the developments in functional genomics are allowing moving beyond the blind trial-and-error approaches, promoting and extending the potential of reverse metabolic engineering.

Functional genomics tools comprise several methodologies: genome and DNA sequencing, transcriptional profiling, proteome analysis, metabolite profiling and flux analysis (Bro and Nielsen 2004; Sauer 2004). The fluxome allows observing the functional output of transcriptome, proteome and metabolome changes and links not only the genotype but also to environmental perturbations, thus closer to the cellular phenotype.

In the last decade, with the widespread use of the *omic* tools, we have been observing a build-up of a vast number of potential genes to be used in cell engineering. Proteomic studies of B cells revealed the importance of genes in the secretory protein pathway such as XBP1 (van Anken et al. 2003) which, when expressed in CHO-K1 cells, resulted in an increased production capacity (Tigges and Fussenegger 2006). Microarrays and transcriptomics have unveiled genes: (i) conferring enhanced viability in serum-free media (*egr1* and *Gas6*) (Jaluria et al. 2008), (ii) involved in cell adhesion (*siat7* and *lama4*) (Jaluria et al. 2007), (iii) conferring superior productivity in myelomas (*SLPI* and *Cdc6*) (Dorai et al. 2007) or (iv) involved in cholesterol biosynthesis in NSO cells (Seth et al. 2005).

Metabolomics (the global study of metabolite changes) has been used successfully in prokaryotes and plant engineering for a long time to improve production and the first steps are being made in animal cells (Kuystermans et al. 2007). It is a vital component area of the Systems Biology reflecting more closely the phenotype of a cell or organism than the other *omics* and therefore is a fundamental piece of the puzzle. It has been used as an assisting tool for media development, characterization of cell

lines, clone selection and identification of metabolic process engineering targets to enhance production processes (Khoo and Al-Rubeai 2007; Oldiges et al. 2007). Yet, the redundancy of metabolite profiling also make it more challenging to be used for gene engineering purposes.

An integrative study that includes more than one *omic* will best address the use of functional genomics. In this thesis transcriptomics and metabolomics were used for a better understanding of the data coming from both methodologies. So far the application of functional genomics in the animal cell culture has been focusing on the production of antibodies, mostly in CHO, and hybridoma cells from murine origin. Thus, the field of virus based biopharmaceuticals comprising a promising market of vaccines, oncolytic virus for cancer treatment and gene therapy viral vectors, has been left underexplored.

5. Metabolic optimization of cell-culture process in virus production

Manufacturing virus based biopharmaceuticals using cell culture processes is highly costly. Together with the demanding downstream processing of viral preparations and stringent quality control on the final product, production of virus based biopharmaceuticals is likely to be the most expensive process in the biopharmaceutical industry. Thereby, increased attention is being given to process and cell engineering strategies maximizing titers and quality of the viral bulks. Yet, the majority of the studies aiming at such optimization are, predominantly, descriptive reports on metabolic alterations induced by the “virus producer state” using elegant flux-analysis schemes to suggest potential media or cell engineering targets. Less work has been done in effectively enhancing virus production by media or cell manipulation. This section reviews some of that work.

5.1. Media design

For adenoviral vectors, T. Ferreira and co-workers were able to increase vector titers by adapting the cells to non-ammonogenic medium, reaching 1.8-fold improvement in vector productivity (Ferreira et al. 2005). However, this was reported to be a volumetric improvement, likely to be related with increased cell density and not cell specific virus production.

Other media design strategies have targeted lipid metabolism, mainly when producing enveloped viruses. Indeed, lipid metabolism is a relatively easy pathway to manipulate as, in the presence of an external source, most of cultured cells readily uptake lipids from the culture media (Spector et al. 1980). Lipid supplementation has been used to improve the production performance of retrovirus (Chen et al. 2009) and lentivirus (Mitta et al. 2005) based vectors. Lipid supplementation combined with design of experiments (DoE) was also used to improve the production of HIV Gag-based VLPs produced in HEK 293 up to 2.4-fold (Cervera et al. 2013).

For the case of retroviral vectors, additional efforts have been undertaken by culture media manipulation. The use of sugar sources alternative to glucose such as fructose and galactose was shown to improve retroviral production in Te FLY A7, Te FLY Ga 18, PG13 and Tel CeB cell lines (Coroadinha et al. 2006a; Merten 2004). The lactate production decreased 2- to 6-fold in galactose and fructose media and the vector titers increased up to 8-fold. Indeed, lactate concentrations above 5 mM can inhibit cell growth of Te Fly Ga18 cells and retroviral production (Merten et al. 2001). Additionally to the metabolic shift induced by an alternative carbon source, the effect of high osmotic pressure was also found to be of relevance in the improvement of viral titers. The high osmotic pressure obtained for some of the alternative sugars altered the lipid composition of cellular and viral envelope membranes decreasing the cholesterol to phospholipids ratio in the viral membrane, thus conferring higher stability to the produced vectors (Coroadinha et al. 2006c). The increment of infectious titers was confirmed to be the result of higher cell specific productivities, higher vector

stability and lower production of defective non-infectious particles (Coroadinha et al. 2006a; Coroadinha et al. 2006c).

More recently, N. Carinhas and colleagues combined experimental data and flux analysis to quantify and environmentally manipulate the energy metabolism of SF9 insect cells, producing baculovirus vectors. Culture medium supplementation with pyruvate or α -ketoglutarate at the time of infection resulted in 6- to 7-fold higher specific baculovirus yields at high cell density (Carinhas et al. 2010).

5.2. Gene engineering

Media optimization can lead to relevant titer improvements; however, it is inherently limited to the cell transcriptional machinery. From this perspective, gene engineering appears as a more powerful tool to improve the productivity of cell-culture based processes. Indeed, average productivity improvements by gene engineering means in mammalian cells, range from 2- to 4-fold for single gene and up to 30-fold for double gene manipulation. No media optimization based in two metabolites or macromolecules has reached identical improvements. The efforts on gene-based mammalian cell engineering for improved production of biopharmaceuticals have been reviewed in Lim et al. (2010). Yet, the work done so far has mainly been conducted in the view of enhanced production of recombinant proteins. Reports on gene engineering strategies for improved manufacture of virus based biopharmaceuticals are rather scarce.

R.Peng and colleagues were able to improve lentiviral vector production by increasing the secretory pathway of HEK 293 cells through the over-expression of the vesicle-trafficking protein munc18b (Peng et al. 2010). Another work falling into the gene engineering category, although not for improved viral titers, was described by (Hansen et al. 2005). The authors conceived a strategy to generate more stable retroviral vectors which, being produced by murine-derived cell lines were rapidly inactivated in human serum. By expressing chimeric glycosyltransferases to reduce α -gal-epitope synthesis, they were able to increase serum stability up to 3.5-fold. More

recently, it was described a 9-fold improvement in influenza A production in MDCK cells by stable down-regulation of interferon 7 (IRF7, (Hamamoto et al. 2013). In fact, the idea behind this strategy – increase virus replication by blocking intracellular innate defense responses – had been previously described as an engineering approach and shown to increase the production of lentiviral and adenoviral vector particles by 5- to 10-fold and up to 100-fold for Sindbis virus (de Vries et al. 2008).

All in all, gene engineering of virus producing factories is an under-explored territory. In fact, despite the encouraging reports on high productivity improvements – unlikely to be paired by media manipulation – gene engineering represents a minor fraction of metabolic optimization strategies conducted for animal cell hosts. The main reason behind it is that, contrarily to media design, gene engineering is less straightforward and very time consuming from the experimental point of view.

6. Scope of this thesis

The work developed during this PhD thesis aimed at studying the metabolic constraints of retroviral vector production in human cell lines and using that knowledge to design gene engineering strategies for improved titers and viral preparation quality. The thesis is comprised by two parts: i) functional genomics analysis of retrovirus production using different cell lines and culture conditions and ii) metabolic engineering by gene manipulation of producer cell metabolism.

In the first part, functional genomics studies were conducted, including the transcriptional profiling and central carbon metabolism analysis, following the changes in the transition 'parental-to-producer' of two human cell lines producing recombinant retrovirus. Eight pathways were identified to be recruited in the virus production state and their ability to modulate viral titers was experimentally validated. Additionally, the physiological determinants behind serum heterotrophy in vector production were also investigated. Serum heterotrophy was identified to be driven by an impairment of lipid metabolism at the level of cholesterol biosynthesis.

In the second part of this project, the knowledge gathered from the initial characterization studies was used to genetically engineering producer cells, combined with a novel method assisting the fast identification of high-producing clones: the single step cloning-titration method. Engineered cells were able to improve vector specific productivity more than 30-fold and serum heterotrophy was reverted by re-activating cholesterol biosynthesis through the over-expression of the enzymatic and transcription factor genes of *de novo* cholesterol biosynthetic pathway.

This thesis comprises a frontier work, bridging fundamentals to applied research, contributing to enlarge the understanding on virus-host metabolic interactions and delivering innovative tools to translate such knowledge on the tailored design of cell hosts for improved manufacture of recombinant enveloped virus.

7. Author contribution

Ana Filipa A. F. Rodrigues wrote this chapter based on the referred bibliography and by adapting the above mentioned publications.

8. References

Abrantes JL, Alves CM, Costa J, Almeida FC, Sola-Penna M, Fontes CF, Souza TM. 2012. Herpes simplex type 1 activates glycolysis through engagement of the enzyme 6-phosphofructo-1-kinase (PFK-1). *Biochim Biophys Acta* 1822(8):1198-206.

Akaike T. 2001. Role of free radicals in viral pathogenesis and mutation. *Rev Med Virol* 11(2):87-101.

Ando T, Imamura H, Suzuki R, Aizaki H, Watanabe T, Wakita T, Suzuki T. 2012. Visualization and measurement of ATP levels in living cells replicating hepatitis C virus genome RNA. *PLoS Pathog* 8(3):e1002561.

Asokan A, Schaffer DV, Samulski RJ. 2012. The AAV vector toolkit: poised at the clinical crossroads. *Mol Ther* 20(4):699-708.

Bachrach U. 2007. Antiviral activity of oxidized polyamines. *Amino Acids* 33(2):267-72.

Bardeletti G. 1977. Respiration and ATP level in BHK21/13S cells during the earliest stages of rubella virus replication. *Intervirology* 8(2):100-9.

Bardell D, Essex M. 1974. Glycolysis during early infection of feline and human cells with feline leukemia virus. *Infect Immun* 9(5):824-7.

Beer C, Meyer A, Muller K, Wirth M. 2003. The temperature stability of mouse retroviruses depends on the cholesterol levels of viral lipid shell and cellular plasma membrane. *Virology* 308(1):137-46.

Berkson BM. 1999. A conservative triple antioxidant approach to the treatment of hepatitis C. Combination of alpha lipoic acid (thioctic acid), silymarin, and selenium: three case histories. *Med Klin (Munich)* 94 Suppl 3:84-9.

Borysiewicz LK, Fiander A, Nimako M, Man S, Wilkinson GW, Westmoreland D, Evans AS, Adams M, Stacey SN, Bournsnel ME and others. 1996. A recombinant vaccinia virus encoding human papillomavirus types 16 and 18, E6 and E7 proteins as immunotherapy for cervical cancer. *Lancet* 347(9014):1523-7.

Bro C, Nielsen J. 2004. Impact of 'ome' analyses on inverse metabolic engineering. *Metab Eng* 6(3):204-11.

Bukh J, Pietschmann T, Lohmann V, Krieger N, Faulk K, Engle RE, Govindarajan S, Shapiro M, St Claire M, Bartenschlager R. 2002. Mutations that permit efficient replication of hepatitis C virus RNA in Huh-7 cells prevent productive replication in chimpanzees. *Proc Natl Acad Sci U S A* 99(22):14416-21.

Carinhas N, Bernal V, Monteiro F, Carrondo MJ, Oliveira R, Alves PM. 2010. Improving baculovirus production at high cell density through manipulation of energy metabolism. *Metab Eng* 12(1):39-52.

Carmo M, Panet A, Carrondo MJ, Alves PM, Cruz PE. 2008. From retroviral vector production to gene transfer: spontaneous inactivation is caused by loss of reverse transcription capacity. *J Gene Med* 10(4):383-91.

Carrondo MJ, Merten OW, Haury M, Alves PM, Coroadinha AS. 2008. Impact of retroviral vector components stoichiometry on packaging cell lines: effects on productivity and vector quality. *Hum Gene Ther* 19(2):199-210.

Carter BJ. 2005. Adeno-associated virus vectors in clinical trials. *Hum Gene Ther* 16(5):541-50.

- Cassells AC, Burke DC. 1973. Changes in the constitutive enzymes of chick cells following infection with Semliki Forest virus. *J Gen Virol* 18(2):135-41.
- Cawood R, Hills T, Wong SL, Alamoudi AA, Beadle S, Fisher KD, Seymour LW. 2012. Recombinant viral vaccines for cancer. *Trends Mol Med* 18(9):564-74.
- Cervera L, Gutierrez-Granados S, Martinez M, Blanco J, Godia F, Segura MM. 2013. Generation of HIV-1 Gag VLPs by transient transfection of HEK 293 suspension cell cultures using an optimized animal-derived component free medium. *J Biotechnol* 166(4):152-65.
- Chang PC, Izumiya Y, Wu CY, Fitzgerald LD, Campbell M, Ellison TJ, Lam KS, Luciw PA, Kung HJ. 2010. Kaposi's sarcoma-associated herpesvirus (KSHV) encodes a SUMO E3 ligase that is SIM-dependent and SUMO-2/3-specific. *J Biol Chem* 285(8):5266-73.
- Chang TH, Kubota T, Matsuoka M, Jones S, Bradfute SB, Bray M, Ozato K. 2009. Ebola Zaire virus blocks type I interferon production by exploiting the host SUMO modification machinery. *PLoS Pathog* 5(6):e1000493.
- Chayavichitsilp P, Buckwalter JV, Krakowski AC, Friedlander SF. 2009. Herpes simplex. *Pediatr Rev* 30(4):119-29; quiz 130.
- Chen CY, Chang YN, Ryan P, Linscott M, McGarrity GJ, Chiang YL. 1995. Effect of herpes simplex virus thymidine kinase expression levels on ganciclovir-mediated cytotoxicity and the "bystander effect". *Hum Gene Ther* 6(11):1467-76.
- Chen Y, Ott CJ, Townsend K, Subbaiah P, Aiyar A, Miller WM. 2009. Cholesterol Supplementation During Production Increases the Infectivity of Retroviral and Lentiviral Vectors Pseudotyped with the Vesicular Stomatitis Virus Glycoprotein (VSV-G). *Biochem Eng J* 44(2-3):199-207.
- Coffin JM, Hughes SH, Varmus H. 1997. *Retroviruses*: Cold Spring Harbor.
- Cornetta K, Matheson L, Ballas C. 2005. Retroviral vector production in the National Gene Vector Laboratory at Indiana University. *Gene Ther* 12 Suppl 1:S28-35.
- Coroadinha AS, Gama-Norton L, Amaral AI, Hauser H, Alves PM, Cruz PE. 2010. Production of retroviral vectors: review. *Curr Gene Ther* 10(6):456-73.
- Coroadinha AS, Ribeiro J, Roldao A, Cruz PE, Alves PM, Merten OW, Carrondo MJ. 2006a. Effect of medium sugar source on the production of retroviral vectors for gene therapy. *Biotechnol Bioeng* 94(1):24-36.
- Coroadinha AS, Schucht R, Gama-Norton L, Wirth D, Hauser H, Carrondo MJ. 2006b. The use of recombinase mediated cassette exchange in retroviral vector producer cell lines: predictability and efficiency by transgene exchange. *J Biotechnol* 124(2):457-68.
- Coroadinha AS, Silva AC, Pires E, Coelho A, Alves PM, Carrondo MJ. 2006c. Effect of osmotic pressure on the production of retroviral vectors: Enhancement in vector stability. *Biotechnol Bioeng* 94(2):322-9.
- Dalba C, Bellier B, Kasahara N, Klatzmann D. 2007. Replication-competent vectors and empty virus-like particles: new retroviral vector designs for cancer gene therapy or vaccines. *Mol Ther* 15(3):457-66.
- de Vries W, Haasnoot J, van der Velden J, van Montfort T, Zorgdrager F, Paxton W, Cornelissen M, van Kuppeveld F, de Haan P, Berkhout B. 2008. Increased virus replication in mammalian cells by blocking intracellular innate defense responses. *Gene Ther* 15(7):545-52.
- Delgado T, Carroll PA, Punjabi AS, Margineantu D, Hockenbery DM, Lagunoff M. 2010. Induction of the Warburg effect by Kaposi's sarcoma herpesvirus is required for the maintenance of latently infected endothelial cells. *Proc Natl Acad Sci U S A* 107(23):10696-701.

- Delgado T, Sanchez EL, Camarda R, Lagunoff M. 2012. Global metabolic profiling of infection by an oncogenic virus: KSHV induces and requires lipogenesis for survival of latent infection. *PLoS Pathog* 8(8):e1002866.
- Diamond DL, Syder AJ, Jacobs JM, Sorensen CM, Walters KA, Proll SC, McDermott JE, Gritsenko MA, Zhang Q, Zhao R and others. 2010. Temporal proteome and lipidome profiles reveal hepatitis C virus-associated reprogramming of hepatocellular metabolism and bioenergetics. *PLoS Pathog* 6(1):e1000719.
- Dorai H, Li K, Huang CC, Bittner A, Galindo J, Carmen A. 2007. Genome-wide analysis of mouse myeloma cell lines expressing therapeutic antibodies. *Biotechnol Prog* 23(4):911-20.
- Eckert HG, Kuhlcke K, Schilz AJ, Lindemann C, Basara N, Fauser AA, Baum C. 2000. Clinical scale production of an improved retroviral vector expressing the human multidrug resistance 1 gene (MDR1). *Bone Marrow Transplant* 25 Suppl 2:S114-7.
- Edelstein ML, Abedi MR, Wixon J, Edelstein RM. 2004. Gene therapy clinical trials worldwide 1989-2004-an overview. *J Gene Med* 6(6):597-602.
- Edelstine M. 2013. The Journal of Gene Medicine Clinical Trial Site, <http://www.wiley.com/legacy/wileychi/genmed/clinical/>.
- Ferreira TB, Ferreira AL, Carrondo MJ, Alves PM. 2005. Effect of re-feed strategies and non-ammonogenic medium on adenovirus production at high cell densities. *J Biotechnol* 119(3):272-80.
- Fischer A, Hacein-Bey-Abina S, Cavazzana-Calvo M. 2013. Gene therapy of primary T cell immunodeficiencies. *Gene* 525(2):170-3.
- Forns X, Purcell RH, Bukh J. 1999. Quasispecies in viral persistence and pathogenesis of hepatitis C virus. *Trends Microbiol* 7(10):402-10.
- Fukasawa M, Tanaka Y, Sato S, Ono Y, Nitahara-Kasahara Y, Suzuki T, Miyamura T, Hanada K, Nishijima M. 2006. Enhancement of de novo fatty acid biosynthesis in hepatic cell line Huh7 expressing hepatitis C virus core protein. *Biol Pharm Bull* 29(9):1958-61.
- Gaunt ER, Cheung W, Richards JE, Lever A, Desselberger U. 2013. Inhibition of rotavirus replication by downregulation of fatty acid synthesis. *J Gen Virol* 94(Pt 9):2140.
- Ghani K, Cottin S, Kamen A, Caruso M. 2007. Generation of a high-titer packaging cell line for the production of retroviral vectors in suspension and serum-free media. *Gene Ther* 14(24):1705-11.
- Ghani K, Garnier A, Coelho H, Transfiguracion J, Trudel P, Kamen A. 2006. Retroviral vector production using suspension-adapted 293GPG cells in a 3L acoustic filter-based perfusion bioreactor. *Biotechnol Bioeng* 95(4):653-60.
- Gibson W, van Breemen R, Fields A, LaFemina R, Irmiere A. 1984. D,L-alpha-difluoromethylornithine inhibits human cytomegalovirus replication. *J Virol* 50(1):145-54.
- Ginn SL, Alexander IE, Edelstein ML, Abedi MR, Wixon J. 2012. Gene therapy clinical trials worldwide to 2012 - an update. *J Gene Med*.
- Ginn SL, Alexander IE, Edelstein ML, Abedi MR, Wixon J. 2013. Gene therapy clinical trials worldwide to 2012 - an update. *J Gene Med* 15(2):65-77.
- Global Industry Analysts Inc. 2012. Gene Therapy - Global Strategic Business Report.
- Gordon EM, Hall FL. 2010. Rixin-G, a targeted genetic medicine for cancer. *Expert Opin Biol Ther* 10(5):819-32.
- Hamamoto I, Takaku H, Tashiro M, Yamamoto N. 2013. High yield production of influenza virus in Madin Darby canine kidney (MDCK) cells with stable knockdown of IRF7. *PLoS One* 8(3):e59892.

- Hansen W, Grabenhorst E, Nimtz M, Muller K, Conradt HS, Wirth M. 2005. Generation of serum-stabilized retroviruses: reduction of alpha1,3gal-epitope synthesis in a murine NIH3T3-derived packaging cell line by expression of chimeric glycosyltransferases. *Metab Eng* 7(3):221-8.
- Heaton NS, Perera R, Berger KL, Khadka S, Lacount DJ, Kuhn RJ, Randall G. 2010. Dengue virus nonstructural protein 3 redistributes fatty acid synthase to sites of viral replication and increases cellular fatty acid synthesis. *Proc Natl Acad Sci U S A* 107(40):17345-50.
- Heaton NS, Randall G. 2010. Dengue virus-induced autophagy regulates lipid metabolism. *Cell Host Microbe* 8(5):422-32.
- Hennet T, Peterhans E, Stocker R. 1992. Alterations in antioxidant defences in lung and liver of mice infected with influenza A virus. *J Gen Virol* 73 (Pt 1):39-46.
- Higashikawa F, Chang L. 2001. Kinetic analyses of stability of simple and complex retroviral vectors. *Virology* 280(1):124-31.
- Hollenbaugh JA, Munger J, Kim B. 2011. Metabolite profiles of human immunodeficiency virus infected CD4+ T cells and macrophages using LC-MS/MS analysis. *Virology* 415(2):153-9.
- Huret C, Desjardins D, Miyalou M, Levacher B, Amadoudji Zin M, Bonduelle O, Combadiere B, Dalba C, Klatzmann D, Bellier B. 2013. Recombinant retrovirus-derived virus-like particle-based vaccines induce hepatitis C virus-specific cellular and neutralizing immune responses in mice. *Vaccine* 31(11):1540-7.
- Ikeda Y, Takeuchi Y, Martin F, Cosset FL, Mitrophanous K, Collins M. 2003. Continuous high-titer HIV-1 vector production. *Nat Biotechnol* 21(5):569-72.
- Jacoby DB, Choi AM. 1994. Influenza virus induces expression of antioxidant genes in human epithelial cells. *Free Radic Biol Med* 16(6):821-4.
- Jaluria P, Betenbaugh M, Konstantopoulos K, Frank B, Shiloach J. 2007. Application of microarrays to identify and characterize genes involved in attachment dependence in HeLa cells. *Metab Eng* 9(3):241-51.
- Jaluria P, Konstantopoulos K, Betenbaugh M, Shiloach J. 2008. Egr1 and Gas6 facilitate the adaptation of HEK-293 cells to serum-free media by conferring enhanced viability and higher growth rates. *Biotechnol Bioeng* 99(6):1443-52.
- Ji WT, Lee LH, Lin FL, Wang L, Liu HJ. 2009. AMP-activated protein kinase facilitates avian reovirus to induce mitogen-activated protein kinase (MAPK) p38 and MAPK kinase 3/6 signalling that is beneficial for virus replication. *J Gen Virol* 90(Pt 12):3002-9.
- Kanatsu-Shinohara M, Toyokuni S, Shinohara T. 2004. Transgenic mice produced by retroviral transduction of male germ line stem cells in vivo. *Biol Reprod* 71(4):1202-7.
- Khoo SH, Al-Rubeai M. 2007. Metabolomics as a complementary tool in cell culture. *Biotechnol Appl Biochem* 47(Pt 2):71-84.
- Kim DG, Du J, Miao C, Jung JH, Park SC, Kim DK. 2008. The possible roles for polyamines in the initiation process of SV40 DNA replication in vitro. *Oncol Rep* 19(2):535-9.
- Knoops K, Kikkert M, Worm SH, Zevenhoven-Dobbe JC, van der Meer Y, Koster AJ, Mommaas AM, Snijder EJ. 2008. SARS-coronavirus replication is supported by a reticulovesicular network of modified endoplasmic reticulum. *PLoS Biol* 6(9):e226.
- Kotani H, Newton PB, 3rd, Zhang S, Chiang YL, Otto E, Weaver L, Blaese RM, Anderson WF, McGarrity GJ. 1994. Improved methods of retroviral vector transduction and production for gene therapy. *Hum Gene Ther* 5(1):19-28.
- Kresse H, Shah M. 2010. Strategic trends in the vaccine market. *Nat Rev Drug Discov* 9(12):913-4.

- Kumar SH, Rangarajan A. 2009. Simian virus 40 small T antigen activates AMPK and triggers autophagy to protect cancer cells from nutrient deprivation. *J Virol* 83(17):8565-74.
- Kuystermans D, Krampe B, Swiderek H, Al-Rubeai M. 2007. Using cell engineering and omic tools for the improvement of cell culture processes. *Cytotechnology* 53(1-3):3-22.
- LaColla P, Weissbach A. 1975. Vaccinia virus infection of HeLa cells. I. Synthesis of vaccinia DNA in host cell nuclei. *J Virol* 15(2):305-15.
- Lambert JE, Bain VG, Ryan EA, Thomson AB, Clandinin MT. 2013. Elevated lipogenesis and diminished cholesterol synthesis in patients with hepatitis C viral infection compared to healthy humans. *Hepatology* 57(5):1697-704.
- Le Doux JM, Davis HE, Morgan JR, Yarmush ML. 1999. Kinetics of retrovirus production and decay. *Biotechnol Bioeng* 63(6):654-62.
- Levy HB, Baron S. 1957. The effect of animal viruses on host cell metabolism. II. Effect of poliomyelitis virus on glycolysis and uptake of glycine by monkey kidney tissue cultures. *J Infect Dis* 100(2):109-18.
- Lewis PF, Emerman M. 1994. Passage through mitosis is required for oncoretroviruses but not for the human immunodeficiency virus. *J Virol* 68(1):510-6.
- Li J, Liu Y, Wang Z, Liu K, Wang Y, Liu J, Ding H, Yuan Z. 2011. Subversion of cellular autophagy machinery by hepatitis B virus for viral envelopment. *J Virol* 85(13):6319-33.
- Lim Y, Wong NS, Lee YY, Ku SC, Wong DC, Yap MG. 2010. Engineering mammalian cells in bioprocessing - current achievements and future perspectives. *Biotechnol Appl Biochem* 55(4):175-89.
- Lindemann D, Schnittler H. 2009. Genetic manipulation of endothelial cells by viral vectors. *Thromb Haemost* 102(6):1135-43.
- Lucas JJ, Ginsberg HS. 1971. Synthesis of virus-specific ribonucleic acid in KB cells infected with type 2 adenovirus. *J Virol* 8(2):203-14.
- Maassab HF, Loh PC, Ackermann WW. 1957. Growth characteristics of poliovirus in HeLa cells: nucleic acid metabolism. *J Exp Med* 106(5):641-8.
- Mankouri J, Harris M. 2011. Viruses and the fuel sensor: the emerging link between AMPK and virus replication. *Rev Med Virol* 21(4):205-12.
- Mankouri J, Tedbury PR, Gretton S, Hughes ME, Griffin SD, Dallas ML, Green KA, Hardie DG, Peers C, Harris M. 2010. Enhanced hepatitis C virus genome replication and lipid accumulation mediated by inhibition of AMP-activated protein kinase. *Proc Natl Acad Sci U S A* 107(25):11549-54.
- Marcus SL, Smith SW, Bacchi CJ. 1981. Polyamines stimulate DNA-directed DNA synthesis catalyzed by mammalian type C retroviral DNA polymerases. *J Biol Chem* 256(7):3460-4.
- McArdle J, Moorman NJ, Munger J. 2012. HCMV targets the metabolic stress response through activation of AMPK whose activity is important for viral replication. *PLoS Pathog* 8(1):e1002502.
- McTaggart S, Al-Rubeai M. 2000. Effects of culture parameters on the production of retroviral vectors by a human packaging cell line. *Biotechnol Prog* 16(5):859-65.
- Merten O, Landric L, Danos O. 2001. Influence of the metabolic status of packaging cells on retroviral vector production. *Recombinant Protein Production with Prokaryotic and Eukaryotic Cells*. Dordrecht: Kluwer Academic Publishers.
- Merten OW. 2004. State-of-the-art of the production of retroviral vectors. *J Gene Med* 6 Suppl 1:S105-24.

- Merten OW, Charrier S, Laroudie N, Fauchille S, Dugue C, Jenny C, Audit M, Zanta-Boussif MA, Chautard H, Radrizzani M and others. 2011. Large scale manufacture and characterisation of a lentiviral vector produced for clinical ex vivo gene therapy application. *Hum Gene Ther*.
- Mettenleiter TC, Klupp BG, Granzow H. 2006. Herpesvirus assembly: a tale of two membranes. *Curr Opin Microbiol* 9(4):423-9.
- Mitchell RS, Beitzel BF, Schroder AR, Shinn P, Chen H, Berry CC, Ecker JR, Bushman FD. 2004. Retroviral DNA integration: ASLV, HIV, and MLV show distinct target site preferences. *PLoS Biol* 2(8):E234.
- Mitta B, Rimann M, Fussenegger M. 2005. Detailed design and comparative analysis of protocols for optimized production of high-performance HIV-1-derived lentiviral particles. *Metab Eng* 7(5-6):426-36.
- Monie A, Hung CF, Roden R, Wu TC. 2008. Cervarix: a vaccine for the prevention of HPV 16, 18-associated cervical cancer. *Biologics* 2(1):97-105.
- Moran N. 2012. First gene therapy nears landmark European market authorization. *Nat Biotechnol* 30(9):807-9.
- Mueller C, Flotte TR. 2008. Clinical gene therapy using recombinant adeno-associated virus vectors. *Gene Ther* 15(11):858-63.
- Munger J, Bajad SU, Collier HA, Shenk T, Rabinowitz JD. 2006. Dynamics of the cellular metabolome during human cytomegalovirus infection. *PLoS Pathog* 2(12):e132.
- Munger J, Bennett BD, Parikh A, Feng XJ, McArdle J, Rabitz HA, Shenk T, Rabinowitz JD. 2008. Systems-level metabolic flux profiling identifies fatty acid synthesis as a target for antiviral therapy. *Nat Biotechnol* 26(10):1179-86.
- Nayak DP, Hui EK, Barman S. 2004. Assembly and budding of influenza virus. *Virus Res* 106(2):147-65.
- Nchoutmboube JA, Viktorova EG, Scott AJ, Ford LA, Pei Z, Watkins PA, Ernst RK, Belov GA. 2013. Increased long chain acyl-Coa synthetase activity and fatty acid import is linked to membrane synthesis for development of picornavirus replication organelles. *PLoS Pathog* 9(6):e1003401.
- Niemialtowski MG, Toka FN, Malicka E, Gierynska, Spohr de Faundez I, Schollenberger A. 1996. Controlling orthopoxvirus infections--200 years after Jenner's revolutionary immunization. *Arch Immunol Ther Exp (Warsz)* 44(5-6):373-8.
- Nystrom K, Biller M, Grahn A, Lindh M, Larson G, Olofsson S. 2004. Real time PCR for monitoring regulation of host gene expression in herpes simplex virus type 1-infected human diploid cells. *J Virol Methods* 118(2):83-94.
- Nystrom K, Grahn A, Lindh M, Brytting M, Mandel U, Larson G, Olofsson S. 2007. Virus-induced transcriptional activation of host FUT genes associated with neo-expression of Ley in cytomegalovirus-infected and sialyl-Lex in varicella-zoster virus-infected diploid human cells. *Glycobiology* 17(4):355-66.
- O'Callaghan PM, James DC. 2008. Systems biotechnology of mammalian cell factories. *Brief Funct Genomic Proteomic* 7(2):95-110.
- Oldiges M, Lutz S, Pflug S, Schroer K, Stein N, Wiendahl C. 2007. Metabolomics: current state and evolving methodologies and tools. *Appl Microbiol Biotechnol* 76(3):495-511.
- Ono A. 2010. HIV-1 assembly at the plasma membrane. *Vaccine* 28 Suppl 2:B55-9.
- Pace GW, Leaf CD. 1995. The role of oxidative stress in HIV disease. *Free Radic Biol Med* 19(4):523-8.
- Paracha UZ, Fatima K, Alqahtani M, Chaudhary A, Abuzenadah A, Damanhoury G, Qadri I. 2013. Oxidative stress and hepatitis C virus. *Virol J* 10(1):251.

- Pearson S, Jia H, Kandachi K. 2004. China approves first gene therapy. *Nat Biotechnol* 22(1):3-4.
- Peng RW, Guetg C, Tigges M, Fussenegger M. 2010. The vesicle-trafficking protein munc18b increases the secretory capacity of mammalian cells. *Metab Eng* 12(1):18-25.
- Perelson AS, Neumann AU, Markowitz M, Leonard JM, Ho DD. 1996. HIV-1 dynamics in vivo: virion clearance rate, infected cell life-span, and viral generation time. *Science* 271(5255):1582-6.
- Pizzato M, Merten OW, Blair ED, Takeuchi Y. 2001. Development of a suspension packaging cell line for production of high titre, serum-resistant murine leukemia virus vectors. *Gene Ther* 8(10):737-45.
- Przybylowski M, Hakakha A, Stefanski J, Hodges J, Sadelain M, Riviere I. 2006. Production scale-up and validation of packaging cell clearance of clinical-grade retroviral vector stocks produced in cell factories. *Gene Ther* 13(1):95-100.
- Qadri I, Iwahashi M, Capasso JM, Hopken MW, Flores S, Schaack J, Simon FR. 2004. Induced oxidative stress and activated expression of manganese superoxide dismutase during hepatitis C virus replication: role of JNK, p38 MAPK and AP-1. *Biochem J* 378(Pt 3):919-28.
- Quiner CA, Jackson WT. 2010. Fragmentation of the Golgi apparatus provides replication membranes for human rhinovirus 1A. *Virology* 407(2):185-95.
- Raina A, Tuomi K, Mantyljarvi R. 1981. Roles of polyamines in the replication of animal viruses. *Med Biol* 59(5-6):428-32.
- Raper SE, Chirmule N, Lee FS, Wivel NA, Bagg A, Gao GP, Wilson JM, Batshaw ML. 2003. Fatal systemic inflammatory response syndrome in a ornithine transcarbamylase deficient patient following adenoviral gene transfer. *Mol Genet Metab* 80(1-2):148-58.
- Renub Research. 2011. World Vaccines Market: Vaccine Segments Analysis, Vaccine Cases and Future Forecast.
- Reks-Ngarm S, Pitisuttithum P, Nitayaphan S, Kaewkungwal J, Chiu J, Paris R, Prem Sri N, Namwat C, de Souza M, Adams E and others. 2009. Vaccination with ALVAC and AIDSVAX to prevent HIV-1 infection in Thailand. *N Engl J Med* 361(23):2209-20.
- Rosenberg SA, Aebersold P, Cornetta K, Kasid A, Morgan RA, Moen R, Karson EM, Lotze MT, Yang JC, Topalian SL and others. 1990. Gene transfer into humans--immunotherapy of patients with advanced melanoma, using tumor-infiltrating lymphocytes modified by retroviral gene transduction. *N Engl J Med* 323(9):570-8.
- Rusert P, Fischer M, Joos B, Leemann C, Kuster H, Flepp M, Bonhoeffer S, Gunthard HF, Trkola A. 2004. Quantification of infectious HIV-1 plasma viral load using a boosted in vitro infection protocol. *Virology* 326(1):113-29.
- Salzman NP, Lockart RZ, Jr., Sebring ED. 1959. Alterations in HeLa cell metabolism resulting from poliovirus infection. *Virology* 9:244-59.
- Samsa MM, Mondotte JA, Iglesias NG, Assuncao-Miranda I, Barbosa-Lima G, Da Poian AT, Bozza PT, Gamarnik AV. 2009. Dengue virus capsid protein usurps lipid droplets for viral particle formation. *PLoS Pathog* 5(10):e1000632.
- Sauer U. 2004. High-throughput phenomics: experimental methods for mapping fluxomes. *Curr Opin Biotechnol* 15(1):58-63.
- Schambach A, Galla M, Maetzig T, Loew R, Baum C. 2007. Improving transcriptional termination of self-inactivating gamma-retroviral and lentiviral vectors. *Mol Ther* 15(6):1167-73.
- Schucht R, Coroadinha AS, Zanta-Boussif MA, Verhoeyen E, Carrondo MJ, Hauser H, Wirth D. 2006. A new generation of retroviral producer cells: predictable and stable virus production by Flp-mediated site-specific integration of retroviral vectors. *Mol Ther* 14(2):285-92.

- Schweizer M, Merten OW. 2010. Large-scale production means for the manufacturing of lentiviral vectors. *Curr Gene Ther* 10(6):474-86.
- Seo JY, Cresswell P. 2013. Viperin Regulates Cellular Lipid Metabolism during Human Cytomegalovirus Infection. *PLoS Pathog* 9(8):e1003497.
- Seronello S, Montanez J, Presleigh K, Barlow M, Park SB, Choi J. 2011. Ethanol and reactive species increase basal sequence heterogeneity of hepatitis C virus and produce variants with reduced susceptibility to antivirals. *PLoS One* 6(11):e27436.
- Seth G, Hossler P, Yee JC, Hu WS. 2006. Engineering cells for cell culture bioprocessing--physiological fundamentals. *Adv Biochem Eng Biotechnol* 101:119-64.
- Seth G, Philp RJ, Denoya CD, McGrath K, Stutzman-Engwall KJ, Yap M, Hu WS. 2005. Large-scale gene expression analysis of cholesterol dependence in NS0 cells. *Biotechnol Bioeng* 90(5):552-67.
- Shimada M, Abe S, Takahashi T, Shiozaki K, Okuda M, Mizukami H, Klinman DM, Ozawa K, Okuda K. 2013. Prophylaxis and treatment of Alzheimer's disease by delivery of an adeno-associated virus encoding a monoclonal antibody targeting the amyloid Beta protein. *PLoS One* 8(3):e57606.
- Silva da Costa L, Pereira da Silva AP, Da Poian AT, El-Bacha T. 2012. Mitochondrial bioenergetic alterations in mouse neuroblastoma cells infected with Sindbis virus: implications to viral replication and neuronal death. *PLoS One* 7(4):e33871.
- Singh VN, Singh M, August JT, Horecker BL. 1974. Alterations in glucose metabolism in chick-embryo cells transformed by Rous sarcoma virus: intracellular levels of glycolytic intermediates. *Proc Natl Acad Sci U S A* 71(10):4129-32.
- Spector AA, Mathur SN, Kaduce TL, Hyman BT. 1980. Lipid nutrition and metabolism of cultured mammalian cells. *Prog Lipid Res* 19(3-4):155-86.
- Speir E, Shibutani T, Yu ZX, Ferrans V, Epstein SE. 1996. Role of reactive oxygen intermediates in cytomegalovirus gene expression and in the response of human smooth muscle cells to viral infection. *Circ Res* 79(6):1143-52.
- Spencer CM, Schafer XL, Moorman NJ, Munger J. 2011. Human cytomegalovirus induces the activity and expression of acetyl-coenzyme A carboxylase, a fatty acid biosynthetic enzyme whose inhibition attenuates viral replication. *J Virol* 85(12):5814-24.
- Staal FJ, Roederer M, Herzenberg LA, Herzenberg LA. 1990. Intracellular thiols regulate activation of nuclear factor kappa B and transcription of human immunodeficiency virus. *Proc Natl Acad Sci U S A* 87(24):9943-7.
- Stacey GN, Merten OW. 2011. Host cells and cell banking. *Methods Mol Biol* 737:45-88.
- Stornaiuolo A, Piovani BM, Bossi S, Zucchelli E, Corna S, Salvatori F, Mavilio F, Bordignon C, Rizzardi GP, Bovolenta C. 2013. RD2-MolPack-Chim3, a Packaging Cell Line for Stable Production of Lentiviral Vectors for Anti-HIV Gene Therapy. *Hum Gene Ther Methods*.
- Tafesse FG, Sanyal S, Ashour J, Guimaraes CP, Hermansson M, Somerharju P, Ploegh HL. 2013. Intact sphingomyelin biosynthetic pathway is essential for intracellular transport of influenza virus glycoproteins. *Proc Natl Acad Sci U S A* 110(16):6406-11.
- Takahashi K, Yamanaka S. 2006. Induction of pluripotent stem cells from mouse embryonic and adult fibroblast cultures by defined factors. *Cell* 126(4):663-76.
- Tanaka S, Furukawa T, Plotkin SA. 1975. Human cytomegalovirus stimulates host cell RNA synthesis. *J Virol* 15(2):297-304.
- Tigges M, Fussenegger M. 2006. Xbp1-based engineering of secretory capacity enhances the productivity of Chinese hamster ovary cells. *Metab Eng* 8(3):264-72.

- Tilton C, Clippinger AJ, Maguire T, Alwine JC. 2011. Human cytomegalovirus induces multiple means to combat reactive oxygen species. *J Virol* 85(23):12585-93.
- van Anken E, Romijn EP, Maggioni C, Mezghrani A, Sitia R, Braakman I, Heck AJ. 2003. Sequential waves of functionally related proteins are expressed when B cells prepare for antibody secretion. *Immunity* 18(2):243-53.
- Vigerust DJ, Shepherd VL. 2007. Virus glycosylation: role in virulence and immune interactions. *Trends Microbiol* 15(5):211-8.
- Vu HN, Ramsey JD, Pack DW. 2008. Engineering of a stable retroviral gene delivery vector by directed evolution. *Mol Ther* 16(2):308-14.
- Wagner EK, Roizman B. 1969. Ribonucleic acid synthesis in cells infected with herpes simplex virus. I. Patterns of ribonucleic acid synthesis in productively infected cells. *J Virol* 4(1):36-46.
- Wallace HM, Fraser AV, Hughes A. 2003. A perspective of polyamine metabolism. *Biochem J* 376(Pt 1):1-14.
- Waris G, Felmlee DJ, Negro F, Siddiqui A. 2007. Hepatitis C virus induces proteolytic cleavage of sterol regulatory element binding proteins and stimulates their phosphorylation via oxidative stress. *J Virol* 81(15):8122-30.
- Welsch S, Miller S, Romero-Brey I, Merz A, Bleck CK, Walther P, Fuller SD, Antony C, Krijnse-Locker J, Bartenschlager R. 2009. Composition and three-dimensional architecture of the dengue virus replication and assembly sites. *Cell Host Microbe* 5(4):365-75.
- Wikstrom K, Blomberg P, Islam KB. 2004. Clinical grade vector production: analysis of yield, stability, and storage of gmp-produced retroviral vectors for gene therapy. *Biotechnol Prog* 20(4):1198-203.
- Willis S, Davidoff C, Schilling J, Wanless A, Doranz BJ, Rucker J. 2008. Virus-like particles as quantitative probes of membrane protein interactions. *Biochemistry* 47(27):6988-90.
- Wodrich H, Guan T, Cingolani G, Von Seggern D, Nemerow G, Gerace L. 2003. Switch from capsid protein import to adenovirus assembly by cleavage of nuclear transport signals. *Embo J* 22(23):6245-55.
- Ye K, Dhiman HK, Suhan J, Schultz JS. 2003. Effect of pH on infectivity and morphology of ecotropic moloney murine leukemia virus. *Biotechnol Prog* 19(2):538-43.
- Zhang HS, Wu MR. 2009. SIRT1 regulates Tat-induced HIV-1 transactivation through activating AMP-activated protein kinase. *Virus Res* 146(1-2):51-7.

Chapter II

METABOLIC PATHWAYS RECRUITED IN THE PRODUCTION OF RECOMBINANT RETROVIRUS

This chapter is adapted from:

Rodrigues AF, Formas-Oliveira AS, Bandeira VS, Alves PM, Hu WS, Coroadinha AS, 2013. Metabolic pathways recruited in the production of a recombinant enveloped virus: mining targets for process and cell engineering. *Metab. Eng.* Nov; 20: 131-145

Abstract

Biopharmaceuticals derived from enveloped virus comprise an expanding market of vaccines, oncolytic vectors and gene therapy products. Thus, increased attention is given to the development of robust high-titer cell hosts for their manufacture. However, the knowledge on the physiological constraints modulating virus production is still scarce and the use of integrated strategies to improve hosts productivity and upstream bioprocess an under-explored territory.

In this work, we conducted a functional genomics study, including the transcriptional profiling and central carbon metabolism analysis, following the metabolic changes in the transition ‘parental-to-producer’ of two human cell lines producing recombinant retrovirus. Results were gathered into three comprehensive metabolic maps, providing a broad and integrated overview of gene expression changes for both cell lines. Eight pathways were identified to be recruited in the virus production state: amino acid catabolism, carbohydrate catabolism and integration of the energy metabolism, nucleotide metabolism, glutathione metabolism, pentose phosphate pathway, polyamines biosynthesis and lipid metabolism. Their ability to modulate viral titers was experimentally challenged, leading to improved specific productivities of recombinant retrovirus up to 6-fold. Within recruited pathways in the virus production state, we sought for metabolic engineering gene targets in the low producing phenotypes. A mining strategy was used alternative to the traditional approach ‘high vs. low producer’ clonal comparison. Instead, ‘high vs. low producer’ from different genetic backgrounds (i.e. cell origins) were compared. Several genes were identified as limiting in the low-production phenotype, including two enzymes from cholesterol biosynthesis, two enzymes from glutathione biosynthesis and the regulatory machinery of polyamines biosynthesis. This is thus a frontier work, bridging fundamentals to technological research and contributing to enlarge our understanding of enveloped virus production dynamics in mammalian cell hosts.

Contents

1. Introduction.....	44
2. Materials and methods	45
2.1. Cell lines and culture conditions	45
2.2. Cell growth and viral production studies	45
2.3. Measurement of infectious and genome containing retrovirus titer	46
2.4. RNA extraction and RT-PCR.....	46
2.5. Amplification, labeling and BeadChip hybridization of RNA samples.....	47
2.6. Determination of intracellular oxidative load	47
2.7. Metabolite profiling	47
2.8. Data processing and analysis.....	48
3. Results and discussion.....	48
3.1. Changes in metabolic transcriptome enrich the virus producer state.....	48
3.2. Metabolic transcriptome fingerprints in high producers.....	50
3.3. Enriched pathways modulate viral production	54
3.4. Media manipulation of enriched pathways increases specific cell productivity without changing virus properties.	64
4. Conclusions.....	67
5. Author contribution	68
6. References.....	69

1. Introduction

Biopharmaceuticals derived from enveloped virus produced in mammalian hosts comprise a myriad of valuable products from vaccines to gene therapy vectors. Such products have been based on different *genus* including gammaretrovirus (Dalba et al. 2007), lentivirus (Cockrell and Kafri 2007; Di Nunzio et al. 2011), alphavirus (Atkins et al. 2008), orthopoxvirus (Walsh and Dolin 2011), avulavirus (Schirrmacher and Fournier 2009), flavivirus (Appaiahgari and Vрати 2010) and respirovirus (Griesenbach et al. 2005). As this market expands (Kresse and Shah 2010; Moran 2012) it increases the interest to develop high-titer production hosts. In this context, metabolic optimization by culture medium and gene manipulation are potential tools to improve both process and cell engineering. But metabolic intervention, particularly at the gene engineering level, requires a broad overview on the physiological constraints modulating the (virus) producing phenotype. In recombinant protein production, mammalian cell culture has profited from 20 years of functional genomics studies from transcriptomics to proteomics and metabolomics (Griffin et al. 2007; Khoo and Al-Rubeai 2007). In the case of recombinant virus production, however, the translation of gathered knowledge for the rational design of process and cell engineering is still scarce.

In this work we mine the bases of virus induced metabolic changes and use that knowledge to boost viral titers. A functional genomics study was conducted – including transcriptional profiling and central carbon metabolism analysis – of the metabolic changes occurring in the transition ‘parental-to-producer’ of two different human cell lines, using recombinant retrovirus as an enveloped virus model. Gathered knowledge was used to increase viral titers by media manipulation and to identify targets for gene metabolic engineering for 293 FLEX cells (Coroadinha et al. 2006; Schucht et al. 2006).

To identify gene engineering targets the traditional approach, regardless the bioproduct, has mainly been based on the comparison ‘producers vs. parental’ or ‘high vs. low producers’ for clonal cells with different productivity levels. While this strategy can certainly identify potential targets, their genetic manipulation may often result in small productivity enhancements. A gene already *recruited* in the transition parental-to-

producer or in the high producing clone, is likely to be *responsive* to that transition or phenotype; it also indicates that the cells have the intrinsic capability to express it, with no need for further over-expression. Thus in the work herein presented, in addition to analyzing the transition ‘parentals-to-producers’, we followed a complementary approach by comparing ‘high vs. low producer’ from different genetic backgrounds (two different cell line origins). Comparing different genetic backgrounds for gene engineering has been used, for instance, to evaluate and manipulate glycosylation patterns of recombinant proteins (for a review see Grabenhorst et al. (1999)). To the best of our knowledge, such approach has never been used to mine high productivity transcriptome signatures.

2. Materials and methods

2.1. Cell lines and culture conditions

Te Fly Ga 18 (Cosset et al. 1995; Duisit et al. 1999) and 293 FLEX (Coroadinha et al. 2006; Schucht et al. 2006) are human derived cell lines producing murine leukemia virus (MLV) based vector harbouring a LacZ reporter gene, pseudotyped with gibbon ape leukemia virus (GaLV). Their corresponding parental cell lines are Te671 (ATCC CCL-136) and HEK 293 (ATCC CRL-1573), respectively. The cells were maintained in Advanced Dulbecco’s modified Eagle’s medium, DMEM (Gibco, Paisley, UK), with 25 mM of glucose, supplemented with 10% (v/v) Foetal Bovine Serum (FBS) (Gibco) and 4 mM of glutamine (Gibco). Te671 cell line was also used to titrate infectious retroviral particles. All cells were maintained in an incubator with a humidified atmosphere of 92% air and 8% CO₂ at 37 °C.

2.2. Cell growth and viral production studies

Two types of virus production studies were performed: a 7-day batch culture for cell growth/virus production kinetics, transcriptome analysis and metabolite profiling and a 48+24 hours production/harvesting process to evaluate media supplementation effect on viral titers. For the 7-day batch cultures, producer and parental cells were inoculated in t-flasks at 2×10^4 cells/cm² for Te671 / Te Fly Ga 18 and 4×10^4 cells/cm² for HEK 293 /

293 FLEX 18. Two samples were collected *per day*: culture supernatant was harvested, filtered through 0.45 µm for clarification, aliquoted and stored at -85°C until analysis. Cell concentration and viability was determined by the trypan blue exclusion method. At day 3, total RNA was extracted for transcriptome analysis. For media supplementation studies, cells were inoculated in media containing one or a combination of the following supplements: i) amino acids (Sigma, Steinheim, Germany); ii) nucleosides (Millipore, Billerica, MA, U.S.A); iii) anti-oxidants (Sigma); iv) polyamines (Sigma); v) reduced glutathione (Sigma); a non-supplemented control was also prepared. Total RNA was extracted and vector infectivity decay kinetics were assessed. A detailed illustration of this experimental setup can be found in (Rodrigues et al. 2013). For both growth curves as well as for supplemented media studies, three biological replicates were used.

2.3. Measurement of infectious and genome containing retrovirus titer

Infectious procedure and viral titer determination were performed by limiting dilution infection assay, as previously described in (Rodrigues et al. 2009). Genome containing particles titer was determined by real-time PCR as described elsewhere (Carmo et al. 2004).

2.4. RNA extraction and RT-PCR

Total RNA was extracted using RNeasy Mini Kit (Qiagen, Valencia, CA) according to the manufacturer's instructions. The resultant RNA pellet was eluted in 100 µL of nuclease-free water (Qiagen) and stored at -85°C until further processing. RNA yields were quantified using NanoDrop 2000 (Thermo Scientific, Waltham, MA, USA) and RNA quality was characterized by the quotient of the 28S to 18S ribosomal RNA electropherogram peak using an Agilent 2100 bioanalyzer and the RNA Nano Chip (Agilent, Santa Clara, CA, USA).

For real time PCR, RPL-22 was chosen as a control gene using as forward primer (F): 5'-CTGCCAATTTTGAGCAGTTT-3' and as reverse primer (R): 5'-CTTTGCTGTAGCAACTACGC-3'. Forward (F) and reverse (R) primer sequences for viral genes were the following: envelope (F) 5'-GGACCAAATAGCGAATGGA-3' / (R) 5'-GGTGAAGTGTACGCCTGGAT-3';

gag-pol (F) 5'-GTCCACTATCGCCAGTTGCT-3' / (R) 5'-CTGGGTCCTCAGGGTCATAA-3';
transgene (F) 5'-ACTATCCCGACCGCCTTACT-3' / (R) 5'-TAGCGGCTGATGTTGAACTG-3'.
The reverse transcription of total RNA and qRT-PCR were performed as described in
(Rodrigues et al. 2012).

2.5. Amplification, labeling and BeadChip hybridization of RNA samples

Illumina HumanHT-12 v4 Expression BeadChip microarray technology (Illumina, San Diego, CA, USA) was used to analyze the transcriptional profile of retrovirus production. Illumina TotalPrep RNA Amplification Kit (Ambion, Austin, TX, USA) was used to transcribe 200 ng of RNA according to the manufacturer's recommendation. A total of 700 ng of cRNA was hybridized at 58°C for 16 hours to the Illumina HumanHT-12 v4 Expression BeadChips (Illumina). BeadChips were scanned using an Illumina BeadArray Reader and the Bead Scan Software (Illumina). Three biological replicates were used.

2.6. Determination of intracellular oxidative load

Intracellular oxidative load was determined by measuring the oxidation rate of 2'-dichlorodihydrofluorescein diacetate probe (H₂DCFDA) (Invitrogen), followed by fluorescence emission (ex/em: 490/520 nm). Briefly, cells were seeded in DMEM phenol red free in 96-well plates. 36 hours later a mild permeabilization was induced by saponin (Sigma) at a final concentration of 0.005% (w/v) during 30 minutes at 37°C, after which the probe was added to a final concentration of 10 µM. Fluorescence was measured every 15 minutes during 4 hours and the rate of probe oxidation (RFU/min) was determined.

2.7. Metabolite profiling

Glucose and lactate concentrations were determined with automated enzymatic assays (YSI 7100 Multiparameter Bioanalytical System, USA). Ammonia was quantified enzymatically using the UV assay kit (NZYTech, Lisbon, Portugal). Amino acids were quantified by high performance liquid chromatography (HPLC) using the protocol described in (Carinhas et al. 2010).

2.8. Data processing and analysis

Data was processed using Environment for Statistical Computing (R) 2.7.0 (R Development Core Team 2008) in combination with Bioconductor 2.2 (Gentleman et al. 2004). The Bioconductor lumi package (Du et al. 2008) was used for quality control. Raw data was log₂-transformed using the *lumiT()* function and no background correction was performed (Schmid et al. 2010). Data was transformed using variance-stabilizing transformation (Lin et al. 2008) and quantile normalized (Bolstad et al. 2003). All methods used are implemented in the R package lumi.

Differentially expressed genes were identified by False Discovery Rate using Significance Analysis of Microarrays (Tusher et al. 2001) and Weighted Average Difference (Kadota et al. 2008). The comparison between the two cell lines was performed using Principal Component Analysis (PCA) in Environment for Statistical Computing (R) 2.7.0 using the function *prcom()* after data transposition with the function *t()*. PCA loadings and scores were obtained with the functions *pca\$rotation()* and *pca\$x()*, respectively. Pathway analysis was performed using Ingenuity Pathway Analysis (IPA) (Ingenuity® Systems, www.ingenuity.com). Probes for pathway analysis were selected based on $|WAD| > 1$ criterion when comparing “parentals vs. producers”. For the comparison between the two cell lines, probes with the absolute highest PCA scores were selected.

3. Results and discussion

3.1. Changes in metabolic transcriptome enrich the virus producer state

To investigate relevant pathways for virus production the transcriptome of two producer cell lines – 293 FLEX and Te Fly – was compared with that of their respective parentals: HEK 293 and Te 671. The use of different genetic backgrounds in the transcriptome profiling could provide robustness and confidence to the analysis as relevant pathways in the producer state should emerge independently of the cell line origin. However, it also presented the challenge of finding a common expression signature in two very different transcriptomes. Two criteria were considered to identify

differentially expressed probes: Significance Analysis of Microarrays (SAM) (Tusher et al., 2001) and Weighted Average Difference (WAD) (Kadota et al., 2008). SAM relies on repeated sample permutations to determine the percentage of genes that are identified as differentially expressed by chance, that is, false discovery rate (FDR). WAD is a fold-change (FC)-based method that ranks differential expression based on average difference (between comparisons) and relative average signal intensity so that highly expressed genes are highly ranked. While the former is strictly mathematical, providing statistical confidence, the later better copes with the biological constraints of gene expression particularly evident in mammalian transcriptome analysis: modest fold-changes – usually not passing FDR cut-offs – can be very relevant in highly expressed genes. WAD was thus used for biological significance – selection of differentially expressed probes for pathway analysis – while FDR was used to attribute statistical significance to differentially expressed genes within the identified pathways.

Differentially expressed probes were inputted in Ingenuity Pathway Analysis Software and the results were grouped into functional categories (Fig. 1A). Metabolic pathways were over-represented in this analysis comprising more than 50% of significantly enriched pathways common to both producers. The canonical pathways were then discriminated highlighting the metabolic pathways of: amino acids, nucleotides, glutathione and detoxification metabolism, lipids, polyamines, vitamins and co-factors, carbohydrate and energy integration, glycosylation and pentose phosphate pathway (Fig. 1B). These comprised the candidate metabolic pathways recruited in the production of a recombinant retrovirus.

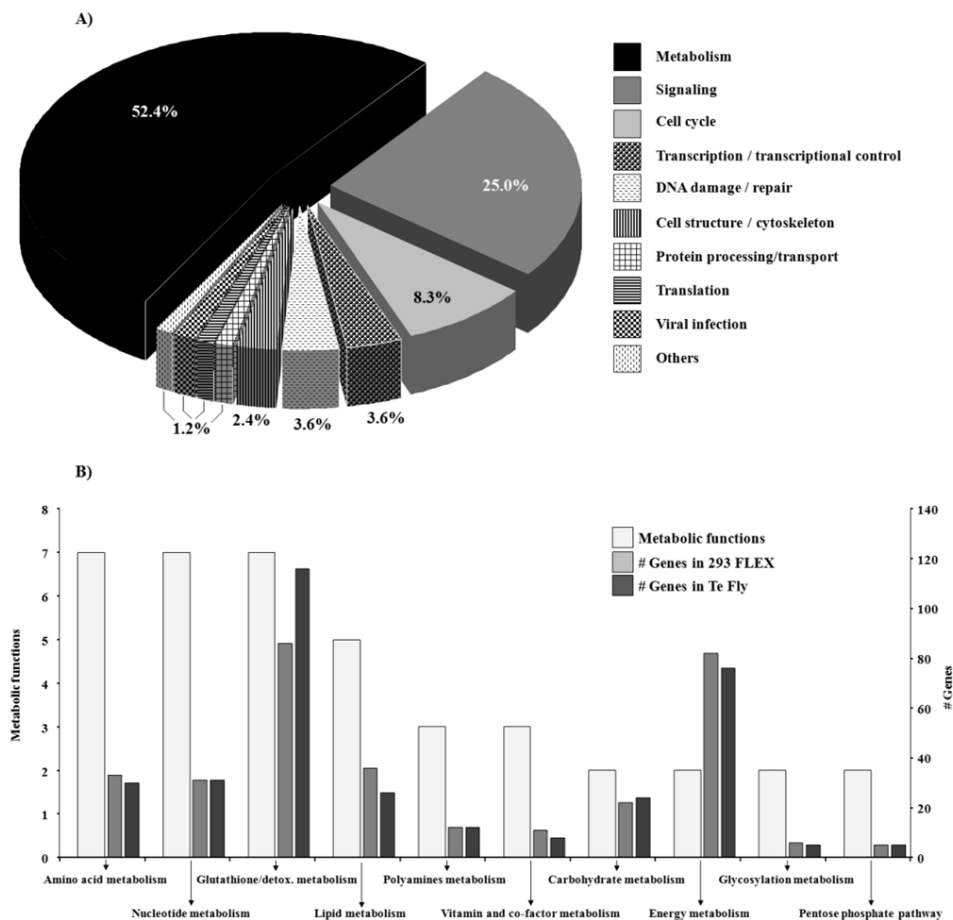


Figure 1 – Enriched pathways in the analysis ‘producers vs. parentals’ for 293 FLEX and Te Fly cells. Biological category distribution of significantly enriched pathways ($p < 0.05$) given by Ingenuity Pathway Analysis of WAD selected data when comparing producers to the respective parental cell lines (A); numbers indicate percentage of significantly enriched pathways common to both producers. Discrimination of pathways comprising the “Metabolism” category (B); left axes refer to number of metabolic functions associated to each pathway and right axes indicates the number of differentially expressed genes enriching such pathways.

3.2. Metabolic transcriptome fingerprints in high producers

The experimental setup in the transcriptional profiling of virus production in Te Fly and 293 FLEX cells comprises the analysis ‘producers vs. parentals’ and the additional assessment of ‘high vs. low producers’, given that Te Fly cells (high-producer) present specific productivity performances one order of magnitude higher than 293 FLEX cells (low-producer). We investigated if this difference was related to specific productivity,

infectious to total particles ratio or limiting expression of the viral components; the results are summarized in Table I.

Table I – Viral productivity performances and viral components expression in 293 FLEX and Te Fly cells

		293 FLEX	Te Fly	FC
Viral production	Infectious particles productivity (I.P./cell.h)	0.016 ± 0.0002	0.36 ± 0.09	20
	Total particles productivity (T.P./cell.h)	8.0 ± 1.1	131 ± 12	16
	I.P./ 1000 T.P.	3.8 ± 0.6	4.6 ± 0.4	NC
Viral components expression	Gag-Pol	5.3 ± 1.2	1.9 ± 0.8	-2.9
	Transgene	1.7 ± 0.6	22 ± 6	13
	Envelope	3.5 ± 0.4	0.8 ± 0.3	-4.2

Specific productivities were calculated by linear fit of infectious or total particles titer vs. the integral of cell number during the exponential growth phase as stated in Rodrigues et al. (2009). Values are shown as average ± standard deviation of three independent replicates. Quantification of viral gene components, gag-pol, transgene and envelope was performed by qRT-PCR; values are shown as average expression (relative to the control gene, RPL22) ± standard deviation of three independent replicates. FC refers to fold-change when comparing high (Te Fly) vs. low (293 FLEX) producers, where positive values denote increases and negative values denote decreases of Te Fly relatively to 293 FLEX; fold-changes are shown for significant changes ($p < 0.05$) based on a two-tailed non-paired t-test, whereas non-significant changes are shown as NC (no change).

Te Fly specific productivity was confirmed to be more than one order of magnitude higher than 293 FLEX both for infectious as well as for total particles. Viral components expression showed significantly lower values of gag-pol and envelope for the Te Fly, demonstrating that none of these is limiting the productivity in the low producer (293 FLEX). Transgene expression, on the other hand, presented a 13-fold increase in Te Fly. Yet, previous work demonstrated that increased transgene expression does not lead to superior productivities in 293 FLEX cells (Carrondo et al. 2008).

The pathways separating high from low producer (Te 671 vs. HEK 293 derived cells) were thus analyzed in the pursuit of potential targets for metabolic engineering in the low producer (293 FLEX) using a principal component analysis (PCA). PCA is multivariate statistical technique that reduces the data dimension to a small number of uncorrelated variables, called principal components, by orthogonal transformations while maximizing the variance captured (Abdi and Williams 2010). As expected, PCA separated HEK 293 from Te 671 derived cell lines, independently of the producer status (data not shown). Thus, the probes with the (absolute) highest PCA scores, those responsible for the highest variability between the two cell lines, were analyzed using Ingenuity Pathway Analysis, to

identify the biological pathways responsible for such separation. Pathway analysis showed signaling pathways to be the most significantly enriched for the comparison ‘high vs. low producers’ (data not shown). Still, metabolism was the scenario most heavily changing the “virus producer state”; its contribution for the increased productivity performance of Te671 derived cells could not be overlooked. Thus, the metabolic pathways found to be enriched in the producer state were scrutinized in the pathways analysis output of PCA filtered data (Table II).

Nucleotide metabolism was considerably different between the two cell lines, with increased (purine) *de novo* biosynthetic capacity for Te 671/Te Fly cells and increased salvage biosynthesis for HEK 293/293 FLEX. For the latter, the majority of the salvage genes were found to be expressed more than 2-fold higher in HEK 293/293 FLEX cells (Table II).

Increased glutathione mediated detoxification and reactive oxygen species scavenging was also found to be a distinctive transcriptional signature of Te 671 derived cells. Genes like glutathione synthase (GSS), glutathione reductase (GSR), isocitrate dehydrogenase 1 (IDH1) and several glutathione transferases (GSTs) were significantly more expressed in these cells, the latter up to 10-fold (Table II).

High producers presented transcriptome changes associated to increased polyamines (putrescine, spermine and spermidine) synthesis, marked by strong down-regulation of ornithine decarboxylase antizyme 1 (OAZ1) – responsible for inhibiting the first and rate-limiting step of polyamine biosynthesis – and increased expression of antizyme inhibitor 1 (AZIN1), promoting the opposite effect (Pegg, 2006)

Finally, increased amino acid catabolism appeared as a distinctive marker in high-producers particularly at the level of branched-chain amino acids (valine, leucine and isoleucine). The first step in this pathway – branched chain aminotransferase 1 (BCAT1) – was found to be over-expressed in high-producers more than 3-fold (Table II). Moreover, branched chain ketoacid dehydrogenase kinase (BCKDK) that inhibits the next step (Harris et al., 1997) (see Fig. 2), presented expression levels 3-fold lower, potentially contributing for increased flux through this route. The hints in the co-factors/vitamins metabolism at

the level of folate transformations are likely to be related to amino acid catabolism (Table II).

Table II – Metabolic pathways distinguishing Te 671 from HEK 293 derived producers

Metabolic pathway	Genes	High vs. low producer (FC q (%))		
		Producer	Parentals	
Nucleotide metabolism	↑ Purines (<i>de novo</i>)	ADSL – adenylosuccinate lyase (ADSL)	1.5 (3.0%)	NC
		IMPDH2 – inosine monophosphate	1.8 (0.3%)	NC
		PAICS – phosphoribosylaminoimidazole	1.4 (2.1%)	1.3 (2.4%)
		PPAT – phosphoribosyl pyrophosphate	1.4 (1.4%)	1.5 (7.2%)
	↓ Purines / pyrimidines (salvage)	PGM2 – phosphoglucomutase 2	-1.6 (0.3%)	NC
		APRT - adenine phosphoribosyltransferase	-2.5 (2.1%)	-2.4 (1.9%)
		HPRT – hypoxanthine	-2.5 (0.1%)	-2.5 (1.9%)
		ADK – adenosine kinase (ADK)	-1.6 (0.7%)	-1.4 (1.4%)
Detoxification metabolism	↑ Glutathione-mediated detoxification	PNP – nucleoside phosphorylase	-2.6 (0.3%)	-2.0 (1.7%)
		UPP1 – uridine phosphorylase 1	-3.4 (0.2%)	-2.9 (4.6%)
		NM3 - non-metastatic cells 3, protein expressed	-2.6 (0.3%)	-2.6 (2.9%)
		IDH1 – isocitrate dehydrogenase 1 (NADP+)	1.3 (1.2%)	NC
		GSTM1 – glutathione S-transferase M1	9.6 (0.0%)	8.3 (1.1%)
	GSTM2 – glutathione S-transferase M2	8.6 (0.1%)	6.5 (0.8%)	
	GSS – Glutathione synthetase	1.6 (2.1%)	1.4 (2.4%)	
	GSR – Glutathione reductase	1.5 (3.0%)	NC	
Amines metabolism	↑ Polyamine biosynthesis	AZIN1 – antizyme inhibitor 1	1.6 (2.1%)	NC
		OAZ1 – ornithine decarboxylase antizyme 1	-1.9 (0.2%)	-1.3 (5.8%)
	↓ Amines catabolism	MAOA - monoamine oxidase A	NC	-2.8 (4.6%)
Amino acid metabolism	↑ Branched chain amino acid catabolism	BCAT1 - branched chain aminotransferase 1	3.1 (0.0%)	4.0 (2.9%)
		BCKDK – branched chain ketoacid	-3.3 (0.1%)	-2.2 (0.3%)
	↑ Citrulline/ornithine	PCCA – propionyl Coenzyme A carboxylase,	4.5 (1.0%)	5.9 (0.4%)
		ASS1 – argininosuccinate synthetase 1	4.0 (0.2%)	3.2 (1.9%)
		↓ Serine catabolism	SDSL – serine dehydratase-like	-2.6 (0.0%)
Cofactors metabolism	↑ Aspartate transamination	GOT2 – glutamic-oxaloacetic transaminase 2	-2.3 (0.3%)	-1.6 (2.9%)
		MTHFD2 – methylenetetrahydrofolate dehydrogenase 2	1.4 (0.3%)	1.8 (0.8%)

Metabolic pathways significantly enriched ($p < 0.05$) given by Ingenuity Pathway Analysis of PCA filtered data. PCA was performed as described in materials and methods and the probes with the absolute highest PCA scores were inputted in Ingenuity software. Up-pointing arrow (↑) indicates up-regulation and down-pointing arrow (↓) indicates down-regulation of the metabolic pathway. FC refers to fold-change when comparing Te671 vs. HEK293 (parentals) and Te Fly vs. 293 FLEX (producers), where positive values denote increases and negative values denote decreases of Te 671 / Te Fly relatively to 293 FLEX / HEK 293 cells. FC values are followed by false discovery rate (q-value %) in-between brackets. FC was considered significant for $q < 10\%$ based on the False Discovery Rate given by Significance Analysis of Microarrays (SAM) (Tusher et al. 2001); NC, indicates no change based on the criteria $q \geq 10\%$. All genes in this table can be mapped to one or more pathways in Figures 2 or 3.

3.3. Enriched pathways modulate viral production

Pathway analysis methods return “enriched pathways” – in which the number of differentially expressed genes is unlikely to be obtained randomly – rather than a direct correlation of such pathways with the phenotype under study. Establishing these relations requires experimental testing a manual analysis on which and how certain genes might be contributing for the observed outputs. Therefore, enriched metabolic pathways in the “producer state” were analyzed to assess possible transcriptome-metabolome correlations and evaluated for their capacity to modulate viral production. Differential expression was gathered into metabolic maps colored to highlight significantly changing genes to better assist a visual interpretation.

Amino metabolism

Amino acid metabolism was one of the top enriched pathways in transcriptome analysis (Fig. 1B). Ammonia production and amino acid uptake/production rates were quantified and are summarized in Table III.

The net amino acid consumption in Te Fly cells remained unchanged relatively to the parentals but ammonia production increased almost 2-fold. This indicated amino acid channeling to energy generation and was supported by increased gene expression particularly in glycine, lysine, and branched chain amino acid catabolic enzymes along with succinate dehydrogenase complex (SDH) – the link to oxidative phosphorylation. 293 FLEX producers also presented identical net consumption of amino acids relatively to the parentals (Table III). But contrarily to Te Fly, ammonia production was decreased by more than 3-fold in 293 FLEX suggesting a preferential channeling of uptake amino acids through ammonia non-generating routes – e.g. protein synthesis. Of notice, Te Fly producers presented consistently higher uptake rates relatively to 293 FLEX producers (Table III). Moreover, some amino acids as phenylalanine, tyrosine and histidine appear to be blocked metabolites as their catabolic enzymes are virtually non-expressed for both cell lines (Fig. 2). Increased consumption can thus suggest increased protein synthesis in

Te Fly cells. In fact, protein synthesis initiation and elongation factors were up-regulated in the producer state and are extensively more expressed in Te Fly (data not shown).

Table III - Growth and central carbon metabolism rates of HEK 293, Te671 and their respective retrovirus producer cell lines, 293 FLEX and Te Fly

	293 derived			Te 671 derived		Producers	
	Parental	Producer		Parental	Producer		
Growth rate (h ⁻¹)	0.019 ± 0.002	0.023 ± 0.004		0.024 ± 0.003	0.026 ± 0.003		
	Specific uptake or production rate (nmol/10 ⁶ cells.h)		FC (a)	Specific uptake or production rate (nmol/10 ⁶ cells.h)		FC (b)	FC (c)
GLC	-219 ± 23	-145 ± 23	-1.5*	-371 ± 50	-320 ± 59		2.2*
LAC	271 ± 45	207 ± 41		590 ± 104	536 ± 118		2.6*
LAC/GLC	1.2 ± 0.1	1.4 ± 0.1		1.6 ± 0.1	1.7 ± 0.1		1.2*
GLN	-44 ± 12	-29 ± 4		-75 ± 6	-79 ± 10		2.8**
AMN	32 ± 7	10 ± 1	-3.2*	29 ± 6	54 ± 10	1.8*	5.4*
AMN/GLN	0.75 ± 0.05	0.35 ± 0.01	-2.1**	0.39 ± 0.05	0.7 ± 0.04	1.8**	2.0**
ASP	-1.2 ± 0.4	-0.59 ± 0.17	-2.0	-0.76 ± 0.09	-0.81 ± 0.25		
GLU	-1.3 ± 0.2	0.35 ± 0.17	3.6**	5.1 ± 2.3	5.4 ± 0.4		15**
SER	-4.6 ± 1.9	-3.8 ± 0.8		-12 ± 1	-10 ± 2		2.8*
ASN	-0.53 ± 0.07	-0.12 ± 0.07	-4.3**	-1.7 ± 0.5	-1.8 ± 0.2		14**
GLY	-1.5 ± 0.2	-2.0 ± 0.2	1.3*	-4.0 ± 1.3	-3.8 ± 0.3		1.9**
HIS	-0.66 ± 0.22	-0.49 ± 0.28		-1.6 ± 0.1	-1.9 ± 0.03		3.9*
THR	-1.3 ± 0.2	-1.8 ± 0.5		-3.3 ± 0.8	-3.0 ± 0.1		1.7
ARG	-4.1 ± 1.2	-2.6 ± 0.5		-7.5 ± 0.4	-6.8 ± 0.6		2.6**
ALA	11 ± 2	5.5 ± 0.9	-1.9*	20 ± 3	25 ± 5		4.6*
PRO	5.0 ± 0.7	3.6 ± 0.2	-1.4*	5.9 ± 0.6	4.8 ± 0.9		
TYR	-0.62 ± 0.24	-0.77 ± 0.29		-2.0 ± 0.9	-2.5 ± 0.4		3.3**
VAL	-2.6 ± 0.5	-2.9 ± 0.44		-5.7 ± 1.0	-6.7 ± 0.3		2.3**
MET	-1.4 ± 0.3	-1.1 ± 0.2		-2.7 ± 0.6	-3.0 ± 0.2		2.7**
ILE	-1.8 ± 0.5	-1.9 ± 0.6		-5.0 ± 1.1	-5.8 ± 0.5		3.1**
LEU	-3.3 ± 0.9	-2.5 ± 0.6		-8.2 ± 0.5	-8.7 ± 0.6		3.4**
LYS	-2.5 ± 0.6	-3.0 ± 0.3		-9.4 ± 2.3	-6.6 ± 1.1		2.2*
PHE	-1.0 ± 0.2	-1.2 ± 0.1		-2.3 ± 0.5	-2.5 ± 0.4		2.1*
TRP	ND	ND		ND	ND		
CYS	ND	ND		ND	ND		
Net a.a uptake ¹	-28 ± 8	-25 ± 6		-66 ± 14	-65 ± 8		2.6*
Net a.a. production	16 ± 3	9 ± 1	-1.6*	31 ± 3	36 ± 3		3.8**

ND: not determined.

¹: excluding glutamine uptake

Specific rates were calculated by linear fit of extracellular metabolite concentration vs. the integral of cell number during the exponential growth phase as stated in Rodrigues et al. (2009). For metabolic rates, negative values denote uptake and positive values denote production rate. FC refers to fold-change in uptake or production rate of (a) 293 FLEX vs. HEK 293, (b) Te Fly vs. Te 671 and (c) Te Fly vs. 293 FLEX. Fold-changes are shown for significantly changing rates (* p<0.05 and ** p<0.005 given by a two-tailed non-paired *t*-test).

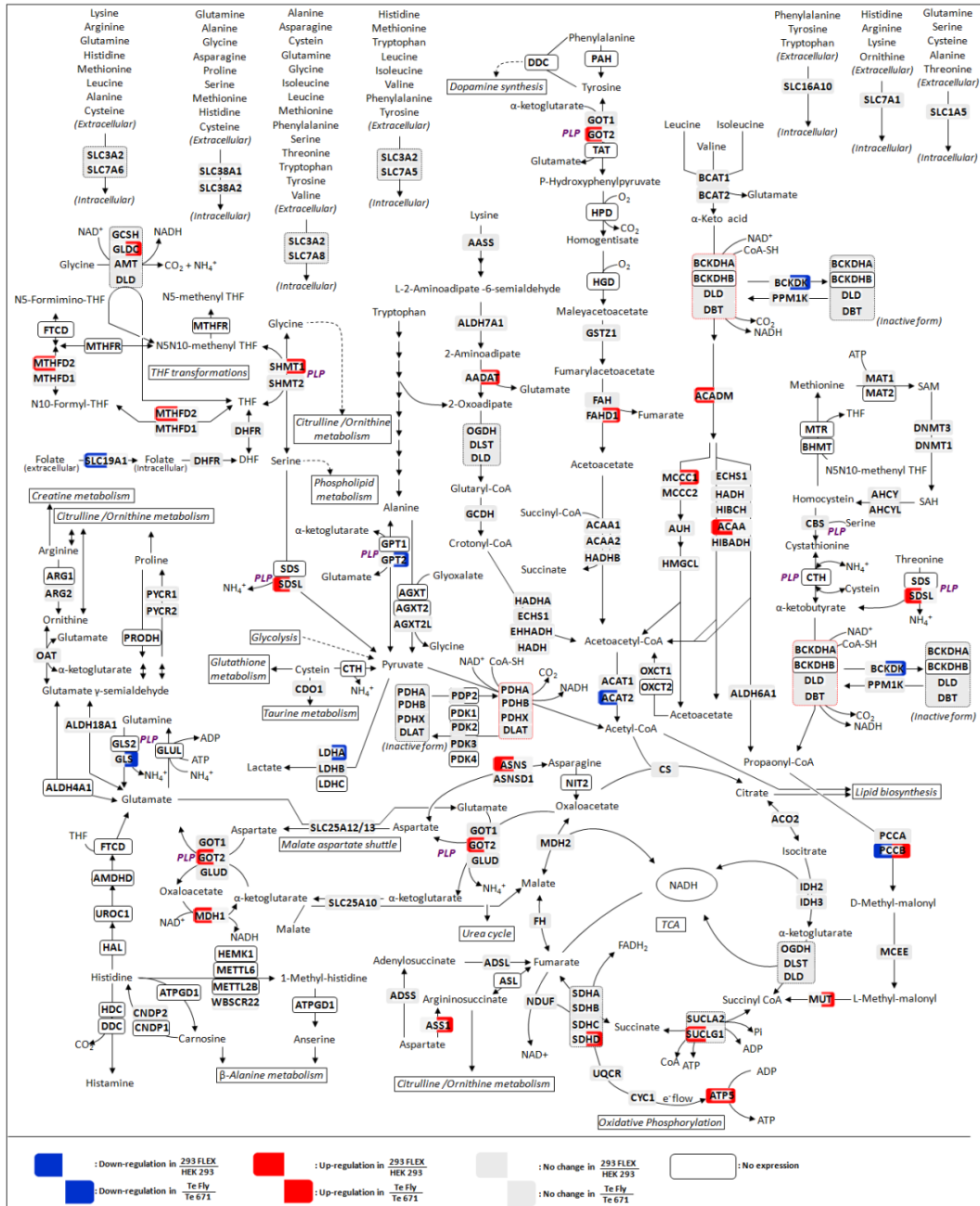
The enrichment in pathway analysis of one-carbon units transfer co-factors – pyridoxal phosphate (PLP), tetrahydrofolate (THF) and S-adenosylmethionine (SAM) (Fig. 1B) – further substantiated the significance of amino acid catabolism enrichment (Nelson and Cox 2000). Gene expression data also suggested the THF transformation cycle to be partially inactive due to the absence (non-expression) of 5,10-methylenetetrahydrofolate reductase (MTHFR) (Fig. 2). The balance between the THF and its oxidized forms should probably be controlled at the level of folate uptake from extracellular medium and/or at the level of serine hydroxymethyltransferase (SHMT) and methylenetetrahydrofolate dehydrogenase (MTHFD1/2). Indeed, the latter are highly expressed enzymes and additionally up-regulated in producer cells (data not shown).

Carbohydrate metabolism

Carbohydrate metabolism, namely glycolysis, was highlighted in the transcriptional profiling analysis of virus production (Fig. 2B and Fig.4). Thus, glucose uptake and lactate production were quantified (Table III). Producer cells presented lower glucose uptake and lactate production rates, very evident in 293 FLEX producers (Table III). Gene expression showed strong down-regulation of aldolase A (ALDOA) up to 2.3-fold and lactate dehydrogenase A (LDHA).

The down-regulation in glycolytic enzymes can only partially explain the reduction in glucose uptake and lactate production in producers as these are highly expressed genes and their enzymatic activity mainly controlled at the post-transcriptional level (Mulukutla et al. 2010). In line, transcriptional controllers of glycolytic metabolism were found to be

Figure 2 – Transcriptome changes in amino acid and integration of energy metabolism pathways. Each arrow represents a single reaction; reversibility is indicated by a two-arrow line according to the BioCyc database (Caspi et al. 2010). Dashed arrows are a general representation of metabolites being channeled from or to the indicated pathways. Reactions are shown as a schematic representation and do not necessarily represent a unique possibility for the presented metabolites. For a matter of simplicity, only the main metabolites and co-factors are shown; thus, the reactions are not necessarily balanced. Not all the reactions (arrows) are assigned to an enzyme, either for clearness purposes or because no specific enzyme has been described in the BioCyc database. Genes are shown in corner-rounded boxes, colored according to fold-change and metabolites are shown unboxed. Fold-changes are shown for the analysis “producer vs. parentals” and were considered significant for $q < 10\%$ based on the False Discovery Rate given by Significance Analysis of Microarrays (SAM) (Tusher et al. 2001). Enzymatic complexes and multi-gene composed →



→ (Figure 2 cont) proteins are identified by a corner-rounded dashed line surrounding the gene set. Gene sets not surrounded by this line represent different enzymes and/or enzyme isoforms catalyzing the same reaction. For multi-protein complexes subject to phosphorylation activation/inactivation mechanisms, the active form is surrounded by a red-colored corner-rounded dashed line. ATP synthase gene (ATP5) is a multi-protein complex comprised by more than 15 subunits; for simplicity purposes, it is represented as a single gene and expression fold-change is shown as the sum-up fold-change of all q<10% subunits. Genes were considered to be expressed for average expression value above 1.5-fold the average expression of the background probes. CoA: coenzyme A; SAH: S-adenosylhomocysteine; SAM: S-adenosylmethionine; THF: tetrahydrofolate; DHF: dihydrofolate; Pi: inorganic phosphate; PLP: pyridoxal-5-phosphate.

changing towards reduced glycolysis, including the down-regulation of HIF1 (hypoxia inducible factor 1), the up-regulation of HIF1AN (hypoxia inducible factor 1, alpha subunit inhibitor) and the down-regulation of AKT1 (v-akt murine thymoma viral oncogene homolog 1).

Polyamines metabolism

Polyamines metabolism and preceding routes appeared as highly changing pathways in the producer state (Fig. 1B and Fig. 3). Up-regulated genes towards citrulline/ornithine biosynthesis – precursor metabolites for polyamines – included dimethylarginine dimethylaminohydrolase 1 (DDAH1) and argininosuccinate synthetase 1 (ASS1), although only in Te Fly producers these changes passed the $q < 10\%$ cut-off (Fig. 3). Spermine synthase (SMS) and spermidine/spermine N1-acetyltransferase 1 (SAT1), were also significantly up-regulated, the former in Te Fly and the latter in 293 FLEX producers (Fig. 3). Te Fly producers also presented gene expression patterns suggesting increased polyamines biosynthesis – already suggested by the comparison “high vs. low producer” (Table II). This difference could then be a metabolic advantage of these cells as a production substrate. To evaluate this hypothesis, polyamine biosynthesis was chemically inhibited using difluoromethylornithine (DFMO) an irreversible inhibitor of ornithine decarboxylase 1 (ODC1) (Fig. 4A).

293 FLEX producers were more susceptible to difluoromethylornithine reducing infectious particles productivity, even in low doses, and the addition of polyamines supplement only partially restored virus production. Te Fly producers were capable of handling higher doses of difluoromethylornithine in polyamine non-supplemented medium with minor reductions in infectious particles productivity and, in polyamine supplemented medium, virus production was completely rescued. This was consistent with the lower expression of ornithine decarboxylase antizyme 1 (OAZ1) and higher expression of antizyme inhibitor 1 (AZIN1) (Table II). As ornithine decarboxylase 1 (ODC1) was found to be identically expressed for both producers these differences point

to the ODC1 regulatory machinery between both cell lines, namely OAZ1 and AZIN1, as the basis for improved polyamine synthesis (Fig. 3).

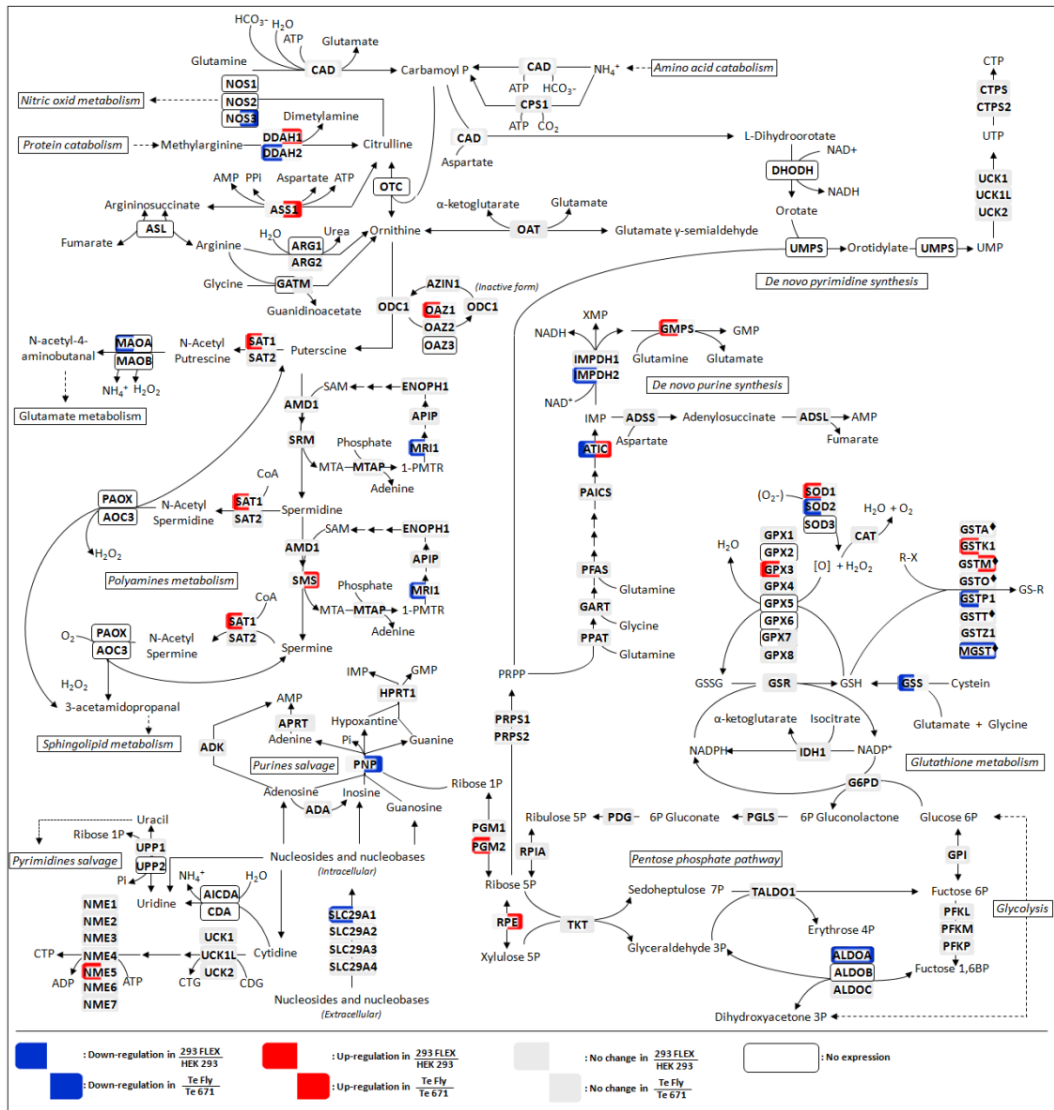


Figure 3 – Transcriptome changes in the metabolic pathways of polyamines, nucleotides, glutathione and pentose phosphate pathway. (Refer to Figure 2 caption for further details on graphical formalisms). ♦: Glutathione S transferases comprise eight (indicated) classes of enzymes the majority of them with several isoforms; for a matter of simplicity, the isoforms numbers were omitted. SAH: S-adenosylhomocysteine; SAM: S-adenosylmethionine; AMP: adenosine monophosphate; CTP: cytidine triphosphate; IMP: inosine monophosphate; GMP: guanosine monophosphate; MTA: methylthioadenosine; 1PMTR: 1-phosphomethylthioribose; PRPP: phosphorybosil pyrophosphate; UMP: uridine monophosphate; UTP: uridine triphosphate; XMP: xanthosine monophosphate; R-X: R may be an aliphatic, aromatic or heterocyclic group, and X may be a sulfate, nitrile or halide group.

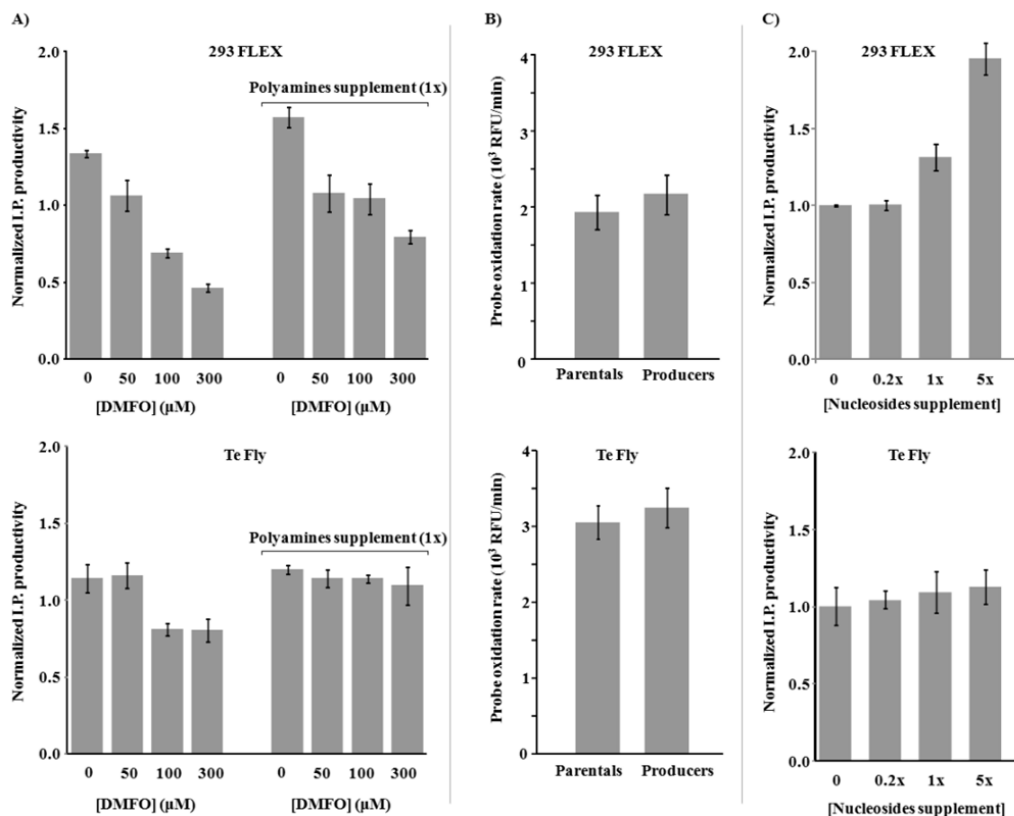


Figure 4 – Effect of polyamines and nucleosides on virus production and oxidative load in virus producing cells. A) Infectious particles production after ornithine decarboxylase 1 inhibition with difluoromethylornithine (DFMO) in polyamine-free or polyamines supplemented (1x) medium. In both cases, medium contains an anti-oxidant (1x) supplement (Sigma), since polyamines present anti-oxidant properties and the inhibition of their synthesis may increase the oxidative burden. Values are shown as average \pm standard deviation (n=3) of infectious particles specific productivity normalized to a polyamines/DFMO/anti-oxidants free control (not shown). B) Intracellular oxidative load of parentals and producer cell, given by the oxidation rate of H₂DCFDA probe (fluorescence) during a 4 hour assay in saponine permeabilized cells; values are shown as average \pm standard deviation (n=12). C) Viral production in nucleosides supplemented medium; values are shown as average \pm standard deviation (n=3) of infectious particles productivity normalized to a nucleoside-free control (shown as [Nucleosides supplement] = 0). For A) and C), cell growth and viral production studies were performed as described in “Materials and methods” for supplemented medium studies.

Glutathione metabolism

Glutathione metabolism and surrounding oxidative stress scavenging machinery was found to be changing in the producer state (Fig. 1B and 3). Comparing to the parentals, reduced glutathione biosynthetic enzymes appeared as down-regulated in 293 FLEX producers including glutathione synthetase (GSS), glutathione reductase (GSR) and

isocitrate dehydrogenase 1 (IDH1), although only GSS passed the $q < 10\%$ cut-off criteria (Fig. 3). Te Fly producers, on the other hand, had their glutathione based defenses increasing, namely several glutathione S-transferases and isocitrate dehydrogenase 1 (IDH1). This led to the hypothesis that Te 671 derived producers would present increased anti-oxidant defenses. Reactive oxygen species were thus quantified in parentals and producers, for both cell lines (Fig. 4B). The results showed higher reactive oxygen species content in producers when compared to the parentals supporting increased oxidative burden in the producer state, although the differences were rather small. However, it was also clear that Te 671 derived cells, our high-producing cell model, presented superior values of intracellular oxidative burden for both parentals and producers (Fig. 4B), questioning the real importance of glutathione in their improved productivity performance. But the over expression of glutathione metabolism genes in 293 FLEX, translated in productivity improvements of more than one order of magnitude (please refer to Chapter VIII). This confirmed the importance of up-regulating glutathione metabolism in the producer state, although its correlation with the oxidative stress was not obvious. Indeed, (reduced) glutathione, in addition to the anti-oxidant properties, plays a role in the pentose phosphate pathway – which provides NADPH for biosynthetic reactions and ribose 5-phosphate for nucleic acid synthesis – and assists protein folding in the endoplasmic reticulum (Chakravarthi et al. 2006). All of these effects are likely to contribute to increased viral production.

Nucleotide metabolism

The enrichment in nucleic acid metabolism occurred extensively in the “virus producer state” (Fig.1B and 3). The two producers behaved differently with WAD sum-up values indicating a predominance of *de novo* synthesis pathways in Te Fly and salvage pathways in 293 FLEX producers (Fig. 3). Both routes are equally capable of providing nucleotide intermediaries. In fact, salvage pathways should represent an advantage as they are energetically less expensive (Berg JM 2002) but they rely on an external nucleosides supply source, a potential disadvantage for 293 FLEX cells. We evaluated this hypothesis

by the addition of nucleoside supplements to the culture medium (Fig. 4C). The results confirmed 293 FLEX producers to be responsive to external nucleoside sources, thus more dependent on salvage pathways. Moreover, specific viral productivity increased almost 2-fold when higher nucleoside concentrations were present, confirming the importance of nucleotide metabolism in virus production.

From *de novo* synthesis, 5-aminoimidazole-4-carboxamide ribonucleotide formyltransferase/IMP cyclohydrolase (ATIC), guanine monophosphate synthetase (GMPS) and IMP dehydrogenase 1 (IMPDH1) were found to be up-regulated in Te Fly. For 293 FLEX producers, salvage pathways seems to be mainly supported at the level of adenine phosphoribosyltransferase (APRT), hypoxanthine phosphoribosyltransferase 1 (HPRT1) and nucleoside phosphorylase (PNP) which, although not differentially expressed in the “producer state”, are consistently more expressed in these cells (Table II).

Pentose phosphate pathway

Pentose phosphate pathway (PPP) appeared as significantly enriched (Fig. 1B), however, the analysis of differential gene expression revealed modest changes for this particular pathway, with only ribulose-5-phosphate-3-epimerase (RPE) being up-regulated in Te Fly producers (Fig. 3). Overall, it was not clear the (up-regulation) recruitment of pentose phosphate pathway in the virus producer state. Still, both salvage and *de novo* nucleotide synthesis will necessarily rely on pentose phosphate pathway to supply ribose 5-phosphate for phosphoribosylpyrophosphate (PRPP) and ribose 1-phosphate synthesis, respectively (Fig. 3)

Lipid metabolism

Lipid metabolism was one of the most significantly enriched pathways in the transcriptional profiling of virus production (Fig. 1B and 5).

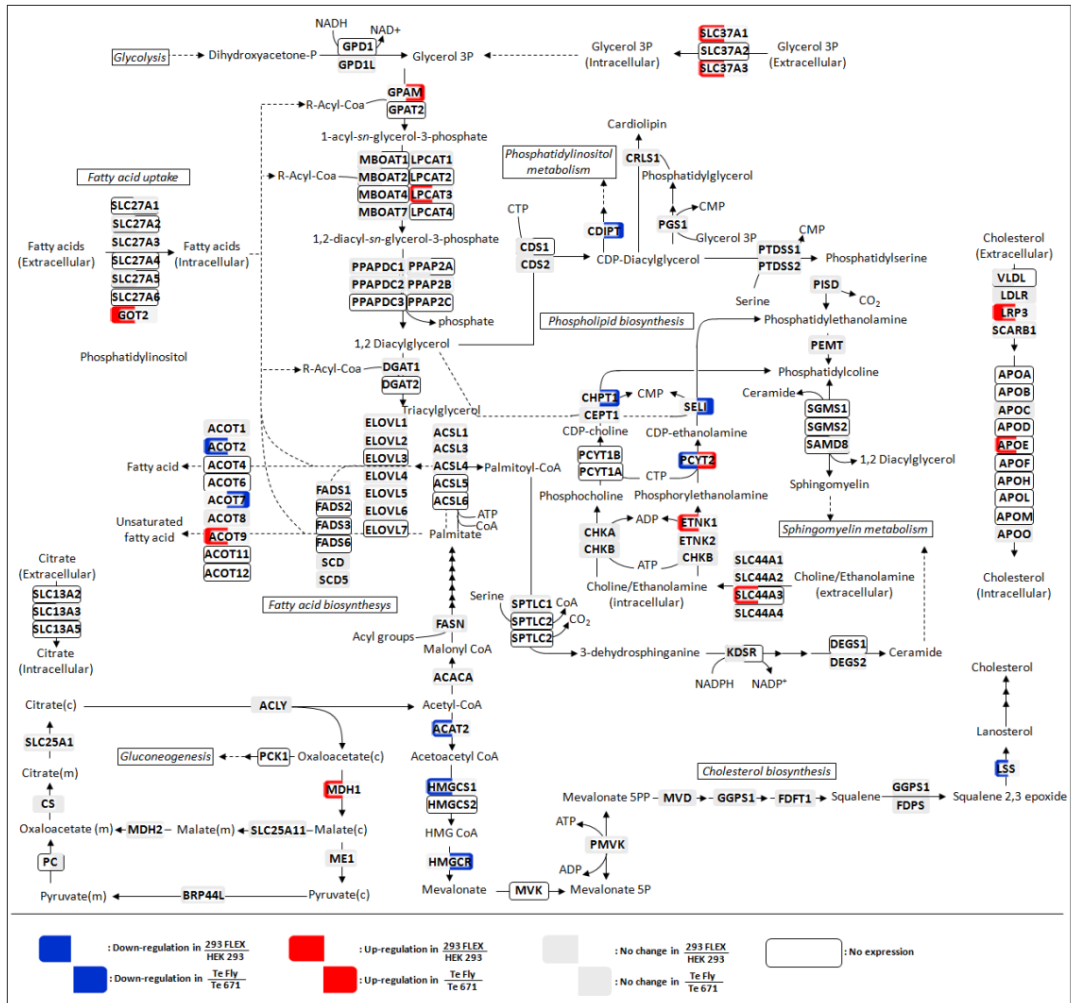


Figure 5 – Transcriptome changes in the lipid metabolism. (Refer to Figure 3 caption for further details on graphical formalisms). CoA: coenzyme A; HMG CoA: 3-hydroxy-3-methylglutaryl-CoA; CMP: cytidine monophosphate; CTP: cytidine triphosphate; '(c)': cytosolic; '(m)': mitochondrial.

Within lipids, we discriminated cholesterol, fatty acids and phospholipids metabolism. In the case of the first two, it was observed a general down-regulation of the biosynthetic pathways, more prominent in 293 FLEX producers, particularly for the case of cholesterol. Down-regulating lipid biosynthesis might seem contradictory in the production of an enveloped virus but it was counterbalanced with the up-regulation of lipid uptaking machinery. Interestingly, this effect seems to be restricted to fatty acids and cholesterol, whereas the enzymes in phospholipid metabolism were tendentially

up-regulated (Fig. 5). Identical results have been reported for hepatitis C virus (Blackham et al. 2010). Further studies on the lipid metabolism and retroviral vector production can be found on Chapters III, IV.

3.4. Media manipulation of enriched pathways increases specific cell productivity without changing virus properties.

In the last part of this work, we questioned how culture medium supplements could modulate viral production and impact vector components, namely at the gene expression level, and whether the increases in viral titers were specific or volumetric. Five classes of culture supplements were tested: nucleosides, amino acids, antioxidants, polyamines and reduced glutathione, alone or combined, mainly targeting the pathways distinguishing high from low producer (Fig. 6).

In 293 FLEX producers, infectious vector specific productivity was improved from 30% to 110% with the different supplementation strategies, reaching a cooperative effect with their combination of 600% (6-fold) increase (Fig. 6). The ratio of infectious to total particles also improved relatively to the control: although there was an increase in total particles formation, the improvement in infectious particles productivity was even higher. For Te Fly cells, the improvements in infectious vector titers were modest and, excluding the cocktail condition with all the supplements, not significantly different from the control (Fig. 6).

By opposite to 293 FLEX, for Te Fly cells the infectious *per* total particles content, was tendentially lower in supplemented cultures mainly derived by higher production of total particles (T.P.) not followed by increased infectious particles (I.P.). The analysis of viral components gene expression showed no significant differences (in gag-pol, transgene or envelope) (Fig. 6), neither any correlation of viral genes expression with vector titers.

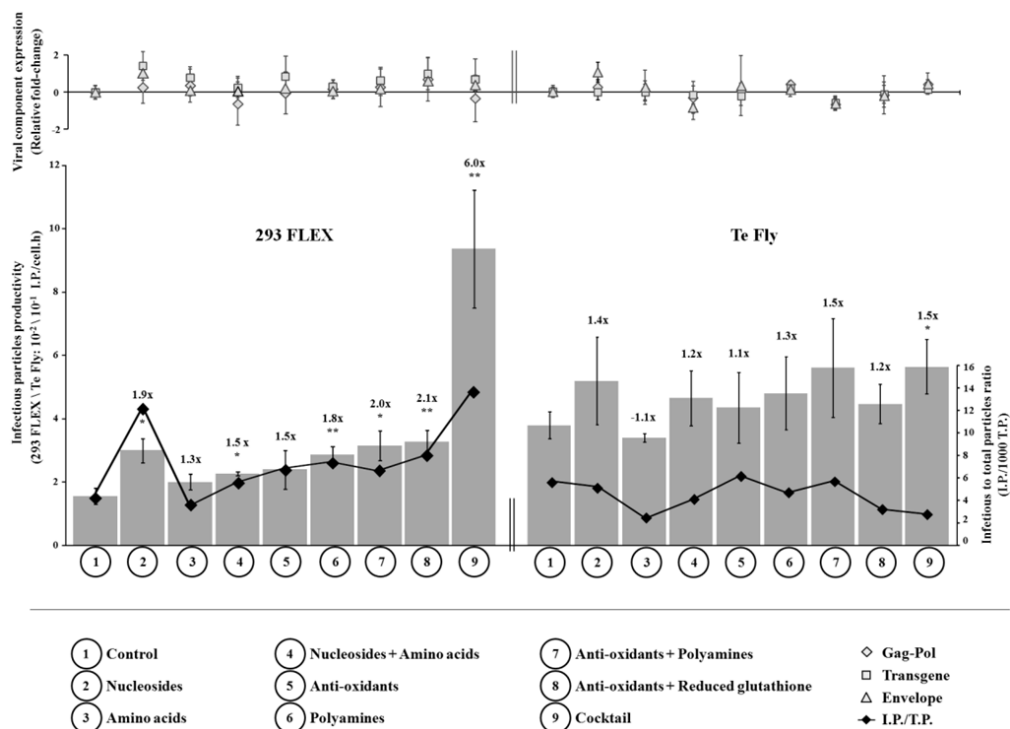


Figure 6 – Effect of culture medium supplementation on viral titers and viral components gene expression for 293 FLEX and Te Fly cells. Bottom left axes: specific infectious titers productivity; the numbers on the top of the bars indicate fold change of infectious titer specific productivity relatively to the control (non-supplemented medium). Bottom right axes: infectious to total particles content. Upper left axes: fold-change gene expression of viral components relatively to the control (non-supplemented medium). All values are shown as average \pm standard deviation of three independent replicates; * $p < 0.05$ and ** $p < 0.005$ given by a non-paired two-tailed t-test. For a matter of simplicity, in infectious to total particles ratio (bottom right-axes) error bars were omitted, ranging 6-30% of the average. In 293 FLEX, all values are significantly different ($p < 0.05$) from the control whereas for Te Fly only “amino acids” and “cocktail” supplementation conditions are different. Supplement concentrations and respective combinations are as described in (Rodrigues et al. 2013).

The pathways targeted by this experimental set up, chosen to improve the low-producer, meet those found to distinguish high from low producer. Probably because of this, improved productivities were achieved for the low producer (293 FLEX) whereas for the high producer (Te Fly), the improvements were neglectable (Fig. 6). For 293 FLEX, the addition of nucleosides yielded the highest titer achieved by the addition of a single supplement: 90% (1.9 fold). As nucleosides are the precursor of nucleotides, building blocks of nucleic acids, they can derive improved synthesis of vector genome, transcription rate of the viral components and/or other important proteins in the producer cell.

Amino acid supplementation yielded the lowest titer improvement (Fig. 6). At a first glance, this was a disappointing result, as amino acid metabolism was one of the most significantly enriched pathways in the transition parentals-to-producers (Fig, 1B and 2), and certainly a major distinctive marker between high and low producer (Table II). As metabolite profiling suggested the preferential channeling of uptaken amino acids for protein synthesis (Table III), these results indicate that infectious vector production is not being restricted at the level of protein synthesis.

Polyamines supplementation yielded 80% (1.8 fold) improvement on viral titers. In addition to cell growth, polyamines can bind to nucleic acids participating in their stabilization, modulate gene transcription events, play a role in membrane rigidity and present anti-oxidant properties (Wallace et al. 2003). These properties can have a beneficial effect on viral production, particularly by stabilizing viral genome leading to improved encapsidation, changing viral membrane rigidity and preventing its lipid peroxidation. They have also been reported to improve viral RNA polymerase activity (Marcus et al. 1981). In fact, the role of polyamines in the replication of animal viruses was studied 3 decades ago (Raina et al. 1981), falling into oblivion afterwards. These results rekindle the importance of polyamines metabolism in virus production, pointing it as a good target for improved titers.

The down regulation of enzymes involved in glutathione metabolism indicated that the “virus producer status” may increase oxidative stress, an event already described for a broad number of viruses (Georgakilas et al. 2010). The addition of anti-oxidant supplements to the culture medium can thus alleviate this burden and led to a 50% (1.5 fold) increase in infectious virus production for 293 FLEX. In theory, this supplement could also influence viral preparation quality by improving particle resistance to oxidative stress; however, virus half-life was not improved (data not shown). When complemented with polyamines or reduced glutathione supplement, viral titers were further increased (100% (2-fold) and 110% (2.1 fold), respectively) when compared to supplementation with anti-oxidants alone.

Although substantial, a 6-fold improvement seems modest for such a high number of identified hints. Nevertheless, it is important to consider the short-lasting effects of many supplements under a batch operation mode, as these are rapidly consumed and/or degraded (for instance, anti-oxidant supplements).

The targeted pathways modulated virus production in low producer cells without changing vector infectivity or viral genes expression: for the same amounts of vector components, supplemented cells managed to produce more. Such results do not necessarily imply a metabolic impairment of HEK 293 derived cells, except perhaps for the specific case of cholesterol metabolism data (Fig. 6). They suggest instead a metabolic *pre-disposition* of Te 671 derived cells for higher titer yields based on potentially more active pathways which, when stimulated in HEK 293 derived cells result in increased titers. The increment in infectious titers occurred without increases in cell growth or extended viability. Thus, the higher infectious titer yields were explicitly obtained by increasing specific and not volumetric productivity, denoting intrinsic changes in the metabolic status of supplemented cultures.

Note: due to space constraints, many of the original publication results were not included on the thesis. For further details see Rodrigues et al. (2013).

4. Conclusions

In the era of Systems Biology, a global view of the biological players and their network integration is increasingly believed as the key to understand and rationally design a phenotype. In the expanding market of virus based biopharmaceuticals, the pursuit of robust and high-producing phenotypes will be leveraged by increasing the understanding on which and how biochemical pathways can drive to improved manufacture processes and cell hosts.

In this work, the transcriptional profiling of an enveloped virus production (retrovirus) in mammalian cells was analyzed and the metabolic constraints underlying this phenotype scrutinized. Eight pathways were identified: amino acid catabolism,

carbohydrate catabolism and integration of energy metabolism, nucleotide metabolism, glutathione metabolism, pentose phosphate pathway, polyamines biosynthesis and lipid metabolism. Their orchestrated manipulation through media supplementation led improved productivities up to 6-fold for the lower producer 293 FLEX, although with minor improvements for the high producer, Te Fly. When targeted alone, nucleotides and polyamines metabolism manipulation resulted in the highest titer improvements.

Analyzing mild transcriptome changes, as those arising from retrovirus production, is a recurrent challenge in the transition parental-to-producer for many bioproducts produced in mammalian hosts. In this work, we demonstrated that such changes can be pulled out of the massive amounts of transcriptomic data using less strict cut-offs, without loss of biological relevance. We additionally propose an alternative mining strategy for the identification of gene engineering targets towards increased titer yields by comparing 'high vs. low producer' derived from different genetic backgrounds. To the best of our knowledge, such approach has never been used, as transcriptome comparison studies seeking for gene engineering targets have traditionally used the 'high vs. low producer' clonal comparison. Several genes were identified as limiting in the low-production phenotype, including two cholesterol biosynthesis enzymes, two glutathione biosynthesis enzymes and the regulatory machinery of polyamines biosynthesis, none of which would be found by the 'high vs. low producer' clonal comparison.

While some of the findings herein discussed can be specifically related to the model virus under study, the majority of the identified pathways are likely to be of relevance for other (enveloped) virus producing cells. And due to the conservation of metabolic pathways and their similar role, regardless the bioproduct, those highlighted in the present work should be a solid starting point.

5. Author contribution

Ana Filipa A. F. Rodrigues participated on the experimental setup and design, performed part of the experiments, analyzed the data and wrote the chapter.

6. References

- Abdi H, Williams LJ. 2010. Principal component analysis. *WIREs Comp Stat* 2(4):433–459.
- Appaihgari MB, Vrati S. 2010. IMOJEV((R)): a Yellow fever virus-based novel Japanese encephalitis vaccine. *Expert Rev Vaccines* 9(12):1371-84.
- Atkins GJ, Fleeton MN, Sheahan BJ. 2008. Therapeutic and prophylactic applications of alphavirus vectors. *Expert Rev Mol Med* 10:e33.
- Berg JM TJ, Stryer L. . 2002. Purine Bases Can Be Synthesized de Novo or Recycled by Salvage Pathways. *Biochemistry*. New York: W H Freeman.
- Blackham S, Baillie A, Al-Hababi F, Remlinger K, You S, Hamatake R, McGarvey MJ. 2010. Gene expression profiling indicates the roles of host oxidative stress, apoptosis, lipid metabolism, and intracellular transport genes in the replication of hepatitis C virus. *J Virol* 84(10):5404-14.
- Bolstad BM, Irizarry RA, Astrand M, Speed TP. 2003. A comparison of normalization methods for high density oligonucleotide array data based on variance and bias. *Bioinformatics* 19(2):185-93.
- Carinhas N, Bernal V, Monteiro F, Carrondo MJ, Oliveira R, Alves PM. 2010. Improving baculovirus production at high cell density through manipulation of energy metabolism. *Metab Eng* 12(1):39-52.
- Carmo M, Peixoto C, Coroadinha AS, Alves PM, Cruz PE, Carrondo MJ. 2004. Quantitation of MLV-based retroviral vectors using real-time RT-PCR. *J Virol Methods* 119(2):115-9.
- Carrondo MJ, Merten OW, Haury M, Alves PM, Coroadinha AS. 2008. Impact of retroviral vector components stoichiometry on packaging cell lines: effects on productivity and vector quality. *Hum Gene Ther* 19(2):199-210.
- Caspi R, Altman T, Dale JM, Dreher K, Fulcher CA, Gilham F, Kaipa P, Karthikeyan AS, Kothari A, Krummenacker M and others. 2010. The MetaCyc database of metabolic pathways and enzymes and the BioCyc collection of pathway/genome databases. *Nucleic Acids Res* 38(Database issue):D473-9.
- Chakravarthi S, Jessop CE, Bulleid NJ. 2006. The role of glutathione in disulphide bond formation and endoplasmic-reticulum-generated oxidative stress. *EMBO Rep* 7(3):271-5.
- Cockrell AS, Kafri T. 2007. Gene delivery by lentivirus vectors. *Mol Biotechnol* 36(3):184-204.
- Coroadinha AS, Schucht R, Gama-Norton L, Wirth D, Hauser H, Carrondo MJ. 2006. The use of recombinase mediated cassette exchange in retroviral vector producer cell lines: predictability and efficiency by transgene exchange. *J Biotechnol* 124(2):457-68.
- Cosset FL, Takeuchi Y, Battini JL, Weiss RA, Collins MK. 1995. High-titer packaging cells producing recombinant retroviruses resistant to human serum. *J Virol* 69(12):7430-6.
- Dalba C, Bellier B, Kasahara N, Klatzmann D. 2007. Replication-competent vectors and empty virus-like particles: new retroviral vector designs for cancer gene therapy or vaccines. *Mol Ther* 15(3):457-66.
- Di Nunzio F, Felix T, Arhel NJ, Nisole S, Charneau P, Beignon AS. 2011. HIV-derived vectors for therapy and vaccination against HIV. *Vaccine* 30(15):2499-509.
- Du P, Kibbe WA, Lin SM. 2008. lumi: a pipeline for processing Illumina microarray. *Bioinformatics* 24(13):1547-8.
- Duisit G, Salvetti A, Moullier P, Cosset FL. 1999. Functional characterization of adenoviral/retroviral chimeric vectors and their use for efficient screening of retroviral producer cell lines. *Hum Gene Ther* 10(2):189-200.
- Gentleman RC, Carey VJ, Bates DM, Bolstad B, Dettling M, Dudoit S, Ellis B, Gautier L, Ge Y, Gentry J and others. 2004. Bioconductor: open software development for computational biology and bioinformatics. *Genome Biol* 5(10):R80.
- Georgakilas AG, Mosley WG, Georgakila S, Ziech D, Panayiotidis MI. 2010. Viral-induced human carcinogenesis: an oxidative stress perspective. *Mol Biosyst* 6(7):1162-72.
- Grabenhorst E, Schlenke P, Pohl S, Nimt M, Conradt HS. 1999. Genetic engineering of recombinant glycoproteins and the glycosylation pathway in mammalian host cells. *Glycoconj J* 16(2):81-97.

- Griesenbach U, Inoue M, Hasegawa M, Alton EW. 2005. Sendai virus for gene therapy and vaccination. *Curr Opin Mol Ther* 7(4):346-52.
- Griffin TJ, Seth G, Xie H, Bandhakavi S, Hu WS. 2007. Advancing mammalian cell culture engineering using genome-scale technologies. *Trends Biotechnol* 25(9):401-8.
- Kadota K, Nakai Y, Shimizu K. 2008. A weighted average difference method for detecting differentially expressed genes from microarray data. *Algorithms Mol Biol* 3:8.
- Khoo SH, Al-Rubeai M. 2007. Metabolomics as a complementary tool in cell culture. *Biotechnol Appl Biochem* 47(Pt 2):71-84.
- Kresse H, Shah M. 2010. Strategic trends in the vaccine market. *Nat Rev Drug Discov* 9(12):913-4.
- Lin SM, Du P, Huber W, Kibbe WA. 2008. Model-based variance-stabilizing transformation for Illumina microarray data. *Nucleic Acids Res* 36(2):e11.
- Marcus SL, Smith SW, Bacchi CJ. 1981. Polyamines stimulate DNA-directed DNA synthesis catalyzed by mammalian type C retroviral DNA polymerases. *J Biol Chem* 256(7):3460-4.
- Moran N. 2012. First gene therapy nears landmark European market authorization. *Nat Biotechnol* 30(9):807-9.
- Mulukutla BC, Khan S, Lange A, Hu WS. 2010. Glucose metabolism in mammalian cell culture: new insights for tweaking vintage pathways. *Trends Biotechnol* 28(9):476-84.
- Nelson DL, Cox MM. 2000. Amino acid oxidation and the production of urea. *Lehninger Principles of Biochemistry*. Ney York: Worth Publishers.
- R Development Core Team. 2008. R: A language and environment for statistical computing. Vienna, Austria: R Foundation for Statistical Computing.
- Raina A, Tuomi K, Mantyjarvi R. 1981. Roles of polyamines in the replication of animal viruses. *Med Biol* 59(5-6):428-32.
- Rodrigues AF, Amaral AI, Verissimo V, Alves PM, Coroadinha AS. 2012. Adaptation of retrovirus producer cells to serum deprivation: Implications in lipid biosynthesis and vector production. *Biotechnol Bioeng* 109(5):1269-79.
- Rodrigues AF, Carmo M, Alves PM, Coroadinha AS. 2009. Retroviral vector production under serum deprivation: The role of lipids. *Biotechnol Bioeng* 104(6):1171-81.
- Rodrigues AF, Formas-Oliveiras AS, Bandeira VS, Alves PM, Hu WS, Coroadinha AS. 2013. Metabolic pathways recruited in the production of a recombinant enveloped virus: mining targets for process and cell engineering. *Metab. Eng. Nov*;20:131-145.
- Schirmmacher V, Fournier P. 2009. Newcastle disease virus: a promising vector for viral therapy, immune therapy, and gene therapy of cancer. *Methods Mol Biol* 542:565-605.
- Schmid R, Baum P, Ittrich C, Fundel-Clemens K, Huber W, Brors B, Eils R, Weith A, Mennerich D, Quast K. 2010. Comparison of normalization methods for Illumina BeadChip HumanHT-12 v3. *BMC Genomics* 11:349.
- Schucht R, Coroadinha AS, Zanta-Boussif MA, Verhoeven E, Carrondo MJ, Hauser H, Wirth D. 2006. A new generation of retroviral producer cells: predictable and stable virus production by Flp-mediated site-specific integration of retroviral vectors. *Mol Ther* 14(2):285-92.
- Tusher VG, Tibshirani R, Chu G. 2001. Significance analysis of microarrays applied to the ionizing radiation response. *Proc Natl Acad Sci U S A* 98(9):5116-21.
- Wallace HM, Fraser AV, Hughes A. 2003. A perspective of polyamine metabolism. *Biochem J* 376(Pt 1):1-14.
- Walsh SR, Dolin R. 2011. Vaccinia viruses: vaccines against smallpox and vectors against infectious diseases and tumors. *Expert Rev Vaccines* 10(8):1221-40.

Chapter III

RETROVIRAL VECTOR PRODUCTION UNDER SERUM DEPRIVATION: THE ROLE OF LIPIDS

This chapter is adapted from:

Rodrigues AF, Carmo M, Alves PM, Coroadinha AS, 2009. Retroviral vector production under serum deprivation: the role of lipids. *Biotechnol Bioeng.* 104(6):1171-81

Abstract

The use of retroviral vectors for gene therapy applications demands high titer preparations and stringent quality standards. However, the manufacturing of these vectors still represents a highly challenging task due to the low productivity of the cell lines and reduced stability of the vector infectivity, particularly under serum-free conditions. With the objective of understanding the major limitations of retroviral vector production under serum deprivation, a thorough study of viral production kinetics, vector characterization and cell growth and metabolic behavior was conducted, for 293 FLEX 18 and Te Fly Ga 18 producer cell lines using different serum concentrations.

The reduction of serum supplementation in the culture medium resulted in pronounced decreases in cell productivity of infectious vector, up to 9-fold in 293 FLEX 18 cells and 7-fold in Te Fly Ga 18 cells. Total particles productivity was maintained, as assessed by measuring viral RNA; therefore, the decrease in infectious vector production could be attributed to higher defective particles output. The absence of the serum lipid fraction was found to be the major cause for this decrease in cell viral productivity. The use of delipidated serum confirmed the requirement of serum lipids, particularly cholesterol, as its supplementation not only allowed the total recovery of viral titers as well as additional production increments in both cell lines when comparing with the standard 10% (v/v) FBS supplementation.

This work identified lower production ratios of infectious particles/ total particles as the main restraint of retroviral vector production under serum deprivation; this is of the utmost importance concerning the clinical efficacy of the viral preparations. Lipids were confirmed as the key serum component correlated with the production of infective retroviral vectors and this knowledge can be used to efficiently design medium supplementation strategies for serum-free production.

Contents

1. Introduction.....	74
2. Materials and methods	75
2.1. Cell lines and cell culture media.....	75
2.2. Cell number	76
2.3. Retroviral vector production	76
2.4. Retroviral vector decay kinetics	77
2.5. Measurement of retrovirus titer	77
2.6. Measurement of retroviral RNA and reverse transcriptase activity .	78
2.7. Serum delipidation and lipid analysis.....	78
2.8. Metabolite Analysis	78
2.9. Cell specific rates determination.....	79
3. Results	79
3.1. Influence of serum on retroviral vector production and cell specific productivity	79
3.2. Influence of serum on retroviral vector properties.....	81
3.3. The role of serum lipids on viral production: delipidated serum and lipid supplements	85
4. Discussion	88
5. Author contribution.....	92
6. References.....	92

1. Introduction

The supplementation of mammalian cell culture media with animal sera has been common practice in biomedical and biotechnological research, since it provides critical nutrients and factors that support cell growth and proliferation. However, the ill-defined composition and high batch-to-batch variability of serum together with its potential source of contaminations, hinders safety and standardization of cell cultures, making it an undesirable supplement in the production of biopharmaceuticals (Falkner et al. 2006). Additionally, most of the animal proteins present in the serum are immunogenic, increasing downstream complexity to eliminate them, implying significant product losses and rising costs up. Regardless of intensive research efforts, serum replacement still constitutes a challenge for specific situations, such as the expansion of morphologically undifferentiated human embryonic stem cells for cell therapy (Chase and Firpo 2007; Chen et al. 2007) and the production of retroviral vectors for gene therapy (Chan et al. 2001; Gerin et al. 1999a; Gerin et al. 1999b; Pizzato et al. 2001).

Retroviral vectors are powerful tools for gene transfer purposes due to their high transduction efficiency, stable transgene integration and expression and low immunogenicity *in vivo* (Mountain 2000). They were the first viral vectors used in gene therapy clinical trials and so far account for the highest number of successful protocols (Edelstein et al. 2007). Nevertheless, retroviral vectors are difficult to manufacture, mainly due to low productivities of the producer cells and reduced stability of the particles in serum-free conditions (Merten 2004). The need for serum on retroviral vector production has controversial evidence. (McTaggart and Al-Rubeai 2000) reported a 10-fold retroviral production increase in FLYRD18 packaging cell line when the percentage of serum in culture medium was reduced from 5% to 1%. The authors suggested that this could be due to the absence of protease inhibitors present in the serum, which are thought to inhibit virus maturation. Nevertheless, the majority of the latest generation of packaging cell lines, especially those derived from HEK293 (human embryonic kidney), seem to require high concentrations (5-10% (v/v)) of serum in the culture medium to support high viral productivities for long term culture (Chan et al. 2001; Gerin et al. 1999a; Gerin et al.

1999b; Pizzato et al. 2001). 293 FLEX cells (Coroadinha et al. 2006) belong to a newly developed generation of modular retroviral producer cell lines. They are based on a tag-and-targeting principle (Schucht et al. 2006), being highly flexible for transgene exchange and thus, constituting a preferential platform for the establishment of production processes for clinical applications. 293 FLEX cells are able to grow in suspension and serum-free media. However, in the absence of serum, cell viral productivities decline abruptly in the first passage and the production completely ceases after a few passages both for suspension, as well as for adherent cell culture systems (unpublished data).

Identifying the limitations of retroviral vector production under serum deprivation was the main goal of this work. A thorough characterization study of viral production with two different human derived packaging cell lines, 293 FLEX 18 and Te Fly Ga 18, in response to serum reduction in the culture medium was conducted. The importance of serum lipids in the production medium of retroviral vectors was demonstrated and correlated with the viral titer.

2. Materials and methods

2.1. Cell lines and cell culture media

Te Fly Ga 18 and 293 FLEX 18 are human derived producer cell lines producing MoMLV based recombinant retroviral vectors expressing GaLV ecotropic envelope and harbouring a LacZ reporter gene (Te Fly Ga 18 are TE 671 (ATCC CCL-136) derived cells established as described in Cosset et al. (1995); 293 FLEX 18 are HEK293 (ATCC CRL-1573) derived cells established as described in Coroadinha et al. (2006). Both cells were maintained in Advanced DMEM (Gibco, Paisley, UK) with 25 mM of glucose, supplemented with 10% (v/v) Foetal Bovine Serum (FBS) (Gibco) and 4 mM of glutamine (Gibco) in an incubator with a humidified atmosphere of 90% air and 10% CO₂ at 37 °C.

Te671 cell line (ATCC CCL-136) was used as the target cell to titrate infectious retroviral particles and was maintained in DMEM (Gibco) with 25 mM of glucose and 4

mM of glutamine supplemented with 10% (v/v) FBS (Gibco) in an incubator with a humidified atmosphere of 95% air and 5% CO₂ at 37 °C.

2.2. Cell number

Cell concentration and viability was determined by the trypan blue exclusion method using a 0.1% (v/v) solution prepared in phosphate-buffered saline (PBS) and counting cells in a Fuchs-Rosenthal hemacytometer (Brand, Wertheim, Germany) on an inverted microscope (Olympus, Japan).

2.3. Retroviral vector production

To study the effect of serum deprivation in cell specific viral productivity and vector particles characteristics, producer cells were inoculated at 2×10^4 cells/cm² and 4×10^4 cells/cm² for Te Fly Ga 18 cells and 293 FLEX 18, respectively. Advanced-DMEM (Gibco) supplemented with 4mM of glutamine (Gibco) and 10, 5, 1 or 0.5% (v/v) of FBS (Gibco) was used. Several samples were collected during the growth curve: viral supernatant was harvested, filtered through 0.45 µm, aliquoted and stored at -85°C until analysis.

To evaluate vector production in delipidated medium (dFBS) with lipid supplements, cells were seeded at the same cell density described above and cultured for three days, in Advanced DMEM supplemented with 4 mM of glutamine (Gibco), a minimum serum percentage of 1% (v/v) for 293 FLEX 18 and 0.5% (v/v) for Te Fly Ga 18 completing the FBS concentration to 10% (v/v) with delipidated FBS. Additionally i) 0.3% (v/v) bovine lipoprotein solution (CellPro-LPS from HyClone, Logan, Utah, USA), ii) 0.1% (v/v) cholesterol supplement (Chemically Defined Cholesterol from Gibco) or iii) 2% (v/v) free fatty acids supplement (Chemically Defined Lipid Concentrate from Gibco) were added. After 3 days in culture, the medium was replaced, and the vectors produced during the following 24 hours were harvested. Sampling was performed as described above. All the studies in this work were performed twice and the results have shown to be reproducible.

2.4. Retroviral vector decay kinetics

To evaluate vector decay kinetic, 24 hour viral vector productions were performed during the late phase of exponential cell growth, corresponding to the highest production period. For this purpose, the culture medium was replaced by fresh one and after 24 hours, the viral supernatant was harvested and filtered through a 0.45 μm filter. Part of this supernatant was 1/10 diluted in Advanced DMEM with 10% (v/v) FBS, and the remaining supernatant was 1/10 diluted in the correspondent production medium. The viral suspensions were then incubated at 37 °C in a 10% CO₂ incubator. Samples were taken at 0, 3, 6, 9, 12, 24, 36, and 48 h and stored at -85 °C for viral titer determination. Decay rate constants and half-lives were calculated according to a first order exponential decay model (Le Doux et al. 1999)

2.5. Measurement of retrovirus titer

For the infectious particle titration, Te671 cells were seeded at 5×10^4 cells/cm² in 96-well plates with DMEM with 10% (v/v) FBS and incubated overnight in a humidified CO₂ incubator at 37 °C. After 24 h, the supernatant was removed and cells were infected with 50 μl of viral suspension. Serial dilutions were performed in DMEM with 10% (v/v) FBS containing 8 $\mu\text{g/ml}$ of polybrene (Sigma, Steinheim, Germany). After 4h of incubation at 37 °C to promote virus adsorption, 150 μl of DMEM with 10% (v/v) FBS were added to each well. Two days after infection, cells were fixed: the culture supernatant was removed and cells were washed with PBS and incubated with formaldehyde at 0.3% (v/v) and glutaraldehyde at 1.35% (v/v) in PBS for 5 min. After a washing step with PBS, staining was carried out using a solution of 0.2 mg/mL x-gal (5-bromo-4-chloro-3-indolyl- β -D-galactopyranoside) (Stratagene, La Jolla, USA), 5 mM K₃Fe(CN)₆, 5 mM K₄Fe(CN)₆, and 1 mM MgCl₂ in PBS. Three replicates were made for each dilution. The viral titer was determined by counting the stained blue cells using an inverted phase contrast microscope, multiplied by the dilution factor.

2.6. Measurement of retroviral RNA and reverse transcriptase activity

The retroviral transgene RNA was determined by real-time reverse transcriptase PCR as described elsewhere (Carmo et al. 2004). To determine DNA polymerase activity the RetroSys C-Type RT activity kit (Innovagen, Lund, Sweden) was used. All reactions were linear with respect to incubation time and amount of virus added. Each measurement was done in duplicate.

2.7. Serum delipidation and lipid analysis

Lipids were removed from FBS by a delipidation method described elsewhere (Cham and Knowles 1976). Two additional steps of i) vacuum evaporation followed by ii) a dialysis against PBS in 100 volumes with three buffer exchanges at 4°C were performed.

Lipid composition of FBS and delipidated FBS was assessed by total lipid extraction as described by Bligh and Dyer (1959), followed by cholesterol, phospholipids, triglycerids and free fatty acids quantification. Concentration of total phospholipids was determined by a colorimetric assay based on complex formation between ammonium ferrothiocyanate and the phospholipid (Stewart 1980). Cholesterol, triacylglycerols and fatty acids were determined by enzymatic assays using: i) for cholesterol determination, the Amplex[®] Red Cholesterol Assay Kit (Invitrogen); ii) for triglycerides, the Serum Triglyceride Determination Kit (Sigma) and iii) for fatty acids, the Free Fatty Acids Half Micro Test kit (Roche Applied Science, Mannheim, Germany). All quantification procedures were carried out following manufacturer's instructions. The lipid extraction efficiency was 95% for phospholipids, 98% for triglycerides and cholesterol and 100% for fatty acids.

2.8. Metabolite Analysis

Glucose, glutamine, lactate and ammonia concentration were determined using Bioprofile 100 plus Analyzer system (Nova Biomedical, Waltham, USA).

2.9. Cell specific rates determination

To determine cell specific growth rate, metabolite uptake/consumption rate, productivities of I.P. (infectious particles), RNA (viral genome) and RT (reverse transcriptase), the Boltzmann equation was considered:

$$\frac{dP}{dt} = \mu_p C \quad (\text{Eq. 1})$$

where P represents the different parameters, either viable cell concentration, metabolite concentration, I.P., RNA or RT, C is the viable cell concentration, t is the time and μ_p is the cell specific rate of each parameter in study. The confidence interval considered was 95%.

3. Results

3.1. Influence of serum on retroviral vector production and cell specific productivity

The effect of serum on retroviral vector production was studied by analyzing the impact of decreasing serum concentration in the culture medium on the infectious and total particles production (Fig. 1). The serum concentration in the culture medium could be reduced from 10% (v/v) to 1% (v/v) for 293 FLEX 18 cells and 0.5% (v/v) for Te Fly Ga 18 without disturbing cell growth and central carbon energy metabolism (Table I).

Cell specific viral productivity decreased when serum concentration was reduced for both producer cell lines (Fig. 1). This was particularly evident for concentrations lower than 5% (v/v) FBS, specially for 293 FLEX 18 cells where this drop was even more pronounced with a 9 fold decrease in cell specific viral productivity being observed as serum concentrations dropped from 10% (v/v) to 1% (v/v) FBS; for Te Fly Ga 18 cells a 7 - fold decrease occurred from 10% (v/v) to 0.5% (v/v) FBS. The maximum viral titers obtained were also approximately one order of magnitude lower at the minimum concentration of serum for both cell lines.

Table I – Cell specific growth rate and central energetic metabolic yields v_{lac}/v_{glc} and v_{amm}/v_{glu}

		Production media FBS % (v/v)			
		10%	5%	1%	0.5%
293 FLEX 18	$\mu_{growth} (h^{-1})$	0.019 ± 0.002	0.022 ± 0.002	0.018 ± 0.002	-
	v_{lac}/v_{glc}	1.1 ± 0.3	1.1 ± 0.3	1.3 ± 0.02	-
	v_{amm}/v_{gln}	0.5 ± 0.1	0.6 ± 0.2	0.6 ± 0.2	-
Te Fly Ga 18	$\mu_{growth} (h^{-1})$	0.020 ± 0.002	0.020 ± 0.001	0.020 ± 0.002	0.018 ± 0.002
	v_{lac}/v_{glc}	1.5 ± 0.4	1.2 ± 0.3	1.4 ± 0.3	1.5 ± 0.3
	v_{amm}/v_{gln}	0.4 ± 0.1	0.5 ± 0.1	0.4 ± 0.1	0.8 ± 0.2

The errors in μ_{growth} correspond to a 95% confidence interval as defined in Material and Methods. The errors in v_{lac}/v_{glc} and v_{amm}/v_{gln} correspond to error propagation; (μ_{growth}) maximum cell specific growth rate, (v_{lac}) lactate production rate, (v_{glc}) glucose uptake rate, (v_{amm}) ammonia production rate, (v_{gln}) glutamine uptake rate.

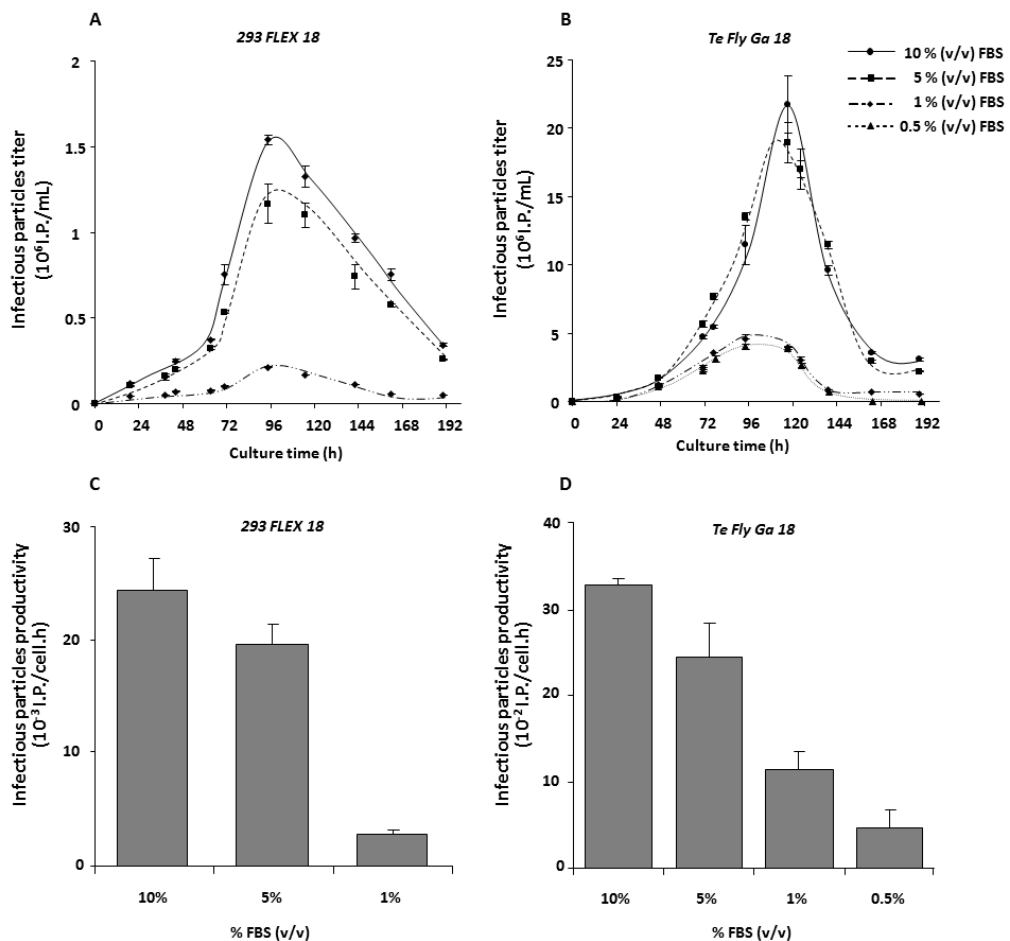


Figure 1 – Effect of serum deprivation on infectious particles titers. Infectious particles production kinetics of 293 FLEX 18 (A) and Te Fly Ga 18 (B) cells in production medium with different serum concentrations; error bars represent standard deviations (n=3). Cell specific infectious particles productivities of 293 FLEX 18 (C) and Te Fly Ga 18 (D) cells in production medium with different serum concentrations; error bars correspond to a 95% confidence interval, as defined in Material and methods.

3.2. Influence of serum on retroviral vector properties

To analyze the effect of serum concentration on vector properties, the number of viral RNA copies, RT activity, as well as vector stability was assessed. Table II summarizes cell productivities ratios calculated based on viral RNA and RT quantifications. Viral RNA in the supernatant was quantified as it corresponds to the encapsidated RNA, it is a measure of total viral particles with infectious potential. However, viral genome RNA measurements disregard the production of empty particles. To account for this, a second measure of total particles was performed, quantifying reverse transcriptase (RT) activity. RT activity in supernatant is also an indirect measurement of *gag-pol* expression and particles assembly.

The ratio infectious particles/total particles (I.P./T.P.) decreased when the serum concentration in the culture medium was reduced, either when considering viral genome RNA or RT as a total particles measure, thus, indicating the production of higher amounts of defective vectors. For both Te Fly Ga 18 and 293 FLEX 18 cells, viral RNA production and encapsidation was not affected by serum deprivation which, besides attesting that there were no limitations in viral genome production and encapsidation, shows that the total number of produced particles was maintained. Conversely, the analysis of RT activity confirms that this is one of the particles' components that was disturbed by serum reduction, but only when 293 FLEX 18 cells are used. Nevertheless, this effect is too low to justify the sharp decrease in infectious particles titer.

Serum contains considerable amounts of albumin, lipoproteins and other molecules that are known to act as stabilizing agents of retroviral vectors. Its presence in the culture medium results in a higher vector half-life, and ultimately, leads to an increase in vector titers. Thus, to confirm that the reduction in infectious vector titers in low-serum conditions was a consequence of limitations at the level of the production of the particles, and not an indirect effect of lower vector stability due to the absence of serum stabilizing agents, a detailed study of vector stability was performed.

Table II – Cell specific productivities of viral RNA and reverse transcriptase (RT) and the corresponding ratios for 293 FLEX 18 and Te Fly Ga 18 cells

		Production media FBS % (v/v)			
		10%	5%	1%	0.5%
293 FLEX 18	β_{RNA} (copy/cell.h)	4.8 ± 0.2	4.4 ± 0.1	4.2 ± 0.1	-
	β_{RT} (10 ⁻⁷ ng/cell.h)	1.1 ± 0.1	0.8 ± 0.1	0.6 ± 0.1	-
	I.P./RNA (10 ⁻³ I.P./copy)	5.1 ± 0.8	4.5 ± 0.5	0.7 ± 0.1	-
	I.P./RT (10 ⁴ I.P./ng)	23 ± 2	23 ± 2	5 ± 1	-
	RT/RNA (10 ⁻⁶ ng /copy)	2.2 ± 0.2	1.9 ± 0.2	1.4 ± 0.1	-
Te Fly Ga 18	β_{RNA} (copy/cell.h)	57 ± 7	54 ± 8	50 ± 8	69 ± 2
	β_{RT} (10 ⁻⁷ ng/cell.h)	1.0 ± 0.3	1.2 ± 0.2	1.2 ± 0.1	1.1 ± 0.2
	I.P./RNA (10 ⁻³ I.P./copy)	5.7 ± 0.9	4.5 ± 1.4	2.3 ± 0.8	0.7 ± 0.3
	I.P./RT (10 ⁴ I.P./ng)	315 ± 32	196 ± 20	98 ± 10	100 ± 10
	RT/RNA (10 ⁻⁶ ng /copy)	0.18 ± 0.01	0.23 ± 0.02	0.24 ± 0.02	0.16 ± 0.01

The errors in β_{RNA} and β_{RT} correspond to a 95% confidence interval as defined in Material and Methods. Errors in I.P./RNA, I.P./RT and RT/RNA represent 10% of maximum variability determined for each ratio. β_{RNA} (cell specific production rate of viral RNA), β_{RT} (cell specific production rate of reverse transcriptase)

Viral infectivity decay kinetics of vectors produced at different serum concentrations were assessed both in: i) the different production media and in ii) 10% (v/v) FBS medium (Fig. 2 and Table III). In this latter case, independently of the production medium, the decaying medium is the same, normalizing possible stabilization effects of medium or serum components. Consequently, a higher half-life indicates that the production condition in study generated intrinsically more stable particles.

A 4-hour reduction in the half-life of vectors produced by Te Fly cells was observed from 10% to 0.5% (v/v) FBS, when assessed in the production medium; however, this difference disappeared when assessed in 10% (v/v) FBS medium, even for particles produced in reduced-serum conditions. This indicates that, for these vectors, either serum concentration in the production medium does not induce intrinsic stability changes, or that the serum stabilization effect surpasses the possible intrinsic effects induced on the produced particles. In the case of the vectors produced by 293 FLEX cells, higher concentrations of serum led to an increased stability originated both by its protective presence in the medium and also by generating intrinsically more stable particles.

When comparing the decay kinetics of viral infectivity of vectors produced in 1% (v/v) FBS, either in 1% (v/v) FBS medium or 10% (v/v) FBS medium, it is evident that serum presence confers stability to the particle, since viral stability was enhanced from 6.5 to 8.1 hours. This is similar to what was observed with the Te Fly Ga 18 derived vectors, and can be explained by the presence of albumin. When analysing the decay kinetics of viral infectivity of vectors produced in different serum concentrations was assessed in the medium supplemented with 10% (v/v) FBS, it was observed that for particles produced both in 5% and 1% (v/v) FBS, the vector half-life was always lower than for the particles produced in 10% (v/v) FBS. Therefore, and in contrast to what was observed with Te Fly Ga 18 derived vectors, vector infectivity decay kinetics was not completely restored when decaying in medium supplemented with 10% (v/v) serum. This indicates that producing at 10% (v/v) FBS generates more stable particles in the case of 293 FLEX 18 cells.

Table III - Half-life of vectors produced by 293 FLEX 18 and Te Fly Ga 18 cells

		Vector half-life (h)							
		293 FLEX 18				Te Fly Ga 18			
		Vector decay medium FBS % (v/v)							
		10%	5%	1%	0.5%	10%	5%	1%	0.5%
Production medium (FBS % (v/v))	10%	9.7 ± 0.4	-	-	-	12.0 ± 0.9	-	-	-
	5%	7.7 ± 0.6	8.4 ± 1.0	-	-	11.7 ± 0.9	10.9 ± 1.1	-	-
	1%	8.1 ± 0.6	-	6.5 ± 0.5	-	12.5 ± 0.3	-	10.6 ± 0.4	-
	0.5%	-	-	-	-	12.3 ± 1.4	-	-	8.1 ± 1.1

Vectors produced by each cell line decay either in the respective production media (diagonal) or in medium supplemented with 10% FBS, independently of the medium they were produced in (vertical). Errors correspond to a 95% confidence interval as defined in Material and methods.

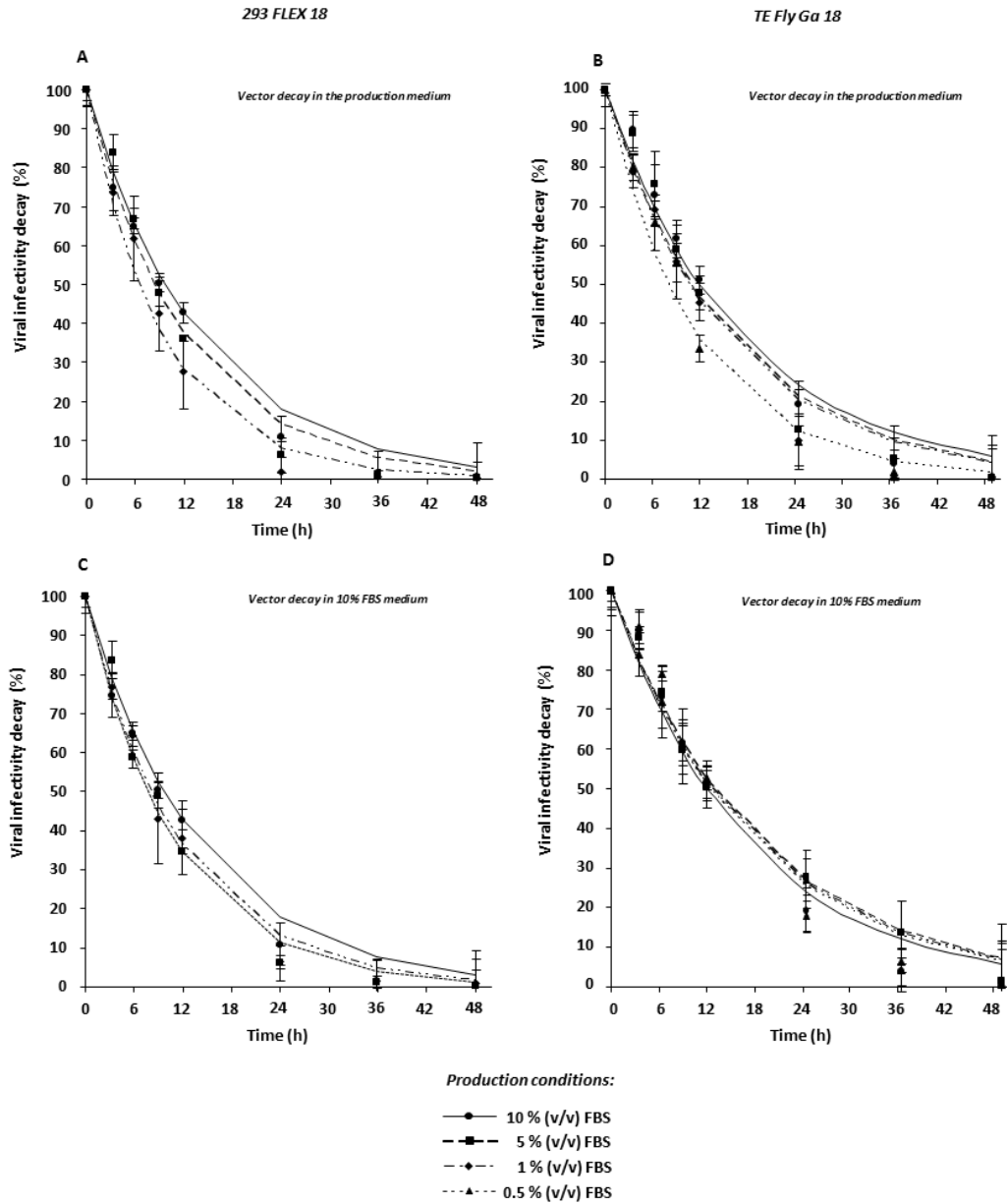


Figure 2 – Effect of serum in retroviral vector stability. Decay kinetics of viral infectivity of 293 FLEX 18 (A and C) and TE Fly Ga 18 (B and D) derived vectors in the production medium (A and B) and in medium supplemented with 10% (v/v) FBS (C and D). In A and B, vectors produced by each cell line decay in the media they were produced in; in C and D, all vectors decay in medium supplemented with 10% FBS, independently of the medium they were produced in; values are shown as average \pm standard deviation (n=3). Curves obtained by fitting with the rate constants calculated as described in Material and methods.

3.3. The role of serum lipids on viral production: delipidated serum and lipid supplements

To evaluate the role of serum lipids in viral production, delipidated FBS (dFBS) was used. After the delipidation process, dFBS was assessed for the protein profile by SDS-PAGE, serum total protein content, pH, osmolarity, and enzyme activity of lactate dehydrogenase and alkaline phosphatase (data not shown). No differences were observed in none of these parameters between delipidated and non-delipidated serum.

To ensure the maintenance of cell growth, the minimum serum percentage previously determined was used: 1% (v/v) FBS for 293 FLEX 18 and 0.5% (v/v) FBS for Te Fly Ga 18 cells. dFBS was added to attain a final serum concentration of 10% (v/v), that is, 9% (v/v) dFBS for 293 FLEX 18 and 9.5% (v/v) dFBS for Te Fly Ga 18 cells. The use of delipidated serum did not perturb either cell growth or central carbon metabolism (data not shown) in agreement with the previous results (Table I) since the minimum serum percentage had already shown to be sufficient to support similar cell growth and metabolic patterns as 10% (v/v) FBS. However, infectious particles titers were not recovered by the addition of delipidated serum, and cell specific viral productivities were comparable to those obtained with the minimum serum percentage (Fig. 3 A and B).

In order to appraise the effects of using delipidated serum on vector half-life a second stability study was conducted. In a first approach, viral infectivity decay kinetics of vector particles produced in 10% (v/v) FBS medium were assessed in medium supplemented with delipidated serum (data not shown). This allowed analyzing the effect of delipidated serum presence in the culture medium upon produced particles. For this case, the presence of delipidated serum in the culture medium was shown not to interfere in viral particles stability thus, confirming that the infectious particles titer drops observed when using dFBS medium were mainly due to limitations in actual vector production. To further investigate if the vectors produced in dFBS media presented intrinsic production changes, viral infectivity decay kinetics of vectors produced in the conditions described (either 10% (v/v) FBS, Min% (v/v) FBS or dFBS medium), were measured in 10% (v/v) FBS medium (Fig. 3 C and D).

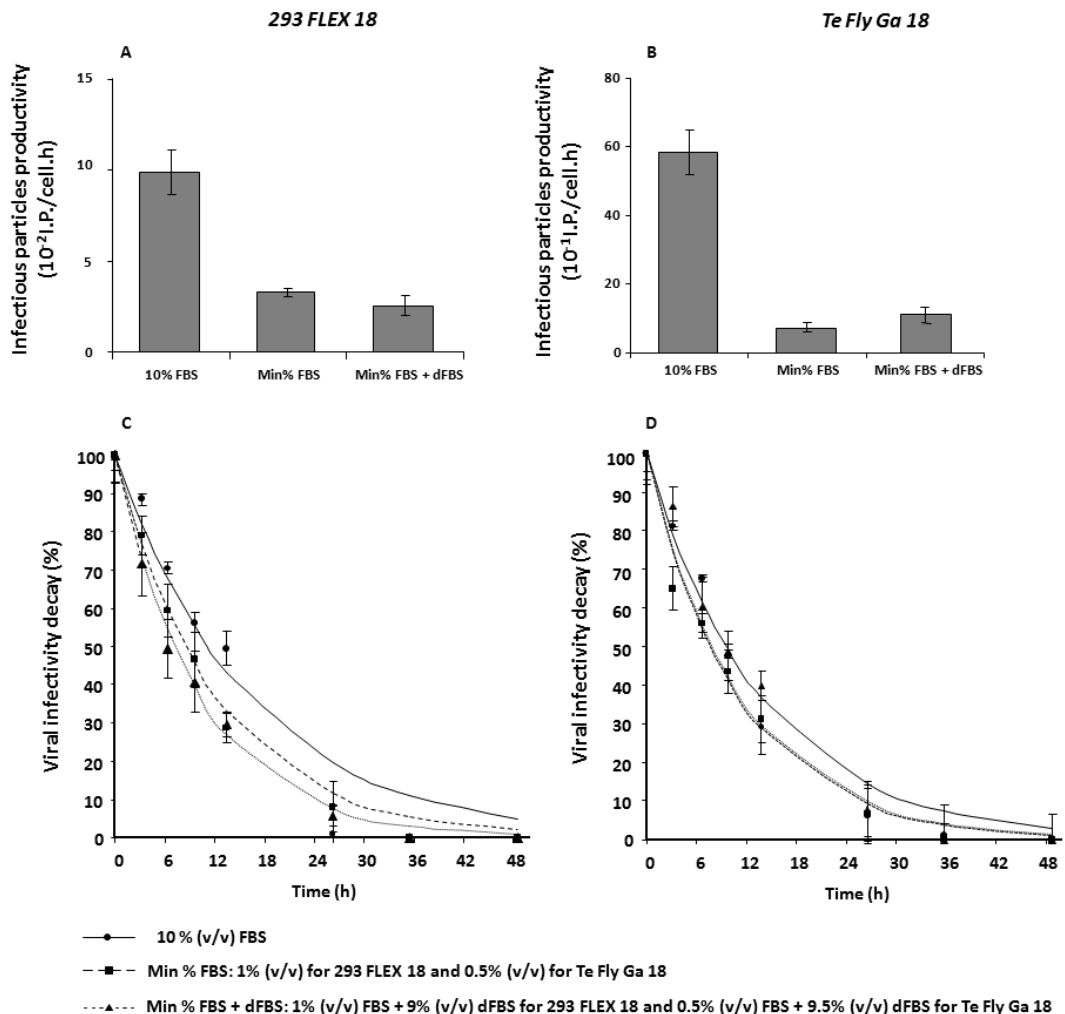


Figure 3 – Effect of delipidated serum in infectious particles titers and stability. Specific productivities of infectious particles of 293 FLEX 18 (A) and Te Fly Ga 18 (B) cells; error bars correspond to 95% confidence interval, as defined in Material and methods. Decay kinetics of viral infectivity of 293 FLEX 18 (C) and Te Fly Ga 18 (D) derived vectors produced in medium with different serum supplementation, and assessed in 10% FBS (v/v) medium; values are shown as average \pm standard deviation (n=3). Curves obtained by fitting with the rate constants calculated as described in Material and methods. Abbreviations: (dFBS) delipidated FBS; (Min% (v/v) FBS) minimum serum percentage corresponding to 1% (v/v) and 0.5% (v/v) FBS for 293 FLEX 18 and Te Fly Ga 18 cells, respectively.

For this second case, the use of delipidated serum resulted in vector particles slightly less stable than those produced at 10% (v/v) FBS. These results are similar and thus, validate, those already found in the previous stability study (Table III): the stability of the viral particles produced in medium with delipidated serum was similar to that of viruses produced in reduced-serum conditions and lower than those produced in 10% (v/v) FBS

medium. Taken all together, these results strongly support the hypothesis that serum lipid fraction is of the utmost importance for viral production, being its deprivation the main cause for infectious particles titer decline.

The removal of serum lipid content is insufficient to establish a quantitative relationship between serum lipids and viral production. Thus, a viral production study was performed in which i) 0.3% (v/v) bovine lipoprotein solution (LPS), ii) 0.1% (v/v) cholesterol supplement (Chol) or iii) 2% (v/v) free fatty acids (FAs) supplement were added to medium already supplemented with delipidated serum (Fig.4).

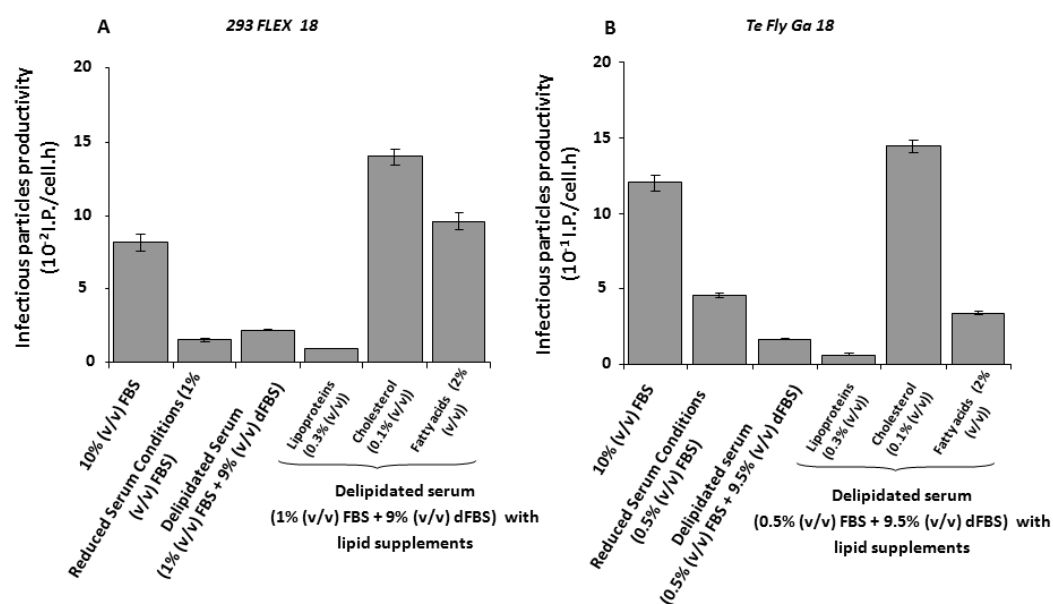


Figure 4 – Recovery of infectious titers by adding lipid supplements. Specific productivities of infectious particles of 293 FLEX 18 (A) and Te Fly Ga 18 (B) cells in production medium with different lipid supplements; error bars represent standard deviation (n=3). Abbreviations: (dFBS) delipidated FBS; (LPS) bovine lipoprotein solution; (Chol) cholesterol supplement; (FAs) free fatty acids supplement

These concentrations correspond, in the case of cholesterol and fatty acids, to the best percentages for viral production (assessed in preliminary studies with reduced-serum media (data not shown)) and, in the case of the lipoprotein supplement, to the percentage that mimics serum concentration.

The addition of lipid supplements, particularly cholesterol, to the medium supplemented with delipidated serum resulted in a 6- and 9-fold increment in viral productivity in 293 FLEX 18 cells and Te Fly Ga 18 cells, respectively. This represents the total recovery of viral titers, with an additional improvements, comparatively to 10% (v/v) FBS supplemented medium, for both cell lines. The use of fatty acids supplements also led to increased productivities, when comparing with the minimum serum percentage but only for 293 FLEX 18 cells. Infectious particles production was very low in lipoprotein supplemented medium, however, viral RNA and RT activity levels were identical to the ones produced in 10% FBS, suggesting a *post*-production interference effect.

Viral RNA and RT productivities were determined for each assay described (data not shown). In agreement with the results already obtained (Table II), there was no evidence of RNA limitations susceptible to justify the decrease in infectious particles productivity. However, slight differences in RT productivity were obtained depending on the lipid supplement used. The general tendency was a decrease in RT productivity in all the conditions, when comparing with the production in 10% (v/v) FBS medium. In fact, the exception is when cholesterol supplemented medium is used where RT productivity is actually increased.

4. Discussion

Serum supplementation of the culture medium is known to be crucial to support long term periods of vector production for the majority of the retroviral producer cell lines (Chan et al. 2001; McTaggart and Al-Rubeai 2000; Pizzato et al. 2001; Shen and Palsson 1996). To understand the role of serum in retroviral vector production in general, and for 293 FLEX and Te Fly cells derived vectors in particular, a thorough study of viral production patterns, vector characteristics and cell growth and metabolic behavior was performed for 293 FLEX 18 and Te Fly Ga 18 retroviral vector producer cell lines, in media supplemented with different serum concentrations. The requirement of serum to support viral production by Te Fly Ga 18 cells had already been reported (Merten 2004) and since the vectors produced by these cells have the same characteristics than those of 293 FLEX

– MoMLV derived, GaLV pseudotyped, harboring *LacZ* reporter gene – they are an adequate comparison in terms of final product.

It was soon realized that some serum components were directly and specifically related with retroviral vector production: although cell growth and the central energetic metabolic profile were similar in all the serum concentrations tested, decreases in infectious particles production were always observed, being the extent of the decline proportional to serum reduction. The stability studies highlighted that though serum reduction in the culture medium could result in slight decreases in vector stability, this effect did not suffice to account for the sharp drop in infectious vector titers. Moreover, similar results were obtained both with 293 FLEX and Te Fly cells, suggesting the pattern to be independent of the producer cell line and confirming that it was vector related.

To identify the serum components which mostly affect viral production, a preliminary study of serum fractioning was conducted; lipoproteins were identified as the most critical serum for the production of infectious particles. This result was in accordance with previous work, where the importance of lipids and lipid metabolism of producer cells in viral production is shown (Amaral et al. 2008; Coroadinha et al. 2006a). Unless other supplements are added, serum is the only lipid source of the culture medium and, although cells should be able to sense lipid absence in the culture medium and activate biosynthetic pathways to stand up to lipid deprivation, the activation of lipid *de novo* synthesis may take hours or days, depending on the cell type (Alberts et al. 1974; Spector et al. 1980). In some cases, cells can no longer synthesize certain lipids, since the long-term synthesis inhibition can induce mechanisms of gene silencing, leading to a complete heterotrophy of some lipid molecules (Seth et al. 2005, 2006). Therefore, changes in serum concentration that disturb cell membrane lipid composition will ultimately affect viral particle membrane properties (Rawat et al. 2003), since it is part of the host cell membrane, possibly resulting in a higher production of non-infectious particles.

RNA and RT quantification results demonstrated that the infectious particles production decrease is actually a problem of *quality*, rather than *quantity*: in reduced-serum conditions, the produced particles are defective and thus non-infectious. The effect

of lipid removal of the membrane of other enveloped virus host cells has already been shown to result in the disruption of the particle structure. Laliberte et al. (2006) demonstrated that cholesterol depletion from the host cell membrane led to the production of structurally damaged particles, with altered “proteins/lipids” ratios, and in some cases resulting in membrane holes. The authors reported also that, although defective and less infectious, the total number of produced particles was maintained, a conclusion that our results further substantiate. Membrane lipids are known to be active players in the complex process of viral assembling and pseudotyping that takes place at the host cell membrane, in which interactions of membrane lipid rafts select both envelope and core proteins, recruiting the later the other viral components by cooperative interaction. The production of infectious particles is known to rely on the efficiency of this process, which is dependent upon a delicate equilibrium of lipid type and amounts, easily disturbed by lipid deprivation (Briggs et al. 2003). In this context, it is noteworthy that, not only the best results for productivity recovery were obtained for cholesterol supplemented medium, but also that these recoveries were associated with an increase in RT amounts quantified in the supernatant, which can be correlated with an improved assembling process of the *gag-pol* elements. Moreover, since the limitations in RT were not sufficient to justify the reduced production of infectious particles, it can also be speculated that part of these non-infectious particles could also be due to protein envelope limitations. These limitations can either be due to restriction in envelope protein amounts or functionality, as the lipid environment in which the protein is anchored is known to exert strong influence on its mobility and also on the linkage strength to the membrane (Carmo et al. 2006).

Retroviral vector production in serum-free conditions was recently reported for the first time by Ghani et al. (2007). However, the major limitations for the production of these particles in serum absence still remained unclear, rendering it difficult to accomplish without decreasing either vector titer or quality. With this study, we identified the serum key component correlated with high vector titers: lipids. Actually, in the work reported by

Ghani et al. (2007), the medium was not protein-free, containing several components, including lipids and lipoproteins.

In this work, we were able to identify the production of non-infectious particles as the main constraint resulting from serum withdrawal from the culture medium of retroviral vector producer cells. Although non-infectious, these particles should be, in terms of general physical structure, identical to the infectious ones, resulting the non-infectious profile from changes in the lipid membrane content/integrity and envelope amounts. However, these changes are not sufficient to be exploited in the current purification protocols in order to separate them from the infectious ones (Rodrigues et al. 2007). This can be important from the clinical application point of view, as a decrease in the transduction efficiency of the viral preparations is expected, since non-infective particles will interfere with and obstruct the infective ones. The outcome of this work is almost certainly susceptible of being extended to lentiviral vector production, concerning their similar biological characteristics with MLV derived vectors (Blesch 2004) particularly, the importance of adequate lipid environment for a correct particle assembling (Briggs et al. 2003). In addition, many of these results are also of interest for the production of other enveloped viruses. The supplementation of the reduced-serum culture medium with cholesterol has shown to be enough to support high viral titers with no need of adding further supplements establishing the potential of using cholesterol supplementation as a bioreaction strategy to support viral production in serum-free medium. But more than the technological relevance of retroviral vector production in serum-free conditions, the findings in this study allow a better comprehension and exploitation of the culture medium supplements used for the production biopharmaceuticals and its effects on the final product titer and quality.

5. Author contribution

Ana Filipa A. F. Rodrigues participated on the experimental setup and design, performed the experiments, analyzed the data and wrote the chapter.

6. References

- Alberts AW, Ferguson K, Hennessy S, Vagelos PR. 1974. Regulation of lipid synthesis in cultured animal cells. *J Biol Chem* 249(16):5241-5249.
- Amaral AI, Coroadinha AS, Merten OW, Alves PM. 2008. Improving retroviral vectors production: Role of carbon sources in lipid biosynthesis. *J Biotechnol* 138(3-4):57-66.
- Blesch A. 2004. Lentiviral and MLV based retroviral vectors for ex vivo and in vivo gene transfer. *Methods* 33(2):164-172.
- Bligh EG, Dyer WJ. 1959. A rapid method of total lipid extraction and purification. *Can J Biochem Physiol* 37(8):911-917.
- Briggs JA, Wilk T, Fuller SD. 2003. Do lipid rafts mediate virus assembly and pseudotyping? *J Gen Virol* 84(Pt 4):757-768.
- Carmo M, Faria TQ, Falk H, Coroadinha AS, Teixeira M, Merten OW, Geny-Fiamma C, Alves PM, Danos O, Panet A and others. 2006. Relationship between retroviral vector membrane and vector stability. *J Gen Virol* 87(Pt 5):1349-1356.
- Carmo M, Peixoto C, Coroadinha AS, Alves PM, Cruz PE, Carrondo MJT. 2004. Quantitation of MLV-based retroviral vectors using real-time RT-PCR. *Journal of Virological Methods* 119(2):115-119.
- Cham BE, Knowles BR. 1976. A solvent system for delipidation of plasma or serum without protein precipitation. *J Lipid Res* 17(2):176-181.
- Chan LM, Coutelle C, Themis M. 2001. A novel human suspension culture packaging cell line for production of high-titre retroviral vectors. *Gene Ther* 8(9):697-703.
- Chase LG, Firpo MT. 2007. Development of serum-free culture systems for human embryonic stem cells. *Current Opinion in Chemical Biology Next-generation therapeutics* 11(4):367-372.
- Chen HF, Kuo HC, Chien CL, Shun CT, Yao YL, Ip PL, Chuang CY, Wang CC, Yang YS, Ho HN. 2007. Derivation, characterization and differentiation of human embryonic stem cells: comparing serum-containing versus serum-free media and evidence of germ cell differentiation. *Hum Reprod* 22(2):567-577.
- Coroadinha AS, Alves PM, Santos SS, Cruz PE, Merten OW, Carrondo MJ. 2006a. Retrovirus producer cell line metabolism: implications on viral productivity. *Appl Microbiol Biotechnol* 72(6):1125-1135.
- Coroadinha AS, Schucht R, Gama-Norton L, Wirth D, Hauser H, Carrondo MJ. 2006b. The use of recombinase mediated cassette exchange in retroviral vector producer cell lines: predictability and efficiency by transgene exchange. *J Biotechnol* 124(2):457-468.
- Cosset FL, Takeuchi Y, Battini JL, Weiss RA, Collins MK. 1995. High-titer packaging cells producing recombinant retroviruses resistant to human serum. *J Virol* 69(12):7430-7436.
- Edelstein ML, Abedi MR, Wixon J. 2007. Gene therapy clinical trials worldwide to 2007--an update. *J Gene Med* 9(10):833-842.

- Falkner E, Appl H, Eder C, Losert UM, Schoffl H, Pfaller W. 2006. Serum free cell culture: the free access online database. *Toxicol In Vitro* 20(3):395-400.
- Gerin PA, Gilligan MG, Searle PF, Al-Rubeai M. 1999a. Improved titers of retroviral vectors from the human FLYRD18 packaging cell line in serum- and protein-free medium. *Hum Gene Ther* 10(12):1965-1974.
- Gerin PA, Searle PF, Al-Rubeai M. 1999b. Production of retroviral vectors for gene therapy with the human packaging cell line FLYRD18. *Biotechnol Prog* 15(5):941-948.
- Ghani K, Cottin S, Kamen A, Caruso M. 2007. Generation of a high-titer packaging cell line for the production of retroviral vectors in suspension and serum-free media. *Gene Ther* 14(24):1705-1711.
- Laliberte JP, McGinnes LW, Peebles ME, Morrison TG. 2006. Integrity of membrane lipid rafts is necessary for the ordered assembly and release of infectious Newcastle disease virus particles. *J Virol* 80(21):10652-10662.
- Le Doux JM, Davis HE, Morgan JR, Yarmush ML. 1999. Kinetics of retrovirus production and decay. *Biotechnol Bioeng* 63(6):654-662.
- McTaggart S, Al-Rubeai M. 2000. Effects of culture parameters on the production of retroviral vectors by a human packaging cell line. *Biotechnol Prog* 16(5):859-865.
- Merten OW. 2004. State-of-the-art of the production of retroviral vectors. *J Gene Med* 6 Suppl 1:S105-24.
- Mountain A. 2000. Gene therapy: the first decade. *Trends Biotechnol* 18(3):119-128.
- Pizzato M, Merten OW, Blair ED, Takeuchi Y. 2001. Development of a suspension packaging cell line for production of high titre, serum-resistant murine leukemia virus vectors. *Gene Ther* 8(10):737-745.
- Rawat SS, Viard M, Gallo SA, Rein A, Blumenthal R, Puri A. 2003. Modulation of entry of enveloped viruses by cholesterol and sphingolipids (Review). *Mol Membr Biol* 20(3):243-254.
- Rodrigues T, Carrondo MJ, Alves PM, Cruz PE. 2007. Purification of retroviral vectors for clinical application: biological implications and technological challenges. *J Biotechnol* 127(3):520-541.
- Schucht R, Coroadinha AS, Zanta-Boussif MA, Verhoeven E, Carrondo MJ, Hauser H, Wirth D. 2006. A new generation of retroviral producer cells: predictable and stable virus production by Flp-mediated site-specific integration of retroviral vectors. *Mol Ther* 14(2):285-292.
- Seth G, Ozturk M, Hu WS. 2006. Reverting cholesterol auxotrophy of NS0 cells by altering epigenetic gene silencing. *Biotechnol Bioeng* 93(4):820-827.
- Seth G, Philp RJ, Denoya CD, McGrath K, Stutzman-Engwall KJ, Yap M, Hu WS. 2005. Large-scale gene expression analysis of cholesterol dependence in NS0 cells. *Biotechnol Bioeng* 90(5):552-567.
- Shen BQ, Palsson BO. 1996. Kinetics of retroviral production from the amphotropic Psi-CRIP murine producer cell line. *Cytotechnology* 22(1-3):185-195.
- Spector AA, Mathur SN, Kaduce TL, Hyman BT. 1980. Lipid nutrition and metabolism of cultured mammalian cells. *Prog Lipid Res* 19(3-4):155-186.
- Stewart JC. 1980. Colorimetric determination of phospholipids with ammonium ferrothiocyanate. *Anal Biochem* 104(1):10-14.

Chapter IV

ADAPTATION OF RETROVIRUS PRODUCER CELLS TO SERUM DEPRIVATION: *IMPLICATIONS IN LIPID BIOSYNTHESIS AND VECTOR PRODUCTION*

This chapter is adapted from:

Rodrigues AF, Amaral AI, Veríssimo V, Alves PM, Coroadinha AS, 2012. Adaptation of retrovirus producer cells to serum deprivation: implications in lipid biosynthesis and vector production *Biotechnol Bioeng.* 109(5):1269-79.

Abstract

The manufacture of enveloped virus, particularly retroviral and lentiviral vectors, faces the challenge of low titers that are aggravated under serum deprivation culture conditions. Also, the scarce knowledge on the biochemical pathways related with virus production is still limiting the design of rational strategies for improved production yields. This work describes the adaptation to serum deprivation of two human RV packaging cell lines, 293 FLEX and Te Fly and its effects on lipid biosynthetic pathways and infectious vector production. Total lipid content as well as cellular cholesterol were quantified and lipid biosynthesis was assessed by ¹³C-NMR spectroscopy; changes in gene expression of lipid biosynthetic enzymes were also evaluated.

The effects of adaptation to serum deprivation in lipid biosynthesis were cell line specific and directly correlated with infectious virus titers: 293 FLEX cells faced severe lipid starvation – up to 50% reduction in total lipid content – along with a 68 fold reduction in infectious vector titers; contrarily, Te Fly cells were able to maintain identical levels of total lipid content by rising *de novo* lipid biosynthesis, particularly for cholesterol – 50 fold increase – with the consequent recovery of infectious vector productivities. Gene expression analysis of lipid biosynthetic enzymes further confirmed cholesterol production pathway to be prominently up-regulated under serum deprivation conditions for Te Fly cells, providing a genotype-phenotype validation for enhanced cholesterol synthesis. These results highlight lipid metabolism dynamics and the ability to activate lipid biosynthesis under serum deprivation as an important feature for high retroviral titers. The mechanisms underlying virus production and its relationship with lipid biosynthesis, with special focus on cholesterol, are discussed as potential targets for cellular metabolic engineering.

Contents

1. Introduction.....	98
2. Materials and methods	99
2.1. Cell lines and culture media	99
2.2. Incubation with ¹³ C-labeled glucose for ¹³ C NMR spectroscopy analysis of lipid content.....	99
2.3. Lipid extraction	100
2.3.1. Lipid extraction for quantification of total lipid and cholesterol in producer cells.....	100
2.3.2. Lipid extraction for ¹³ C-NMR spectroscopy analysis	101
2.4. ¹³ C NMR spectroscopy	101
2.5. Retroviral vector production	101
2.5.1. Adaptation to reduced serum conditions	101
2.6. Retrovirus titration	102
2.7. Metabolite analysis and cholesterol quantification	102
2.8. RNA extraction and real-time quantitative PCR	102
2.9. Cell specific rates determination.....	103
3. Results	104
3.1. Adaptation to reduced-serum conditions	104
3.2. Study of lipid biosynthesis by ¹³ C-NMR spectroscopy.....	107
3.3. Total lipid and cholesterol content of RV and producer cells	109
3.4. Gene expression of lipid biosynthetic enzymes under reduced serum conditions.....	109
4. Discussion.....	111
5. Author contribution	115
6. References.....	115

1. Introduction

Enveloped viruses, in particular retroviral derived vectors, have been extensively used for therapeutic purposes. Recombinant retroviral vectors have been widely used as gene transfer tools in gene therapy protocols (Edelstein et al. 2007). Genome free particles have already demonstrated promising results in the vaccinology field and replication-competent-particles were developed and efficiently used as oncolytic agents for cancer therapy (Bellier et al. 2006; Dalba et al. 2007; Dalba et al. 2005). Retrovirus manufacture is still a challenging task, due to the low titers of packaging cells, reduced vector stability and, the requirement of high amounts of serum to support high infectious particles production during long-term cultures (Merten 2004; Rodrigues et al. 2009). Retrovirus, have been manufactured using mammalian cells, due to the inherent complexity of the biochemical pathways required for viral components production and assembly (Barrett et al. 2010; Delenda 1999). Among several cell lines, the selection of a particular host may constraint bioprocess and final product characteristics. The ultimate goal aims at understanding and controlling the physiological traits driving to high viral titers and quality, allowing for a tailored design or educated choice of cell substrates for virus production.

From the biochemical pathways closely related to virus replication, lipid biosynthesis has gained increased attention in recent years, not only for the specific case of enveloped virus production (Sagan et al. 2006) but also for protein production (Sriburi et al. 2004) and cellular growth in general (Whitford and Manwaring 2004). Recent works have shown that lipid metabolism of cells infected with enveloped viruses, such as hepatitis C (HCV), human cytomegalovirus (HCMV) and human immunodeficiency virus I (HIV-1) plays a crucial role in viral replication. Both HIV-1 and HCV infection increases lipogenesis, in particular, cholesterol biosynthesis (Giri et al. 2006; Syed et al. 2009). HCMV infection appears to stimulate sphingolipid biosynthesis and to increase metabolic flux of citrate through the tricarboxylic cycle (TCA) and its efflux to the fatty acid biosynthesis pathway as malonyl-CoA (Munger et al. 2008). In all the cases, the modification of the host lipid metabolism seems to support viral replication both by

providing building blocks to the newly formed virion progeny, as well as sustaining the functionality of lipid microdomains where viral assembly occurs (for a review see Chan et al. (2010)).

This work aimed to better understand the physiological changes occurring in two human cell lines producing recombinant Murine Leukemia Virus (MLV) vector, under serum deprivation conditions. We show that lipid metabolism dynamics of the producer cells is directly related to serum deprivation response and can constrain retroviral infectious vector production. Therefore, lipid biosynthetic pathways emerge as an appealing target for metabolic engineering in order to improve vector titers.

2. Materials and methods

2.1. Cell lines and culture media

Te Fly Ga 18 and 293 FLEX 18 are human derived cell lines producing MLV based vector expressing Gibbon Ape Leukemia Virus (GaLV) ecotropic envelope and harbouring a LacZ reporter gene. Te Fly Ga 18 are Te 671 (ATCC CCL-136) derived (Cosset et al. 1995, Duisit et al. 1999) and 293 FLEX 18 are HEK 293 (ATCC CRL-1573) derived cells established as described in Coroadinha et al. (2006a). Both cells were maintained in Advanced Dulbecco's modified Eagle's medium, DMEM, (Gibco, Paisley, UK) with 25 mM of glucose, supplemented with 10% (v/v) Foetal Bovine Serum (FBS) (Gibco) and 4 mM of glutamine (Gibco). Te671 cell line was used as the target cell to titrate infectious retroviral particles and was maintained in DMEM (Gibco) with 25 mM of glucose and 4 mM of glutamine supplemented with 10% (v/v) FBS (Gibco).

2.2. Incubation with ¹³C-labeled glucose for ¹³C NMR spectroscopy analysis of lipid content

For ¹³C-Nuclear Magnetic Resonance (NMR) spectroscopy analysis of lipid content, cells were inoculated at a density of 2×10^4 cells/cm² and 4×10^4 cells/cm² for Te Fly Ga 18 and 293 FLEX 18 cells, respectively. Final FBS concentrations were 10%, 7.5%, 3% (v/v) or

the corresponding reduced serum conditions for which both adapted and non-adapted cells were used. 72 hours later, the culture supernatant was replaced by medium supplemented with 8 mM of [U-¹³C] glucose (Cambridge Isotope Laboratories Inc, Andover, MA, USA), and incubated for further 24 hours after which lipid extraction was performed. The glucose concentration used during this period was previously determined to be sufficient to avoid depletion. The new medium was prepared from DMEM (Gibco) with no glucose, no glutamine and no sodium pyruvate, and supplemented to mimic Advanced DMEM formulation. The supplements used were non-essential amino acids solution (Gibco), reduced glutathione (Sigma, Steinheim, Germany), insulin-transferrin-selenium-X solution (Gibco), ascorbic acid (Sigma), albuMAXII® (Gibco), sodium pyruvate (Gibco) and glutamine (Gibco). All NMR cultures were performed using this formulation including the 10% (v/v) FBS control.

2.3. Lipid extraction

2.3.1. Lipid extraction for quantification of total lipid and cholesterol in producer cells

To determine the total lipid content of both producer cells and viruses, cells were seeded as described previously. Final FBS concentration was 10% (v/v) or the corresponding reduced serum conditions (RSC) for which both adapted and non-adapted cells were used. 96 hours later, cell culture supernatant containing retroviral vector was harvested, filtered through 0.45 µm for clarification and concentrated by ultracentrifugation as described in (Coroadinha et al. 2006b) and stored at -85°C until further analysis. Simultaneously, cells were harvested by trypsinization, washed twice by successive centrifugation-ressuspension in phosphate-buffered saline (PBS) to remove culture medium traces and stored at -20°C until total lipid extraction. Total lipid content was extracted from the cellular pellets as described in (Bligh and Dyer 1959) and the lipid containing chloroform phase was evaporated using a speed-vac. The final lipid pellet was weighted and used as a total lipid content measurement. For cholesterol quantification, the lipid pellet was solubilised in PBS (Gibco) + 0.1% (v/v) Tween-80 (Sigma).

2.3.2. Lipid extraction for ^{13}C -NMR spectroscopy analysis

For ^{13}C -NMR spectroscopy analysis, cells were seeded as described previously; after 24 hours of incubation with medium containing 8 mM of [$\text{U-}^{13}\text{C}$] glucose, lipid extraction was performed as described in Amaral et al. (2008).

2.4. ^{13}C NMR spectroscopy

Lipid extracts were prepared as described in section 2.4.2 and a known amount of dioxane 10% (v/v) in CDCl_3 was added as an internal standard to all samples. Proton-decoupled ^{13}C NMR spectra were acquired in a Bruker AVANCE II 500 MHz spectrometer operating at a frequency of 125.77 MHz, using the following parameters: 30° pulse angle, 25 kHz spectral width, 64-K data points, acquisition time of 1.3 s and a 0.5 s relaxation delay. The number of scans was typically 40.000. Relevant peaks in the spectra were identified and integrated. The amounts of ^{13}C were quantified from the integrals of the peak areas, using dioxane at 67.40 ppm as internal standard. Assignments were made by comparison with chemical shifts reported in the literature (Pollesello et al. 1996; Tugnoli et al. 2003). The values were compared after biomass normalization and are relative to the total amount of glucose consumed during the incubation time.

2.5. Retroviral vector production

2.5.1. Adaptation to reduced serum conditions

To analyse the long-term effects of serum deprivation in cell physiology and vector production, cells were seeded as described previously. The final concentration of FBS was either 10% (v/v) FBS or the correspondent to reduced serum conditions (1% (v/v) for 293 FLEX 18 cells and 0.5% (v/v) for Te Fly Ga 18). Reduced serum conditions had been previously determined for each cell line, as the minimum serum concentration allowing for the same cell growth and central energy metabolism profile than 10% (v/v) FBS (Rodrigues et al. 2009). During 9 sequential passages, a new splitting was performed, twice a week, maintaining the initial inoculums. In each split, the viral

supernatant was harvested, filtered through 0.45 µm pore membrane for clarification, aliquoted and stored at -85°C for further analysis. At the 10th passage, the curve of cell growth and vector production was analyzed for each case: 10% (v/v) FBS, and RSC for both adapted and non-adapted cells. Several samples were collected during the growth curve and the viral supernatant was treated as described above.

2.6. Retrovirus titration

For the infectious particle titration, Te671 were used as target cells. Infectious procedure and viral titer determination were performed by serial dilution infection assay, as previously described in Rodrigues et al. (2009).

2.7. Metabolite analysis and cholesterol quantification

Glucose, glutamine, lactate and ammonia concentration were determined using Bioprofile 100 plus Analyzer system (Nova Biomedical, Waltham, USA). Cholesterol was quantified in purified virus and cellular total lipid content by an enzymatic assay (Cayman Chemical, Ann Arbor, MI, USA), following the manufacturer's instructions.

2.8. RNA extraction and real-time quantitative PCR

To assess gene expression of lipid biosynthetic enzymes, cells were inoculated as described previously either in 10% (v/v) FBS or reduced serum conditions. For reduced serum conditions both adapted and non-adapted cells were used. 96 hours later, corresponding to middle exponential phase of the growth curve, total RNA was extracted using RNeasy Mini Kit (Qiagen, Valencia, CA) according to the manufacturer's instructions. For real time PCR, RPL-22 was chosen as a control gene. Forward (F) and reverse (R) primer sequences for control and lipid enzyme genes are given in Table I. The reverse transcription of total RNA was performed according to Transcriptor High Fidelity cDNA Synthesis Kit (Roche Applied Science, Mannheim, Germany) protocol for cDNA synthesis using 2 µg of total RNA and oligo dT primer for total mRNA reverse transcription. The reverse transcribed (RT) product was aliquoted and stored at -20°C until further processing. SYBR Green I dye chemistry was used to detect the PCR

products using LightCycler® 480 SYBR Green I Master (Roche Applied Science) according to the manufacturer's instructions using LightCycler® 480 Real Time PCR System (Roche Applied Science). cDNA samples were run along with a no RT-reaction control and a no cDNA template sample. Three independent cultures (biological replicates) were analyzed, each of them run in three (technical) replicates.

Table I – Primers used in Real-Time PCR

Gene	Primer orientation	5' to 3' sequence
RPL22	Forward	CTGCCAATTTTGAGCAGTTT
	Reverse	CTTTGCTGTTAGCAACTACGC
ATP citrate synthase	Forward	TGTAACAGAGCCAGGAACCC
	Reverse	CTGTACCCAGTGGCTGTT
Acetyl-CoA carboxylase	Forward	AACTCCAAGGACACAGTCACCAT
	Reverse	CAGCTGCTCCACGAACTCAA
Fatty acid synthase	Forward	GCACCAACTCCATGTTTGG
	Reverse	TGGAGATCACATGCGGTTTA
HMG-CoA reductase	Forward	ACAATAAGATCTGTGGTTGGAATTATGA
	Reverse	GCTATGCATCGTTATTGTCAGAA
HMG-CoA synthase (S)	Forward	CCATTGAAGAGGCTTCTGGT
	Reverse	CTGCCCTATTCTTCCCTTC
Acetoacetyl-CoA thiolase	Forward	AAAAGCAGGTTGGTCACTGG
	Reverse	CGACTTCTGCCATTCTCTC

2.9. Cell specific rates determination

To determine specific rates of cell growth, metabolite production/consumption and infectious particles (I.P.) productivities, the Boltzmann equation was considered:

$$\frac{dP}{dt} = \mu_p C \quad (\text{Eq. 1})$$

where P represents the different parameters, either viable cell concentration, metabolite concentration or I.P., C is the viable cell concentration, t is the culture time and μ_p is the cell specific rate of each parameter in study. The confidence interval considered was 95%.

3. Results

3.1. Adaptation to reduced-serum conditions

293 FLEX 18 and Te Fly Ga 18 cell lines had been shown to significantly decrease infectious vector production when serum was reduced in the culture medium; this decrease was found to be due to a reduction in the infectious particles production, as the number of total particles remained unchanged, and therefore suggesting biochemical limitations in the viral assembly line resulting in defective particles (Rodrigues et al. 2009). To further investigate the physiologic response to serum deprivation, cell growth and infectious vector production were monitored for 9 sequential passages under reduced serum conditions (Fig. 1). At the 10th passage, cell growth, central energy metabolism and infectious vector productivity were assessed (Fig. 2 and Table II).

Table II – Cell specific growth rate and central energetic metabolic yields ν_{lac}/ν_{glc} and ν_{amm}/ν_{glu} of 293 FLEX 18 and Te Fly Ga 18

		Culture media FBS % (v/v)		
		10%	RSC	RSC-Ad
293 FLEX 18	$\mu_{growth} (h^{-1})$	0.019 ± 0.002	0.018 ± 0.002	0.020 ± 0.001
	ν_{lac}/ν_{glc}	1.1 ± 0.3	1.3 ± 0.2	1.3 ± 0.3
	ν_{amm}/ν_{gln}	0.5 ± 0.1	0.6 ± 0.2	0.5 ± 0.2
Te Fly Ga 18	$\mu_{growth} (h^{-1})$	0.020 ± 0.002	0.018 ± 0.002	0.018 ± 0.002
	ν_{lac}/ν_{glc}	1.5 ± 0.4	1.5 ± 0.3	1.6 ± 0.3
	ν_{amm}/ν_{gln}	0.4 ± 0.1	0.8 ± 0.2	0.5 ± 0.1

RSC (*reduced serum conditions*) correspond to 1% (v/v) FBS for 293 FLEX 18 cells and 0.5% (v/v) FBS for Te Fly Ga 18. RSC-Ad are cells under reduced serum conditions after an adaptation period of 10 passages, as described in Materials and Methods. The errors in μ_{growth} correspond to a 95% confidence interval as defined in Material and Methods; the errors in ν_{lac}/ν_{glc} and ν_{amm}/ν_{gln} correspond to error propagation; (μ_{growth}) maximum cell specific growth rate, (ν_{lac}) lactate production rate, (ν_{glc}) glucose uptake rate, (ν_{amm}) ammonia production rate, (ν_{gln}) glutamine uptake rate.

No relevant changes were observed in cell growth or central energy metabolism patterns either during or after the adaptation period for both cell lines (Fig. 1A and B, Fig 2. A and B and Table II).

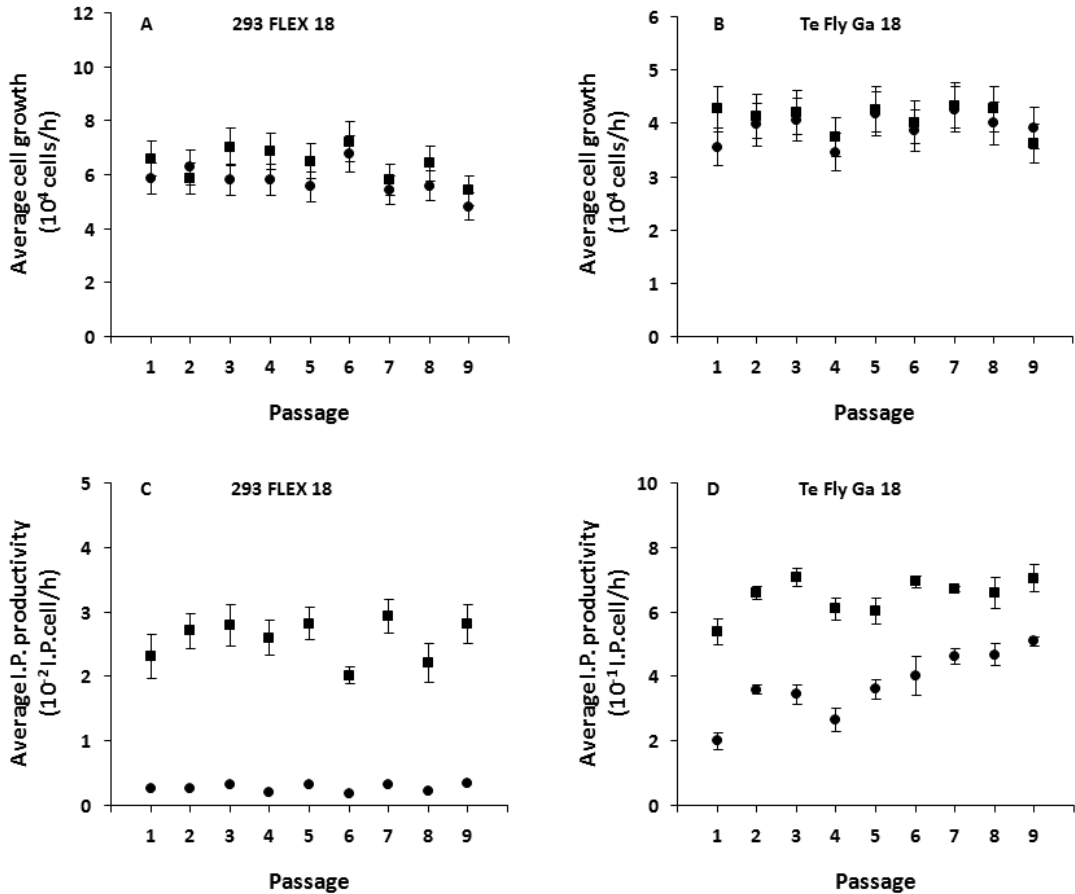


Figure 1 – Effect of passage number upon cell growth and vector productivity of 293 FLEX 18 and Te Fly Ga 18. Average cell growth (A and B) and infectious vector productivity (C and D) of 293 FLEX 18 (A and C) and Te Fly Ga 18 (B and D) cell lines during the adaptation period to reduced serum conditions (●) (RSC); 10% (v/v) FBS is shown as a control (■). Reduced serum conditions correspond to 1% (v/v) FBS for 293 FLEX 18 cells and 0.5% (v/v) FBS for Te Fly Ga 18 as defined in Rodrigues et. al. (2009). Error bars in A and B correspond to 10% error in cell counting, and in C and D correspond to standard deviation (n=3).

However the patterns of RV production were markedly altered during the adaptation period to serum deprivation and opposite responses were observed for the two cell lines (Fig. 1C and D, Fig. 2C and D). For 293 FLEX cells, the average infectious vector titer decreased abruptly since the first passage under RSC, and the values were found to be nearly identical in subsequent passages (Fig. 1C). Infectious vector productivity dropped 9 fold when compared with the standard 10% (v/v) FBS conditions and 68 fold for the adapted cells (Fig. 2C). On the other hand, Te Fly cells adapted to serum deprivation and recovered infectious vector production (Fig 1D). The first passage

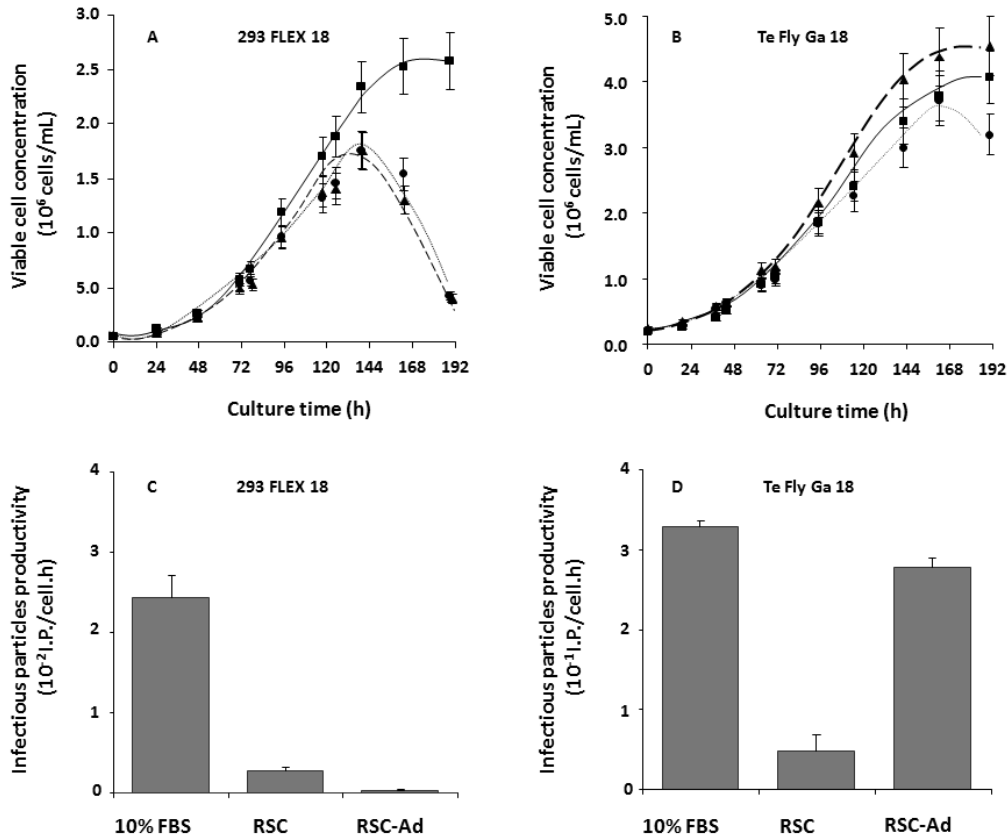


Figure 2 – Cell growth and vector productivity of 293 FLEX 18 and Te Fly Ga 18. Cell growth (A and B) and infectious vector productivity (C and D) of 293 FLEX 18 (A and C) and Te Fly Ga 18 (B and D) cell lines in standard 10% (v/v) FBS supplementation (—■—) and in reduced serum conditions before (RSC) (···●···) and after the adaptation period (RSC-Ad) (---▲---). Reduced serum conditions correspond to 1% (v/v) FBS for 293 FLEX 18 cells and 0.5% (v/v) FBS for Te Fly Ga 18. Error bars in A and B correspond to 10% error, for cell counting, and in C and D correspond to a 95% confidence interval, as defined in Material and methods.

was, indeed, where the highest decrease in infectious vector titer occurred, followed by an increase in the second passage; viral titers kept improving until the passage 6 and thereafter the average infectious vector titers remained nearly unaltered (Fig. 1D). Without adaptation, infectious vector productivity of Te Fly cells, decreased 7 fold under RSC comparatively to 10% (v/v) FBS but recovered to almost identical values after the adaptation period (Fig. 2D). Altogether, these results depicted a very distinct cellular/metabolic behavior for Te Fly and 293 FLEX cells when responding to serum deprivation, resulting in different viral production outcomes.

3.2. Study of lipid biosynthesis by ^{13}C -NMR spectroscopy

The absence of the serum lipid fraction had previously been correlated with the decrease in infectious vector productivity for both Te Fly Ga 18 and 293 FLEX 18 cells (Rodrigues et al. 2009). Therefore, the recovery of infectious vector production for Te Fly Ga 18 after the adaptation period led to hypothesize changes in producer cells lipid metabolism to be the basis for the recovery in infectious vector production. Glucose is the major carbon source for lipid biosynthesis in cultured mammalian cells (Spector et al. 1980); thus, uniformly labeled glucose ($[\text{U-}^{13}\text{C}]$ glucose) was used to probe lipid biosynthetic pathways by ^{13}C -NMR spectroscopy and to assess quantitative lipid biosynthesis in response to serum deprivation for both Te Fly Ga 18 and 293 FLEX 18 cells. Table III summarizes the results of ^{13}C incorporation into lipid molecules from cells cultured using different serum concentrations, including RSC for both adapted and non-adapted cells.

From a quantitative point of view, glucose channeling through lipid biosynthetic pathways occurred to a higher extent in 293 FLEX than in Te Fly cells, that is, for the same serum concentration in the culture medium, 293 FLEX synthesized higher amounts of lipids (Table III). However, these values needed to be analyzed in the context of 10% (v/v) FBS basal synthesis; this would translate the fold change relatively to the conditions under which a minimum lipid synthesis from glucose is known to occur and that corresponds to the lipid biosynthesis increase/capacity in response to serum deprivation comparable between both cell lines (Figure 3).

The increase in lipid biosynthesis was higher in Te Fly cells for all the lipid molecules considered. This was particularly evident in the case of cholesterol synthesis, which had a 35 fold increase from 10% (v/v) to the minimum serum concentration of 0.5% (v/v) FBS. This value increased even further, to 50 fold in Te Fly cells adapted to RSC, suggesting that metabolic changes were induced by such conditions. Conversely, 293 FLEX cells showed no appreciable changes in cholesterol synthesis neither in the remaining lipid molecules analyzed both before and after the adaptation period to serum withdrawal.

Table III – ¹³C incorporation in 293 FLEX 18 and Te Fly Ga 18 lipid content after [U-13C] glucose metabolism in the presence of different serum concentrations.

¹³ C relative* incorporation (10 ⁻⁶ /mg protein)	293 FLEX 18					
	10% FBS	7.5% FBS	3% FBS	1% (v/v) FBS		
				Non-adapted cells	Adapted cells	
Cholesterol	0.19 ± 0.02	0.20 ± 0.02	0.24 ± 0.02	0.41 ± 0.04	0.46 ± 0.05	
Cholesteryl Esters	0.9 ± 0.1	1.1 ± 0.1	1.9 ± 0.2	2.4 ± 0.2	2.6 ± 0.3	
Fatty Acids	2.9 ± 0.3	4.8 ± 0.5	5.4 ± 0.5	5.9 ± 0.6	6.1 ± 0.6	
Triacylglycerols	0.24 ± 0.02	0.35 ± 0.04	0.42 ± 0.04	0.59 ± 0.06	0.58 ± 0.06	
Phospholipids	2.6 ± 0.3	3.3 ± 0.3	3.7 ± 0.4	4.0 ± 0.4	4.0 ± 0.4	
¹³ C relative* incorporation (10 ⁻⁶ /mg protein)	Te Fly Ga 18					
	10% FBS	7.5% FBS	3% FBS	0.5% (v/v) FBS		
				Non-adapted cells	Adapted cells	
Cholesterol	0.004 ± 0.0004	0.02 ± 0.002	0.05 ± 0.01	0.15 ± 0.02	0.21 ± 0.02	
Cholesteryl Esters	0.39 ± 0.04	0.66 ± 0.07	1.5 ± 0.2	2.2 ± 0.2	2.4 ± 0.2	
Fatty Acids	0.79 ± 0.8	1.2 ± 0.1	1.8 ± 0.2	2.5 ± 0.3	3.0 ± 0.3	
Triacylglycerols	0.08 ± 0.01	0.12 ± 0.01	0.24 ± 0.02	0.28 ± 0.03	0.32 ± 0.03	
Phospholipids	1.0 ± 0.1	1.5 ± 0.2	1.8 ± 0.2	2.1 ± 0.2	2.4 ± 0.2	

The synthesis of each lipid was assessed by choosing one characteristic carbon and the values were compared using the same mark. (*) Values are relative to glucose consumption as described in Materials and methods. Errors correspond to 10%, the error associated to the NMR quantification method.

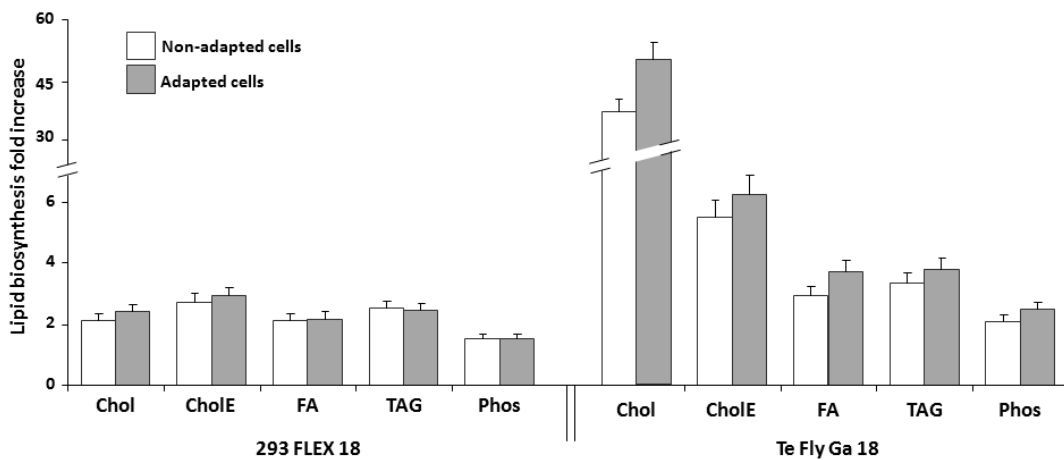


Figure 3 – Lipid biosynthesis in 293 FLEX 18 and Te Fly Ga 18. For reduced serum conditions, both adapted and non-adapted cells were used; fold increase is relative to 10% (v/v) FBS. Reduced serum conditions correspond to 1% (v/v) FBS for 293 FLEX 18 cells and 0.5% (v/v) FBS for Te Fly Ga 18. Abbreviations: (Chol) cholesterol, (CholE) cholesteryl esters, (FA) fatty acids, (TAG) triacylglycerols, (Phos) phospholipids. Error bars correspond to 10% error of NMR spectroscopy quantifications.

3.3. Total lipid and cholesterol content of RV and producer cells

To further analyze the effects of serum deprivation adaptation total cellular lipid and cholesterol content was quantified (Table IV).

Table IV – Lipid content of 293 FLEX 18 and Te Fly Ga 18 cells.

		Total lipids (pg/cell)	Cholesterol (pg/cell)
293 FLEX 18	10% FBS	0.34 ± 0.004	0.031 ± 0.006
	RSC	0.22 ± 0.009	0.020 ± 0.005
	RSC Adapted cells	0.15 ± 0.003	0.016 ± 0.002
Te Fly Ga 18	10% FBS	0.31 ± 0.03	0.029 ± 0.001
	RSC	0.34 ± 0.02	0.017 ± 0.003
	RSC Adapted cells	0.29 ± 0.02	0.029 ± 0.003

Reduced serum conditions (RSC) correspond to 1% (v/v) FBS for 293 FLEX 18 cells and 0.5% (v/v) FBS for Te Fly Ga 18. Values are shown as average ± standard deviation (n=5).

Although both cell lines activated lipid biosynthesis under RSC, in the case of FLEX cells, it was not enough to maintain neither the total lipid nor the cholesterol content at the same levels than in 10% (v/v) FBS. For Te Fly cells, this decrease was only observed for the cholesterol content. Actually, serum withdrawal induced a cholesterol deprivation scenario for both cell lines. This pattern was reverted after the adaptation period for Te Fly cells, but not for FLEX cells, further substantiating NMR spectroscopy data (Fig. 3) and evidencing distinct metabolic fingerprints between these two cell lines. This was ultimately correlated with vector production, as these changes also affected viral lipid content (data not shown).

3.4. Gene expression of lipid biosynthetic enzymes under reduced serum conditions

¹³C-NMR spectroscopy and lipid quantification showed unequivocally distinct profiles of lipid biosynthesis and lipid content, respectively, between Te Fly and FLEX cells under RSC and, more importantly, in the ability of these cells to adapt to serum deprivation maintaining high infectious vector titers. Thus, we further investigated if

such differences were based in gene expression changes of key lipid biosynthetic enzymes (Fig. 5).

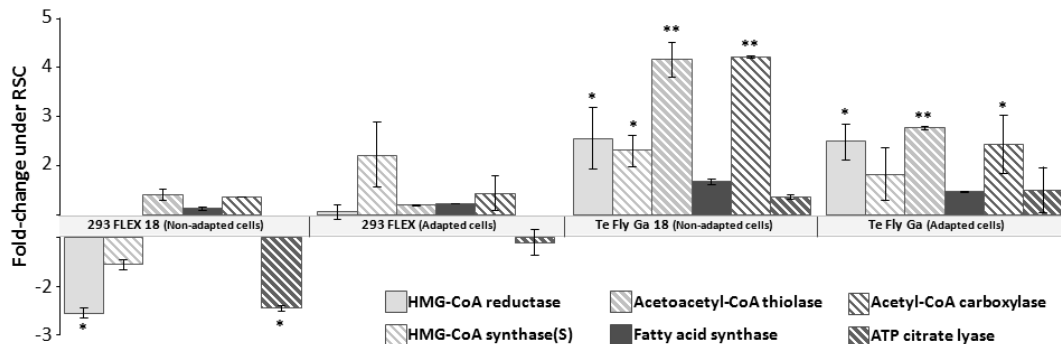


Figure 4 – Gene expression changes of lipid biosynthetic enzymes of 293 FLEX 18 and Te Fly Ga 18 cells. Gene expression changes induced by reduced-serum conditions of six key enzymes in lipid biosynthesis: HMG-CoA reductase, HMG-CoA synthase (cytosolic form), acetoacetyl-CoA thiolase, acetyl-CoA carboxylase, fatty acid synthase and ATP citrate lyase. Fold change under reduced serum conditions (RSC) for both adapted and non-adapted cells relatively to 10% (v/v) FBS conditions. Reduced serum conditions correspond to 1% (v/v) FBS for 293 FLEX 18 cells and 0.5% (v/v) FBS for Te Fly Ga 18. For relevant fold-changes (greater than 2 or -2) * and ** give the significance of a two-tailed non-paired *t*-test, between three independent replicates; * $p < 0.05$, ** $p < 0.005$.

For 293 FLEX cells, none of the lipid biosynthetic enzymes was significantly up-regulated. Actually, non-adapted cells presented a 2 fold down-regulation of HMG-CoA reductase and ATP-citrate lyase whereas adapted cells had no significant changes in none of the six enzymes analyzed when compared to 10% (v/v) FBS. By opposite, (non-adapted) Te Fly cells showed a significant up-regulation in four of the six enzymes analyzed; for acetoacetyl-CoA thiolase and acetyl-CoA carboxylase the changes were higher than 4 fold increase. Interestingly, for both Te Fly and FLEX cells, changes in gene expression were more pronounced for non-adapted than for adapted cells, suggesting it to have a stress response component, which tends to be diluted after the adaptation. After the adaptation, only Te Fly cells sustained higher expression levels of lipid biosynthetic enzymes, namely HMG-CoA reductase, acetoacetyl-CoA thiolase and acetyl-CoA carboxylase.

4. Discussion

In previous work, it was demonstrated that lipids are the main serum component correlated with infectious retroviral vector production and its absence under reduced serum conditions a major cause for the accentuated decrease of titers and viral preparation quality (Rodrigues et al. 2009). In this work, we analyzed the physiologic response of the same two retrovirus producer cell lines, 293 FLEX 18 and Te Fly Ga 18, to serum deprivation and its effects on lipid biosynthetic pathways and infectious vector production. The drop in infectious viral titer occurred immediately after the first passage (Fig. 1) evidencing it to be based on short-term mechanisms. On the other hand, the ability of Te Fly cells to respond to serum starvation rescuing viral productivity after adaptation to serum withdrawal pointed that intrinsic metabolic or biochemical factors could provide a natural foundation for vector production in the absence of serum.

The analysis of lipid biosynthesis for different serum concentrations (Table III) showed that both cell lines were able to activate *de novo* lipid synthesis when challenged by the lipid source removal, in accordance to what has previously been described (Alberts et al. 1974; Spector et al. 1980). Nevertheless, this was insufficient to maintain cellular lipid content in 293 FLEX cells, particularly cholesterol, at levels identical to those observed for 10% (v/v) FBS (Table III). Deficiency in cholesterol content of host cells has already been shown to impair viral infectivity of other enveloped viruses resulting in defective structurally damaged particles, with altered “proteins/lipids” ratios and/or membrane holes (Laliberte et al. 2006). Thus, it is not surprising that changes in cellular lipid content resulting from serum withdrawal could impair infectious vector production. The differences between the two cell lines after the adaptation to serum deprivation were, however, unexpected (Fig. 2). The response dynamics of lipid biosynthesis under RSC was higher in Te Fly cells than in 293 FLEX cells, with additional changes induced by the adaptation period particularly for cholesterol (Fig. 3). The ability of cholesterol synthesis under RSC can provide an explanation for the recovery of infectious vector production, as we have previously shown that the addition of cholesterol supplements under RSC is sufficient to achieve infectious vector titers

identical to those obtained with 10% (v/v) FBS for both cell lines (Rodrigues et al. 2009). Thus, the inability of 293 FLEX cells to synthesize cholesterol was probably the major cause of the very low titers obtained.

Limitations in cholesterol biosynthesis have been previously described for cultured mammalian cells (Seth et al. 2006; Seth et al. 2005) and may explain the different adaptation profile between Te Fly and FLEX cells and consequent infectious vector production performances. Cholesterol biosynthesis relies on tight regulation mechanisms mainly targeting the LDL (low density lipoprotein) receptors and key enzymes of the cholesterol biosynthetic pathway such as HMG-CoA synthase and particularly HMG-CoA reductase (Horton et al. 2002; Rudney and Sexton 1986). Thus, gene expression of six key lipid biosynthetic enzymes was analyzed under RSC (Fig. 4). Figure 6 shows a schematic representation of lipid biosynthesis from glucose and the main intervenient enzymes. ATP-citrate synthase (d) converts citrate to oxaloacetate and acetyl-CoA thus contributing to the flux of glucose towards lipid biosynthesis. Acetyl-CoA carboxylase and acetoacetyl-CoA thiolase convert acetyl-CoA to malonyl-CoA and acetoacetyl-CoA, initiating its commitment to fatty acid and cholesterol biosynthesis, respectively. Both enzymes were significantly up-regulate under RSC for Te Fly but not in 293 FLEX cells. HMG-CoA synthase and HMG-CoA reductase, considered the rate limiting enzyme in cholesterol biosynthesis definitely committing HMG-CoA to cholesterol production, were also increased in Te Fly cells (Fig. 4). Such results support the hypothesis of increased glucose flux towards cholesterol production occurring in these cells under RSC (Fig. 3) to be accomplished by enhanced gene expression of cholesterol biosynthetic enzymes induced by serum withdrawal. The up-regulation in gene expression of these enzymes, could be readily seen after 96 hours under RSC (Fig. 4, Te Fly Ga 18 non-adapted cells), which goes in agreement with NMR data showing enhanced cholesterologenesis even before the adaptation period (Fig. 3); still, infectious vector productivity recovery only begins to be evident in the second passage under RSC (Fig. 1) suggesting a time-shifting between lipid metabolism rearrangements and recovery in infectious vector production. 293 FLEX cells failed to increase gene

expression of lipid biosynthetic enzymes in response to serum deprivation (Fig. 4), which can explain the lower lipid biosynthesis (Fig. 3), reflected in their absolute lipid content (Table IV) and ultimately in infectious vector production (Fig. 1 and 2).

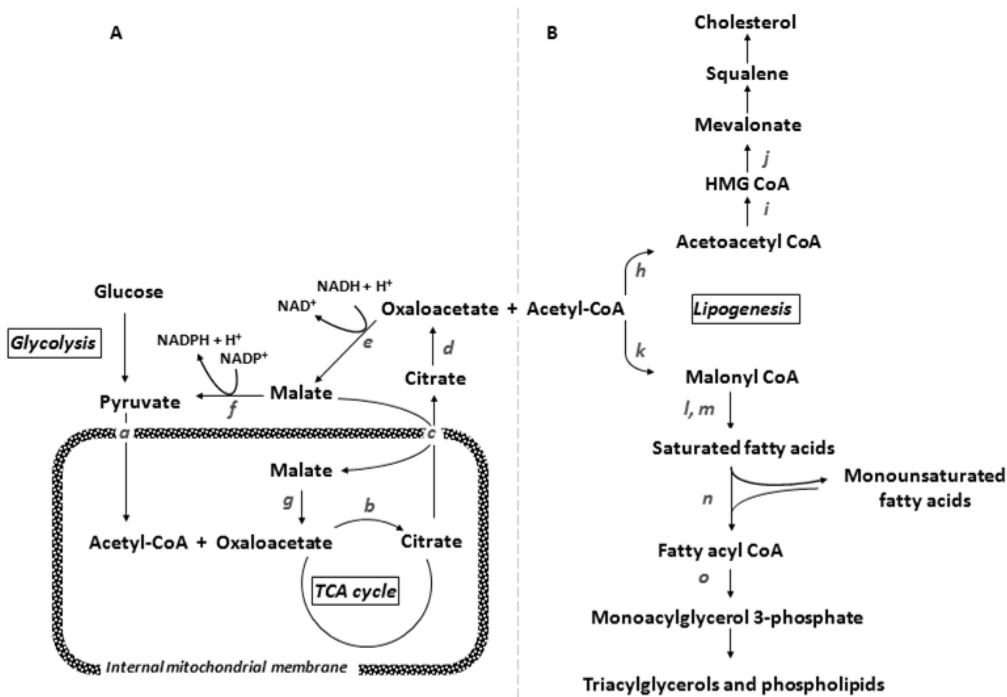


Figure 5 – Lipid biosynthesis from glucose in mammalian cells. (a) pyruvate dehydrogenase, (b) citrate synthase, (c) citrate carrier, (d) ATP-citrate lyase, (e) cytosolic malate dehydrogenase, (f) malic enzyme, (g) mitochondrial malate dehydrogenase, (h) acetoacetyl-CoA thiolase, (i) HMG-CoA synthase, (j) HMG-CoA reductase, (k) acetyl-CoA carboxylase, (l) fatty acid synthase, (m) long-chain fatty acyl elongase, (n) stearoyl-CoA desaturase, (o) glycerol 3-phosphate acyl transferase. Abbreviations: SREBPs (SRE binding proteins), TCA (tricarboxylic acids cycle). Adapted from Horton et al. (2002) and Gnani et al (2009). For a matter of simplicity, only the major reactions and corresponding enzymes are indicated

The distinct cellular origin between Te Fly and 293 FLEX cells can provide a hypothesis for the observed differences in cholesterol biosynthesis dynamics. 293 FLEX cells are derived from kidney tissue, being characterized by a modest cell turnover and presenting low activity of cholesterol biosynthetic enzymes with a consequent low capacity of cholesterol synthesis (Tosi and Tugnoli 2005). Conversely, Te Fly cells are tumor-derived cells, retaining high proliferation markers such as enhanced cholesterol synthesis and cholesteryl esters synthesis (Coleman 1986; Tosi and Tugnoli

2005), which were observed for these cells (Fig. 3). In this context, it is interesting to notice that long term serum free production of retro or lentiviral vectors has been based not only on lipid supplemented media (Broussau et al. 2008; Ghani et al. 2007) but also, in the case of transient systems, on highly transformed cells, namely 293T, transformed with SV40 large T antigen (T-Ag) or 293 EBNA, transformed with Nuclear Antigen of Epstein-Barr Virus (Schweizer and Merten 2010). These cells exhibit very different physiological features and gene expression patterns when compared to their counterparts, HEK 293 potentially facilitating serum independence for vector production (unpublished results); indeed, SV40 transformation was shown to facilitate serum-independent proliferation (Ahuja et al. 2005). Regarding vector production, Gama-Norton et al. (2011) have recently shown that even low levels of constitutive T-Ag expression can significantly increase lentiviral vectors titers in HEK 293; this effect was found not be exerted at the level of vector transcriptional activity but rather at the cellular/physiological level, through an indirect and unidentified mechanism. In fact, not much is known about the long-term metabolic modifications induced by T-Ag or EBNA transformation. However, it is probable that some of those changes target lipid biosynthetic pathways, given that oncogenic neoplastic transformation is typically characterized by an increase in lipid biosynthesis and turnover (Barger and Plas 2010; Swinnen et al. 2006).

In this work we show that lipid biosynthesis and its connection to central carbon metabolism is more dynamic and regulated in Te Fly cell line than in 293 FLEX cells; this resulted in an increased capability to respond to serum deprivation and a consequent improvement in infectious vector production performance. The results herein presented highlight the need of understanding the metabolic fingerprints of producer hosts keeping the perspective of virus biology. Studies addressing relevant metabolic pathways for high-titer vector production, as the one herein presented should provide important knowledge to choose new cell substrate hosts, to design metabolic engineering strategies – genetic or environmental – and establish optimal bioprocess framings towards maximum vector yields and quality.

5. Author contribution

Ana Filipa A. F. Rodrigues participated on the experimental setup and design, performed the experiments, analyzed the data and wrote the chapter.

6. References

- Ahuja D, Saenz-Robles MT, Pipas JM. 2005. SV40 large T antigen targets multiple cellular pathways to elicit cellular transformation. *Oncogene* 24(52):7729-45.
- Alberts AW, Ferguson K, Hennessy S, Vagelos PR. 1974. Regulation of lipid synthesis in cultured animal cells. *J Biol Chem* 249(16):5241-9.
- Amaral AI, Coroadinha AS, Merten OW, Alves PM. 2008. Improving retroviral vectors production: Role of carbon sources in lipid biosynthesis. *J Biotechnol* 138(3-4):57-66.
- Barrett PN, Portsmouth D, Ehrlich HJ. 2010. Developing cell culture-derived pandemic vaccines. *Curr Opin Mol Ther* 12(1):21-30.
- Bellier B, Dalba C, Clerc B, Desjardins D, Drury R, Cosset F-L, Collins M, Klatzmann D. 2006. DNA vaccines encoding retrovirus-based virus-like particles induce efficient immune responses without adjuvant. *Vaccine* 24(14):2643-2655.
- Bligh EG, Dyer WJ. 1959. A rapid method of total lipid extraction and purification. *Can J Biochem Physiol* 37(8):911-7.
- Broussau S, Jabbour N, Lachapelle G, Durocher Y, Tom R, Transfiguracion J, Gilbert R, Massie B. 2008. Inducible packaging cells for large-scale production of lentiviral vectors in serum-free suspension culture. *Mol Ther* 16(3):500-7.
- Chan RB, Tanner L, Wenk MR. 2010. Implications for lipids during replication of enveloped viruses. *Chem Phys Lipids* 163(6):449-59.
- Coleman PS. 1986. Membrane cholesterol and tumor bioenergetics. *Ann N Y Acad Sci* 488:451-67.
- Coroadinha AS, Schucht R, Gama-Norton L, Wirth D, Hauser H, Carrondo MJ. 2006a. The use of recombinase mediated cassette exchange in retroviral vector producer cell lines: predictability and efficiency by transgene exchange. *J Biotechnol* 124(2):457-68.
- Coroadinha AS, Silva AC, Pires E, Coelho A, Alves PM, Carrondo MJ. 2006b. Effect of osmotic pressure on the production of retroviral vectors: Enhancement in vector stability. *Biotechnol Bioeng* 94(2):322-9.
- Cosset FL, Takeuchi Y, Battini JL, Weiss RA, Collins MK. 1995. High-titer packaging cells producing recombinant retroviruses resistant to human serum. *J Virol* 69(12):7430-6.
- Dalba C, Bellier B, Kasahara N, Klatzmann D. 2007. Replication-competent vectors and empty virus-like particles: new retroviral vector designs for cancer gene therapy or vaccines. *Mol Ther* 15(3):457-66.
- Dalba C, Klatzmann D, Logg CR, Kasahara N. 2005. Beyond oncolytic virotherapy: replication-competent retrovirus vectors for selective and stable transduction of tumors. *Curr Gene Ther* 5(6):655-67.
- Delenda CC, M; Douar, A-M; Merten, O-W. 1999. Cells for gene therapy and vector production. In: Jenkins N, editor. *Animal Cell Biotechnology: Methods and Protocols*. Totowa, NJ: Human Press Inc.
- Duisit G, Salvetti A, Moullier P, Cosset FL. 1999. Functional characterization of adenoviral/retroviral chimeric vectors and their use for efficient screening of retroviral producer cell lines. *Hum Gene Ther* 10(2):189-200.
- Edelstein ML, Abedi MR, Wixon J. 2007. Gene therapy clinical trials worldwide to 2007- an update. *J Gene Med* 9(10):833-42.

- Gama-Norton L, Botezatu L, Herrmann S, Schweizer M, Alves PM, Hauser H, Wirth D. 2011. Lentivirus Production Is Influenced by SV40 Large T-Antigen and Chromosomal Integration of the Vector in HEK293 Cells. *Hum Gene Ther* 22(10):1269-79
- Ghani K, Cottin S, Kamen A, Caruso M. 2007. Generation of a high-titer packaging cell line for the production of retroviral vectors in suspension and serum-free media. *Gene Ther* 14(24):1705-11.
- Giri MS, Nebozhyn M, Showe L, Montaner LJ. 2006. Microarray data on gene modulation by HIV-1 in immune cells: 2000-2006. *J Leukoc Biol* 80(5):1031-43.
- Goldstein JL, Brown MS. 1990. Regulation of the mevalonate pathway. *Nature* 343(6257):425-30.
- Horton JD, Goldstein JL, Brown MS. 2002. SREBPs: activators of the complete program of cholesterol and fatty acid synthesis in the liver. *J Clin Invest* 109(9):1125-31.
- Laliberte JP, McGinnes LW, Peeples ME, Morrison TG. 2006. Integrity of membrane lipid rafts is necessary for the ordered assembly and release of infectious Newcastle disease virus particles. *J Virol* 80(21):10652-62.
- Merten OW. 2004. State-of-the-art of the production of retroviral vectors. *J Gene Med* 6 Suppl 1:S105-24.
- Munger J, Bennett BD, Parikh A, Feng XJ, McArdle J, Rabitz HA, Shenk T, Rabinowitz JD. 2008. Systems-level metabolic flux profiling identifies fatty acid synthesis as a target for antiviral therapy. *Nat Biotechnol* 26(10):1179-86.
- Pollesello P, Eriksson O, Hockerstedt K. 1996. Analysis of total lipid extracts from human liver by ¹³C and ¹H nuclear magnetic resonance spectroscopy. *Anal Biochem* 236(1):41-8.
- Rodrigues AF, Carmo M, Alves PM, Coroadinha AS. 2009. Retroviral vector production under serum deprivation: The role of lipids. *Biotechnol Bioeng* 104(6):1171-81.
- Rudney H, Sexton RC. 1986. Regulation of cholesterol biosynthesis. *Annu Rev Nutr* 6:245-72.
- Sagan SM, Rouleau Y, Leggiadro C, Supekova L, Schultz PG, Su AI, Pezacki JP. 2006. The influence of cholesterol and lipid metabolism on host cell structure and hepatitis C virus replication. *Biochem Cell Biol* 84(1):67-79.
- Schweizer M and Merten OW. 2010. Large-scale production means for the manufacturing of lentiviral vectors. *Curr Gene Ther* 10(6):474-86.
- Seth G, Ozturk M, Hu WS. 2006. Reverting cholesterol auxotrophy of NS0 cells by altering epigenetic gene silencing. *Biotechnol Bioeng* 93(4):820-7.
- Seth G, Philp RJ, Denoya CD, McGrath K, Stutzman-Engwall KJ, Yap M, Hu WS. 2005. Large-scale gene expression analysis of cholesterol dependence in NS0 cells. *Biotechnol Bioeng* 90(5):552-67.
- Spector AA, Mathur SN, Kaduce TL, Hyman BT. 1980. Lipid nutrition and metabolism of cultured mammalian cells. *Prog Lipid Res* 19(3-4):155-86.
- Sriburi R, Jackowski S, Mori K, Brewer JW. 2004. XBP1: a link between the unfolded protein response, lipid biosynthesis, and biogenesis of the endoplasmic reticulum. *J Cell Biol* 167(1):35-41.
- Syed GH, Amako Y, Siddiqui A. 2009. Hepatitis C virus hijacks host lipid metabolism. *Trends Endocrinol Metab* 21(1):33-40.
- Tosi MR, Tugnoli V. 2005. Cholesteryl esters in malignancy. *Clin Chim Acta* 359(1-2):27-45.
- Tugnoli V, Bottura G, Fini G, Reggiani A, Tinti A, Trincherio A, Tosi MR. 2003. ¹H-NMR and ¹³C-NMR lipid profiles of human renal tissues. *Biopolymers* 72(2):86-95.
- Whitford W, Manwaring J. 2004 Lipids in cell culture media. *Art To Science - HyClone Laboratories, Inc.*:1-5.

Chapter V

Part A

LIPID BIOSYNTHESIS BOTTLENECKS UNDERLYING SERUM HETEROTROPHY

Chapter V is divided into two parts following the two main sections of this thesis: i) understanding the metabolic constraints of retroviral vector production and ii) use the gathered knowledge for rational gene engineering. Therefore, Chapter V – part A comprises transcriptome analysis of serum deprivation and Chapter V – part B focuses metabolic engineering of lipid biosynthesis.

Both parts will be combined to be published as:

Reversion of serum heterotrophy in retrovirus replicating cells:

Reactivation of cholesterol biosynthesis

Ana F. Rodrigues, Ana S. Formas-Oliveira, Paula M. Alves, Wei-Shou Hu,

Ana S. Coroadinha, *(in preparation)*

Abstract

The need of animal blood sera to support infectious vector titers has challenged retroviral vector production in HEK 293 derived cells. Lipid starvation under reduced serum conditions was demonstrated to be a main cause for the loss of infectious vector titers while the ability to reactivate lipid biosynthesis, particularly cholesterol, was shown to allow the reversion of serum heterotrophy phenotype. Yet, HEK 293 derived retroviral vector producer cells seem to have this pathway impaired, unable to rescue cholesterol biosynthesis in response to the removal of the external lipid supply.

In the first part of this work, we aimed at understanding the metabolic impairments underlying lipid heterotrophy of 293 FLEX retroviral vector producer cells. Transcriptional profiling identified three potential bottlenecks in the pathway of *de novo* cholesterol biosynthesis: mevalonate kinase (MVK), lanosterol synthase (LSS) and sterol regulatory element binding factor 2 (SREBF2).

In the second part of this work (refer to Chapter V Part B), these targets were over-expressed in 293 FLEX in an attempt to reactivate cholesterol biosynthesis and revert serum heterotrophy. When individually over-expressing MVK and LSS, serum heterotrophy was mildly alleviated. When in combination, it was totally reverted. The over-expression SREBF2 alone, not only promoted the complete reversion of serum heterotrophy, as it resulted in higher infectious titers than those of standard serum supplementation conditions.

The work herein described focuses the tailored design of retroviral vector producer cells in the pursuit of a serum-independent phenotype based on educated guesses driven by functional genomics studies. The results also represent, to the best of our knowledge, the first metabolic engineering manipulation of cholesterolgenesis in mammalian cell culture.

Contents

1. Introduction.....	120
2. Materials and methods	121
Cell lines and culture conditions	121
Cell growth and viral production studies	122
RNA extraction, amplification, labeling and BeadChip hybridization	122
Data processing and analysis.....	122
3. Results	123
3.1. Transcriptional profiling of retroviral vector production under serum deprivation	123
4. Discussion	126
5. Author contribution.....	128
6. References.....	129

1. Introduction

Retro and lentiviral vectors are powerful gene delivery tools comprising the most widely used viral vectors for the treatment of monogenic diseases and hematopoietic cell modification in gene and cell therapy (Edelstine 2013; Ginn et al. 2013). As gene therapy moves from clinical to market (Moran 2012; Sheridan 2011), increased pressure is put on the development of stable cell lines and robust manufacture processes for vector production. However, long-term vector production is dependent on animal blood serum, an ill-defined culture supplement and potential source of pathogen contamination, hindering the safety and standardization required in clinical-grade manufacture processes.

In previous work we demonstrated that reducing serum in the culture medium of two human cell lines producing recombinant retrovirus leads to sharp reductions in infectious but not total particles titer (Rodrigues et al. 2009). Thus, serum withdrawal results in high contamination content of non-infectious particles likely to obstruct the therapeutic potential of the infectious ones. Lipids, in particular cholesterol, were confirmed as the key serum component correlated with the production of infectious retroviral vectors (Rodrigues et al. 2009). Following these findings, an adaptation to serum deprivation was conducted for these two cell lines, and the effects on lipid biosynthetic pathways and infectious vector production were analyzed. Such effects were found to be cell line specific and directly correlated with infectious virus titers. Cells facing lipid starvation nearly inhibited infectious vector production while cells rising *de novo* lipid biosynthesis, particularly cholesterol, recovered infectious vector titers (Rodrigues et al. 2012). Yet, recruiting biosynthetic machinery and starting *de novo* lipogenesis, is the expectable phenotype of cultured mammalian cells in response to the removal of the external lipid source (Alberts et al. 1974; Spector et al. 1980). Also, the cells found to be unable to rise up lipid biosynthesis – 293 FLEX – are derived from HEK 293, a cell line that has been cultured under serum-free conditions in the past two decades (Berg et al. 1993). Therefore, retroviral vector production

appears to induce a particular serum heterotrophy phenotype, not derived from the original parental cells.

The hint on the possible source of serum heterotrophy arose from the transcriptome comparison between producer and non-producer parental cells (Rodrigues et al. 2013). Retroviral vector production was found to induce a general down-regulation of the lipid biosynthetic pathways, more prominent in case of cholesterol; this effect appeared to be counterbalanced with the up-regulation of lipid uptaking machinery partially explaining the heavy reliance of retroviral vector producer cells on external lipid sources. More importantly, two particular enzymes were found to be limiting the pathway function. One was mevalonate kinase (MVK), with gene expression values near the non-transcription threshold. The other was lanosterol synthase (LSS) as it was strongly down-regulated in the transition “parental-to-producer” in 293 derived producers (Rodrigues et al. 2013).

In the first part of this work, we conducted transcriptome analysis for the two retroviral vector producer cells of the above mentioned studies – 293 FLEX and Te Fly Ga – under serum deprivation conditions. The results were crossed with those of the transcriptional profile of “parental-to-producer” transition. We found that the re-activation of both enzymes, MVK and LSS, is an exclusive ability of Te Fly producers, those capable of rescuing cholesterol biosynthesis in response to serum depletion. Therefore, these enzymes appear as over-expression targets to revert cholesterol (serum) heterotrophy in 293 FLEX producers.

2. Materials and methods

Cell lines and culture conditions

Te Fly Ga 18 (Cosset et al. 1995; Duisit et al. 1999) and 293 FLEX (Coroadinha et al. 2006; Schucht et al. 2006) are human derived cell lines producing murine leukemia virus (MLV) based vector harbouring a LacZ reporter gene, pseudotyped with gibbon ape leukemia virus (GaLV). The cells were maintained in Advanced Dulbecco’s

modified Eagle's medium, DMEM (Gibco, Paisley, UK), with 25 mM of glucose, supplemented with 10% (v/v) Foetal Bovine Serum (FBS) (Gibco) and 4 mM of glutamine (Gibco). The final concentration of FBS was changed for the different studies of retroviral vector production. Te671 (ATCC CCL-136) cell line was used to titrate infectious retroviral particles. All cells were maintained in an incubator with a humidified atmosphere of 92% air and 8% CO₂ at 37 °C.

Cell growth and viral production studies

Cells were inoculated at a density of 2×10^4 cells/cm² and 4×10^4 cells/cm² for Te Fly Ga 18 and 293 FLEX 18 cells, respectively. Final FBS concentrations were 10% (v/v) or the corresponding reduced serum conditions (RSC). Reduced serum conditions had been previously determined for each cell line, as the minimum serum concentration allowing for the same cell growth and central energy metabolism profile than 10% (v/v) FBS (Rodrigues et al. 2009). Two samples were collected *per* day: culture supernatant was harvested, filtered through 0.45 µm for clarification, aliquoted and stored at -85°C until analysis. Cell concentration and viability was determined by the trypan blue exclusion method. At day 3, total RNA was extracted for transcriptome analysis.

RNA extraction, amplification, labeling and BeadChip hybridization

RNA extraction, amplification, labeling and BeadChip hybridization were performed as described in Chapter II (Rodrigues et al. 2013).

Data processing and analysis

Data was processed by log₂ and variance-stabilizing transformation and quantile normalized as described in Chapter II (Rodrigues et al. 2013).

Differentially expressed genes were considered for a $|FC| \geq 1.5$ fold-change criterion. Pathway analysis was performed using Ingenuity Pathway Analysis (IPA) (Ingenuity® Systems, www.ingenuity.com).

3. Results

3.1. Transcriptional profiling of retroviral vector production under serum deprivation

To evaluate the effects of serum deprivation on global gene expression of 293 FLEX and Te Fly retroviral vector producer cells, a whole-transcriptome microarray analysis was conducted comparing 10% (v/v) FBS standard conditions to reduced serum conditions for each of the cell lines: 1% (v/v) for 293 FLEX and 0.5% (v/v) for Te Fly (Rodrigues et al. 2009). A fold-change (FC) criterion was set, considering as differentially expressed genes those for which $|FC| \geq 1.5$ -fold. Differentially expressed genes were analyzed by Ingenuity Pathway Analysis software. Figure 1 shows metabolic pathways significantly enriched for each of the cell lines.

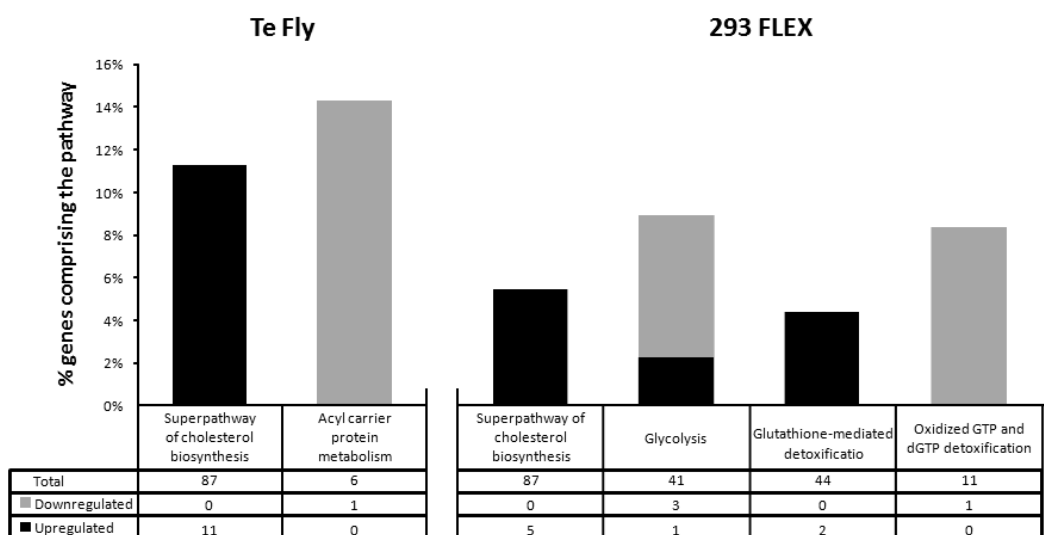


Figure 1 – Metabolic pathways enriched under serum deprivation. Significantly enriched pathways ($p < 0.05$) given by Ingenuity Pathway Analysis of differentially expressed genes under serum deprivation and number of genes enriching the pathways. Note that only *metabolic*, and not *signaling*, pathways are shown. Differentially expressed genes were considered for a $|FC| \geq 1.5$ criterion for each of the comparisons 10% (v/v) FBS vs. reduced serum conditions for Te Fly and 293 FLEX cells. FC: fold-change.

Cholesterol biosynthesis was the top significantly enriched metabolic pathway under serum deprivation. It was also the only category common to 293 FLEX and Te Fly. All of these genes were cholesterol biosynthetic enzymes, reporting to up-

regulation and, thus, indicating strong activation of the pathway under serum deprivation. The number of up-regulated genes in Te Fly producers (11) substantially exceeded those in 293 FLEX (5).

Since both 293 FLEX and Te Fly up-regulated cholesterol biosynthesis gene in response to serum deprivation, we further inquired on gene expression patterns specific to each producer that could explain the impairment of cholesterol biosynthesis in 293 FLEX. Cholesterol biosynthetic proteins were analyzed in terms of absolute expression and fold-change, between 10% (v/v) FBS and reduced serum conditions (Fig. 2). Given our previous results indicating cholesterol biosynthesis arrestment in the transition “parental-to-producer” (Rodrigues et al. 2013), gene expression in parental cells was also analyzed.

The results confirmed that producer cells down-regulated cholesterol biosynthesis enzymes – relatively to non-producers. Mevalonate kinase (MVK) appeared as nearly non-expressed in both producers and non-producers. A very drastic reduction was observed for lanosterol synthase (LSS) in 293 FLEX also near to the non-expression threshold, comparatively to the parents HEK 293 (Fig. 2). These results have been previously reported (Rodrigues et al. 2013). When challenged by serum withdrawal, Te Fly cells up-regulated the vast majority of cholesterol biosynthetic enzymes not only to values identical to those of the parents but, to even higher values. The same happened in 293 FLEX with two exceptions: LSS and MVK. It was additionally noteworthy that the transcription factor mainly associated to cholesterol biosynthesis activation, sterol regulatory element binding protein 2 (SREBP2), was poorly expressed in both cell lines – although higher in Te Fly – and was not up-regulated in response to serum removal. The results from Figure 2 evidence gene expression patterns in Te Fly cells to favor cholesterol biosynthesis under serum deprivation.

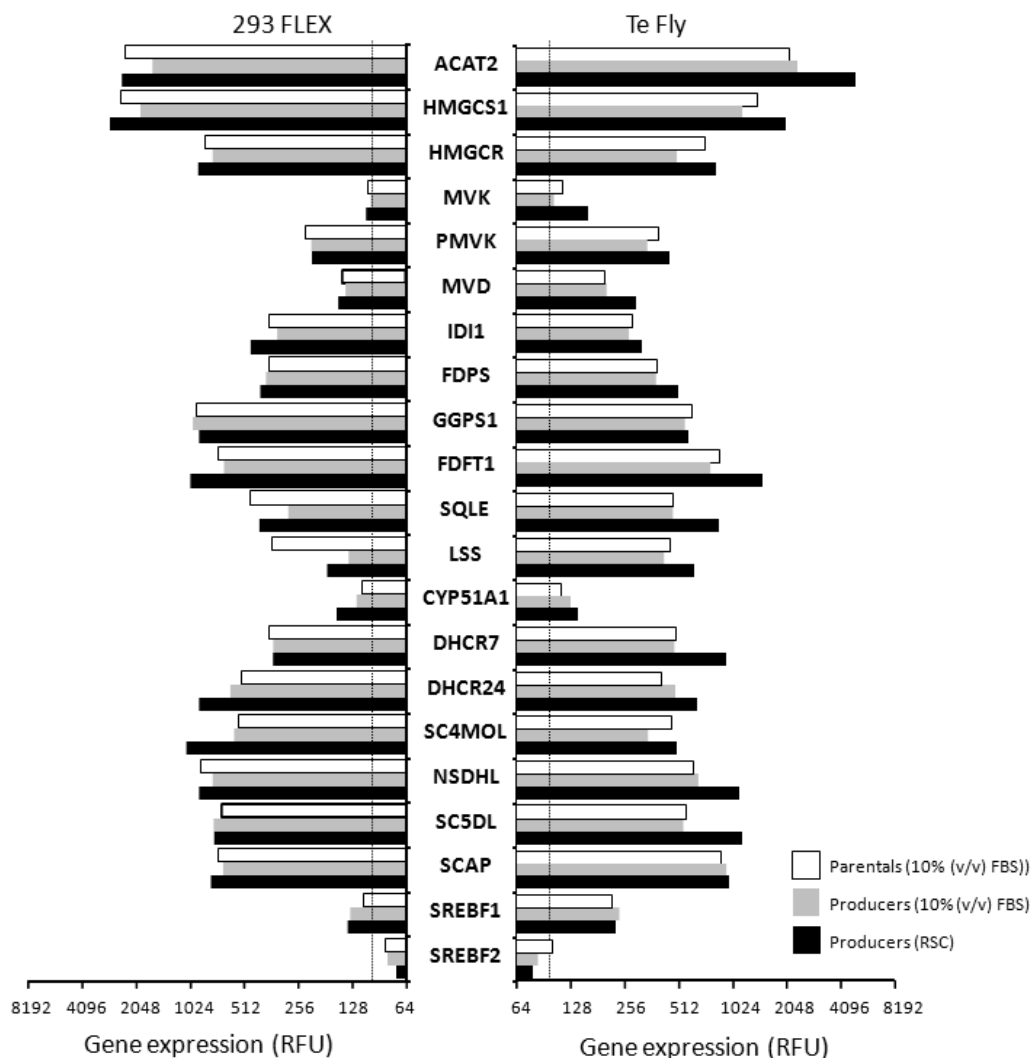


Figure 2 – Gene expression of cholesterol biosynthesis enzymes. Expression values of cholesterol biosynthetic enzymes of 293 FLEX (left side) and Te Fly (right side) retroviral vector producers and respective parental cells (HEK 293 and Te 671). Values are relative fluorescence units (RFU) from Illumina BeadChip microarray after variance-stabilizing transformation and quantile normalization as defined in Materials and methods. Genes are shown in the order that pathway proceeds from acetyl-CoA to cholesterol. Note that the three last proteins (SCAP and SREBF 1 and 2) are not biosynthetic enzymes. SREBF 1 and 2 are transcription factors related to lipid biosynthesis control and SCAP is the chaperone of these factors. The vertical dashed line indicates the expression value corresponding to 1.5-fold higher than the background probes. This value can be used as cut-off to distinguish expressed from non-expressed genes. ACAT2: acetyl-Coenzyme A acetyltransferase 2; CYP51A1: cytochrome P450, family 51, subfamily A, polypeptide 1; DHCR7: 7-dehydrocholesterol reductase; DHCR24: 24-dehydrocholesterol reductase; FDFT1: farnesyl-diphosphate farnesyltransferase 1; FDPS: farnesyl diphosphate synthase; GGPS1: geranylgeranyl diphosphate synthase 1; HMGCR: 3-hydroxy-3-methylglutaryl-Coenzyme A reductase; HMGCS1: 3-hydroxy-3-methylglutaryl-Coenzyme A synthase 1; IDI1: isopentenyl-diphosphate delta isomerase 1; LSS: lanosterol synthase; MVD: mevalonate (diphospho) decarboxylase; MVK: mevalonate kinase; NSDHL: NAD(P) dependent steroid dehydrogenase-like; PMVK: phosphomevalonate kinase; SCAP: SREBF chaperone; SC4MOL: sterol-C4-methyl oxidase-like; SC5DL: sterol-C5-desaturase; SQLE: squalene epoxidase; SREBF1: sterol regulatory element binding transcription factor 1; SREBF2: sterol regulatory element binding transcription factor 2.

4. Discussion

The need of animal blood sera to support infectious vector titers has challenged retroviral vector production in HEK 293 derived cells. Lipid starvation under reduced serum conditions was shown as a main cause for this problem (Rodrigues et al. 2012; Rodrigues et al. 2009). In fact, previous publications on serum-free retroviral vector production report the supplementation of the culture medium with lipids and lipoproteins (Ghani et al. 2007). The problem is likely to extend to lentiviral vector, although the transient nature of lentiviral vector production hinders a fair comparison since the main effects of serum deprivation are felt on a long-term culture period (Rodrigues et al. 2012). Indeed, the only publication of long-term serum-free lentiviral vector production also reports lipid supplementation of the culture medium (Broussau et al. 2008).

At the lab-scale, lipid supplements may be an interesting alternative to serum. At larger scales, however, animal-free derived lipid supplements translate into substantial manufacture costs. Also, lipids are extremely sensitive molecules, easily peroxidable, and a potential source of oxidative burden in the culture (Esterbauer et al. 1991). Therefore, understanding serum (lipid) heterotrophy is an important landmark to deliver improved cell lines and robust manufacture processes for retroviral, and most likely, lentiviral vector production.

By using retroviral vector producer cells derived from two different origins (293 FLEX and Te Fly), we have shown that, for both cell lines, the heavy reliance on an external lipid source results from the “viral producer state” which leads to a strong down-regulation of the lipid synthesizing machinery while up-regulating the lipid uptaking machinery (Rodrigues et al. 2013). But we have also shown that serum heterotrophy is cell line dependent, dictated by the ability to revert this “viral producer state” induced arrestment of lipid biosynthesis and reactivate cholesterol synthesis in response to serum depletion (Rodrigues et al. 2012). Therefore, in this

work, we conducted transcriptome analysis under serum deprivation conditions of these two cell lines, in an attempt to identify cholesterol biosynthesis bottlenecks in 293 FLEX.

Pathway analysis of differentially expressed genes readily identified *cholesterol biosynthesis* as the most significantly enriched metabolic pathway under serum depletion conditions (Fig. 1). In fact, for Te Fly cells, this and *acyl carrier protein metabolism* were the only enriched metabolic pathways under serum deprivation. We have previously hypothesized this robustness of Te Fly cells to derive from its cancer origin (Rodrigues et al. 2012). Interestingly, *acyl carrier protein metabolism* pathway was enriched by the down-regulation of amino adipate-semialdehyde dehydrogenase-phosphopantetheinyl transferase (AASDHPPT). This enzyme transfers the 4'-phosphopantetheine moiety of coenzyme A (CoA) to conserved serine residues of several synthase enzymes (Joshi et al. 2003), thereby, reducing the available pool of CoA. CoA, is actually the co-factor used in the synthesis of acetyl-CoA from citrate in *de novo* lipid biosynthesis. Down-regulating the expression of AASDHPPT appears, thus, a potential mechanism to reduce the draining of CoA to other pathways, favouring acetyl-coA synthesis for lipogenesis.

Pathway analysis only retrieves significantly enriched pathways, those in which the number of differentially expressed genes is unlikely to be obtained randomly. Thereby, all the genes comprising cholesterol biosynthesis pathway were individually analyzed, not only in terms of fold-change under, but also for absolute expression (Fig. 2). This analysis identified mevalonate kinase (MVK) and lansterol synthase (LSS) as the two potential blocking points of cholesterol biosynthesis in 293 FLEX producers. The former, given the very low values, near to non-expression threshold, and the latter since it was abruptly down-regulated from parental-to-producer, and only minorly up-regulated in response to serum deprivation.

At a first glance, arresting lipid biosynthesis might seem contradictory for cells replicating an enveloped virus. Yet, the up-regulation of lipid up-taking machinery should counter balance this effect (Rodrigues et al. 2013). From the cell point-of-

view, lipid uptake is more advantageous since lipids are very *expensive* molecules to synthesize, both in terms of carbon and energy and, thereby increasing intracellular reactive oxygen species. In fact, in the presence of an external lipid source, most mammalian cell lines readily uptake lipids from the culture medium, *pacifying-down* *de novo* biosynthesis (Alberts et al. 1974; Spector et al. 1980). From the virus point-of-view, it can also be conceived as advantageous. Carrying a chronic/latent infection, retroviruses do not rely on fast membrane turnover for the maximum progeny production in the shortest period of time. Instead, they would better benefit from a cell host capable of channeling the spare resources to other pathways serving viral replication and living longer due to the lower oxidative burden. However, when facing lipid deprivation, this scenario should be rapidly reverted to assure cell survival, as found for Te Fly producers (Fig. 2 and Chapter IV). The reason 293 FLEX could not reactivate MVK and LSS to cope with the need of *de novo* cholesterol biosynthesis is still not clear. Yet, the low expression levels of sterol regulatory element binding factor 2 (SREBF2), the transcription factor activated under cholesterol depletion conditions to recruit the biosynthetic machinery, might be a possible explanation. Therefore, in the second part of this work, MVK, LSS and SREBP2 were over-expressed in 293 FLEX in an attempt to reactivate cholesterol biosynthesis.

(Please refer to chapter V part B for the continuation of this work).

5. Author contribution

Ana Filipa A. F. Rodrigues participated on the experimental setup and design, performed part of the experiments, analyzed the data and wrote the chapter.

6. References

- Alberts AW, Ferguson K, Hennessy S, Vagelos PR. 1974. Regulation of lipid synthesis in cultured animal cells. *J Biol Chem* 249(16):5241-9.
- Berg DT, McClure DB, Grinnell BW. 1993. High-level expression of secreted proteins from cells adapted to serum-free suspension culture. *Biotechniques* 14(6):972-8.
- Broussau S, Jabbour N, Lachapelle G, Durocher Y, Tom R, Transfiguracion J, Gilbert R, Massie B. 2008. Inducible packaging cells for large-scale production of lentiviral vectors in serum-free suspension culture. *Mol Ther* 16(3):500-7.
- Coroadinha AS, Schucht R, Gama-Norton L, Wirth D, Hauser H, Carrondo MJ. 2006. The use of recombinase mediated cassette exchange in retroviral vector producer cell lines: predictability and efficiency by transgene exchange. *J Biotechnol* 124(2):457-68.
- Cosset FL, Takeuchi Y, Battini JL, Weiss RA, Collins MK. 1995. High-titer packaging cells producing recombinant retroviruses resistant to human serum. *J Virol* 69(12):7430-6.
- Duisit G, Salvetti A, Moullier P, Cosset FL. 1999. Functional characterization of adenoviral/retroviral chimeric vectors and their use for efficient screening of retroviral producer cell lines. *Hum Gene Ther* 10(2):189-200.
- Edelstine M. 2013. The Journal of Gene Medicine Clinical Trial Site (<http://www.wiley.com/legacy/wileychi/genmed/clinical>).
- Esterbauer H, Schaur RJ, Zollner H. 1991. Chemistry and biochemistry of 4-hydroxynonenal, malonaldehyde and related aldehydes. *Free Radic Biol Med* 11(1):81-128.
- Ghani K, Cottin S, Kamen A, Caruso M. 2007. Generation of a high-titer packaging cell line for the production of retroviral vectors in suspension and serum-free media. *Gene Ther* 14(24):1705-11.
- Ginn SL, Alexander IE, Edelstein ML, Abedi MR, Wixon J. 2013. Gene therapy clinical trials worldwide to 2012 - an update. *J Gene Med* 15(2):65-77.
- Joshi AK, Zhang L, Rangan VS, Smith S. 2003. Cloning, expression, and characterization of a human 4'-phosphopantetheinyl transferase with broad substrate specificity. *J Biol Chem* 278(35):33142-9.
- Moran N. 2012. First gene therapy nears landmark European market authorization. *Nat Biotechnol* 30(9):807-9.
- Rodrigues AF, Amaral AI, Verissimo V, Alves PM, Coroadinha AS. 2012. Adaptation of retrovirus producer cells to serum deprivation: Implications in lipid biosynthesis and vector production. *Biotechnol Bioeng* 109(5):1269-79.
- Rodrigues AF, Carmo M, Alves PM, Coroadinha AS. 2009. Retroviral vector production under serum deprivation: The role of lipids. *Biotechnol Bioeng* 104(6):1171-81.
- Rodrigues AF, Formas-Oliveiras AS, Bandeira VS, Alves PM, Hu WS, Coroadinha AS. 2013. Metabolic pathways recruited in the production of a recombinant enveloped virus: mining targets for process and cell engineering. *Metab. Eng. Nov* (20):131-145 .
- Schucht R, Coroadinha AS, Zanta-Boussif MA, Verhoeven E, Carrondo MJ, Hauser H, Wirth D. 2006. A new generation of retroviral producer cells: predictable and stable virus production by Flp-mediated site-specific integration of retroviral vectors. *Mol Ther* 14(2):285-92.
- Sheridan C. 2011. Gene therapy finds its niche. *Nat Biotechnol* 29(2):121-8.
- Spector AA, Mathur SN, Kaduce TL, Hyman BT. 1980. Lipid nutrition and metabolism of cultured mammalian cells. *Prog Lipid Res* 19(3-4):155-86.

Chapter V

Part B

REACTIVATION OF CHOLESTEROL BIOSYNTHESIS REVERTS SERUM HETEROTROPHY

Chapter V is divided into two parts following the two main sections of this thesis: i) understanding the metabolic constraints of retroviral vector production and ii) use the gathered knowledge for rational gene engineering. Therefore, Chapter V – part A comprises transcriptome analysis of serum deprivation and Chapter V – part B focuses metabolic engineering of lipid biosynthesis.

Both parts will be combined to be published as:

Reversion of serum heterotrophy in retrovirus replicating cells:

Reactivation of cholesterol biosynthesis

Ana F. Rodrigues, Ana S. Formas-Oliveira, Paula M. Alves, Wei-Shou Hu,

Ana S. Coroadinha, *(in preparation)*

Abstract

The need of animal blood sera to support infectious vector titers has challenged retroviral vector production in HEK 293 derived cells. Lipid starvation under reduced serum conditions was demonstrated to be a main cause for the loss of infectious vector titers while the ability to reactivate lipid biosynthesis, particularly cholesterol, was shown to allow the reversion of serum heterotrophy phenotype. Yet, HEK 293 derived retroviral vector producer cells seem to have this pathway impaired, unable to rescue cholesterol biosynthesis in response to the removal of the external lipid supply.

In the first part of this work (refer to chapter V Part A), we aimed at understanding the metabolic impairments underlying lipid heterotrophy of 293 FLEX retroviral vector producer cells. Transcriptional profiling identified three potential bottlenecks in the pathway of *de novo* cholesterol biosynthesis: mevalonate kinase (MVK), lanosterol synthase (LSS) and sterol regulatory element binding factor 2 (SREBF2).

In the second part of this work, these targets were over-expressed in 293 FLEX in an attempt to reactivate cholesterol biosynthesis and revert serum heterotrophy. When individually over-expressing MVK and LSS, serum heterotrophy was mildly alleviated. When in combination, it was totally reverted. The over-expression SREBF2 alone, not only promoted the complete reversion of serum heterotrophy, as it resulted in higher infectious titers than those of standard serum supplementation conditions.

The work herein described focuses the tailored design of retroviral vector producer cells in the pursuit of a serum-independent phenotype based on educated guesses driven by functional genomics studies. The results also represent, to the best of our knowledge, the first metabolic engineering manipulation of cholesterolgenesis in mammalian cell culture.

Contents

1. Introduction.....	134
2. Materials and methods	134
2.1. Cell lines and culture conditions	134
2.2. Cell growth and viral production studies	135
2.3. Plasmids for lipid gene expression and lentiviral vector production	135
2.4. Cell transduction with lipid genes lentiviral vector	136
2.5. Titration of infectious particles	136
3. Results	137
3.1. Over-expression of cholesterol biosynthesis genes reverts serum heterotrophy	137
4. Discussion.....	139
5. Author contribution.....	141
6. References.....	141

1. Introduction

The need of animal blood sera to support infectious vector titers has challenged retroviral vector production in HEK 293 derived cells. Lipid starvation under reduced serum conditions was shown as a main cause for this problem (Rodrigues et al. 2009). The ability to reactivate lipid biosynthesis, particularly cholesterol, allows the reversion of serum heterotrophy. Yet, HEK 293 derived retroviral vector producer cells seem to have this pathway impaired, unable to rescue cholesterol biosynthesis in response to the removal of the external lipid supply (Rodrigues et al. 2012).

In the first part of this work, transcriptome analysis was used to identify the lipid biosynthesis bottlenecks underlying serum heterotrophy in 293 FLEX retroviral vector producer cells. Mevalonate kinase (MVK) and lanosterol synthase (LSS) were identified as the potential blocking points in the pathway of *de novo* cholesterol biosynthesis. The poor expression of cholesterol biosynthesis transcription factor – sterol regulatory element binding factor 2 (SREBF2) – was also hypothesized to contribute to this impairment. Therefore, in the second part of this work, MVK, LSS and SREBP2 were over-expressed in 293 FLEX in an attempt to reactivate cholesterol biosynthesis and revert serum heterotrophy.

2. Materials and methods

2.1. Cell lines and culture conditions

293 FLEX S11 were used for gene engineering of lipid metabolism. These cells derive from 293 FLEX 18 (Coroadinha et al. 2006) by recombinase mediated cassette exchange as described in Chapter VII. In these cells, the original LacZ transgene was exchanged by a fusion of LacZ with S11 fragment of the split-GFP® SandiaBiotech (Albuquerque, NM, U.S.A). The cells were maintained in Advanced Dulbecco's modified Eagle's medium, DMEM (Gibco, Paisley, UK), with 25 mM of glucose, supplemented with 10% (v/v) Foetal Bovine Serum (FBS) (Gibco) and 4 mM of

glutamine (Gibco). The final concentration of FBS was changed for the different studies of retroviral vector production.

HEK 293T (ATCC CRL-11268) is a HEK 293 derived cell line expressing large T antigen from SV40 (simian vacuolating virus 40) and was used to transiently produce the lentiviral vectors for lipid gene delivery. Te 671 is a human rhabdomyosarcoma derived cell line (ATCC CCL-136) used to titrate infectious retroviral particles by LacZ staining. Te 671 S10 is a Te 671 derived cell line stably expressing the S10 fragment of the split-GFP® (SandiaBiotech) established as described in Chapter VII, used to titrate lipid gene lentiviral vector stocks. HEK 293T, Te 671 and Te 671 S10 cells were maintained in DMEM (Gibco, Paisley, UK), with 25 mM of glucose and 4mM of glutamine, supplemented with 10% (v/v) (FBS) (Gibco). All cell lines were maintained in an incubator with a humidified atmosphere of 92% air and 8% CO₂ at 37 °C.

2.2. Cell growth and viral production studies

293 FLEX S11 engineered for the over-expression of lipid metabolism genes were analyzed for cell growth and vector production using a 48+24 hours production/harvesting operation mode described in Chapter II (Rodrigues et al. 2013). Final FBS concentrations were 10% (v/v), or the corresponding reduced serum conditions: 0.5% (v/v) for Te Fly Ga 18 and 1% (v/v) for 293 FLEX 18 (and S11).

2.3. Plasmids for lipid gene expression and lentiviral vector production

Mevalonate kinase (MVK), lanosterol synthase (LSS), sterol regulatory element binding factor 1 and 2 (SREBF1 and 2) cDNAs were acquired through DNASU Plasmid Repository (Biodesign Institute, Arizona State University) and cloned into a lentiviral backbone (*pRRLSIN LacZS11*, refer to Chapter VII), after removal of the LacZ as described in Chapter VII. S11 fragment was maintained for titer determination. A mock vector was obtained by re-ligating the lentiviral backbone after LacZ removal.

For lentiviral transient production the third generation lentiviral packaging system and the transfection procedure described in Dull et al. (1998) were used. Viral vector supernatants were filtered through 0.45 µm cellulose acetate filter for clarification, aliquoted and stored at -85°C until further use.

2.4. Cell transduction with lipid genes lentiviral vector

Lipid genes were delivered by lentiviral vector infection of 293 FLEX S11. The cells were seeded at a density of 4×10^4 cells/cm² 24 hours before infection in 6-well plates. Transduction was performed by removing the cell supernatant and infecting with 2 mL of viral suspension using the appropriate dilution to achieve multiplicities of infection (infectious particles *per* cell) of 1, 3 and 5. Dilutions were made in fresh DMEM (Gibco) with 10% (v/v) FBS (Gibco) and 8 µg/mL of polybrene (Sigma). Cells were incubated at 37°C overnight after which medium was exchanged. Two days after infection, cells were amplified to 75 cm² t-flasks in Advanced DMEM (Gibco) with 1% (v/v) FBS and re-passaged 3-4 days after. At this point, part of the cells was frozen and the other part was seeded to assess infectious particles production of transduced populations (section 2.2).

2.5. Titration of infectious particles

For LacZ based staining titration, infectious procedure and viral titer determination were performed by limiting dilution infection assay, as previously described in chapter III (Rodrigues et al. 2009). Lipid-gene delivery lentiviral vector, were titrated by GFP transcomplementation in Te 671 S10 target cells as described in Chapter VII.

3. Results

3.1. Over-expression of cholesterol biosynthesis genes reverts serum heterotrophy

The over-expression of mevalonate kinase (MVK), lanosterol synthase (LSS) and sterol regulatory element binding factor 2 (SREBF2) was conducted in our recently established 293 FLEX S11 (please refer to Chapter VII for cell line establishment details). This cell line derives from 293 FLEX 18, for which ^{13}C -NMR lipid biosynthesis (Chapter IV) and transcriptome analyses were conducted (Chapters II and V.a), by recombinase mediated cassette exchange. In these cells, the original LacZ transgene was exchanged by a fusion of LacZ with the S11 fragment of the split-GFP (Cabantous et al. 2005). As described in Chapter VII, these cells are suited to be used with the single step cloning-titration method for fast identification of high-producing phenotypes. Therefore, these were chosen for genetic manipulation since the resulting population can be further screened for high-titer clones under reduced serum conditions.

The genes from lipid biosynthesis pathways were delivered through lentiviral vector infection at increasing multiplicities of infection (MOI). Infectious vector titers of the transduced populations under reduced serum conditions were evaluated; as a control, non-transduced cells were also analyzed both under 10% and 1% (v/v) serum supplementation (Fig. 1). MVK transduced cells exhibited titer increase responsive to the MOI, although not able to achieve titers similar to those of 10% FBS. LSS transduced cells also partially recovered infectious vector titers but did not exhibit this MOI responsiveness. However, by conjugating MVK and LSS over-expression infectious particles titers were recovered to levels identical to those of 10% (v/v) FBS (Fig.1A). More impressively, SREBF2 over-expression allowed for achieving the same performances and also to exceed the titers obtained with 10% (v/v) FBS. The over-expression of SREBF1 did not result in titer increases.

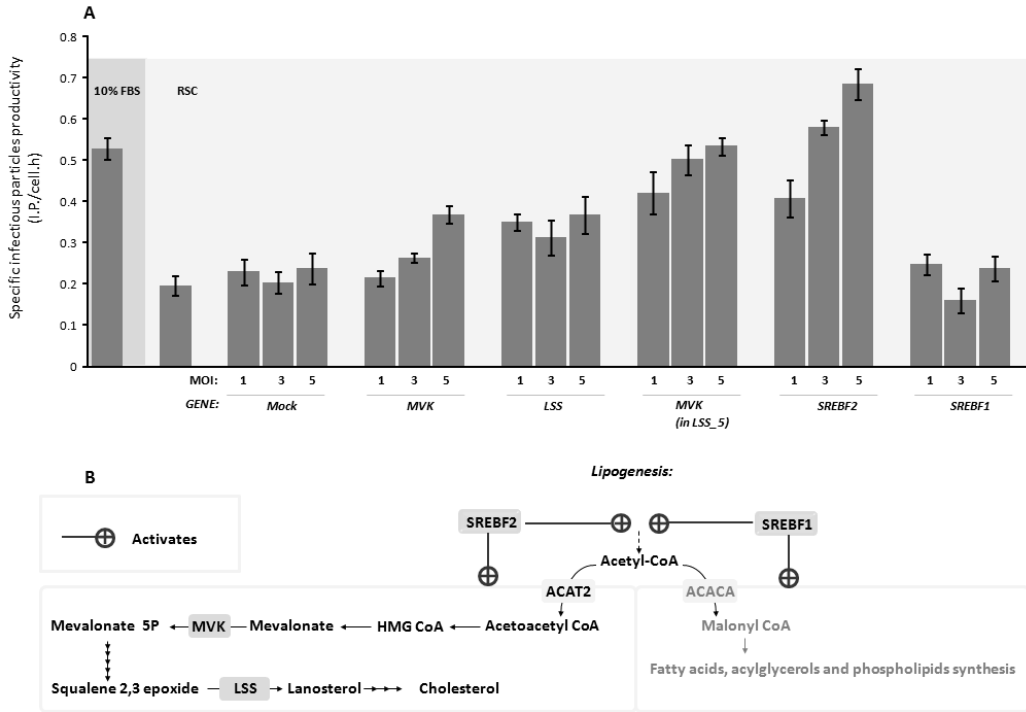


Figure 1 – Over-expression of cholesterol biosynthesis enzymes reverts serum heterotrophy in 293 FLEX retroviral vector producer cells. Specific productivity of infectious particles titer of 293 FLEX S11 under serum deprivation manipulated for the over-expression of cholesterol biosynthesis genes **(A)**. Specific productivities were calculated based on infectious particles titers after 48 hours culture at 1% (v/v) FBS. 10% (v/v) FBS is shown as a control. Values are shown as average ± standard deviation (n=3). 293 FLEX S11 were transduced with lentiviral vector carrying the lipid gene at increasing multiplicities of infection (MOI). The mock control corresponds to the same lentiviral backbone without the lipid gene, as described in Materials and methods. Schematic representation of lipogenesis from acetyl-Coa **(B)**, featuring cholesterol biosynthesis on the left side, fatty acid/phospholipid biosynthesis on the right side and the transcriptional control exerted by sterol regulatory element binding factors. ACACA: acetyl-Coenzyme A carboxylase alpha; ACAT2: acetyl-Coenzyme A acetyltransferase 2; LSS: lanosterol synthase; MVK: mevalonate kinase; SREBF 1 and 2: sterol regulatory element binding factor 1 and 2.

4. Discussion

In the first part of this work, we conducted transcriptome analysis to identify the bottlenecks in cholesterolgenesis of 293 FLEX retroviral vector producer cells (Chapter V.a). Mevalonate kinase (MVK), lanosterol synthase (LSS) and sterol regulatory element binding factor 2 (SREBF2) were identified as potential targets to reactivate *de novo* cholesterol biosynthesis.

In the second part of this work, these targets were over-expressed aiming at reverting serum heterotrophy (Fig. 1). One of the first evidences in the results from Figure 1 was the decrease in infectious particles titer to be smaller between 10% serum and reduced serum conditions than previously found in Chapter III (Rodrigues et al. 2009). Although this might indicate increased robustness of 293 FLEX S11 to serum deprivation – relatively to 293 FLEX 18 – it is more likely to be related to the short culture period used in this assays (48 hours). In fact, when analyzing viral production kinetics during a growth curve we observe that, in the first 48 hours, the differences in infectious particles titers between standard and reduced serum conditions does not exceed 3-fold (Chapter III).

When individually over-expressing MVK and LSS, serum heterotrophy was mildly alleviated. When combined, it was totally reverted (Fig. 1A). The over-expression SREBF2 alone not only promoted the complete reversion of serum heterotrophy but resulted in higher infectious titers than those of standard serum supplementation conditions. SREBF2 is expressed in response to cholesterol-depletion conditions activating the whole cholesterol biosynthesis machinery (Weber et al. 2004). This orchestrated and upstreamly regulated effect might explain not only the total reversion of serum heterotrophy but also the additional titer improvements relatively to MVK/LSS combined over-expression and even 10% FBS conditions (Fig. 1A). In fact, SREBP2 over-expression induces all enzymes of the cholesterol biosynthetic pathway (Sakakura et al. 2001), most notably the mRNA for HMG

Coenzyme A reductase (HMGCR), which may increase as many as 75-fold (Horton et al. 1998).

Reversion of serum heterotrophy was confirmed to be cholesterolgenesis-specific since the over-expression of sterol regulatory binding factor 1 (SBRF1), more related to fatty-acid biosynthesis (Eberle et al. 2004), had no effect neither on viral productivity nor in the capability of reverting serum heterotrophy (Fig. 1A and B).

In the follow-up of this work, manipulated cells will be analyzed for gene expression to evaluate the effects of these over-expressions in the whole cholesterol biosynthetic pathway. Lipid biosynthesis, in particular, cholesterolgenesis, will also be evaluated. Taking advantage of the S11 fusion transgene, manipulated cells will be subjected to the single step cloning-titration method (see Chapter VII), conducted under serum deprivation conditions to isolate serum-independent high-titer clones. These clones should be challenged for vector production using serum-free media formulations.

The work herein described focuses the tailored design of retroviral vector producer cells in the pursuit of a serum-independent phenotype based on educated guesses driven by functional genomics studies. By opposite to a more traditional trial-and-error approach, our results engage a Systems Biology concept on a global understanding of the biological players and their network integration to rationally design a phenotype. They also represent, to the best of our knowledge, the first gene-based metabolic engineering manipulation of cholesterolgenesis in mammalian cell culture.

5. Author contribution

Ana Filipa A. F. Rodrigues participated on the experimental setup and design, performed part of the experiments, analyzed the data and wrote the chapter.

6. References

- Broussau S, Jabbour N, Lachapelle G, Durocher Y, Tom R, Transfiguracion J, Gilbert R, Massie B. 2008. Inducible packaging cells for large-scale production of lentiviral vectors in serum-free suspension culture. *Mol Ther* 16(3):500-7.
- Cabantous S, Terwilliger TC, Waldo GS. 2005. Protein tagging and detection with engineered self-assembling fragments of green fluorescent protein. *Nat Biotechnol* 23(1):102-7.
- Coroadinha AS, Schucht R, Gama-Norton L, Wirth D, Hauser H, Carrondo MJ. 2006. The use of recombinase mediated cassette exchange in retroviral vector producer cell lines: predictability and efficiency by transgene exchange. *J Biotechnol* 124(2):457-68.
- Dull T, Zufferey R, Kelly M, Mandel RJ, Nguyen M, Trono D, Naldini L. 1998. A third-generation lentivirus vector with a conditional packaging system. *J Virol* 72(11):8463-71.
- Eberle D, Hegarty B, Bossard P, Ferre P, Foufelle F. 2004. SREBP transcription factors: master regulators of lipid homeostasis. *Biochimie* 86(11):839-48.
- Esterbauer H, Schaur RJ, Zollner H. 1991. Chemistry and biochemistry of 4-hydroxynonenal, malonaldehyde and related aldehydes. *Free Radic Biol Med* 11(1):81-128.
- Ghani K, Cottin S, Kamen A, Caruso M. 2007. Generation of a high-titer packaging cell line for the production of retroviral vectors in suspension and serum-free media. *Gene Ther* 14(24):1705-11.
- Horton JD, Shimomura I, Brown MS, Hammer RE, Goldstein JL, Shimano H. 1998. Activation of cholesterol synthesis in preference to fatty acid synthesis in liver and adipose tissue of transgenic mice overproducing sterol regulatory element-binding protein-2. *J Clin Invest* 101(11):2331-9.
- Rodrigues AF, Amaral AI, Verissimo V, Alves PM, Coroadinha AS. 2012. Adaptation of retrovirus producer cells to serum deprivation: Implications in lipid biosynthesis and vector production. *Biotechnol Bioeng* 109(5):1269-79.
- Rodrigues AF, Carmo M, Alves PM, Coroadinha AS. 2009. Retroviral vector production under serum deprivation: The role of lipids. *Biotechnol Bioeng* 104(6):1171-81.
- Rodrigues AF, Formas-Oliveiras AS, Bandeira VS, Alves PM, Hu WS, Coroadinha AS. 2013. Metabolic pathways recruited in the production of a recombinant enveloped virus: mining targets for process and cell engineering. *Metab. Eng. Nov* (20):131-145 .
- Sakakura Y, Shimano H, Sone H, Takahashi A, Inoue N, Toyoshima H, Suzuki S, Yamada N. 2001. Sterol regulatory element-binding proteins induce an entire pathway of cholesterol synthesis. *Biochem Biophys Res Commun* 286(1):176-83.
- Schucht R, Coroadinha AS, Zanta-Boussif MA, Verhoeven E, Carrondo MJ, Hauser H, Wirth D. 2006. A new generation of retroviral producer cells: predictable and stable virus production by Flp-mediated site-specific integration of retroviral vectors. *Mol Ther* 14(2):285-92.
- Weber LW, Boll M, Stampfl A. 2004. Maintaining cholesterol homeostasis: sterol regulatory element-binding proteins. *World J Gastroenterol* 10(21):3081-7.

Chapter VI

ON THE DOWN-REGULATION OF THE WARBURG EFFECT IN RETROVIRUS REPLICATING CELLS: *BEYOND THE LACTOGENIC PHENOTYPE*

This chapter is based on data to be published as:

**On the down-regulation of the Warburg effect in retrovirus replicating
cells: beyond the lactogenic phenotype**

Ana F. Rodrigues, Miguel R. Guerreiro, Ana S. Formas-Oliveira, Paulo Fernandes, Anne-K. Blechert, Yvonne Genzel, Paula M. Alves, Wei-Shou Hu, Ana S. Coroadinha, *(in preparation)*

Abstract

Many cultured mammalian cell lines used in research and biopharmaceuticals manufacture exhibit a Warburg effect phenotype with enhanced glycolytic fluxes predominantly channeled to lactate formation, which reduces culture viability and can also affect product quality. In this work, we conducted a proof-of-concept metabolic engineering study in HEK 293 derived retroviral vector producer cells, based on the down-regulation of two key molecular effectors of the Warburg effect-like lactogenic phenotype: hypoxia inducible factor 1 (HIF1) and pyruvate dehydrogenase kinase (PDK). This strategy would simultaneously tackle reduced lactate accumulation and enhanced channeling of the glycolytic intermediates into the tricarboxylic acids cycle.

For single gene manipulation, (HIF1 or PDK), clones producing, on average, 20-fold higher titers of infectious particles were isolated. Without substantial differences in glucose consumption, lactate production was diminished up to 4-fold, indicating the channeling of the consumed glucose into non-lactogenic routes. The physiological fingerprints associated to high-titer HIF1 down-regulated clones indicated significant recruitment of metabolic pathways related to virus production such as biological amines metabolism, detoxification routes – including glutathione metabolism – and pentose phosphate pathway. High titer clones also presented substantial transcriptional increases of viral components. However, this could only be translated into increased vector titers when conjugated with the improved metabolic status arising from these manipulations. The results herein presented demonstrate the down-regulation of the Warburg effect phenotype as a successful approach to improve the productivity performance of a mammalian cell line producing a highly complex and lactate-sensitive bioproduct, potentially extendable to other cell and/or products. They additionally unveiled the importance of secondary pathways affected in the Warburg effect which can further be explored towards an *improved metabolic status beyond the lactogenic phenotype*.

Contents

1. Introduction.....	146
2. Materials and methods	148
2.1. Cell lines and culture media	148
2.2. Plasmids and shRNA sequences	148
2.3. Cell growth and viral production studies	150
2.4. Titration of infectious and total particles.....	150
2.5. Cell transduction and selection.....	150
2.6. Measurement of central carbon enzymes activity.....	151
2.7. Metabolite profiling.....	151
2.8. RNA extraction and RT-PCR.....	151
2.9. Amplification, labelling and BeadChip hybridization of RNA samples .	152
2.9. Microarray data processing and analysis	152
3. Results	153
3.1. Down-regulation of HIF1	153
3.2. Downstream effects of HIF1 down-regulation in high-titer clones.....	158
Transcriptional profiling pathway analysis.....	158
Central carbon enzymes activity	160
3.3. Down-regulation of PDK.....	161
3.4. Double HIF1 – PDK1/3 down-regulation	165
3.5 Impact of shHIF1 and shPDK1/3 in viral batch quality	168
4. Discussion	170
5. Author contribution.....	174
6. References	175

1. Introduction

Many cultured mammalian cell lines exhibit a Warburg effect-like lactogenic phenotype with enhanced glycolytic fluxes and high lactate formation. However, this phenotype is typically not ascribed to a hypoxic environment, as originally described by Otto Warburg for cancer cells, but to a set of genetic transformations underlying cell immortalization – induced or spontaneous – and adaptation to the *in vitro* culture (Kondoh 2008). The over-expression of hypoxia inducible factor 1 (HIF1) is a major hallmark and inducer of those transformations (Fig. 1).

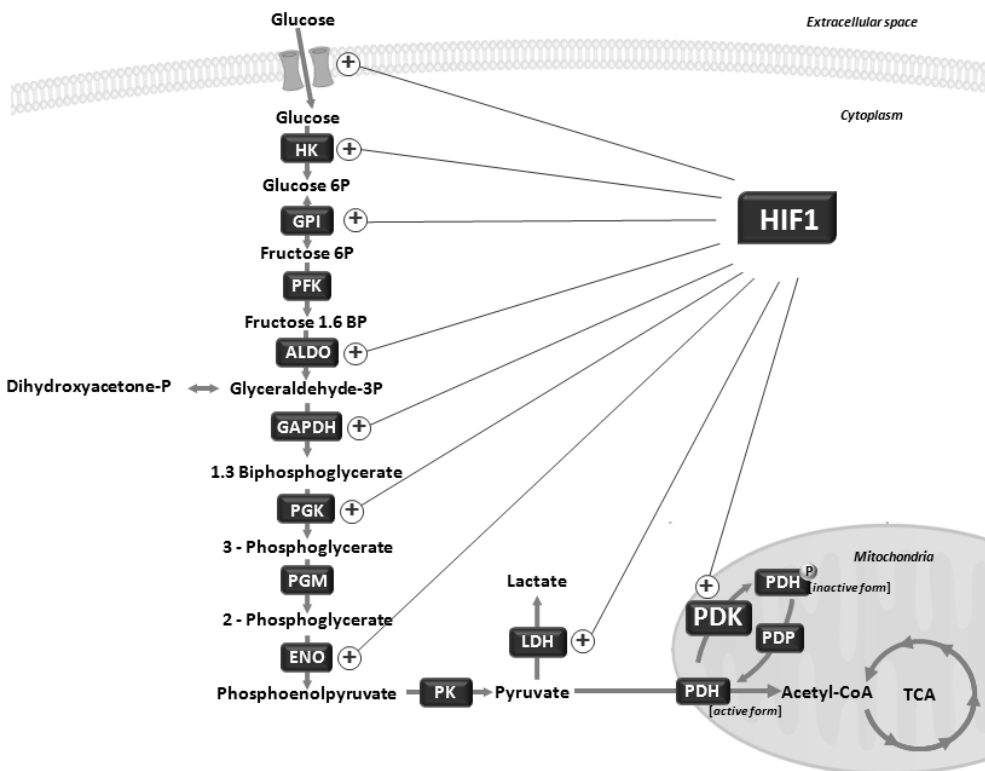


Figure 1 – The Warburg effect-like lactogenic phenotype. HIF1 transcriptionally activates several glycolytic enzymes, lactate dehydrogenase (LDH) and pyruvate dehydrogenase kinase (PDK). The latter inactivates pyruvate dehydrogenase complex (PDH) by phosphorylation, blocking the entrance of pyruvate into the TCA at the level of acetyl-CoA which, combined with the enhanced expression of LDH, increases the glycolytic flux towards lactate. Adapted from Kondoh (2008). ALDO: aldolase; LDH: lactate dehydrogenase; ENO: enolase; GAPDH: glyceraldehyde-3-phosphate dehydrogenase; GPI: glucose phosphate isomerase; HIF1: hypoxia inducible factor 1; HK: hexokinase; PDH: pyruvate dehydrogenase; PDK: pyruvate dehydrogenase kinase; PDP: pyruvate dehydrogenase phosphatase; PGM: phosphoglycerate mutase; PGK: phosphoglycerate kinase; PK: pyruvate kinase; PFK: phosphofruktokinase.

While the Warburg effect-like lactogenic phenotype in cultured mammalian cell lines seems to offer a proliferative advantage for *in vitro* cell survival (Shlomi et al. 2011), it is undesirable from the biotechnology view-point as the accumulation of lactate reduces culture viability (Lao and Toth 1997; Ozturk et al. 1992) and can also impact product quality (Chee Fung Wong et al. 2005).

Reducing lactate production in mammalian cell lines producing recombinant biopharmaceuticals has been a major goal of cell culturists. To this end, the majority of the approaches has focused on: i) using carbon sources alternative to glucose, with or without over-expressing the respective transporters (Jimenez et al. 2011; Wlaschin and Hu 2007); ii) over-expressing anaplerotic enzymes by-passing the entrance of pyruvate into the TCA via pyruvate dehydrogenase (Elias et al. 2003; Irani et al. 2002) or iii) down-regulating LDHA (Kim and Lee 2007). In this work, we conducted a proof-of-concept metabolic engineering study based on the down-regulation of two key molecular effectors of the Warburg effect: hypoxia inducible factor 1 (HIF1) and pyruvate dehydrogenase kinase (PDK), simultaneously targeting reduced lactate accumulation and enhanced channeling of the glycolytic intermediates into the tricarboxylic acid cycle (TCA). These are widely described upstream effectors of the Warburg effect-like lactogenic phenotype in cultured mammalian cell lines although no attempts, up to date, have been conducted in the view of their combined down-regulation. Down-regulating pyruvate dehydrogenase kinase has been reported for CHO cells producing recombinant monoclonal antibody (Zhou et al. 2011b).

The study herein presented was conducted using retroviral vector producer cells since these particles are particularly sensitive to high lactate concentrations (McTaggart and Al-Rubeai 2000; Merten et al. 2001). Also, using alternative carbon sources steering a reduced lactogenic phenotype has previously been shown to improve virus production up to 6-fold (Coroadinha et al. 2006a; Coroadinha et al. 2006b). Identical observations were reported for other complex

biopharmaceuticals, including recombinant protein (Altamirano et al. 2004). Thus, retroviral vector production appeared as a good study model to evaluate the impact of down-regulating the Warburg effect-like lactogenic phenotype in mammalian cells producing complex biopharmaceuticals. Additionally, for the particular case of the producer cells herein used – 293 FLEX – a previous functional genomics study suggested the reduction of the glycolytic metabolism as a potential target to improve viral titers (Rodrigues et al. 2013).

2. Materials and methods

2.1. Cell lines and culture media

293 FLEX GFP is a human embryonic kidney (HEK293, ATCC CRL-1573) derived cell line producing murine leukemia virus (MLV) based vector harboring a GFP reporter gene, pseudotyped with gibbon ape leukemia virus (GaLV) (Coroadinha et al. 2006c). These cells were maintained in Advanced modified Eagle's medium, DMEM, (Gibco, Paisley, UK) with 25 mM of glucose, supplemented with 10% (v/v) Foetal Bovine Serum (FBS) (Gibco) and 4 mM of glutamine (Gibco). Te 671 (ATCC CCL-136) cell line was used as the target cell to titrate infectious retroviral particles and HEK 293T cell line (ATCC CRL-11268) was used for producing and titrating shRNA lentiviral vector stocks. Both were maintained in DMEM (Gibco) with 25 mM of glucose and 4 mM of glutamine supplemented with 10% (v/v) FBS (Gibco). All cells were maintained in an incubator with a humidified atmosphere of 92% air and 8% CO₂ at 37 °C.

2.2. Plasmids and shRNA sequences

Short hairpin (sh) RNA lentiviral vectors based on pLKO.1-puro (Moffat et al. 2006) containing a puromycin resistance gene and targeting sequences on the human HIF1 (shHIF1) gene, PDK1/3 (shPDK1/3) gene and a non-target shRNA (ntshRNA) vector were purchased from Sigma Mission® RNAi (Sigma, St. Louis, MO, USA). shHIF1 hairpin sequence corresponds to the first version of the shRNA library

from The RNAi Consortium (TRC 1) (Broad Institute, Cambridge, MA, USA). The shPDK1/3 hairpin sequences were custom made and designed to target isoform 1 (sequences A and B) and isoform 1 and 3 of the human pyruvate dehydrogenase kinase (sequence C). For sequences C the first 19 nucleotides hybridize with isoform 3 and all the 21 nucleotides hybridize with isoform 1. The sequences were: (A) 5'-CTGTCACCAGCCAGAATGTTCCCTCGAGGAACATTCTGGCTGGTGACAG-3'; (B) 5'-TAGGCGTCTGTGTGATTTGTA CTGAGTACAAATCACACAGACGCCTA-3' and (C) 5'-GTGATTGAATACAAGGAGAGCCTCGAGGCTCTCCTTGTATTCAATCAC-3', in which the first 21 nucleotides constitute the sense sequence, the last 21 nucleotides constitute the anti-sense sequence and the intermediate 6 nucleotides constitute the hairpin loop. All sequences are additionally flanked by 5'-CCGG-3' at the 5' and by 5'-TTTTT-3' at the 3' (for further details on general vector construct please consult [http://www.sigmaaldrich.com/life-science/functional-genomicsandrna/library-information/vector-map.html](http://www.sigmaaldrich.com/life-science/functional-genomicsandrna/shrna/library-information/vector-map.html)). The original custom made plasmids contained a dsRED fluorescence selectable marker additional to the puromycin resistance, which was replaced by mCherry to minimize the cytotoxicity associated to the former (Zhou et al. 2011a). The vector backbone was amplified by PCR to exclude dsRED sequence and mCherry was cloned in its place using In-Fusion® HD Cloning Kit (Clontech Laboratories, Inc., Terra Bella Avenue, CA, USA). The non-target control used was Sigma Mission® RNAi Cat. No SHC002. This vector was used as provided and also modified to introduce mCherry as a second selectable marker, by replacing the original puromycin. In both cases, the second fluorescence selectable markers were conceived to perform double shRNA transduction. Cells transduced with mCherry containing constructions were selected by flow cytometry activated sorting (MoFlo High-Speed Cell Sorter, Dako Cytomation, Glostrup, Denmark). For each of the shRNA, lentiviral vector stocks were produced by transient co-transfection of HEK 293T cells with pSPAX2 and pMD2G (kindly provided by Didier Trono from the Swiss Federal Institute of Technology (EPFL) through Addgene plasmid repository,

Cambridge, MA, USA), providing the packaging and the envelope functions, respectively.

2.3. Cell growth and viral production studies

Two types of virus production studies were performed: a 7-day batch culture for cell growth/virus production kinetics, transcriptome analysis and metabolite profiling and a 48+24 hours production/harvesting operation mode to screen individual clone productivity.

For the 7-day batch culture studies, cells were inoculated at 4×10^4 cells/cm². Two samples were collected *per day*: culture supernatant was harvested, filtered through 0.45 µm for clarification, aliquoted and stored at -85°C until analysis. Cell concentration and viability was determined by the trypan blue exclusion method. At day 3, total RNA was extracted for transcriptome analysis. For further details on the second operation mode, please refer to Chapter II (Rodrigues et al. 2013).

2.4. Titration of infectious and total particles

For titrating infectious retroviral particles Te 671 cells were seeded at 5×10^4 cells/cm² in 24-well plates one day before infection. Cell concentration was determined at the time of infection. Transduction was performed in duplicates by removing the cell supernatant and infecting with 0.2 mL of viral suspension using several dilutions in fresh medium with 10% (v/v) FBS and 8 µg/mL of polybrene (Sigma). Cells were incubated at 37°C overnight after which 0.5 mL medium was added. Two days after infection, cells were harvested and analyzed for GFP fluorescence by flow cytometry (CyFlow-space, Partec GmbH). Physical (total) particles were assessed by Nanoparticle Tracking Analysis using NanoSight® NS500 (NanoSight Ltd., Wiltshire, UK).

2.5. Cell transduction and selection

Short hairpin (shRNA) genes were delivered by lentiviral vector infection of 293 FLEX GFP. The cells were seeded at a density of 1×10^5 cells/cm² 24 hours before

infection in 6-well plates. Transduction was performed by removing the cell supernatant and infecting with 1 mL of viral suspension using the appropriate dilution to achieve multiplicity of infections of approximately 1 infectious particles *per* cell. Dilutions were made in fresh DMEM (Gibco) with 10% (v/v) FBS (Gibco) and 8 µg/mL of polybrene (Sigma). Cells were incubated at 37°C overnight after which medium was exchanged. Two days after infection, the cells were amplified to 75 cm² t-flasks in puromycin containing medium (1.5 µg/mL) and cultured for 21 additional days, exchanging culture medium at each 2-3 days. Selected populations were analyzed as such and also cloned by limiting dilution. For double transduction, an identical procedure was followed, but instead of antibiotic pressure, mCherry expressing cells (clones and population) were isolated by flow cytometry activated sorting (MoFlo High-Speed Cell Sorter, Dako Cytomation, Glostrup, Denmark).

2.6. Measurement of central carbon enzymes activity

The activity of 13 central carbon metabolism enzymes was quantified by an adapted version of the method described by Janke et al. (2010). Briefly, the modifications included: CS: specific assay mix with pH 8; IDH: pH 7.0; incubation time 60 min; FH: pH 7.5; GPT: pH 8.5; incubation time 30 min; GOT: pH 7.5; HK: incubation time 70 min; G6P standards up to 0.4 nmol; G6PD: incubation time 60 min; PFK: pH 8.5; PK: pH 8.0; GPI: pH 8.5; MDH: pH 8.5; PDH: pH 8.0.

2.7. Metabolite profiling

Glucose and lactate concentrations were determined with automated enzymatic assays (YSI 7100 Multiparameter Bioanalytical System, USA). Ammonia was quantified enzymatically using the UV assay kit (NZYTech, Lisbon, Portugal).

2.8. RNA extraction and RT-PCR

Total RNA was extracted using RNeasy Mini Kit (Qiagen, Valencia, CA) according to the manufacturer's instructions. The resultant RNA pellet was eluted in 100 µL of

nuclease-free water (Qiagen) and stored at -85°C until further processing. RNA yields were quantified using NanoDrop 2000 (Thermo Scientific, Waltham, MA, USA) and RNA quality was characterized by the quotient of the 28S to 18S ribosomal RNA electropherogram peak using an Agilent 2100 bioanalyzer and the RNA Nano Chip (Agilent, Santa Clara, CA, USA).

For real time PCR, RPL-22 was chosen as a control gene using as forward primer (F): 5'-CTGCCAATTTTGAGCAGTTT-3' and as reverse primer (R): 5'-CTTTGCTGTTAGCAACTACGC-3'. Forward (F) and reverse (R) primer sequences for viral genes were the following: envelope (F) 5'-GGACCAAAATAGCGAATGGA-3' / (R) 5'-GGTGAAGTGTACGCCTGGAT-3'; gag-pol (F) 5'-GTCCACTATCGCCAGTTGCT-3' / (R) 5'-CTGGGTCCTCAGGGTCATAA-3'; transgene (F) 5'-CAGAAGAACGGCATCAAGGT-3' / (R) 5'-CTGGGTGCTCAGGTAGTGG-3'. The reverse transcription of total RNA and qRT-PCR were performed as described in Rodrigues et al. (2012).

2.9. Amplification, labelling and BeadChip hybridization of RNA samples

RNA extraction, amplification, labelling and BeadChip hybridization were performed as described in Chapter II (Rodrigues et al. 2013). Three biological replicates were used.

2.9. Microarray data processing and analysis

Data was processed by log₂ and variance-stabilizing transformation and quantile normalized as described in Chapter II (Rodrigues et al. 2013). Differentially expressed genes were identified by False Discovery Rate using Significance Analysis of Microarrays (Tusher et al. 2001) and Weighted Average Difference (Kadota et al. 2008) as previously described in Rodrigues et al. (2013). Pathway analysis was performed using Ingenuity Pathway Analysis (IPA) (Ingenuity® Systems, www.ingenuity.com).

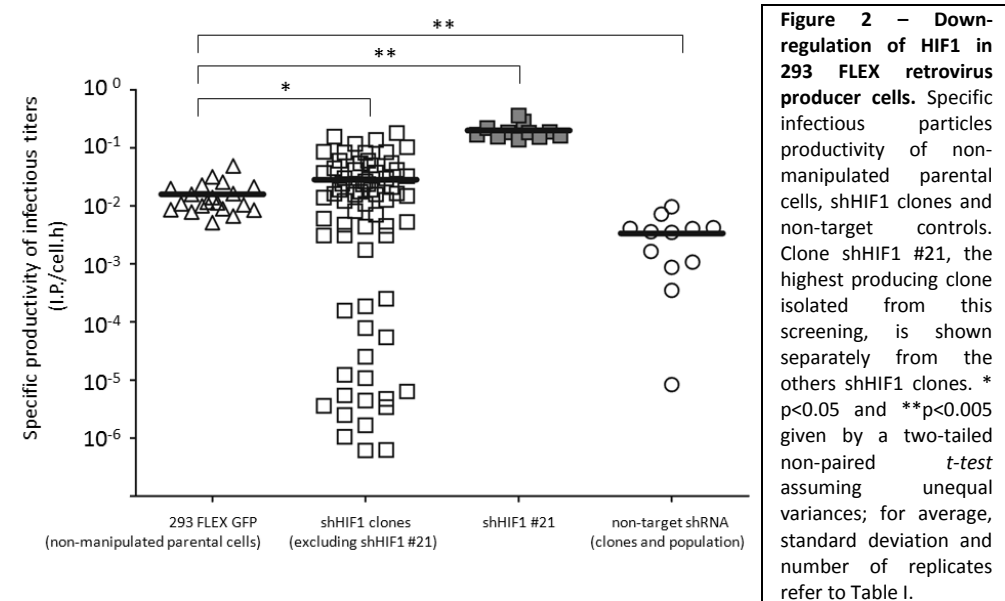
3. Results

3.1. Down-regulation of HIF1

Down regulation of hypoxia inducible factor 1 α -subunit (HIF1) was performed by short-hairpin RNA interference (shRNAi) delivered by lentiviral infection. To minimize extensive activation of the RNAi pathway and/or interferon response (Fish and Kruihof 2004; Rodrigues et al. 2011), low multiplicity of infection (approximately 1) was used. The transduced population was cloned by limiting dilution and more than 80 clones were isolated (Fig. 2).

Many of the HIF1 down-regulated clones presented titer reduction, however, the analysis of the non-target shRNA clones (and population), revealed that this was an off-target effect, probably derived from the activation of the RNA interference pathway (Fig. 2). Notably, non-target shRNA clones and populations consistently delivered titer reductions, while for some shHIF1 clones productivity improvement up to 30-fold, relatively to the parental cells, was observed. The magnitude of titer increase was considerable higher when analyzed comparatively to the non-target control, up to 100-fold. Some of these clones were analyzed for HIF1 gene expression (Fig. 3A). The results showed titer increases in response to HIF1 down-regulation in a pyramid-like layout, in which high-titer clones appear in the upper apex corresponding to gene expression reductions around -2.5-fold. Above and below this value, titers were significantly reduced. Of notice, HIF1 expression in non-transduced cells was relatively low and the maximum down-regulation obtained (-3.1-fold) corresponds to nearly gene knock-out.

Despite the fact that high-titer clones consistently presented down-regulations in the order of -2 to -2.5-fold, other clones with identical extension of HIF1 down-regulation did not demonstrated titer improvements or, in some cases, even presented evident titer reductions.



Therefore, we analyzed the downstream effects of HIF1, particularly, the Warburg effect-like lactogenic phenotype and quantified lactate dehydrogenase A (LDHA) gene expression (Fig. 3B), its impact on the ratio lactate production to glucose consumption (LAC/GLC) (Fig. 3C) and how it correlated with infectious particles titers (Fig. 3D).

LDH expression correlated with HIF1 down-regulation, although some clones presented an outlier behaviour (Fig. 3B). Moreover, all shHIF1 clones presented LAC/GLC ratios lower than those of non-manipulated cells, clearly showing that HIF1 down-regulation diminishes the lactogenic phenotype (Fig. 3C). This output was based on reduced lactate production (20% less, Table I) rather than in less glucose consumption, evidencing the channelling of the consumed glucose into non-lactogenic routes. Increased oxygen consumption supported part of this channelling to be directed into the TCA cycle (data not shown). By opposite, non-target controls clearly presented enhanced glucose consumption and slightly increased LAC/GLC ratios. Interestingly, even for the same clone (shHIF1 #21), the ratio LAC/GLC was found to vary from 1.2 to 1.5. This variation might be related to the oscillatory

expression behaviour of shRNAs during cell growth that we have previously reported (Rodrigues et al, 2011).

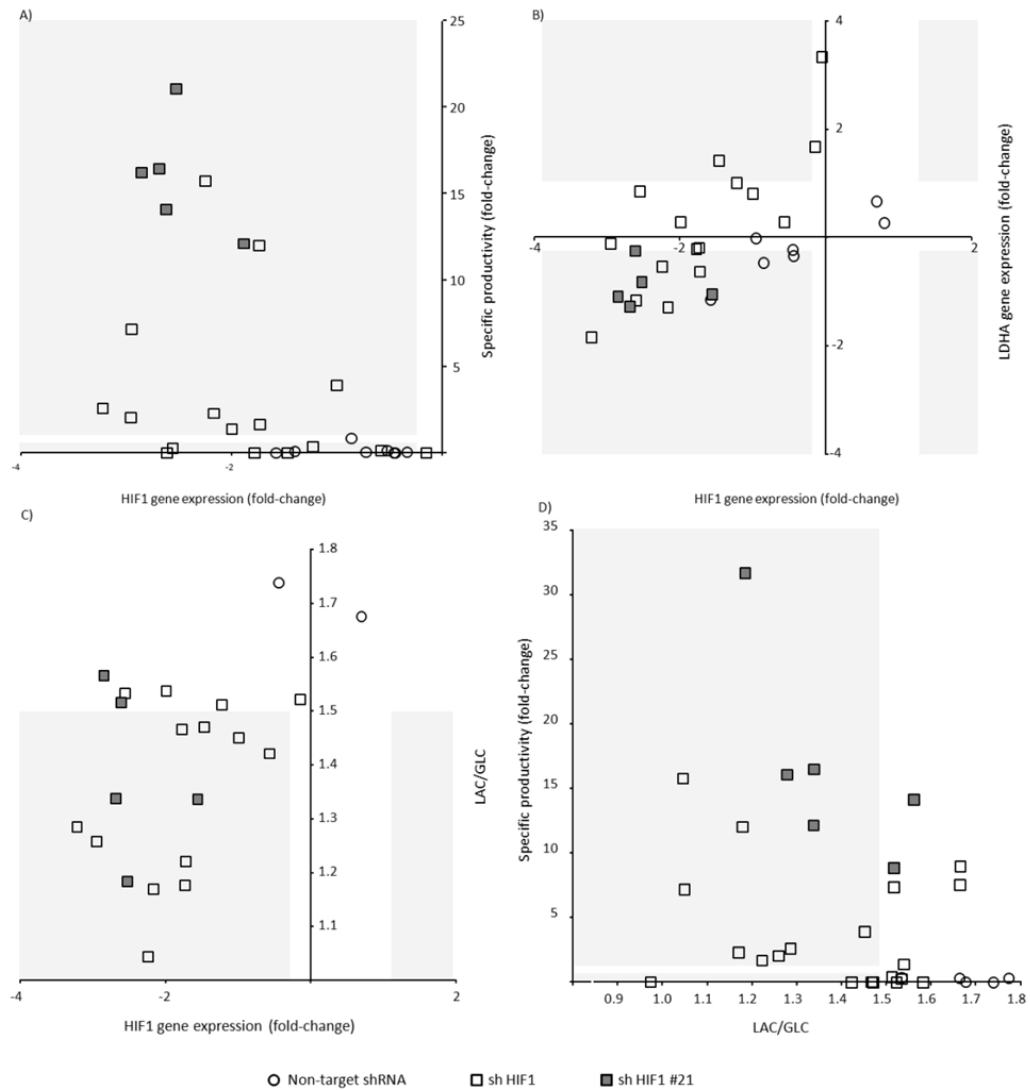
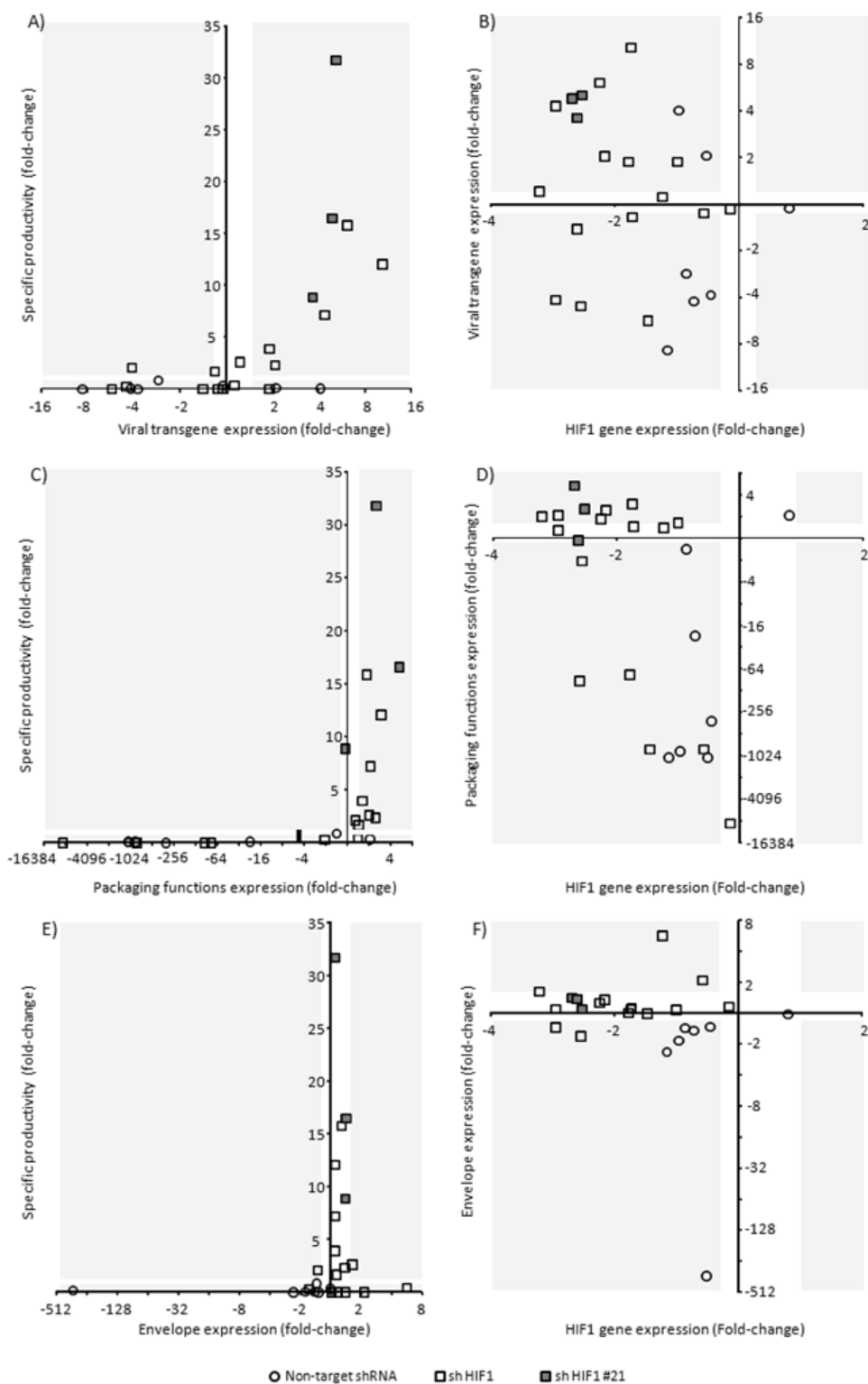


Figure 3 – Virus productivity and lactogenic phenotype in response to HIF1 down-regulation. Specific productivity of infectious retroviral particles (A), lactate dehydrogenase A (LDHA) gene expression (B) and ratio lactate production to glucose consumption (LAC/GLC) (C) of HIF1 down-regulated clones and non-target controls vs. HIF1 gene expression. Values are shown as fold-change relatively to (average) non-manipulated cells. Specific infectious particles productivity vs. ratio lactate production to glucose consumption (LAC/GLC) (D). For all (A) – (D) grey shadowed area represents values outside the range “average \pm standard deviation” of the controls (refer to Table I for further details). Gene expression represents average expression level normalized to the RPL22 housekeeping control and relatively to non-manipulated cells ($2^{\Delta\Delta CT}$) (n=3).

Some of the shHIF1 clones, although presenting substantial HIF1 down-regulation and significant LAC/GLC reduction, saw their specific productivity drastically diminished. Thereby, the clones were analyzed for viral components expression (Fig. 4). The results showed that the viral transgene (Fig. 4A and B) and, to less extent, the gag-pol (Fig. 4C and D) suffered substantial expression changes. The envelope remained relatively unaltered (Fig. 4E and F). These changes, however, did not correlate with HIF1 gene expression (Fig. 4B, D and F). The changes in viral transgene presented some correlation with vector titers (Fig. 4A). Even some of the non-target controls presented increased transgene expression (Fig. 4A and B). Expectably, all clones with substantial decrease of viral components, whether it was the viral transgene, the gag-pol or the envelope, saw the infectious vector titers drastically reduced. Therefore, titer reduction both for shHIF1 and non-target shRNA cells was unequivocally related to viral components loss of expression.

Figure 4 – Vector components expression in shHIF1 cells. Specific productivity of infectious retroviral particles of shHIF1 clones and non-target controls vs. viral transgene (A), gag-pol (C) and envelope (E) gene expression. Viral transgene (B), gag-pol (D) and envelope (F) gene expression vs. HIF1 gene expression. For all (A) – (F) grey shadowed area represents values outside the range of “average \pm the standard deviation” of the controls (please refer to Table I for further details). Gene expression represents average expression level normalized to the RPL22 housekeeping control and relatively to non-manipulated cells ($2^{\Delta\Delta CT}$) (n=3). →



3.2. Downstream effects of HIF1 down-regulation in high-titer clones

Transcriptional profiling pathway analysis

Among HIF1 down-regulated clones, shHIF1 #21 consistently delivered titer improvements of more than one order of magnitude. Therefore, this clone was subjected to a whole-genome transcriptome analysis in an attempt to identify the biological pathways recruited in this high-titer phenotype. Clone shHIF1 #64, also delivering high-titers, the parental non-manipulated and the non-target control cells were also analyzed. Figure 5 shows significantly enriched metabolic pathways given by Ingenuity Pathway Analysis of differentially expressed genes. For all the cells, pathways such as amino acid catabolism, fatty acid oxidation and cholesterol biosynthesis appear extensively enriched, suggesting these to be pathways changing in response to any short hairpin expression, most probably, to the activation of RNA interference pathway. For the case of amino acid catabolism, gene expression patterns suggested increased activity of these pathways, while for fatty acid oxidation and cholesterol biosynthesis, indicated pathway inhibition. Pathways specifically associated to shHIF1 clones were the inhibition of biological amines catabolism, increased detoxification metabolism – including thioredoxin pathway, ascorbate recycling and glutathione redox reactions – increased pentose phosphate pathway, TCA cycle, acetyl-CoA biosynthesis by pyruvate dehydrogenase complex (PDH), and dolichyl-diphosphooligosaccharide biosynthesis. Some aspects of nucleotides/nucleosides metabolism appeared also as specific of shHIF1 clones.

We additionally found the transcriptional neighbouring of the “glucose 6P ↔ fructose 6P” reaction to be changing substantially (Fig. 6). Given the reversibility of this reaction, the analysis of gene expression patterns suggested a reduced draining of fructose 6P to downstream routes, favouring those fed by glucose 6P: pentose phosphate pathway and those using glucose 1P.

Glycolysis activation was exclusive of non-target cells, supporting the enhanced glucose consumption rates observed for these cells (Table I).

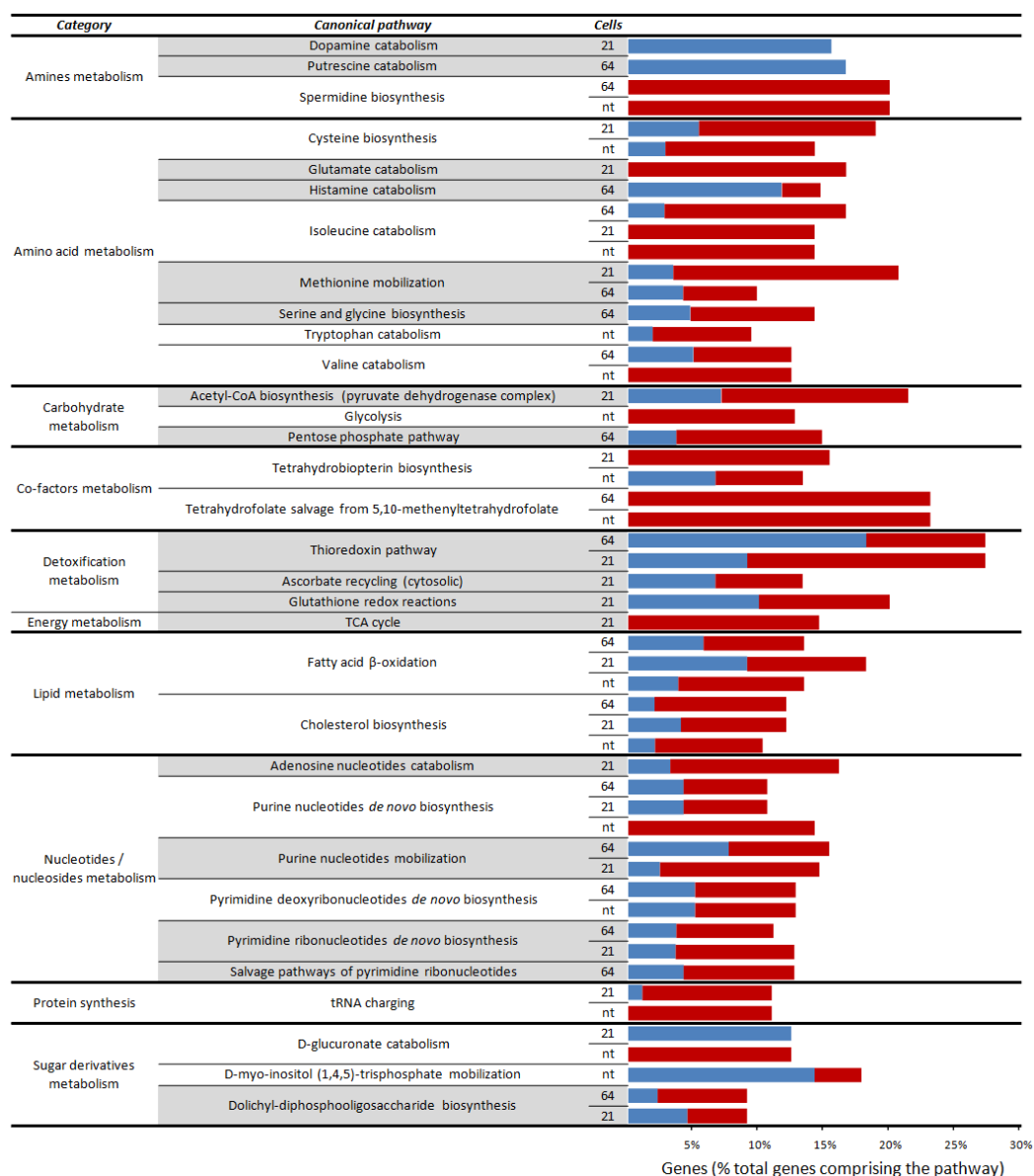


Figure 5 – Enriched metabolic pathways in shHIF1 and non-target shRNA cells. Significantly enriched pathways ($p < 0.05$) given by Ingenuity Pathway Analysis of WAD filtered data and percentage of differentially expressed genes enriching such pathways. Up-regulated genes are indicated in red and down-regulated genes in blue. Note that up-regulated (or down-regulated) genes do not necessarily imply pathway activation (or inhibition): for example, down-regulation of inhibitory genes should lead to pathway activation. Grey shadowed pathways indicate enriched pathways exclusive of shHIF1 clones. For shHIF1, the clones #21 and #64 were analyzed whereas the non-target shRNA corresponds to the cell population. For further details on data filtering for pathway analysis and WAD algorithm please refer to Chapter II (Rodrigues et al, 2013).

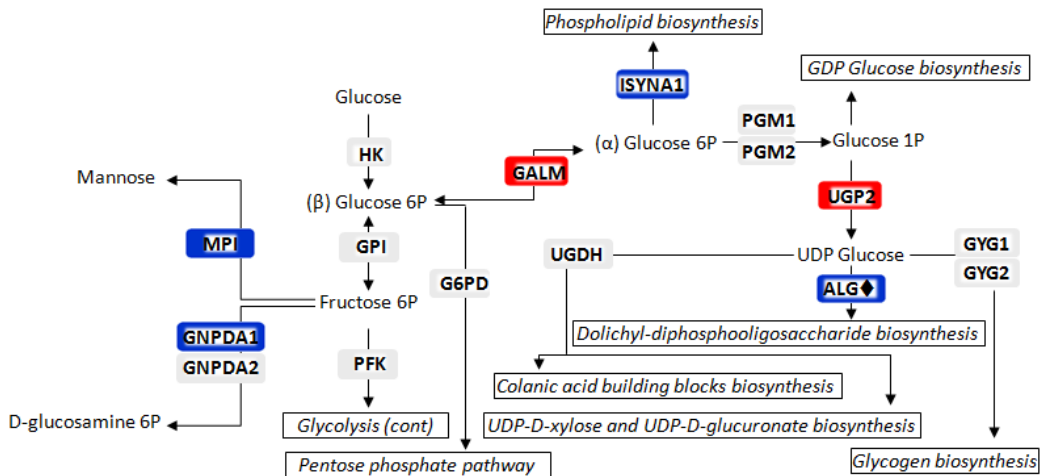


Figure 6 – Schematic representation of significant transcriptional changes of metabolic pathways from glucose/fructose 6P. Each arrow represents a single reaction; reversibility is indicated by a two-arrow line according to the BioCyc database (Caspi et al. 2010). For a matter of simplicity, only the main metabolites are shown; thus, the reactions are not necessarily balanced. Changes are shown for the analysis shHIF1 vs. parentals and were considered significant for $q < 10\%$ based on the False Discovery Rate given by Significance Analysis of Microarrays (SAM) (Tusher et al. 2001). Only gene changes occurring in shHIF1 but not in non-target shRNA are shown. Red indicates up-regulation and blue indicates down-regulation. ALG♦: members of glycosyltransferases attaching glycans to asparagine residues (asparagine-liked glycosylation); GALM: galactose mutarotase; GYG: glycogenin; GPI: glucose-6-phosphate isomerase; GNPDA: glucosamine-6-phosphate deaminase; HK: hexokinase; ISYNA: inositol-3-phosphate synthase; MPI: mannose-6-phosphate isomerase; PGM: phosphoglucomutase; UGP: UDP-glucose 6-dehydrogenase; G6PD: glucose-6-phosphate dehydrogenase. Note that the reaction catalyzed by GALM can also occur spontaneously.

Central carbon enzymes activity

Given the differences in the lactogenic phenotype of shHIF1 clones and also the non-target controls – although in opposite trends – we further enquired on possible changes on enzymes activity steering such phenotypes. Therefore, clone shHIF1 #21, the non-target shRNA population and non-manipulated cells were further characterized in terms of enzymes activity of central carbon metabolism (Fig. 7). Non-target shRNA cells presented increased activity of the early glycolytic enzymes, particularly evident for phosphofruktokinase (PFK) substantiating transcriptome analysis (Fig. 5) and the observed enhanced glucose consumption (Table I). This confirms a more active glycolytic metabolism in non-target control cells, one of the most evident off-target effects associated to short-hairpin RNA expression (Table I). While down-regulating HIF1 should lead to reduced glycolytic activity, these off-

target effects can skew such phenotype. Independently of that, a significant decrease of LDH activity in shHIF1 #21 clone was obtained (Fig. 7), in line with the reduction in LAC/GLC ratio obtained for this clone as well as for all the shHIF1 clones presenting lower LAC/GLC ratios (Fig. 3). Clone shHIF1 #21 also presented enhanced activity of glucose-6-phosphate dehydrogenase (G6PD) indicating increased channeling of the glycolytic intermediaries into the pentose phosphate pathway (PPP). Pathway analysis also indicated activation of acetyl-CoA biosynthesis at the level of pyruvate dehydrogenase complex (PDH) (Fig. 5) although no evidence of enhanced enzyme activity was found at this level. However, this enzyme could not be accurately quantified in none of the (manipulated and non-manipulated) cells, suggesting it to be out of the method sensitivity (Fig 7). Finally, for shHIF1 and non-target control, the amino acid aminotransferases – glutamic-pyruvate aminotransferase (GTP) and aspartate aminotransferase (GOT) – were found to be substantially more active. This phenotype further substantiates the hints on increased amino acid catabolism given by pathway analysis (Fig. 6) and suggests enhanced amino acid mobilization to feed the TCA cycle in shRNA expressing cells (shHIF1 and non-target shRNA). The analysis of metabolite profiling, to be performed in the follow-up of this work, should enlighten these findings.

3.3. Down-regulation of PDK

In 293 FLEX, the PDK isoforms found to be expressed were PDK 1 and PDK3, evaluated by transcriptome analysis (Chapter II). Thereby, a short-hairpin RNAi sequence was designed to target homology zones between these two isoforms (see Materials and methods). Similarly to the approach on HIF1 down-regulation, PDK silencing was conducted by delivering this hairpin by lentiviral infection using low multiplicity of infection (MOI). The transduced population was cloned by limiting dilution and simultaneously screened for high-titer clones using a simpler version of our recently implemented single-step cloning titration method. For method details, please refer to Chapter VII.

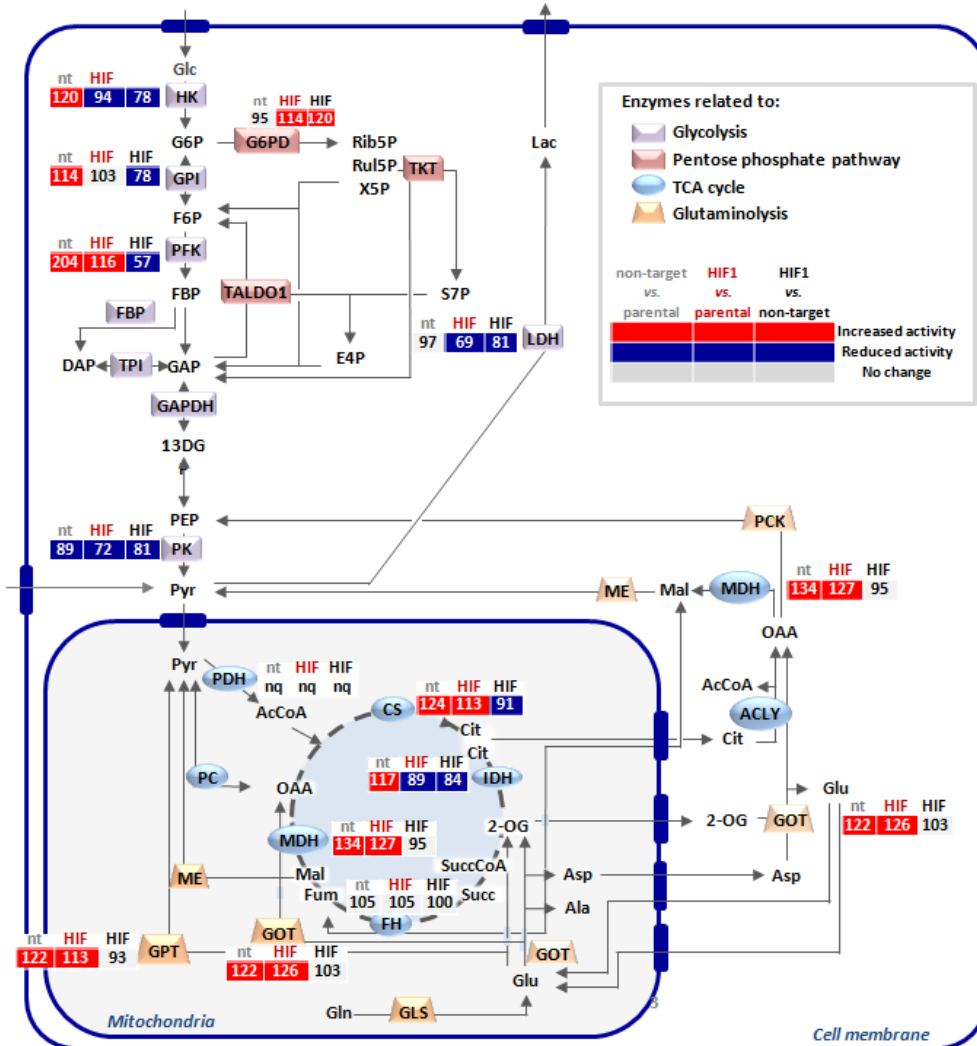
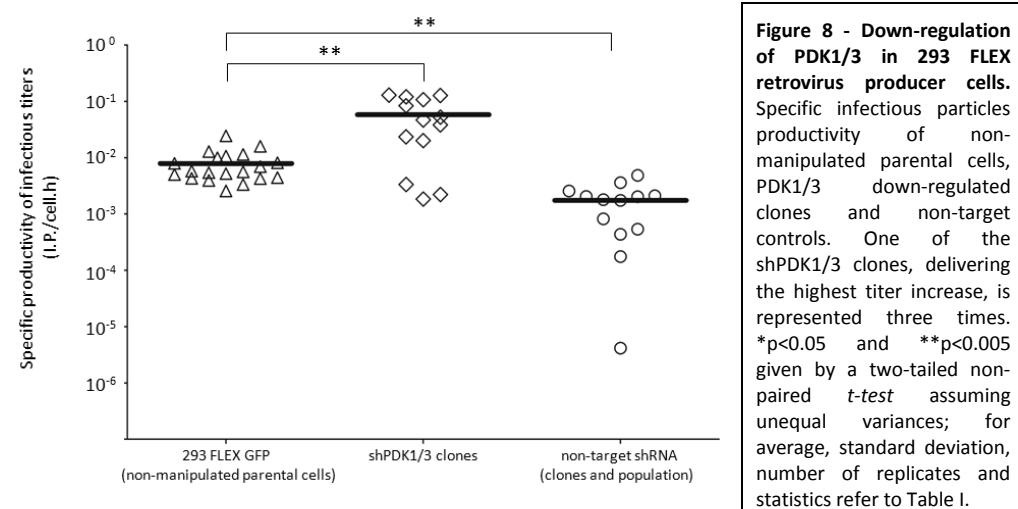


Figure 7 – Central carbon enzymes activity in shHIF1 and non-target shRNA cells. Schematic representation of central carbon reactions and respective enzymes activity of non-target shRNA cells or shHIF1 #21. Values are shown as activity (%) relatively to parental non-manipulated cells (first two columns) or to non-target control (last column) and represent average \pm standard deviation of 4 to 8 replicates. Enzyme activity changes $> 5\%$ were considered of relevance. nq: non-quantifiable; HK: hexokinase; PGI: glucose-6-phosphate isomerase; PFK: phosphofructokinase; FBP: fructose-1,6-bisphosphatase; TPI: triosephosphate isomerase; GAPDH: glyceraldehyde-3-phosphate dehydrogenase; PK: pyruvate kinase; PDH: pyruvate dehydrogenase complex; PC: pyruvate carboxylase; CS: citrate synthase; ME: malic enzyme; GPT: glutamic-pyruvate transaminase; GOT: glutamic-oxaloacetic transaminase 1; MDH: malate dehydrogenase; FH: fumarate hydratase; IDH: isocitrate dehydrogenase; ACLY: ATP citrate lyase; PCK: LDH: lactate dehydrogenase.

Although this simplified version delivers more than 90% of false positives, these can be discriminated by visual inspection of the cloning wells using a

fluorescence microscope, allowing the isolation of high-titer clones with comfortable confidence. Eleven clones were isolated (Fig. 8)



The majority of the isolated clones were found to be high producers relatively to non-manipulated cells (Fig. 8). Even those for which titer reduction was observed, it occurred in small extension. These clones were analyzed for PDK1, PDK3, LDHA gene expression and LAC/GLC ratio (Fig. 9).

All analyzed clones revealed significant PDK1/3 down-regulation although the pattern did not correlate with the extension of productivity increase (Fig. 9A). Except for one (low-titer) clone, all clones presented substantial reduction of the lactogenic phenotype (Fig. 9D), correlated with PDK1/3 down-regulation (Fig. 9C). LDHA gene expression was also found to be reduced, on average -1.4-fold, for all the clones but with no evident correlation with PDK1/3 down-regulation (Fig. 9B).

The analysis of glucose consumption and lactate production rates revealed that the reduced lactogenic phenotype in shPDK1/3 clones was prominently based on diminished lactate production, 44% less (Table I). Lactate production rates were also significantly lower than those of shHIF1 #21. Non major changes were detected neither in glutamine consumption nor in ammonia production (data not shown).

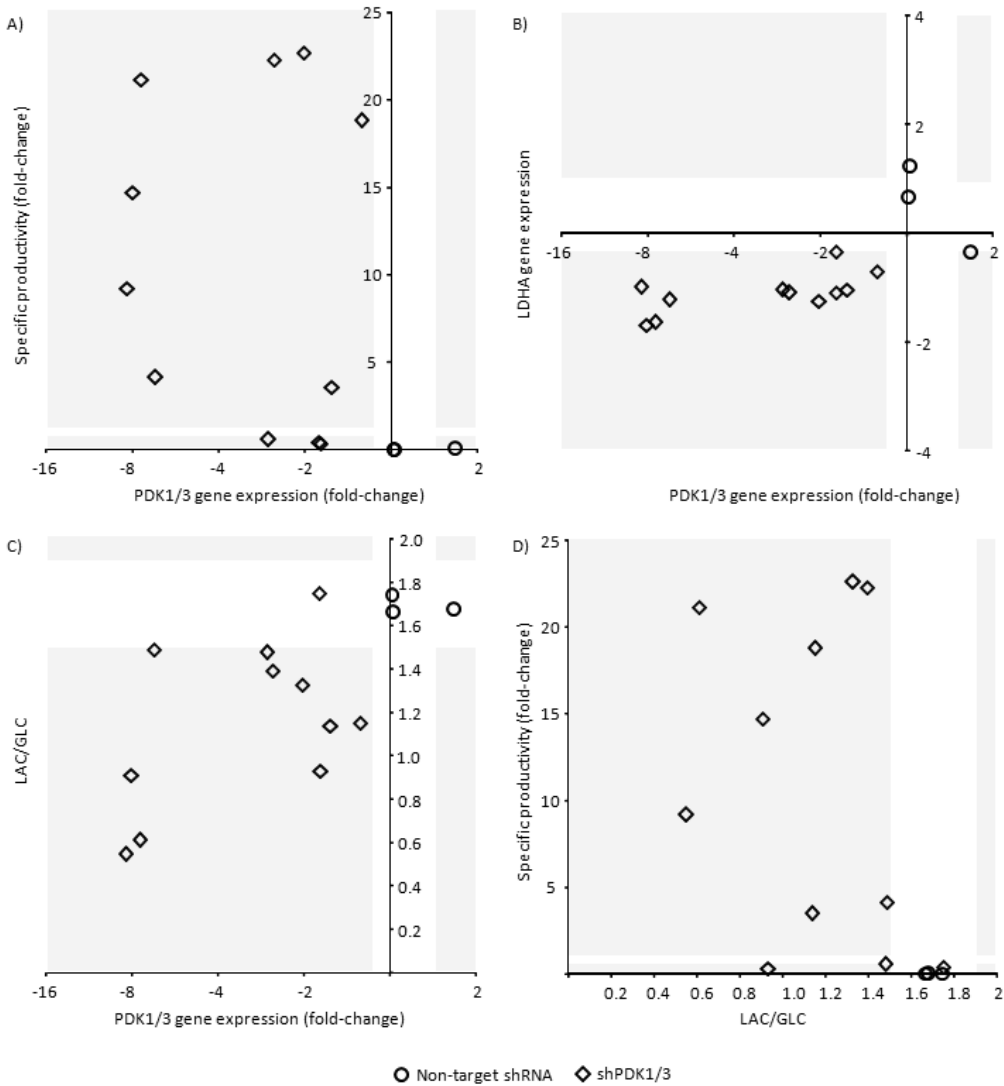


Figure 9 – Virus productivity and lactogenic phenotype in response to PDK1/3 down-regulation. Specific productivity of infectious retroviral particles (A), lactate dehydrogenase A (LDHA) gene expression (B) and ratio lactate production to glucose consumption (LAC/GLC) (C) of shPDK1/3 clones and non-target controls vs. PDK1/3 gene expression. Values are shown as fold-change relatively to non-manipulated cells. For a matter of simplicity, PDK1/3 refers to the average PDK1 and PDK3 genes expression (for individual values please refer to Table I) (D) Specific productivity of infectious retroviral particles vs. ratio lactate production to glucose consumption (LAC/GLC). For all (A) – (D) grey shadowed area represents values outside the range “average \pm the standard deviation” of the controls (please refer to Table I for further details). Gene expression represents average expression level normalized to the RPL22 housekeeping control and relatively to non-manipulated cells ($2^{\Delta\Delta CT}$) (n=3).

Clones delivering titer reduction, were, similarly to what had been observed for shHIF1, those losing the expression of viral components (Fig. 10A). Also here, the viral transgene and the gag-pol components were found to be changing substantially (Fig. 10B and D), with an evident positive correlation between the viral transgene and infectious viral titers (Fig. 10A). Once again, the changes in envelope expression were modest and with no evident correlation with infectious vector titers (Fig. 10E) nor with the extension of PDK1/3 down-regulation (Fig. 10F).

3.4. Double HIF1 – PDK1/3 down-regulation

In the third part of this work, HIF1 and PDK1/3 down-regulations were combined seeking for synergistic effects in infectious particles productivity. Clone shHIF1 #21 was transduced with shPDK1/3 delivered by lentiviral vector infection. Two control populations were additionally analyzed: double transduction with non-target shRNA and clone shHIF1#21 transduced with non-target shRNA. For HIF1#21-PDK1/3 double transduced clones, the simpler version of the single step cloning-titration method was also used to select high titer clones (Fig. 11). All clones delivered relevant titer improvement, relatively to non-manipulated parental cells. Yet, considering that the starting point was clone shHIF1 #21, producing on average 20-fold higher, the magnitude of improvement was rather modest.

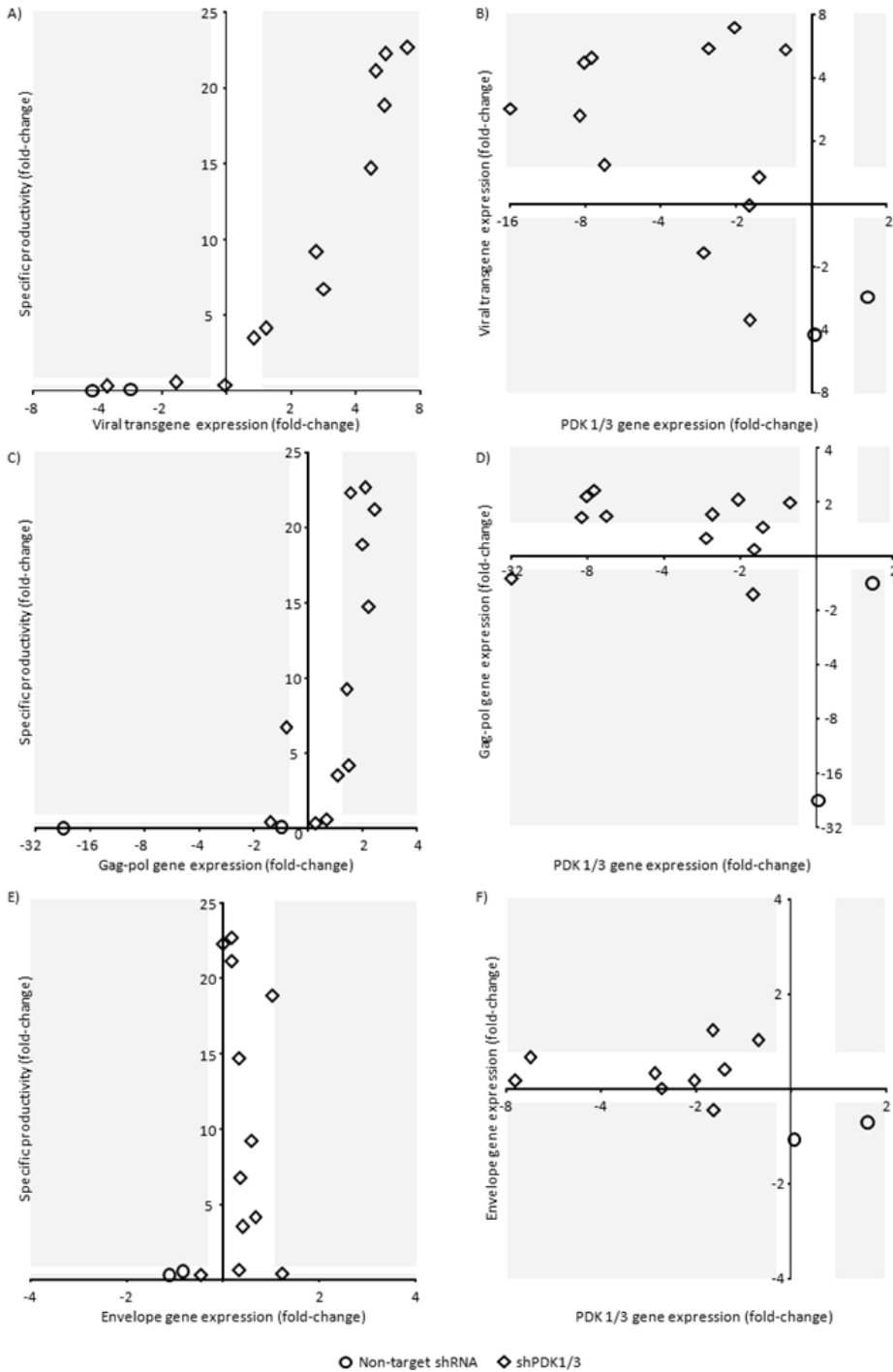


Figure 10 – Vector components expression of PDK1/3 down-regulated cells. Specific productivity of infectious retroviral particles of shPDK1/3 and non-target controls vs. viral transgene (A), gag-pol (C) and envelope (E) gene expression. Viral transgene (B), gag-pol (D) and envelope (F) gene expression vs. PDK1/3 gene expression. →

Indeed, no significant difference was detected between shHIF1 #21 and their derived shPDK1/3 clones (Fig. 11). One clone (#P6C6), with a 32-fold productivity increase relatively to non-transduced cells, was the exception. However, it cannot be disregarded the fact that double non-target shRNA loading further reduced infectious particles titers relatively to single non-target shRNA transduction (Fig. 11 and Table I).

Although PDK1/3 expression was not assessed for the majority of these clones, the relatively unchanged LAC/GLC ratios suggested the magnitude of shPDK1/3 expression to be relatively small (Table I). It should be noted, however, that shPDK1/3 transduction was selected by flow cytometry activated sorting (see Materials and methods), thus excluding the possibility that the clones were not transduced with shPDK1/3 lentiviral vector. All clones were confirmed to express mCherry, the selectable marker of shPDK1/3 construction (data not shown).

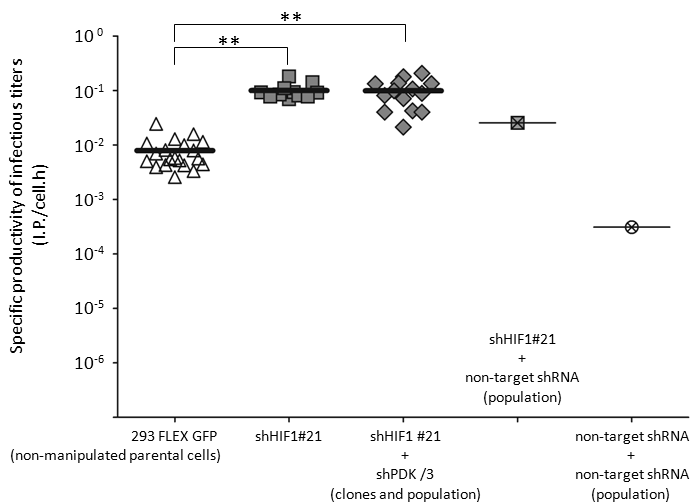


Figure 11 - Down-regulation of PDK1/3 in shHIF1 #21 retrovirus producer cells. Specific infectious particles productivity of non-manipulated parental cells, HIF1 down-regulated clones, double shHIF1#21 – shPDK1/3 clones and non-target controls. For double non-target control, only the population was analyzed, shown as a single point on the right side of the chart. * p<0.05 and **p<0.005 given by a two-tailed non-paired *t*-test assuming unequal variances; for average, standard deviation, number of replicates and p-value statistics refer to Table I.

→ **(Figure 10 continued)** For a matter of simplicity, PDK1/3 refers to the average PDK1 and PDK3 genes expression (for individual values please refer to Table I). For all **(A) – (F)** grey shadowed area represents values outside the range “average \pm standard deviation” of the controls (refer to Table I for further details). Gene expression represents average expression level normalized to the RPL22 housekeeping control relatively to non-manipulated cells ($2^{\Delta\Delta CT}$) (n=3).

3.5 Impact of shHIF1 and shPDK1/3 in viral batch quality

The best clones from each manipulation and corresponding controls were analyzed for virus production in terms of total and infectious particles (Fig. 12).

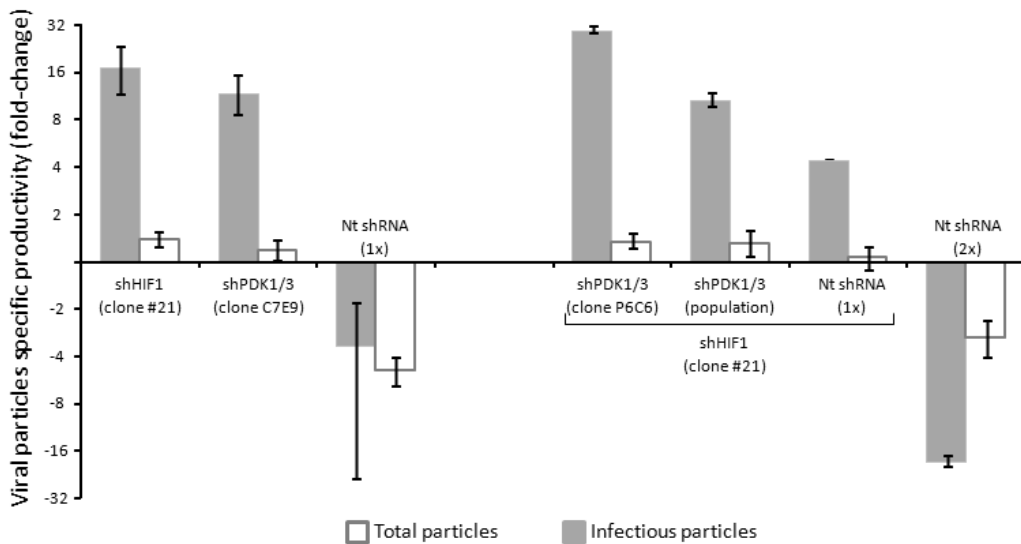


Figure 12 – Specific productivity of infectious and total particles of shRNA manipulated cells. Specific productivity of infectious particles (grey bars) and total particles (white bars). Values are shown as fold-change relatively to non-manipulated cells. Error bars represent standard deviation (“n” between 2 and 11). Total particles assessed by Nanoparticle tracking analysis.

The loss of infectious particles titers in non-target shRNA controls was found to be derived from sharp decreases in total particles production. In fact, for single non-target shRNA transduction, the decrease in infectious particles arised from the reduction in total particles. By opposite, both shHIF1 and shPDK1/3 clones were shown to produce higher content of total particles, being the infectious particles titers those improving more significantly.

Table I – Resume of the parameters analyzed during this work

	Parental cells	shHIF1	shHIF1 #21	shPDK1/3	shHIF1#21 + shPDK1/3	Nt shRNA (1x)	Nt shRNA (2x)	
Specific infectious particles production (I.P./cell.h)	μ	0.0057	0.011	0.100	0.058	0.100	0.002	0.0003
	SD	0.0052	0.025	0.033	0.049	0.054	0.001	-
	#	20	69	11	13	15	11	1
	FC	-	1.9 (*)	17.6 (**)	10.2 (**)	16.9 (**)	-3.4 (**)	-
Specific glucose consumption rate (μmol/10 ⁶ cells.h)	μ	0.18	0.16	0.16	0.14	0.15	0.29	0.17
	SD	0.05	0.03	0.04	0.03	0.04	0.06	-
	#	13	32	11	11	15	5	1
	FC	-	-	-	-	-	2 (*)	-
Specific lactate consumption rate (μmol/10 ⁶ cells.h)	μ	0.31	0.25	0.25	0.17	0.22	0.48	0.23
	SD	0.08	0.06	0.06	0.09	0.06	0.11	-
	#	12	32	11	11	15	5	1
	FC	-	-1.2 (**)	-1.3 (*)	-1.8 (**)	-1.4 (**)	2.7 (*)	-
HIF1 gene expression (2 ^{ΔCT})	μ	0.15	0.08	0.06	-	0.05	0.14	0.11
	SD	0.04	0.03	0.01	-	0.02	0.04	-
	#	6	16	5	-	3	9	1
	FC	-	-2.0 (**)	-2.4 (**)	-	-3.0 (**)	-	-
LDHA gene expression (2 ^{ΔCT})	μ	0.74	0.68	0.51	0.54	0.49	0.86	0.68
	SD	0.16	0.25	0.07	0.07	0.11	0.17	-
	#	8	16	5	11	3	9	1
	FC	-	-	-1.4 (**)	-1.4 (*)	-1.5 (*)	-	-
PDK1 gene expression (2 ^{ΔCT})	μ	0.033	0.034	0.035	0.013	0.014	0.039	0.036
	SD	0.006	0.005	0.008	0.007	0.002	0.013	-
	#	6	11	4	11	3	4	1
	FC	-	-	-	-2.4 (**)	-2.3 (**)	-	-
PDK3 gene expression (2 ^{ΔCT})	μ	0.043	-	0.057	0.016	0.023	0.056	-
	SD	0.008	-	0.002	0.014	0.005	0.014	-
	#	4	-	2	11	3	2	1
	FC	-	-	-	-2.7 (**)	-1.8 (*)	-	-
Viral transgene expression (2 ^{ΔCT})	μ	1.8	4.8	9.5	5.4	11.9	1.5	0.6
	SD	0.4	6.3	1.9	3.8	6.1	1.8	-
	#	6	15	3	12	2	7	1
	FC	-	-	5.2 (*)	3.0 (*)	-	-	-
Gag-pol gene expression	μ	0.5	0.5	1.2	0.7	0.6	0.2	0.03
	SD	0.2	0.5	0.3	0.2	0.1	0.4	-
	#	6	15	3	12	2	7	1
	FC	-	-	2.3 (*)	-	-	-	-
Envelope gene expression (2 ^{ΔCT})	μ	1.8	2.8	2.3	1.8	1.5	1.1	1.1
	SD	0.3	2.2	0.5	0.3	0.2	0.6	-
	#	6	15	3	12	2	7	1
	FC	-	-	-	-	-	-	-

μ: general designation for the parameter under analysis.

SD: standard deviation

#: number of replicates. When only "1" replicate is shown, it refers to the cell population

FC: fold-change, where negative values denote reduction and positive values denote increase, relatively to non-manipulated parental cells.

(*) p<0.05 and (**) p<0.005, given by a non-paired two-tailed *t*-test assuming unequal variances when comparing with non-manipulated parental cells.

In non-target (Nt) shRNA controls (1x) refers to single transduction and (2x) refers to double transduction.

Gene expression represents average expression level normalized to the RPL22 housekeeping control (2^{ΔCT}) (n=3).

4. Discussion

Reducing lactate production in mammalian cell culture producing recombinant biopharmaceuticals has been a major goal of cell culturists. In this work, we conducted a proof-of-concept metabolic engineering study in HEK 293 derived retroviral vector producer cells, based on the down-regulation of two key molecular effectors of the Warburg effect-like lactogenic phenotype: hypoxia inducible factor 1 (HIF1) and pyruvate dehydrogenase kinase 1 and 3 (PDK1/3). This strategy would simultaneously tackle reduced lactate accumulation and enhanced channeling of glycolytic intermediates into the tricarboxylic acid cycle (TCA) (Fig. 1).

Down-regulation of hypoxia inducible factor 1 (HIF1) originated clones with productivity improvements up to 20-fold whereas strong inhibitory effects were observed for non-target shRNA transduced cells (Fig. 2). These results evidenced the beneficial effects of diminishing HIF1 expression. The magnitude of titer increase was considerable higher when analyzed comparatively to the non-target control, up to 100-fold. However, it is difficult to state whether these were affected by the off-target effects observed in the controls – thus corresponding to real 100-fold increase mediated by HIF1 silencing – or if these were simply particular clones less affected by the off-target effects. From the clones analyzed for HIF1 gene expression, HIF1 down-regulation appeared to be correlated with titer increased in a pyramid-like layout suggesting a fine-tuned expression value for which HIF1 reduction delivers improved virus production (Fig. 3A). However, this *fine-tuned* HIF1 down-regulation was a necessary, but not sufficient, condition for high viral titers. The combination of downstream effects of HIF1 silencing, particularly the reduction of the lactogenic phenotype (Fig. 3C) and relevant increases in viral components gene expression (Fig. 4), can be the reason behind the high-titers. However the latter did not correlate with HIF1 expression (Fig. 4 B, D and F). In fact, even some of the non-target controls presented increased vector components expression, suggesting some degree of randomness associated to these results. Yet, only shHIF1 clones – and not non-target

controls – delivered titer increases (Fig. 2). Thereby, even if clonal variability is the explanation for the dispersion of vector components expression, it might only be translated into improved titers when conjugated with the downstream physiological effects of HIF1 down-regulation. Although, when starting this work, we were seeking for a reduction in the lactogenic phenotype, these downstream effects revealed to be broader. Microarray analysis indicated significant recruitment of metabolic pathways non-lactogenesis related, such as biological amines metabolism, detoxification routes – including glutathione metabolism – and pentose phosphate pathway. We have previously shown these pathways to be actively recruited in the production of recombinant retrovirus (Rodrigues et al. 2013). The results from both transcriptional profile as well as central carbon enzymes activity (Figs. 5, 6 and 7), also revealed the glycolytic flux to be partially drained from glycolysis towards pentose phosphate pathway and glucose 1P biosynthesis.

In the second part of this work, the cells were manipulated for the down-regulation of PDK1/3. While for shHIF1 a manual screening, shPDK1/3 clones were selected based on a simplified version of a method allowing for the isolation of high-titer phenotypes. In line, the majority of the isolated clones were found to be high producers relatively to non-manipulated cells (Fig. 8). All analyzed clones revealed significant PDK1/3 down-regulation although the pattern did not correlate with the extension of productivity increase (Fig. 9A). However, as stated above, these clones were not randomly isolated, but chosen based on high-titers. Thus, more than the extension of PDK1/3 down-regulation, they reflect the *advantageous* (from this *selection* point of view) downstream effects of the manipulation, including the ameliorated lactogenic phenotype (Fig. 9). Interestingly, LDHA gene expression was found to be reduced in all shPDK1/3 (Fig. 9B). These results, support previous findings on a feed-back loop mechanism in which reduced lactate accumulation contributes to less stabilization of HIF1, potentially simulating the effects of its down-regulation, including lowering LDH expression/activity (Lu et al. 2002). It was noteworthy that lactate production rates from shPDK1/3 clones were significantly

lower than those of shHIF1 #21, a pertinent result since LDHA down-regulation occurred in identical extension in both cases (Fig. 3, 9 and Table I). This evidenced increased metabolization of pyruvate through pyruvate dehydrogenase (PDH) to occur in higher extension in shPDK cells than in shHIF1, being less dependent on the LDH levels. Indeed, even if no LDH reduction occurs, being PDH sufficiently active, the channeling of pyruvate into the TCA is favored since PDH has much higher affinity for pyruvate than LDH (Nakae and Stoward 1997; Strumilo et al. 1999).

Similarly to shHIF1, for shPDK1/3 clones, relevant changes in viral components gene expression were observed, with an evident positive correlation between viral transgene expression and infectious particles titers (Fig. 10A). For HIF1, a transcription factor targeting several hundreds of genes (Benita et al. 2009) one could hypothesize a transcriptional dynamics affecting the expression of many genes, including the viral cassettes. For PDK1/3 down-regulation, however, the transcriptional effects are expected to be rather limited. Still, among silenced clones, high expression variability was found for the viral transgene and, to less extent, for the gag-pol. This can be rationalized in two ways. One, by assuming that gene expression changes in viral components are randomly derived from the genetic manipulation as it could happen to any other gene. Yet, such variability occurred in evidently greater extension for the viral transgene and gag-pol, whereas envelope remained relatively unchanged. Thus, even assuming some degree of randomness, a second hypothesis reports to a dynamic transcriptional behaviour of retrovirus long-terminal repeats (LTRs) promoter. In 293 FLEX GFP, both the viral transgene as well as the gag-pol are under the control of an LTR. Pertinently, the viral transgene is an MFG-LTR, known to be transcriptionally more active (Byun et al. 1996), thereby substantiating the greater expression changes, relatively to the non-MFG LTR deriving the expression of gag-pol. What leads to such high fold-changes in the mRNA levels of this cassette is not clear. From our results, we hypothesize a dynamic response of the vector cassettes steered by an *improved metabolic status*. This hypothesis arises from the observation that solely the over-expression of gag-pol or

the viral transgene in 293 FLEX does not translate into improved titers (Carrondo et al. 2008). Therefore, high titer clones should present increased vector components not as the cause for the enhanced productivities but as a consequence: cells with higher productive performance derived from an improved metabolic status are capable of using the extra viral components delivering higher titers (Fig. 12).

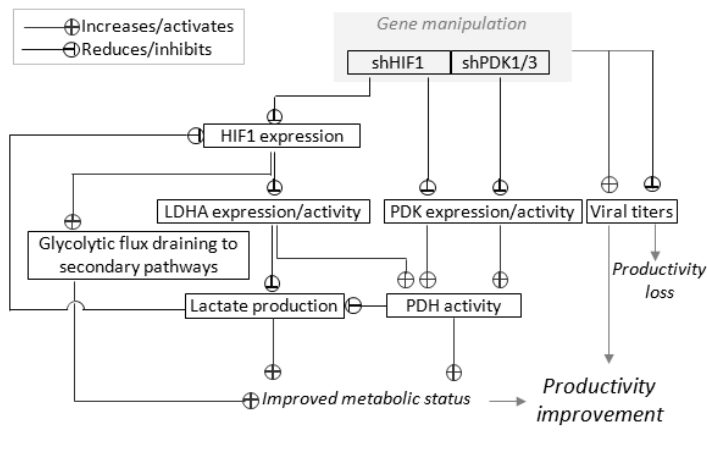


Figure 12 – Improving infectious retrovirus production through the down-regulation of the Warburg effect: beyond the lactogenic phenotype. Reduced HIF1 expression diminishes LDH expression/activity leading to reduced lactate production which also feed-back represses HIF1 stabilization (Lu et al. 2002). LDH reduction additionally stimulates enhanced metabolism of pyruvate through PDH since PDH has a higher affinity for pyruvate than LDH (Nakae and Stoward 1997; Strumilo et al. 1999). Increased flux through PDH leads

to an *improved metabolic status* by feeding TCA-fed routes (e.g.: lipid biosynthesis). Reduced PDK expression results in similar effects although these are exerted at a downstream stage with the additional direct activation of PDH. Reduced HIF1 expression also appeared to stimulate the draining of part of the glycolytic flux to secondary pathways – such as pentose phosphate pathway – known to be recruited in retrovirus producer cells (Rodrigues et al. 2013). Therefore, also this contributes to an *improved metabolic status*. On the other hand, significant variability in viral components expression occurred. When relevant increases occur in clones presenting an *improved metabolic status*, it translates in improved titers. The conjugation of these two factors – *improved metabolic status* and increased vector components – translates in higher titers. Note that *improved metabolic status* refers to a conjugation of active pathways that favours virus production. It does not imply that shHIF1 or shPDK1/3 manipulated cells are, in general, metabolically more active or *superior* to non-manipulated cells.

In the third part of this work, shHIF1 and shPDK1/3 were combined seeking for synergistic effects in enhancing infectious particles productivity. Yet, the improvement was rather modest (Fig. 11). However, one cannot disregard the fact that double non-target shRNA loading further reduced infectious particles titers relatively to single non-target shRNA transduction (Fig. 11). In fact, not only for viral titer, but also for the lactogenic phenotype, non-target shRNA transduced cells revealed marked opposite behavior relatively to the clones. This was evident in infectious vector titers (Figs. 1 and 12), lactate production (Fig. 10 and 4) and central

carbon enzymes activity (Fig. 7). If such effects are also occurring in shHIF1 and shPDK1/3, they might bias the real extension of their down-regulation in the reduction of the lactogenic phenotype and improvement of infectious particles titers. To this end, it might also explain the hurdle in combining the expression of these two hairpins seeking for a synergistic (or even simply, cumulative) effect.

The results herein presented demonstrate the down-regulation of the Warburg effect-like lactogenic phenotype as a successful approach to improve the productivity performance of a human cell line producing a highly complex and lactate-sensitive bioproduct, potentially extendable to other mammalian systems producing recombinant biopharmaceuticals. Given the evident deleterious effects observed for shRNA throughout this work, for the extension of this strategy to other production systems, avoiding RNA interference as a knock-down tool will be preferable. Regardless that, the results herein reported constitute, to the best of our knowledge, the highest fold-increase in specific productivity of a mammalian cell line producing complex biopharmaceuticals for single gene manipulation (20-fold, on average, for both shHIF1 and shPDK1/3). They have also highlighted secondary pathways affected in the Warburg effect, including pentose phosphate pathway and glucose 1P biosynthesis. Such pathways can further be explored towards an *improved metabolic status beyond the lactogenic phenotype*.

5. Author contribution

Ana Filipa A. F. Rodrigues conceived the experimental setup and design, performed part of the experiments, analyzed the data and wrote the chapter.

6. References

- Altamirano C, Paredes C, Illanes A, Cairo JJ, Godia F. 2004. Strategies for fed-batch cultivation of t-PA producing CHO cells: substitution of glucose and glutamine and rational design of culture medium. *J Biotechnol* 110(2):171-9.
- Benita Y, Kikuchi H, Smith AD, Zhang MQ, Chung DC, Xavier RJ. 2009. An integrative genomics approach identifies Hypoxia Inducible Factor-1 (HIF-1)-target genes that form the core response to hypoxia. *Nucleic Acids Res* 37(14):4587-602.
- Byun J, Kim SH, Kim JM, Yu SS, Robbins PD, Yim J, Kim S. 1996. Analysis of the relative level of gene expression from different retroviral vectors used for gene therapy. *Gene Ther* 3(9):780-8.
- Carrondo MJ, Merten OW, Haury M, Alves PM, Coroadinha AS. 2008. Impact of retroviral vector components stoichiometry on packaging cell lines: effects on productivity and vector quality. *Hum Gene Ther* 19(2):199-210.
- Caspi R, Altman T, Dale JM, Dreher K, Fulcher CA, Gilham F, Kaipa P, Karthikeyan AS, Kothari A, Krummenacker M and others. 2010. The MetaCyc database of metabolic pathways and enzymes and the BioCyc collection of pathway/genome databases. *Nucleic Acids Res* 38(Database issue):D473-9.
- Chee Fung Wong D, Tin Kam Wong K, Tang Goh L, Kiat Heng C, Gek Sim Yap M. 2005. Impact of dynamic online fed-batch strategies on metabolism, productivity and N-glycosylation quality in CHO cell cultures. *Biotechnol Bioeng* 89(2):164-77.
- Coroadinha AS, Alves PM, Santos SS, Cruz PE, Merten OW, Carrondo MJ. 2006a. Retrovirus producer cell line metabolism: implications on viral productivity. *Appl Microbiol Biotechnol* 72(6):1125-35.
- Coroadinha AS, Ribeiro J, Roldao A, Cruz PE, Alves PM, Merten OW, Carrondo MJ. 2006b. Effect of medium sugar source on the production of retroviral vectors for gene therapy. *Biotechnol Bioeng* 94(1):24-36.
- Coroadinha AS, Schucht R, Gama-Norton L, Wirth D, Hauser H, Carrondo MJ. 2006c. The use of recombinase mediated cassette exchange in retroviral vector producer cell lines: predictability and efficiency by transgene exchange. *J Biotechnol* 124(2):457-68.
- Elias CB, Carpentier E, Durocher Y, Bisson L, Wagner R, Kamen A. 2003. Improving glucose and glutamine metabolism of human HEK 293 and *Trichoplusia ni* insect cells engineered to express a cytosolic pyruvate carboxylase enzyme. *Biotechnol Prog* 19(1):90-7.
- Fish RJ, Kruithof EK. 2004. Short-term cytotoxic effects and long-term instability of RNAi delivered using lentiviral vectors. *BMC Mol Biol* 5:9.
- Irani N, Beccaria AJ, Wagner R. 2002. Expression of recombinant cytoplasmic yeast pyruvate carboxylase for the improvement of the production of human erythropoietin by recombinant BHK-21 cells. *J Biotechnol* 93(3):269-82.
- Janke R, Genzel Y, Wahl A, Reichl U. 2010. Measurement of key metabolic enzyme activities in mammalian cells using rapid and sensitive microplate-based assays. *Biotechnol Bioeng* 107(3):566-81.
- Jimenez NE, Wilkens CA, Gerdtsen ZP. 2011. Engineering CHO cell metabolism for growth in galactose. *BMC Proc* 5 Suppl 8:P119.
- Kadota K, Nakai Y, Shimizu K. 2008. A weighted average difference method for detecting differentially expressed genes from microarray data. *Algorithms Mol Biol* 3:8.

- Kim SH, Lee GM. 2007. Down-regulation of lactate dehydrogenase-A by siRNAs for reduced lactic acid formation of Chinese hamster ovary cells producing thrombopoietin. *Appl Microbiol Biotechnol* 74(1):152-9.
- Kondoh H. 2008. Cellular life span and the Warburg effect. *Exp Cell Res* 314(9):1923-8.
- Lao MS, Toth D. 1997. Effects of ammonium and lactate on growth and metabolism of a recombinant Chinese hamster ovary cell culture. *Biotechnol Prog* 13(5):688-91.
- Lu H, Forbes RA, Verma A. 2002. Hypoxia-inducible factor 1 activation by aerobic glycolysis implicates the Warburg effect in carcinogenesis. *J Biol Chem* 277(26):23111-5.
- McTaggart S, Al-Rubeai M. 2000. Effects of culture parameters on the production of retroviral vectors by a human packaging cell line. *Biotechnol Prog* 16(5):859-65.
- Merten O, Landric L, Danos O. 2001. Influence of the metabolic status of packaging cells on retroviral vector production. *Recombinant Protein Production with Prokaryotic and Eukaryotic Cells*. Dordrecht: Kluwer Academic Publishers.
- Moffat J, Grueneberg DA, Yang X, Kim SY, Kloepper AM, Hinkle G, Piqani B, Eisenhaure TM, Luo B, Grenier JK and others. 2006. A lentiviral RNAi library for human and mouse genes applied to an arrayed viral high-content screen. *Cell* 124(6):1283-98.
- Nakae Y, Stoward PJ. 1997. Kinetic parameters of lactate dehydrogenase in liver and gastrocnemius determined by three quantitative histochemical methods. *J Histochem Cytochem* 45(10):1427-31.
- Ozturk SS, Riley MR, Palsson BO. 1992. Effects of ammonia and lactate on hybridoma growth, metabolism, and antibody production. *Biotechnol Bioeng* 39(4):418-31.
- Rodrigues AF, Amaral AI, Verissimo V, Alves PM, Coroadinha AS. 2012. Adaptation of retrovirus producer cells to serum deprivation: Implications in lipid biosynthesis and vector production. *Biotechnol Bioeng* 109(5):1269-79.
- Rodrigues AF, Formas-Oliveiras AS, Bandeira VS, Alves PM, Hu WS, Coroadinha AS. 2013. Metabolic pathways recruited in the production of a recombinant enveloped virus: mining targets for process and cell engineering. *Metab. Eng. Nov*; 20:131-145.
- Rodrigues AF, Guerreiro MR, Santiago VM, Dalba C, Klatzmann D, Alves PM, Carrondo MJ, Coroadinha AS. 2011. Down-regulation of CD81 tetraspanin in human cells producing retroviral-based particles: tailoring vector composition. *Biotechnol Bioeng* 108(11):2623-33.
- Shlomi T, Benyamini T, Gottlieb E, Sharan R, Ruppin E. 2011. Genome-scale metabolic modeling elucidates the role of proliferative adaptation in causing the Warburg effect. *PLoS Comput Biol* 7(3):e1002018.
- Strumilo S, Czerniecki J, Dobrzyn P. 1999. Regulatory effect of thiamin pyrophosphate on pig heart pyruvate dehydrogenase complex. *Biochem Biophys Res Commun* 256(2):341-5.
- Tusher VG, Tibshirani R, Chu G. 2001. Significance analysis of microarrays applied to the ionizing radiation response. *Proc Natl Acad Sci U S A* 98(9):5116-21.
- Wlaschin KF, Hu WS. 2007. Engineering cell metabolism for high-density cell culture via manipulation of sugar transport. *J Biotechnol* 131(2):168-76.
- Zhou J, Lin J, Zhou C, Deng X, Xia B. 2011a. Cytotoxicity of red fluorescent protein DsRed is associated with the suppression of Bcl-xL translation. *FEBS Lett* 585(5):821-7.
- Zhou M, Crawford Y, Ng D, Tung J, Pynn AF, Meier A, Yuk IH, Vijayasankaran N, Leach K, Joly J and others. 2011b. Decreasing lactate level and increasing antibody production in Chinese Hamster Ovary cells (CHO) by reducing the expression of lactate dehydrogenase and pyruvate dehydrogenase kinases. *J Biotechnol* 153(1-2):27-34.

Chapter VII

SINGLE STEP CLONING-TITRATION METHOD

A HIGH-THROUGHPUT SCREENING TOOL FOR MULTI-GENE ENGINEERING

This chapter is based on data submitted as:

Single step cloning-titration method: fast cell line development and dynamic study of the physiological traits in high-titer retrovirus producer cells

Ana F. Rodrigues, Ana S. Formas-Oliveira, Miguel R. Guerreiro, Hélio A. Tomás,
Paula M. Alves, Ana S. Coroadinha, (*submitted*)

Abstract

Mammalian cell line development for the production of complex biopharmaceuticals is a laborious and time-consuming work due to the need to screen for high-titer clones. The challenge increases in the case of virus producer stable cell lines as viral components are usually split in several expression cassettes for engineering and/or safety purposes. Herein, we describe a novel method for fast screening of high-titer retrovirus producer cells by merging cell cloning and virus titration.

The method makes use of split-GFP®, a green fluorescent protein separated in two fragments – S10 and S11 – which fluoresce only upon transcomplementation. A cell population producing infectious virus with a S11 transgene is cloned and co-cultured with a target cell line harboring the S10 fragment. S11 viruses produced by the clone infect the target cells and reconstitute the GFP signal. Only the clones yielding high signal are isolated, avoiding cell expansion, cell banking and posterior growth/titration studies, wasteful for the majority of the (low titer) clones.

The method was validated by establishing a retrovirus producer from a nude cell line reducing a one year process of sequential transfection/screening of three viral expression cassettes to three months. Clones producing up to 1×10^8 infectious particles *per* mL were isolated. As transcomplemented fluorescence data provides direct estimation of clone's productivity it can be analyzed in terms of density distribution, offering valuable information on the average productivity of the cell population. Thereby, it was additionally used to evaluate the production performance of different cell substrates – HEK 293 vs. HEK 293T – showing that the later sustain increased titers.

The method was established using a 96-well fluorometer plate reader, giving a manual throughput of 200-500 clones *per* analysis in two weeks; if coupled to an automated device, this could be increased. Moreover, it should be directly applicable to stable cell lines producing other types of infectious virus and, with the proper modifications, may be extended to transient systems. We expect this approach to contribute to the progress of vaccine and gene therapy vector fields by accelerating cell line development and engineering.

Contents

1. Introduction.....	180
2. Materials and methods	182
2.1 Plasmids.....	182
2.2 Cell lines and culture conditions	183
2.3 Target cell line and retroviral vector producer cell line establishment ..	184
2.4 Quantification of vector transgene genomic copies	185
2.5 RNA extraction and quantitative real-time PCR for gene expression	185
2.6 Viral vectors production	186
2.7 Titration of infectious, genome-containing and total particles	186
2.8 Single-step cloning titration method procedure	187
2.9 Data analysis and density distribution curves.....	188
3. Results	189
3.1 Target cell line establishment and titer calibration	190
3.2 Method implementation and validation	192
3.2.1. Establishment of 293 FLEX GP S11 and 293 FLEX S11	192
3.2.2. Method validation – fast isolation of high-producing clones from a cell population	195
3.3 Method applications	196
3.3.1. <i>De novo</i> cell line establishment.....	196
3.3.2 Screening the production performance of alternative cell substrates ..	199
4. Discussion	201
5. Author contribution	204
6. References.....	204

1. Introduction

Retroviral and lentiviral vectors are efficient gene delivery tools and the most widely used viral vectors for the treatment of monogenic diseases and hematopoietic cell modification in gene and cell therapy (Edelstine 2013). As gene therapy moves from clinical to market (Moran 2012; Sheridan 2011), there is an increased pressure in the development of stable producer cell lines to meet the demands of vector production standardization. For the case of retroviral vector, stable production is common practice. For lentiviral vector, it has been more difficult to achieve due to the cytotoxicity of some viral proteins namely, the protease. Still, stable and continuous lentiviral vector productions have also been achieved (Ikeda et al. 2003; Stornaiuolo et al. 2013). For both vectors, infectious titers are usually low – 10^5 - 10^6 infectious particles *per* mL – requiring dozens to hundreds of liters of viral supernatant for a single patient (for a review see Coroadinha et al. (2010) and Schweizer and Merten (2010) for vector titers and Seymour and Thrasher (2012) for vector dose *per* patient). The use of high-titer stable producer cells is thus an important consideration for reducing the production costs, increasing quality by diminishing batch-to-batch variability and improving the efficiency of clinical protocols. Yet, stable cell line development is laborious and time consuming requiring from six months to one year.

In this work, we present a novel method for fast and high-throughput screening of retroviral vector producer cells by merging the two most time consuming steps in cell line development: cell cloning and virus titration. The method makes use of split-GFP®, a green fluorescent protein separated in two fragments – S10 and S11 – which fluoresce only upon transcomplementation. A cell population producing infectious virus with a S11 transgene is cloned and co-cultured with a titration cell line harboring the S10 fragment. During the period of clone expansion, S11 viruses infect the target cells and reconstitute the GFP signal. Only the clones yielding high signal are isolated, avoiding cell expansion, cell banking and posterior growth/titration studies of the low titer clones. Finally, S11 vector transgene is carried in a tagging construct, allowing for rapid

exchange to any therapeutic gene by Recombinase Mediated Cassette Exchange (RCME) (Coroadinha et al. 2006; Gama-Norton et al. 2011; Schucht et al. 2006).

Transcomplementing fluorescent proteins were initially conceived for intracellular localization studies (Cabantous et al. 2005). Herein, we used a transcomplementing GFP as a reporter gene to monitor and quantify viral infection in a co-culture system constituted by a virus producing colony and a layer of target cells (see Fig. 1). This setup provides a functional titration method, non-invasive for the producer cells and amenable to scale-down for high-throughput operation. A high-throughput screening method for retrovirus producer cells has been described by Green and Rasko (2002). Yet, this method needs the time to titrate clones supernatant upon the cloning procedure and makes use of fluorescent proteins that are expressed in the producer cell line, unlikely to be used in a clinical context. Another transcomplementing assay has been described based on the reconstitution of β -lactamase (Ou et al. 2012). This method, however, requires enzyme activity quantification upon substrate addition further analyzed by flow cytometry, limiting its high-throughput potential. The method implemented in this work reduces the time and manipulation required for the generation of high-titer producing clones since it ensures the titration and cloning procedures in one single step. The fluorescence signal arises exclusively and directly from viral infection without the need of any chemical substrate addition. Finally, the flexibility and swiftness of the implemented method demonstrated its usefulness for applications other than cell line establishment, namely, for screening for high-producing cell substrates and as a metabolic manipulation supporting tool, for studying the effects of external gene over-expression in the production dynamics of a cell population and allowing the isolation high-producing clones (please refer to Chapter VIII for metabolic engineering using this method).

2. Materials and methods

2.1 Plasmids

For all the plasmids constructed in this work primers and templates are listed in Table I (please refer to the end of Materials and Methods section). *pCMV mGFP S10* and *pCMV mGFP S11* contain a mammalian codon-optimized version of the GFP under the control of a CMV promoter, split in GFP S10 coding for the first 214 amino-acids, and GFP S11 for the last 15, respectively. These plasmids were acquired through SandiaBiotech (Albuquerque, NM, U.S.A). *pIRES GALEO* (kindly provided by Dr. Dagmar Wirth, Model Systems for Infection Research, HZI, Germany) is a murine stem cell virus (MSCV) based retroviral vector where LacZ is under the control of a LTR promoter and a fusion protein gene hygromycin B phosphotransferase/thymidine kinase (hygTk) is under the control of the encephalomyocarditis virus-internal ribosome entry site (EMCV-IRES). This vector contains two flippase recognition target (FRT) sites in the U3 of 3'LTR, a wild type FRT site (wt) and a spacer mutant FRT site followed by an ATG defective neomycin phosphotransferase gene (neo) (Verhoeven et al. 2001). This construction is present as a single copy in the genome of 293 FLEX and 293 FLEX GP (Coroadinha et al. 2006). *pEmMFG* (also kindly provided by Dr. Dagmar Wirth) is a recombinase mediated cassette exchange (RCME) targeting vector containing a FRT wt, an MLV based retroviral vector with an MFG-LTR deriving the expression of GFP followed by an EMCV-IRES element next to an ATG and F5 FRT site. ATG sequence and the F5 mutant FRT site complementing the neo gene in *pIRES GALEO* after targeting and subsequent cassette exchange (Coroadinha et al. 2006). *pTAR LacZ S11* was derived from *pEmMFG* in which GFP was replaced by LacZ-S11 obtained from *pCMV mGFP LacZS11*. *pCMV mGFP LacZS11* codes for a fusion protein LacZ-S11 under the control of a CMV promoter and was obtained by cloning LacZ gene (from *pIRES GALEO*) into the multiple cloning site (MCS) of *pCMV mGFP S11*. LacZ was amplified by PCR and introduced into the MCS at AgeI site. Both retroviral backbone and LacZ-S11 were amplified by PCR, using primers with NotI recognition site. *pRRLSIN LacZS11* and *pRRLSIN S10* were derived from

pRRLSIN GFP backbone, kindly provided by Dr. D. Trono from the Swiss Federal Institute of Technology (EPFL) through Addgene plasmid repository (Cambridge, MA, USA). This backbone is a 3rd generation lentiviral transgene vector, driving the expression of GFP from the hPGK promoter (human phosphoglycerate kinase) as described in Dull et al. (1998). For *pRRLSIN LacZS11* and *pRRLSIN S10*, GFP was replaced by LacZ-S11 or GFP S10 obtained from *pCMV mGFP LacZS11* or *pCMV mGFP S10*, respectively, isolated by PCR with primers carrying the NheI restriction site. *pRRLSIN* backbone was amplified in two fragments by PCR, with primers carrying NheI and PciI restriction sites. The cloning step involved three fragments: two fragments corresponding to the vector (PciI cloning site) and the insert (NheI cloning site). *pSVFLPe* contains FLP recombinase gene under a SV40 promoter as described in Coroadinha et al. (2006). *pCeB* is a vector containing MLV gag-pol and a blasticidin resistance gene (bsr) both driven by the MLV 5'LTR as described in Cosset et al. (1995). *pGalV* expresses the Gibbon Ape Leukemia virus (GalV) envelope protein and a zeocin (Zeo) (Coroadinha et al. 2006). *pMDLg/pRRE* and *pRSV-REV* are 3rd generation lentiviral vector packaging constructs containing HIV1 gag-pol and the second and third exons of HIV-1 REV, respectively. *pMD2G* expresses the envelope G glycoprotein of the vesicular stomatitis virus (VSV-G) under the control of CMV promoter. The three plasmids were kindly provided by Dr. D. Trono through Addgene and used for transient lentiviral vector production of *pRRLSIN* derived vectors as described in Dull et al. (1998).

2.2 Cell lines and culture conditions

HEK 293 is a Human Embryonic Kidney derived cell line (ATCC CRL-1573) used to establish HEK 293 derived retroviral vector producer cell lines in *de novo* cell line establishment. HEK 293T (ATCC CRL-11268) is a HEK 293 derived cell line expressing large T antigen from SV40 (simian vacuolating virus 40) used to transiently produce lentiviral vectors and also in *de novo* cell line establishment. Te 671 is a human rhabdomyosarcoma derived cell line (ATCC CCL-136) used to establish S10 target cell line and as target cells in LacZ staining titration protocol. 293 FLEX cell line is a HEK 293

derived cell line producing MLV based recombinant retroviral vectors expressing GaLV ecotropic envelope and harboring a LacZ reporter gene. 293 FLEX GP is the precursor cell line of 293 FLEX prior to envelope insertion; both cell lines have been described in (Carrondo et al. 2008; Coroadinha et al. 2006). 293 FLEX and 293 FLEX GP were used to establish retroviral vector LacZ-S11 transgene containing producer cells by RCME.

All cells were maintained in Dulbecco's modified Eagle's medium, DMEM, (Gibco, Paisley, UK) with 25 mM of glucose, 4 mM of glutamine, supplemented with 10% (v/v) Foetal Bovine Serum (FBS) (Gibco) at 37 °C in a humidified atmosphere containing 8% CO₂. In the case of fluorometer assays, DMEM without phenol red was used, containing 20% (v/v) FBS (Gibco) and (1X) B27 supplement (Gibco).

2.3 Target cell line and retroviral vector producer cell line establishment

The target cell line was developed by stable expression of GFP S10 gene mediated by lentiviral vector infection into Te 671 using *pRRLSIN S10* vector. Since this vector does not contain a selectable marker, a multiplicity of infection (MOI) of 30 – to assure synchronous infection and multiple copies *per* cell – was used. Cells were cloned by limiting dilution and clones were analyzed for GFP transcomplementation after infection with LacZ-S11 retrovirus to select high transcomplementation clones.

Two types of retroviral vector producer cells were developed in this work. For method validation, site-specific recombinase mediated cassette exchange (RCME) was used to exchange 293 FLEX GP transgene from LacZ to LacZ S11 using *pTAR LacZ S11* plasmid; transfection and selection procedure is described in Coroadinha et al. (2006). The clones were amplified and analysed for correct cassette exchange and number of copies of *pTAR LacS11* integrated. A cell population producing GaLV pseudotyped infectious retroviral vector was finally established by stable transfection of *pGaLV* (5 µg of DNA *per* million of cells), after 3 weeks under zeocin selective pressure. This population was used to validate to the Single-Step Cloning Titration method.

For *de novo* cell line establishment, HEK 293 and HEK 293 T were chemically transfected using polyethylenimine (PEI) with the retroviral vector constructions, *pCeB*

and *pGalV* and infected with a transiently produced stock of LacZ-S11 retrovirus. 5 µg of DNA *per* million of cells were used for each plasmid and MOI of 8 was used for vector infection.

2.4 Quantification of vector transgene genomic copies

For the quantification of genomic copies of vector transgene, genomic DNA was isolated using the QIAamp® DNA Mini and Blood Mini Kit (Qiagen, Valencia, CA, USA) according to manufacturer's instructions. PCR with specific primers for LacZ and Neo gene (Table I, please refer to the end of Materials and methods section) was performed and PCR amplification products were separated in agarose gel. Depending on the PCR product size it was possible to confirm if cassette exchange was successful. To estimate the number of copies *per* cell, genomic DNA was quantified by qRT-PCR using primers for LacZ gene (Table I) on a thermocycler LightCycler® 480 Real-Time PCR System (Roche Applied Science) using LightCycler® 480 SYBR Green I Master (Roche Applied Science) PCR kit. The number of copies *per* cell was quantified relatively to a single copy control (293 FLEX) after normalization to a control gene (RPL22) using $2^{-\Delta\Delta CT}$ method (Livak and Schmittgen 2001). Single copy was considered for values below 1.4 (Bodin et al. 2005).

2.5 RNA extraction and quantitative real-time PCR for gene expression

Total RNA was extracted using RNeasy Mini Kit (Qiagen, Valencia, CA) according to the manufacturer's instructions. The resultant RNA pellet was eluted in 100 µL of nuclease-free water (Qiagen) and stored at -85°C until further processing. RNA yields were quantified using NanoDrop 2000 (Thermo Scientific, Waltham, MA, USA). For real time PCR, RPL-22 was chosen as a control gene. Forward (F) and reverse (R) primer sequences for all the genes assessed are given in Table I (please refer to the end of Materials and methods section). The reverse transcription of total RNA was performed according to Transcriptor High Fidelity cDNA Synthesis Kit (Roche Applied Science, Mannheim, Germany) protocol for cDNA synthesis using 2 µg of total RNA and oligo dT primer for total mRNA reverse transcription. The reverse transcribed (RT) product was

aliquoted and stored at -20°C until further processing. SYBR Green I dye chemistry was used to detect the PCR products using LightCycler® 480 SYBR Green I Master (Roche Applied Science) according to the manufacturer's instructions using LightCycler® 480 Real Time PCR System (Roche Applied Science). cDNA samples were run along with a no RT-reaction control and a no cDNA template sample.

2.6 Viral vectors production

For lentiviral vector transient production the 3rd generation lentiviral packaging system and the transfection procedure described in Dull et al. (1998) were used.

The stocks of retroviral vector used in *de novo* cell line establishment harboring the LacZ-S11 reporter gene were obtained by polyethylenimine (PEI) mediated transient transfection using *pCeB* to provide the packaging functions, *pMD2G* for the VSV-G envelope and *pTAR LacZ S11* for the transgene. A total of 5 µg of DNA *per* million of cells was used with a DNA ratio of 2:1:3.

For retroviral vector produced with stable cell lines, clones and populations were screened using a 48+24 hours production/harvesting operation described in Chapter II (Rodrigues et al. 2013).

In all the cases, viral vector supernatants were filtered through 0.45 µm cellulose acetate filter for clarification, aliquoted and stored at -85°C until further use.

2.7 Titration of infectious, genome-containing and total particles

For LacZ based staining titration, infectious procedure and viral titer determination were performed by limiting dilution infection assay, as described in Rodrigues et al. (2009). Genome-containing particles were quantified by qRT-PCR using the method described in Carmo et al. (2004) but using LacZ primer set for qRT-PCR given in Table I. Physical (total) particles were assessed by nanoparticle tracking analysis using NanoSight® NS500 (NanoSight Ltd., Wiltshire, UK).

For GFP transcomplementation titration, Te 671 S10 target cells were seeded at 5×10^4 cells/cm² in 24-well plates 24 hour before infection. Transduction was performed by

removing the cell supernatant and infecting with 0.2 mL of viral suspension using several dilutions in fresh DMEM (Gibco) with 10% (v/v) FBS and 8 µg/mL of polybrene (Sigma). Cells were incubated at 37°C overnight after which 0.5 mL of fresh supplemented DMEM was added. Two days after infection, cells were harvested and analyzed for GFP fluorescence by flow cytometry (CyFlow-space, Partec GmbH).

2.8 Single-step cloning titration method procedure

Producer cells were cloned by limiting dilution in Corning CoStar black-wallet with clear bottom 96-well plates (Corning, New York, NY, USA). The final volume was 150 µL/well and border-wells were avoided for cloning, filled with 280 µL of PBS to minimize medium evaporation from the cloning wells. Typically, 10 cloning plates were prepared, thereby corresponding to a total of 600 cloning wells. Cell seeding inoculum was 0.7 cells/well. Under these conditions (see also section 2.2 for culture medium and supplements), the cloning efficiency was found to be around 50%, thus corresponding to approximately 200 clones *per* analysis. A negative control plate was prepared (to assess background) using the same cloning medium/conditions but without containing the cells to be cloned. After 6 days, the target cells were added at a seeding density of 250 cells/well to all plates (including the negative control) corresponding to 50 µL of target cell suspension at 5×10^3 cells/mL. At day 7, day 9 and day 11 polybrene (Sigma) was added at a final concentration of 5 µg *per* mL on day 7 and 9 and 10 µg *per* mL on day 11. At day 11 it was also performed an agitation period of 15-30 minutes using a rocking table to potentiate the spreading of viral infection through the well. At day 15 culture medium was aspirated off and replaced by 50 µL of PBS containing 5% (v/v) FBS (Gibco). Fluorescence reading was performed in a fluorometer plate reader FLx800 (Biotek, Vermont, USA) using a 485/20 emission and a 528/20 absorption filters (Biotek).

2.9 Data analysis and density distribution curves

Fluorescence values were ordered from smaller to largest. High-GFP yielding wells were microscopically inspected to guarantee single colony and those containing double colonies were eliminated from the raw data. Raw data was background subtracted. Background corresponds to the average fluorescence value of the control plate containing only target cells, prepared and treated as the cloning plates. Background subtracted values yielding negative values were also removed from the raw data. The remaining were processed for density distribution curve generation in MATLAB™ 7.10 (The MathWorks Inc., Natick, MA, 2000), using the function *ksdensity()*. Kernel density distribution was chosen as it is a non-parametric method allowing density estimation without imposing any curve distribution type; for further detailed on kernel smoothing see Wand and Jones (1995).

Table I – Primers for cloning, PCR and qRT-PCR

Cloning primers				
Final Construct	Insert		Cloning vector	Primers (5' → 3' sequence)
	Fragment	Source		
pCMV mGFP LacZ S11	LacZ	pIRES GALEO	pCMV mGFP S11	F - ATCCTACCGGTATCCAGCCCTCACTCCTTCTC R - CGACTACCGGTTGACACCAGACCAACTGGTAAT
pTAR LacS11	LacZ-S11	pCMV mGFP LacZ-S11	pEM MFG	F - GCGTGTACGGTGGGAGGTCTAT R - GGGGAGGTGTGGGAGGTTTT
pRRlsin S10	GFP 1-10	pCMV mGFP S10	pRRlsin eGFP	F - GTGAACCGTCAGATCCGCTAGCCG R - GGCTGGCTAGCATCAGTTATCTAGATCCG
pRRsin LacZ S11	LacZ-S11	pCMV mGFP LacZ-S11		R - GGGGAGGTGTGGGAGGTTTT R - GTTTTGCTAGCCAAGTAAACCTCTACA
PCR for cassette exchange evaluation				
Hybridization site	Amplicon size (kb)		Primers (5' → 3' sequence)	
	Before RCME	After RCME		
LacZ (end)	3.8	2.3	F - CTACCGGATTGATGGTAGTGGT	
Neomycin (beginning)			R - AGCCATGATGGATACTTTCTCG	
qRT-PCR				
Gene	Primers (5' → 3' sequence)			
Viral transgene (LacZ)	F - ACTATCCCGACCGCCTTACT			
	R - TAGCGGCTGATGTTGAACTG			
Gag-pol	F - GTCCAATATCGCCAGTTGCT			
	R - CTGGTCTCAGGGTCATAA			
Envelope	F - GGACAAAATAGCGAATGGA			
	R - GGTGAACTGTACGCCTGGAT			
RPL22	F - CTGCCAATTTTGAGCAGTTT			
	R - CTTTGCTGTTAGCAACTACGC			

3. Results

To reduce the clone screening time in virus producer cell line development, a protocol merging the steps of cloning and titration was implemented – the single step cloning-titration method, SSCT, from herein on. Taking advantage of stable cell lines used in retroviral vector production, which favours protocol design, the method is based on a transcomplementation assay using a Split GFP[®], where part of it is encoded by the retroviral vector transgene and the other part stably expressed in the cells to be infected (target cells) (Fig. 1).

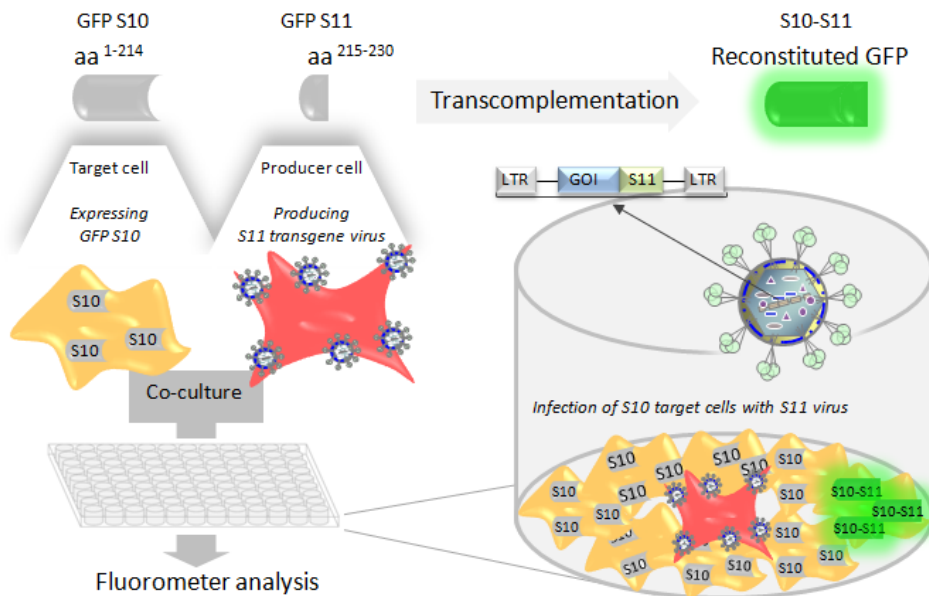


Figure 1 – Schematic representation of the single-step cloning titration method. Viral transgene carries S11 fragment fused to a gene of interest, in this case, a second reporter – LacZ. S10 fragment is stably expressed in the titration cell substrate. Producer cells are cloned and co-cultured with the target cells (S10 titration substrate) and during the period of clones expansion (two weeks) target cells are infected with the viruses produced by the clone reconstituting the GFP signal. Clones and target cells are cultured in black-wallet 96 well plates with clear bottom analyzable in a fluorometer plate reader using the 485/20 emission filter and 528/20 absorption filters. High producing clones originate high GFP signals. The Split GFP[®] used in this work is a mammalian codon-optimized version of the one described in Cabantous et al. (2005), a green fluorescent protein under the control of a CMV promoter separated in GFP S10 coding for the first 214 amino acids (aa) and GFP S11 for the last 15, respectively. GOI: gene of interest, in this case, a second report – LacZ – for method validation.

The method makes use of black-wallet 96 well plates with clear bottom where the retroviral vector producer clone is seeded followed by two-week incubation for cell

expansion. During this period target cells are co-cultured in each well being infected by S11 viruses produced by the clone and reconstituting the GFP signal. After two weeks the clones are selected based on the highest GFP signal using a fluorometer plate reader. The GFP signal arises from the target cell line after GFP S10 transcomplementation with GFP S11 fragment delivered through infection of the retrovirus produced by the clone (Fig. 1). High producing clones can be isolated from the target cells by any of the viral components selectable markers.

3.1 Target cell line establishment and titer calibration

To establish the target cell line (titration substrate), Te 671 cell line routinely used for titrating GaLV pseudotyped retrovirus was used. Chemical transfection by polyethylenimine (PEI) was initially used to deliver *pCMV mGFP S10*, followed by neomycin selection of the transfected population. However, the population and its derived clones did not present sufficient S10 expression levels for high transcomplemented GFP signals (data not shown). Therefore, GFP S10 was cloned into a lentiviral vector (*pRRLSIN S10*) and used to infect Te 671 cells at high multiplicity of infection (MOI, approximately 30). This ensured a high number of GFP S10 gene copies being delivered to each cell. From this population, 21 clones were screened for GFP transcomplementation (Fig.2A).

The key parameters in this screening were: i) a high number of transcomplemented cells for low multiplicity of infection (approx. 0.2), to guarantee a detectable signal under the protocol conditions (higher number of target relatively to producer cells), and ii) a high signal to noise ratio, to minimize the number of false positive wells. The latter is of particular importance as S10 expression was found to increase the background signal. The majority of the clones presenting high signal to noise ratio (>10), failed to deliver the expected percentage of GFP⁺ cells (approximately 20%, according to the MOI). This was due to low noise rather than to high signal, thus, suggesting low S10 levels. Also, none of the clones delivered 20% of infected cells, being the maximum

percentage around 6%. However, the MOI was calculated based on LacZ determined titer which was found to over-estimate GFP transcomplementation in about 5-fold (Fig. 2B). Thereby, 4-6% of GFP⁺ cells should correspond to the maximum expectable, which was in fact observed (Fig. 2A). Among the clones delivering at least 4% of GFP⁺ cells, the best signal to ratio was achieved with clone #27.

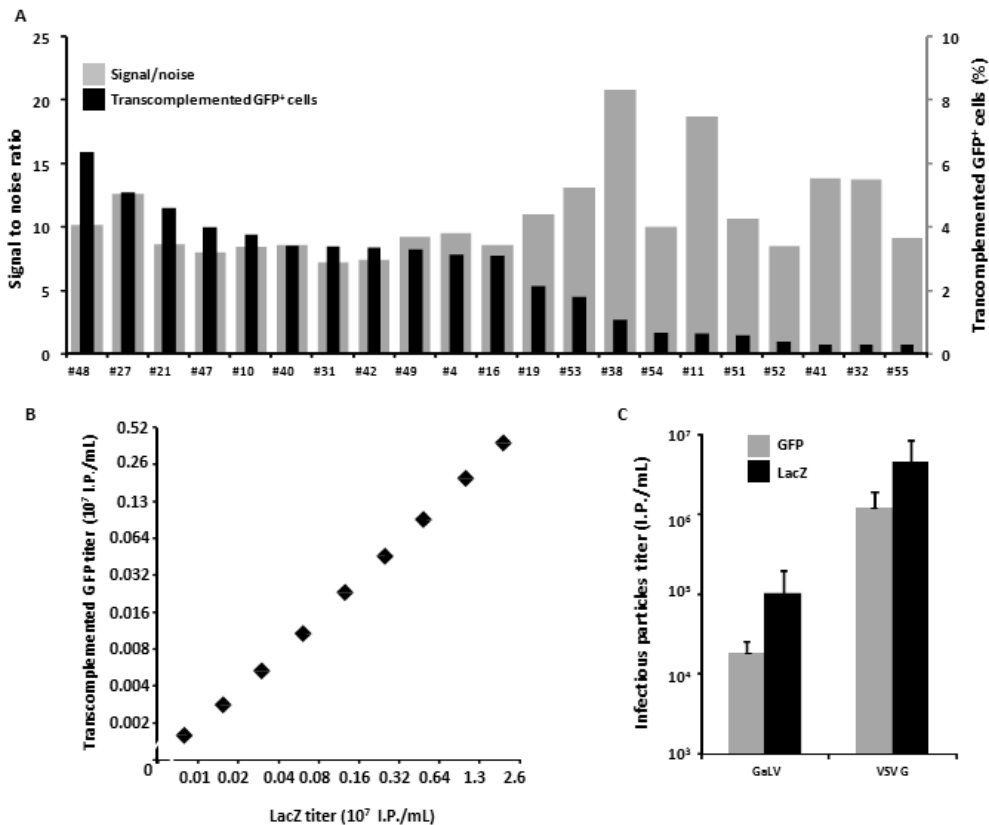


Figure 2 – Establishment of S10 titration cell substrate and comparison of GFP transcomplementation vs. LacZ titers. Signal to noise ratio and GFP transcomplemented positive cells of the different Te 671 S10 clones (A). Signal to noise was defined as the ratio of mean fluorescence intensity of GFP positive (infected) cells to non-infected cells, analyzed by flow cytometry. Infection was performed at multiplicity of infection of 0.2 using a defined dilution of a transiently produced stock of VSV-G pseudotyped retroviral particles. Serial dilutions of a stably produced LacZ_S11 retrovirus stock were titrated by traditional LacZ staining in Te 671 cells or by GFP transcomplementation using Te 671 S10 #27 target cells (B). Correlation coefficient (R^2) = 0.999, given by least squares linear regression. Linear regression fit with slope=0.2 indicating a 5-fold underestimation of GFP transcomplementation relatively to LacZ titer. Average titer of triplicates; for a matter of simplicity error bars were omitted ranging from 1 to 6% in transcomplemented GFP and 5 to 17% in LacZ determinations. Average infectious particles titers of the two reporter proteins encoded by *LacZ-S11* transgene of retrovirus transiently produced and pseudotyped with GalV and VSV-G envelope (C). Error bars represent standard deviation (n=3). GalV – Gibbon Ape Leukemia Virus; VSV-G – Vesicular Stomatitis Virus G Protein.

Using Te 671 S10 #27, LacZ titers were compared to those obtained by GFP transcomplementation (Fig. 2B). Although presenting high correlation coefficient ($R^2=0.999$), GFP transcomplementation yielded an absolute titer under-estimation of 5-fold relatively to LacZ (Fig. 2B). This was also observed for different envelopes – GaLV and VSV-G – with an underestimation of approximately 5- and 4-fold, respectively (Fig. 2C). Since GFP titers were lower than those obtained by LacZ we hypothesized that GFP titration was affected by insufficient levels of GFP S10 expression in Te 671 S10 #27 cells. Thus clone #27 was re-infected with lentivirus containing GFP S10 transgene (MOI of 30) and analyzed for GFP transcomplementation. However, GFP transcomplementation titers were found to be identical between Te 671 S10 #27 and its S10 re-infected derived population (data not shown), suggesting that the underestimation obtained by GFP transcomplementation was not due to insufficient S10 expression. This underestimation is, however, an advantage since GFP signal saturation will only occur for very high titer clones.

3.2 Method implementation and validation

3.2.1. Establishment of 293 FLEX GP S11 and 293 FLEX S11

Two retroviral vector producer cell lines were established in this work: i) 293 FLEX GP S11 and 293 FLEX S11. Both cell lines derive from 293 FLEX cell line (Coroadinha et al. 2006), after recombinase mediated cassette exchange (RMCE) from LacZ to LacZ-S11 fusion retroviral transgene. 293 FLEX GP is the envelope-free precursor cells of 293 FLEX and was used for method validation (section 3.2.2). 293 FLEX S11 were used as a control of cassette exchange from LacZ to LacZ-S11.

For method validation, recombinase mediated cassette exchange (RMCE) technology was used to target 293 FLEX GP and exchange the LacZ retroviral vector transgene to LacZ-S11 fusion transgene, establishing the 293 FLEX GP LacZ S11 (Fig. 3). More than 60 clones were analyzed from the exchanged population and tested for GFP transcomplementation. Among transcomplementing competent clones, 10 were

isolated and analyzed by PCR and qRT-PCR for correct targeting and copy number (Fig. 3D).

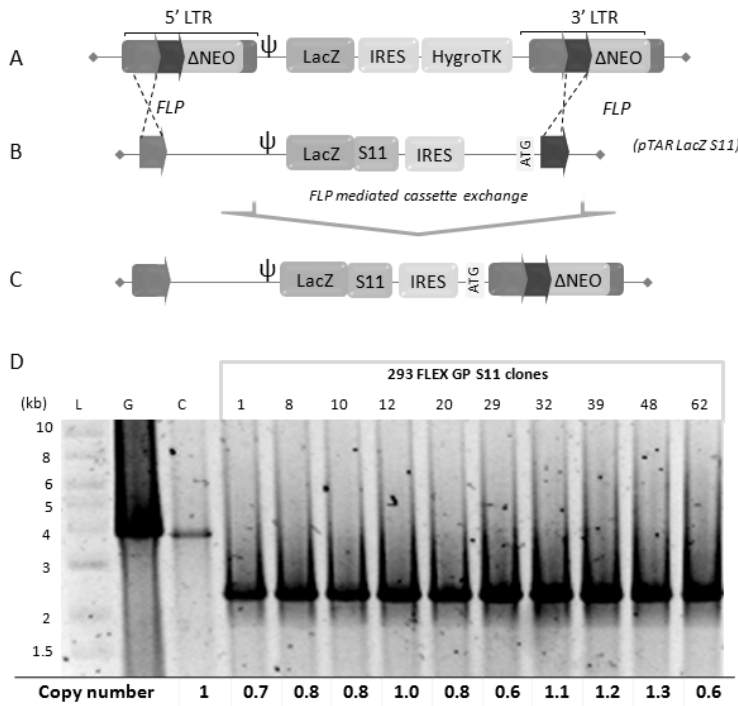


Figure 3 – Cassette exchange in 293 FLEX GP. Tagged vector transgene in 293 FLEX as described in (Coroadinha et al. 2006; Schucht et al. 2006) (A). Target construct (*pTAR LacZ S11*), used to exchange 293 FLEX GP and 293 FLEX viral transgene (B). Integrated targeting cassette after flp mediated cassette exchange (C). Correct cassette exchange is indicated by the loss of 1.5 kb in the integrated cassette, relatively to the tagging cassette (A). Electrophoresis in 0.7% (w/v) agarose gel of the PCR reaction performed to amplify the transgene sequence from genomic DNA of 293 FLEX GP after transgene exchange from LacZ to LacZ-S11 (D). Numbers above the lanes correspond to targeted clones

293 FLEX GP S11 (after cassette exchange). The numbers below the lanes indicate the ratio of copy number relatively to a single copy control (293 FLEX) of targeted transgene given by genomic DNA quantification by qRT-PCR using primers for LacZ gene. The number of copies per cell was quantified after normalization to a control gene (RPL22) using the $2^{-\Delta\Delta Ct}$ method as defined in Materials and methods. L – ladder; G – *pIRES GALEO* plasmid (tagging construct); C – positive control of 293 FLEX GP (before cassette exchange).

Transgene exchange was confirmed by the loss of approximately 1.5 kb in amplicon size in all 293 FLEX GP S11 clones while maintaining single copy. One of the exchanged clones (clone #32) was selected to establish an envelope-containing retroviral vector producer population by stable transfection of *pGalV*. This population was used for method validation (please refer to section 3.2.2).

As part of a control, 293 FLEX, the retroviral vector producer cell line derived from 293 FLEX GP by stable insertion of the GalV envelope (clone #18, Coroadinha et al. (2006)) was also subjected to RCME to exchange the LacZ retroviral vector transgene to LacZ-S11 fusion transgene. As described for 293 FLEX GP S11, exchanged clones were

tested for GFP transcomplementation and analyzed by PCR and qRT-PCR for correct targeting and copy number (data not shown). Finally, the selected exchanged clones, both from 293 FLEX GP S11 and 293 FLEX S11 were analyzed for retroviral vector particles production and vector components gene expression and compared to their respective parental non-exchanged cell lines (Table II).

Table II - Retroviral vector particles production and vector components gene expression of 293 FLEX, 293 FLEX GP and derived S11 exchanged clones

		293 FLEX	293 FLEX S11	FC	293 FLEX GP	203 FLEX GP S11	FC
Cell growth	Duplication time (h)	36 ± 4	36 ± 3	-	33 ± 3	28 ± 3	-
Viral particles	I.P./mL (10 ⁶)	1.6 ± 0.4	13.0 ± 2.5	8	N/A	N/A	N/A
	I.P./Cell.h	0.03 ± 0.01	0.33 ± 0.08	10	N/A	N/A	N/A
	G.P./Cell.h	14 ± 3	17 ± 4	-	19 ± 4	32 ± 6	2
Gene expression (2 ^{-ΔCT})	Transgene	0.7 ± 0.3	2.2 ± 0.3	3	0.9 ± 0.1	3.9 ± 0.2	4
	Gag-Pol	2.6 ± 0.8	1.9 ± 0.2	-	4.1 ± 0.3	2.4 ± 0.1	-
	Envelope	1.1 ± 0.4	1.5 ± 0.1	-	N/A	N/A	N/A

I.P.: Infectious particles

G.P.: genome-containing particles

FC: fold-change relatively to non-exchanged parental cells (293 FLEX for 293 FLEX S11 and 293 FLEX GP for 293 FLEX GP S11)

N/A: not applicable

Cell growth kinetics was found to be relatively unchanged after cassette exchange for both 293 FLEX S11 and 293 FLEX GP S11. However, infectious particles production of 293 FLEX S11 increased almost one order of magnitude relatively to the non-exchanged cell line. Genome-containing particles titer remained identical for 293 FLEX S11, suggesting that the total number of produced particles was the same. Indeed, gag-pol expression levels, the vector component related to the amount of physical particles produced, remained unaltered. Similar results were found for 293 FLEX GP S11, although presenting a slight increase (2-fold) in genome-containing particles titer. Envelope expression levels in 293 FLEX S11 remained unchanged. Vector transgene expression, on the other hand, was increased 3 and 4-fold for 293 FLEX S11 and 293 FLEX GP S11, respectively. These differences might be explained by the use of an MFG retroviral vector for the targeting construct (*pTAR LacZ S11*). Expression of a transgene from MFG vectors can be 10- to 50-fold higher sustained on high levels of genomic RNA (Byun et al.

1996). These observations are in line with the results from Table II and may explain the reason why, for the same amount of genome containing particles, those from MFG-expressed backbones appear to be transcriptionally more active (higher titers).

3.2.2. Method validation – fast isolation of high-producing clones from a cell population

For method validation, the envelope-free precursor cells of 293 FLEX (293 FLEX GP, Coroadinha et al. (2006)), were used (Fig. 3). These cells produce transgene containing but non-infectious murine leukemia virus (MLV) based virions as they lack the envelope. Upon envelope integration, a cell population containing clones with different productivity levels should be obtained. One of the exchanged clones of 293 FLEX GP S11 was selected to establish an envelope-containing retroviral vector producer population by stable transfection of *pGalV*. The method was validated using this selected population; cloning wells were microscopically inspected and the density distribution profile of the producing population was evaluated (Fig. 4).

This distribution comprises about 200 clones originating, the majority of them, low to medium transcomplemented GFP signals (500-3000 RFU) whereas only a minority of them fell in high fluorescence signal range (>4000 RFU). Note that it cannot be confidently defined the minimum fluorescence value for which a cloning well contains a colony, since this would imply microscopically inspecting all the 600 wells. While the selected population presented an average titer of 1.6×10^6 I.P./mL, when isolating clones from the different fluorescence ranges, it was possible to discriminate productivity levels between 1×10^5 to 1×10^8 infectious particles *per* mL (Fig.4). Moreover, transcomplemented GFP signal was found to estimate well the clone productivity as colony size variation was considerably lower (between 0.5 and 3x the average) than titer variation (between 0.1 and 100x the average).

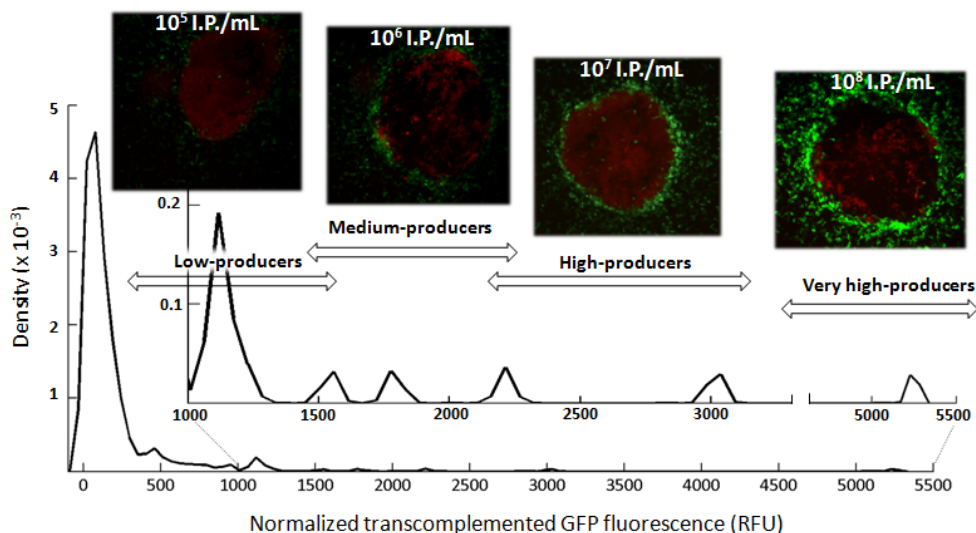


Figure 4 – Density distribution of 293 FLEX GP S11 GaLV population. Kernel density distribution curve of 293 FLEX GP S11 after GaLV envelope stable transfection. The distribution comprises approximately 200 clones corresponding to 10 cloning plates, of 60 wells each, at a seeding density of 0.7 cells/well assuming 50% cloning efficiency. Normalized fluorescence indicates background subtracted values, being background the average relative fluorescence units of a plate containing only target cells. Fluorescence microscopy pictures show colonies of 293 FLEX GP S11 GaLV clones (in red) and the Te 671 S10 target cells infected with retrovirus carrying LacZ-S11 transgene produced by the clone (in green) after the two-week expansion period. For imaging purposes, producer cells express mCherry for a better visualization of the colonies. Arrows indicate typical fluorescence range associated to the mentioned titers (note that these are approximations) and the clones from the pictures were isolated from these ranges.

3.3 Method applications

3.3.1. *De novo* cell line establishment

In the first part of this work, the SSCT method was implemented and validated using 293 FLEX GP S11, after envelope stable transfection. However, 293 FLEX have been developed based on a stoichiometry optimization strategy of the vector components – for high infectious particles titer and high infectious to total particles content – and have required extensive clone screening in-between viral cassettes insertion (Carrondo et al. 2008). The potential of SSCT method was thus tested to search for identical performances, without the need of stoichiometric optimization or clone selection in-between the intermediate steps of integration of the viral components. Transgene, gag-

pol and envelope were sequentially transfected and selected into nude HEK 293. The final population was subjected to the SSCT. As a control, 293 FLEX S11 were also subjected to SSCT. 293 FLEX S11 were derived from 293 FLEX 18 (Coroadinha et al. 2006) through RCME to exchange the LacZ transgene to LacZ-S11 fusion as described for 293 FLEX GP (section 3.2.1). The results are shown in Figure 5.

Even without stoichiometric optimization, clones producing up to 1×10^8 infectious particles *per* mL were isolated. It was also evident that transcomplemented GFP signal is not a direct measurement of clone titer but instead an estimation. Indeed, the highest-titer clone isolated was not the one yielding the highest transcomplemented GFP signal but the one before (Fig. 5B). These variations arise mainly from variations in colony location on the well: centered colonies yield GFP signal concentrated in the middle of the well where the readings are performed. Also, high-transcomplemented GFP yielding clones (RFU>3000) were those presenting the highest ratios of infectious to total particles, suggesting that the method not only allows the identification of high-titer clones but also low defective particles content.

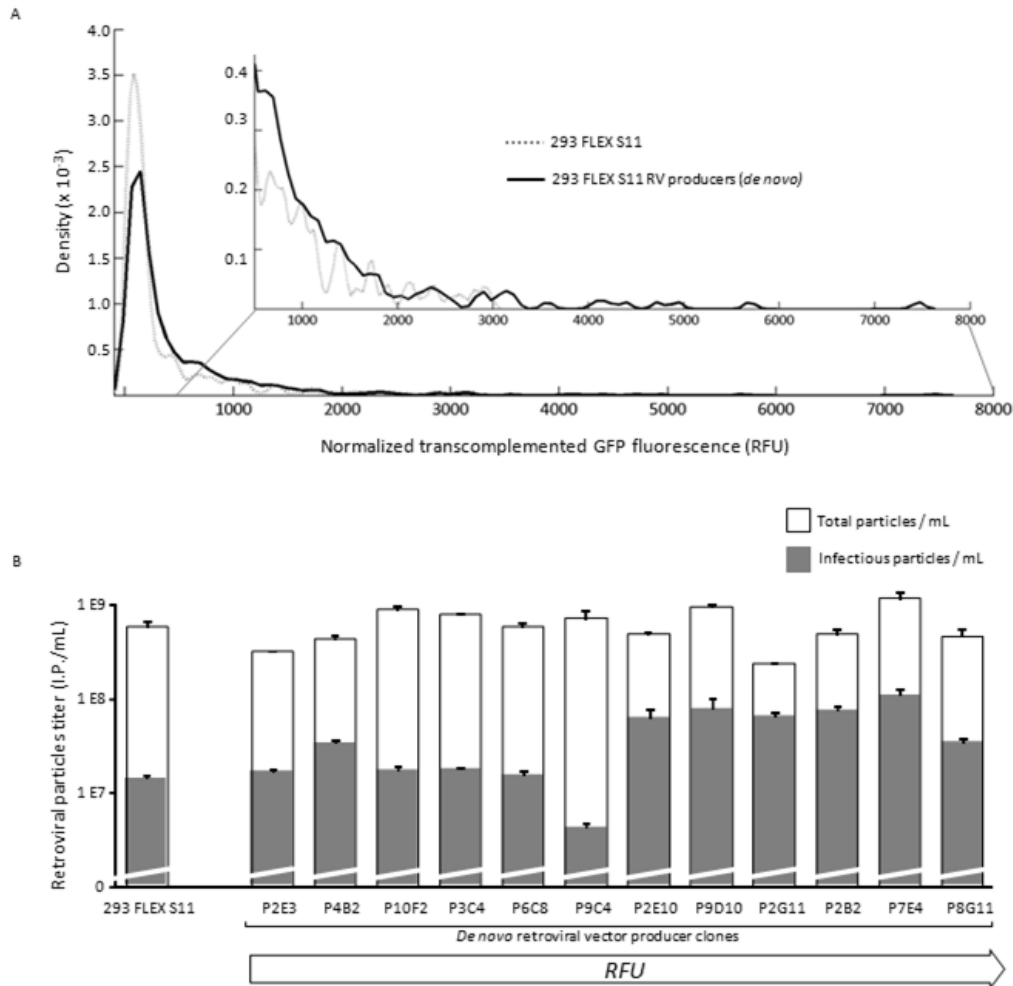


Figure 5 – Applications of SSCT method: *de novo* cell line establishment. Kernel density distribution curve of retroviral vector producer cells established from nude HEK 293 cells (A). Normalized fluorescence indicates background subtracted values. Cells were established by transfecting the three vector components (gag-pol, envelope and vector transgene) without clone screening and isolation in-between intermediated steps. 293 FLEX S11, derived from 293 FLEX 18 (Coroadinha et al. 2006) through RCME to exchange the LacZ transgene to LacZ-S11 fusion as described for 293 FLEX GP (section 3.2.1), is shown as a control. Gag-pol and envelope were delivered by PEI chemical transfection using 5 μ g of DNA per million of cells for each component, separately and sequentially, followed by the respective antibiotic selection. Vector transgene was delivered by infection, MOI of 8, using a transiently produced retrovirus stock pseudotyped with VSV-G envelope and using *pTAR LacZ S11* viral transgene. High-titer clones isolated from *de novo* cell line establishment using viral transgene from *pTAR LacZ S11* (B). Clones are ordered by (normalized) fluorescence. White bars represent average total particles and error bars represent standard deviation ($n=4$) quantified by nanoparticle tracking analysis. Gray bars represent average infectious particles and error bars represent standard deviation ($n=3$) quantified by LacZ staining. RFU: relative fluorescence units. Clones are named after the plate and well number (e.g.:P2E3: cloning plate 2; well E3).

3.3.2 Screening the production performance of alternative cell substrates

The density distribution curve provides valuable information on the productivity performance of a cell population, both by the identification of high-producing clones, as well as by the density (amount of clones) falling into high transcomplemented GFP ranges. With this in mind, the SSCT method was used to evaluate the retroviral vector production performance of two different cell substrates: HEK 293 and HEK 293T. Recently, Gama-Norton and colleagues demonstrated that HEK 293T deliver increased lentiviral titers comparatively to HEK 293 (Gama-Norton et al. 2011). The authors suggested that this improved performance was due to physiological changes induced by the expression of large T antigen itself rather than by a more favorable episomal replication of SV40 *ori* containing plasmids, typically used in retro and lentiviral vector constructions in transient production. These observations were tested using the SSCT method. A *de novo* cell population producing retroviral vector was established as described in 3.3.1, using HEK 293 and HEK 293T. After selecting for each of the viral components, the productivity performance of both populations was assessed by the SSCT method (Fig 6A).

The distribution curve of HEK 293T population presented four times higher clone density (8% of the population) in the range RFU>3000 – corresponding to the high-titer clones – than the one of HEK 293 (2% of the population). Indeed, when analyzing those clones, we found 3 from the 12 HEK 293T derived clones producing in the order of 10^8 infectious particles *per* mL. For those derived from HEK 293, only 1 out of 12 produced in the same order of magnitude. It should be noted, however, that, in this case, the colony size bias a direct comparison of the fluorescence values between HEK 239 and HEK 293T since the later grow considerably faster than the former. Still, even when a factor for colony size normalization was applied, the density of high-fluorescence clones in HEK 293T was about three times higher than in HEK 293. To eliminate the advantage of a more favorable episomal replication in HEK 293T, none of the viral constructions contained SV40 *ori* sequences. Still, HEK 293T present higher transfection efficiencies

than HEK 293, potentially favoring increased amounts of DNA integration into a stably selected population and derived clones. Thus, gene expression of the viral components was quantified by qRT-PCR (Fig.6B).

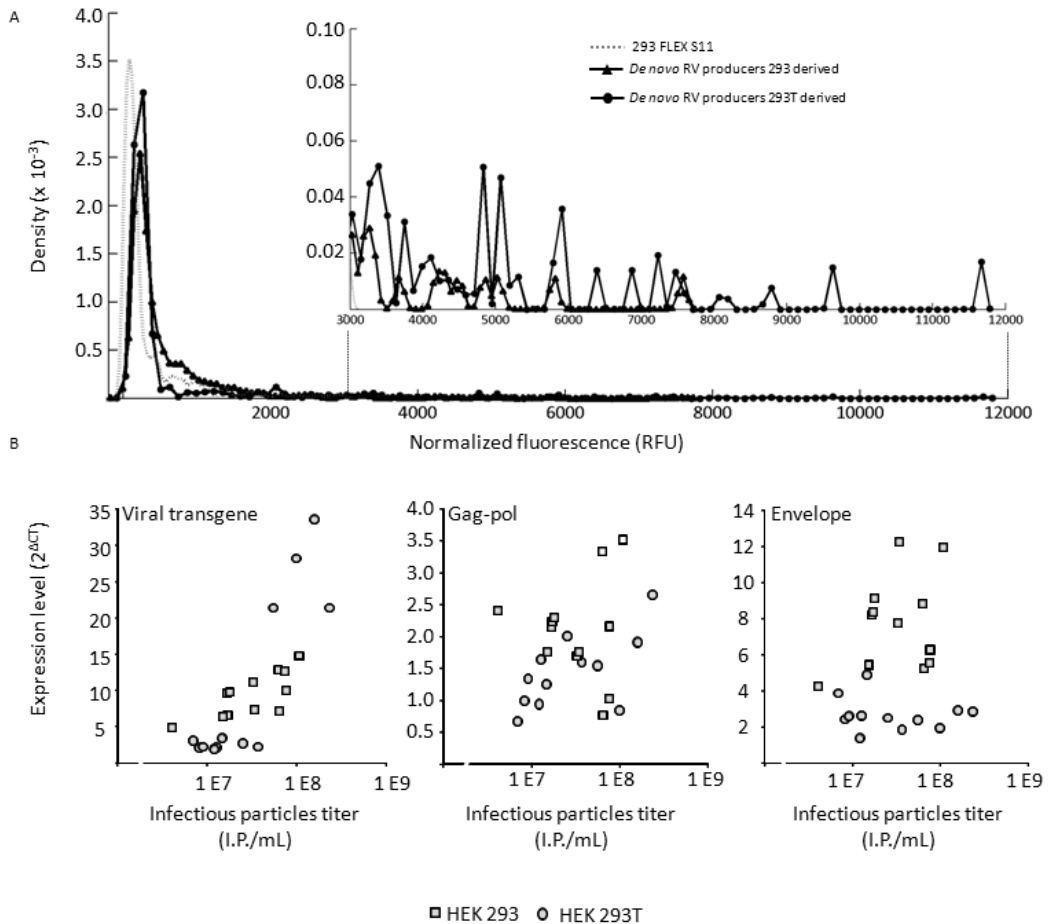


Figure 6 – Applications of SSCT method II: cell substrate comparison. Kernel density distribution curves comparing the production performance of HEK 293 vs. HEK 293T (A). Each distribution comprises approximately 200 clones corresponding to 10 cloning plates, of 60 wells each, at a seeding density of 0.7 cells/well assuming 50% cloning efficiency. Normalized fluorescence indicates background subtracted values, being background the average relative fluorescence units of a plate containing only target cells. For both substrates, a cell population was established as described in Fig. 5. Viral components expression vs. infectious particles titer of high-titer clones isolated from *de novo* cell line establishment using HEK 293 (□) and HEK 293T (○) cell substrates (B). Viral titers represent average infectious particles (n=3) quantified by LacZ staining as described in (Rodrigues et al. 2009) and vector components expression represents average expression level normalized to the RPL22 housekeeping control ($2^{\Delta CT}$) (n=2). Packaging (gag-pol) and envelope expression significantly higher ($p < 0.005$) in HEK 293 than in HEK 293T clones, given by a one-tailed *t*-test assuming unequal variance.

The results showed that, the increased titers obtained with HEK 293T clones are not due to an increased viral components expression, relatively to HEK 293. Although high-titer clones presented higher expression levels of viral transgene in HEK 293T, this was the exception as HEK 293 clones presented, on average, increased viral components expression, particularly evident in the case of the envelope and gag-pol (Fig.6B).

Another application of the SSCT method is as a metabolic manipulation supporting tool, for studying the effects of external gene over-expression in the viral production dynamics and allowing the isolation high-producing clones (please refer to Chapter VIII for metabolic engineering using this method).

4. Discussion

The development of stable retroviral vector producer cell lines is a laborious and time consuming process. Additionally, stable cell lines deliver relatively lower titers than, for instance, transient production processes, translated in dozens to hundreds of viral supernatant liters for each patient to be treated (Stacey and Merten 2011). Strategies assisting the identification of high-producing clones will alleviate the drawbacks of the low-titers and the heavy time-frames in stable cell line development. On the other hand, cell engineering approaches (Rodrigues et al. 2013), new vector designs (Schambach et al. 2007) and strategies based on mutagenesis (Vu et al. 2008) are also contributing for improved titers, attractive viral properties (e.g., thermal stability) and increased safety. In all the cases, a high-throughput screening tool is of the utmost importance to identify high-producing clones and high-titer generating mutations or other genetic manipulations.

In this work, we sought for implementing a high-throughput method handling the analysis of hundreds of retroviral vector producing clones in a relatively short period of time, to assist *de novo* cell line establishment, and cell/vector engineering approaches. This method reduces the time and manipulation required for the identification of high-

titer clones since it ensures that the titration and cloning procedures are performed in one single step. Cell viability and sterility is maintained during the analysis and high-titer clones can be further isolated after the assay. The viral transgene can be exchanged to other gene of interest by recombinase mediated cassette exchange (Coroadinha et al. 2006; Schucht et al. 2006). The LacZ-S11 transgene enables the expression of a fluorescence protein exclusively upon viral infection of the target cells. This is particularly relevant since, from our experience, conducting the SSCT method using producer cells carrying a complete GFP as viral transgene, increased the number of false positives up to 90%. The method was conceived to provide high-throughput screening in an academic/research environment, using commercially available plates and suited to any fluorometer plate reader. A single operator can easily achieve a manual throughput of 200-500 clones *per* analysis in two weeks. If coupled to an automated device, this output could be increased.

The method was used to establish a retrovirus producer from a nude cell line reducing a one year process of sequential transfection and screening of the three viral expression cassettes to three months. Clones producing up to 10^8 infectious particles *per* mL could be isolated, on average, two orders of magnitude higher than the highest state-of-the-art titers obtained for stable production of GaLV pseudotyped retroviral vectors (Coroadinha et al. 2010) (Fig. 5). Of important notice, clones isolated based on the SSCT method, delivered high quality of viral bulks, characterized by high ratios of infectious to total particles content. This parameter is of the utmost importance for clinical-grade viral preparations. SSCT method transcomplemented fluorescence data allows the identification of high-titer clones and can additionally be treated as an estimation of each clone's productivity and analyzed in terms of density distribution (Figs. 4, 5 and 6). This method combines the power of single-cell resolution with the dynamics of cell population analysis and might be used to evaluate the effect of genetic manipulations into viral titers. This method was the pillar for the multi-gene manipulation performed in Chapter VIII. Herein it was also used it to compare infectious vector productivity performance of HEK 293 vs. HEK 293T cell lines, as recent data

suggested large T antigen expression to support enhanced viral titers, not at the level of vector transcriptional activity but rather by indirect physiological effects on the cell (Gama-Norton et al. 2011). Indeed, HEK 293T derived from HEK 293 by stable insertion of the SV40 large T antigen acquiring distinct phenotypic characteristics, including higher transfectability and yielding higher titers (DuBridgde et al. 1987; Rio et al. 1985). This performance is usually attributed to a more favorable episomal replication when SV40 *ori* containing plasmids are used. However, none of the vector constructions used in *de novo* cell line establishment contained SV40 *ori* sequence, neither the HEK 293T derived clones presented obvious increased viral components expression comparatively to those derived from HEK 293 (Fig. 6B). Therefore, HEK 293T cells do not seem to sustain higher retroviral vector titers on increased vector components expression. Together with the data from Gama-Norton et al. (2011), our results support that higher viral titers in large T antigen expressing cells are, at least in part, derived from physiological traits of the cells themselves, making them a better substrate for virus production. The analysis of such changes should be an interesting research area, particularly in the growing field of lentiviral vector production that traditionally uses HEK 293T cells (Merten et al. 2011).

The single step cloning-titration method herein described, demonstrated its applicability in important aspects of viral vector production from high-titer clone selection in cell line development to studying and manipulating cell metabolism (please refer to Chapter VIII). Other applications can be envisaged: for example, in combination with mutagenesis, it can be used for screening randomly generated vector component libraries. Moreover, although it was firstly established for retroviral vector production, it should be directly applicable to stable cell lines producing other types of infectious virus and, with the proper modifications, may be extended to transient systems. We expect this approach to contribute to the progress of gene therapy by accelerating vector and cell line development.

5. Author contribution

Ana Filipa A. F. Rodrigues participated on the experimental setup and design, performed part of the experiments, analyzed the data and wrote the chapter.

6. References

Bodin L, Beaune PH, Lorient MA. 2005. Determination of cytochrome P450 2D6 (CYP2D6) gene copy number by real-time quantitative PCR. *J Biomed Biotechnol* 2005(3):248-53.

Byun J, Kim SH, Kim JM, Yu SS, Robbins PD, Yim J, Kim S. 1996. Analysis of the relative level of gene expression from different retroviral vectors used for gene therapy. *Gene Ther* 3(9):780-8.

Cabantous S, Terwilliger TC, Waldo GS. 2005. Protein tagging and detection with engineered self-assembling fragments of green fluorescent protein. *Nat Biotechnol* 23(1):102-7.

Carmo M, Peixoto C, Coroadinha AS, Alves PM, Cruz PE, Carrondo MJ. 2004. Quantitation of MLV-based retroviral vectors using real-time RT-PCR. *J Virol Methods* 119(2):115-9.

Carrondo MJ, Merten OW, Haury M, Alves PM, Coroadinha AS. 2008. Impact of retroviral vector components stoichiometry on packaging cell lines: effects on productivity and vector quality. *Hum Gene Ther* 19(2):199-210.

Coroadinha AS, Gama-Norton L, Amaral AI, Hauser H, Alves PM, Cruz PE. 2010. Production of retroviral vectors: review. *Curr Gene Ther* 10(6):456-73.

Coroadinha AS, Schucht R, Gama-Norton L, Wirth D, Hauser H, Carrondo MJ. 2006. The use of recombinase mediated cassette exchange in retroviral vector producer cell lines: predictability and efficiency by transgene exchange. *J Biotechnol* 124(2):457-68.

Cosset FL, Takeuchi Y, Battini JL, Weiss RA, Collins MK. 1995. High-titer packaging cells producing recombinant retroviruses resistant to human serum. *J Virol* 69(12):7430-6.

DuBridge R, Tang P, Hsia H, Leong P, Miller J, Calos M. 1987. Analysis of mutation in human cells by using an Epstein-Barr virus shuttle system. *Mol Cell Biol*. 7(1):379-87.

Dull T, Zufferey R, Kelly M, Mandel RJ, Nguyen M, Trono D, Naldini L. 1998. A third-generation lentivirus vector with a conditional packaging system. *J Virol* 72(11):8463-71.

Edelstine M. 2013. The Journal of Gene Medicine Clinical Trial Site (<http://www.wiley.com/legacy/wileychi/genmed/clinical>).

Gama-Norton L, Botezatu L, Herrmann S, Schweizer M, Alves PM, Hauser H, Wirth D. 2011. Lentivirus production is influenced by SV40 large T-antigen and chromosomal integration of the vector in HEK293 cells. *Hum Gene Ther* 22(10):1269-79.

Green BJ, Rasko JE. 2002. Rapid screening for high-titer retroviral packaging cell lines using an in situ fluorescence assay. *Hum Gene Ther* 13(9):1005-13.

Ikeda Y, Takeuchi Y, Martin F, Cosset FL, Mitrophanous K, Collins M. 2003. Continuous high-titer HIV-1 vector production. *Nat Biotechnol* 21(5):569-72.

Livak KJ, Schmittgen TD. 2001. Analysis of relative gene expression data using real-time quantitative PCR and the 2(-Delta Delta C(T)) Method. *Methods* 25(4):402-8.

- Merten OW, Charrier S, Laroudie N, Fauchille S, Dugue C, Jenny C, Audit M, Zanta-Boussif MA, Chautard H, Radrizzani M and others. 2011. Large-scale manufacture and characterization of a lentiviral vector produced for clinical ex vivo gene therapy application. *Hum Gene Ther* 22(3):343-56.
- Moran N. 2012. First gene therapy nears landmark European market authorization. *Nat Biotechnol* 30(9):807-9.
- Ou W, Marino MP, Lu C, Reiser J. 2012. Rapid titration of retroviral vectors using a beta-lactamase protein fragment complementation assay. *Gene Ther* 20(1):43-50.
- Rio D, Clark S, Tjian R. 1985. A mammalian host-vector system that regulates expression and amplification of transfected genes by temperature induction. *Science* 227(4682)(4382):23-28.
- Rodrigues AF, Carmo M, Alves PM, Coroadinha AS. 2009. Retroviral vector production under serum deprivation: The role of lipids. *Biotechnol Bioeng* 104(6):1171-81.
- Rodrigues AF, Formas-Oliveiras AS, Bandeira VS, Alves PM, Hu WS, Coroadinha AS. 2013. Metabolic pathways recruited in the production of a recombinant enveloped virus: mining targets for process and cell engineering. *Metabolic Engineering* 20:131-145.
- Schambach A, Galla M, Maetzig T, Loew R, Baum C. 2007. Improving transcriptional termination of self-inactivating gamma-retroviral and lentiviral vectors. *Mol Ther* 15(6):1167-73.
- Schucht R, Coroadinha AS, Zanta-Boussif MA, Verhoeven E, Carrondo MJ, Hauser H, Wirth D. 2006. A new generation of retroviral producer cells: predictable and stable virus production by Flp-mediated site-specific integration of retroviral vectors. *Mol Ther* 14(2):285-92.
- Schweizer M, Merten OW. 2010. Large-scale production means for the manufacturing of lentiviral vectors. *Curr Gene Ther* 10(6):474-86.
- Seymour LW, Thrasher AJ. 2012. Gene therapy matures in the clinic. *Nat Biotechnol* 30(7):588-93.
- Sheridan C. 2011. Gene therapy finds its niche. *Nat Biotechnol* 29(2):121-8.
- Stacey GN, Merten OW. 2011. Host cells and cell banking. *Methods Mol Biol* 737:45-88.
- Stornaiuolo A, Piovani BM, Bossi S, Zucchelli E, Corna S, Salvatori F, Mavilio F, Bordignon C, Rizzardi GP, Bovolenta C. 2013. RD2-MolPack-Chim3, a Packaging Cell Line for Stable Production of Lentiviral Vectors for Anti-HIV Gene Therapy. *Hum Gene Ther Methods*.
- Verhoeven E, Hauser H, Wirth D. 2001. Evaluation of retroviral vector design in defined chromosomal loci by Flp-mediated cassette replacement. *Hum Gene Ther* 12(8):933-44.
- Vu HN, Ramsey JD, Pack DW. 2008. Engineering of a stable retroviral gene delivery vector by directed evolution. *Mol Ther* 16(2):308-14.
- Wand MP, Jones MC. 1995. Kernel Smoothing (Chapman & Hall/CRC Monographs on Statistics & Applied Probability). Boca Raton, FL, USA: Chapman and Hall/CRC.

Chapter VIII

MULTI-GENE ENGINEERING RETROVIRUS PRODUCER CELLS

This chapter is based on data to be published as:

**Multi-gene engineering of mammalian cell metabolism through iterative
optimization: walking the road to hyperproductivity**

Ana F. Rodrigues, Ana S. Formas-Oliveira, Miguel R. Guerreiro,
Paula M. Alves, Wei-Shou Hu, Ana S. Coroadinha, *(in preparation)*

Abstract

Metabolic gene engineering holds the potential to develop high-producing hosts for the manufacture of complex biopharmaceuticals. Hyperproductivity has been conceptualized as the orchestrated combination of superior attributes from different biochemical pathways. But metabolic manipulation involves labor-intensive steps, from the introduction of the target gene to the isolation and characterization of the candidate clones, turning multiple manipulations extremely difficult.

In this work, we established the basis for multi-gene engineering of mammalian cell metabolism using, as study model, a human cell line producing recombinant retrovirus. To face the challenge of clone screening, a novel method for fast screening of high-titer clones was established by merging cell cloning and virus titration: the single step cloning-titration method (Chapter VII). Assisted by a previous study on the metabolic networks recruited when establishing a retrovirus producer cell line (Chapter II), more than 30 candidates, including metabolic and regulatory genes, were chosen for manipulation. Herein, 13 of those candidates have been evaluated including polyamines metabolism, glutathione metabolism, protein processing in the endoplasmic reticulum, apoptosis and energy generation metabolism. Productivity improvements up to 15-fold increased were obtained. Genes found to yield high-producing phenotypes are now being combined and the resulting clones characterized.

The diversity of metabolic pathways targeted in this study is likely to be of relevance to several biopharmaceuticals produced in mammalian hosts, including complex proteins and other types of recombinant viruses. Moreover, this work encompasses pioneering steps of a multi-gene manipulation approach, being the most extensive metabolic engineering study performed in mammalian cells, so far, further enlightening virus-host metabolic interaction.

Contents

1. Introduction.....	210
2. Materials and methods	212
2.1 Cell lines and culture medium	212
2.2 Metabolic genes expression vectors and lentiviral production	213
2.3 Cell growth and viral production studies	213
2.4 Retro and lentiviral vector titration	213
2.5 Cell transduction for metabolic gene delivery	214
2.6 Quantification of vector transgene genomic copies, RNA extraction and quantitative real-time PCR for gene expression	214
2.7 Single step cloning-titration procedure.....	215
2.8 Data analysis and density distribution curves.....	215
3. Results	215
3.1 Controls	217
3.2 Polyamines metabolism	219
3.3 Glutathione metabolism.....	221
3.4 Protein processing in the ER.....	223
3.5 Apoptosis.....	225
3.6 Energy metabolism.....	227
3.7 Overall analysis and curve validation	229
3.8 Impact of metabolic genes on viral production dynamics – a preliminary analysis with the CBS case study.....	231
4. Discussion	232
5. Author contribution.....	241
6. References.....	241

1. Introduction

Metabolic engineering by gene manipulation holds the promise of developing robust and high-yield cell-based production systems. In the *omics* era, gene engineering in simpler organisms has become more straightforward and, with the appearance of genome-scale metabolic models in the late 90's, achieved high levels of predictability (Edwards and Palsson 1999; Kim et al. 2011). By opposite, eukaryotic cells, particularly mammalian's, were found to be difficult to manipulate with similar levels of predictability. The productivity improvements obtained by gene manipulation have been modest, typically from 2- to 4-fold and, many times, based on volumetric, rather than specific, productivity. The most outstanding achievement was accomplished by Fussenegger et al. (1998), a productivity increase of 30-fold in CHO cells producing a secreted alkaline phosphatase by co-expressing Bcl-xL survival gene with a cell cycle regulator gene, cyclin-dependent kinase inhibitor (p27).

Metabolism is redundant (Palsson 2006): the same metabolite profiling can be generated by different combinations of reactions not conceptualized as a *pathway*. Therefore, point manipulations are often absorbed by the network and *diluted* without obvious phenotypic differences. The problem gains relevance with the complexity, tight regulatory control and high level of compartmentalization of mammalian cells. The datasets available suggest that hyperproductivity is conferred by a collection of positive physiological traits encompassing changes of several genes with a broad spectrum of functions (Fig. 1, Seth et al. (2007)). On the other hand, gene manipulation involves labor-intensive steps, from the introduction of the target genes to the isolation and characterization of candidate clones. Moreover, high-producing phenotypes are typically rare events. Even when the delivered gene might contribute to high-productivity, its effect will depend on the number of integrated copies, integration loci – dictating gene expression levels – and on a combination of favorable downstream effects arising from that manipulation. Many times, this combinatorial effect can only be achieved by multiple gene manipulations (Seth et al. 2007).

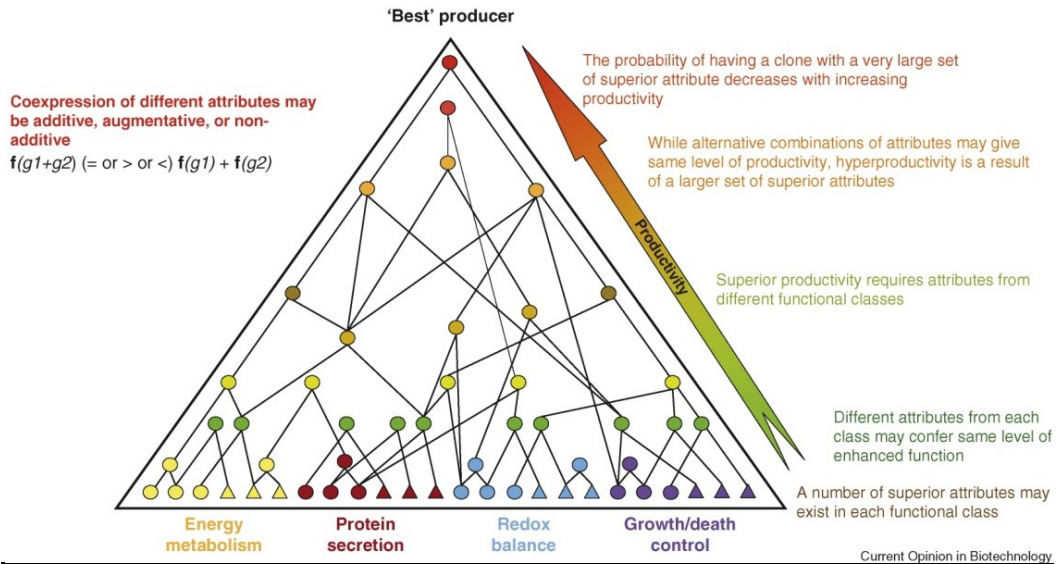


Figure 1 – Multiple routes to hyperproductivity. Hyperproductivity requires the accumulation of multiple superior characteristics. While the productivity is low, acquiring some elements from one or more favorable functional classes (only four potential classes are shown) will enhance the productivity. Thus, many different routes can give the same level of productivity. To achieve a higher productivity level a large number of attributes, arising from multiple favorable pathways may be needed. Hyperproducers are rare, as they must acquire many attributes. In addition, there are possibly multiple routes that lead to the top (Seth et al. 2007).

While the theoretical concept illustrated in Figure 1 is easy to understand, its experimental execution can be rather difficult. For a single gene, the process may take several months implying the screening of several hundreds of clones. For multiple genes, it rapidly becomes impracticable.

In this work, we experimentally challenge the theoretical concept of ‘the multiple routes hyperproductivity’ to improve a mammalian cell host producing recombinant retrovirus. To face the burden of clone screening, a novel method was established for fast screening of high-titer clones by merging cell cloning and virus titration: the single step cloning-titration method (SSCT, Chapter VII). Assisted by a previous study on the metabolic networks recruited when establishing a producer cell line (Chapter II), more than 30 candidates, including enzymatic and regulatory genes, were chosen for manipulation. These candidates span across multiple pathways including energy generation, amino acid metabolism, glutathione metabolism, apoptosis, protein processing, lipid biosynthesis and nucleotide metabolism (Rodrigues et al. 2013). For

the genes evaluated in this work, specific productivity could be increased up 15-fold. High producing clones are being characterized and genes found to yield high-producing phenotypes are starting to be combined to mimic the *routes to hyperproductivity*.

In this work the basis for a pioneering multi-gene manipulation approach were established. For the more than 30 genes identified as potential targets to improve virus production, 17 have, by now, been evaluated comprising the most extensive metabolic engineering study so far performed in mammalian cells.

2. Materials and methods

2.1 Cell lines and culture medium

293 FLEX S11 were used for gene manipulation. These cells derive from 293 FLEX 18 (Coroadinha et al. 2006) by recombinase mediated cassette exchange as described in Chapter VII. In these cells, the original LacZ transgene was exchanged by a fusion of LacZ with S11 fragment of the split-GFP® (SandiaBiotech, Albuquerque, NM, U.S.A), making them suitable to be screened for infectious virus production using the single step cloning-method. HEK 293T (ATCC CRL-11268) is a HEK 293 derived cell line expressing large T antigen from SV40 (simian vacuolating virus 40) used to transiently produce the lentiviral vectors for metabolic gene delivery. Te 671 is a human rhabdomyosarcoma derived cell line (ATCC CCL-136) used to titrate infectious retroviral particles by LacZ staining. Te 671 S10 is a Te 671 derived cell line stably expressing the S10 fragment of the split-GFP® (SandiaBiotech) established as described in Chapter VII. These cells were used as titration cell substrate in the single step cloning-titration method and also to titrate metabolic gene lentiviral vector stocks.

All cells were maintained in DMEM (Gibco, Paisley, UK), with 25 mM of glucose and 4mM of glutamine, supplemented with 10% (v/v) (FBS) (Gibco). For the single step cloning titration method, phenol red-free DMEM supplemented with 20% FBS (Gibco) and 1X B27 supplement (Gibco) was used, as previously described in Chapter VII. All cell lines were maintained in a humidified atmosphere of 92% air and 8% CO₂ at 37 °C.

2.2 Metabolic genes expression vectors and lentiviral production

The cDNAs of all genes used in this work were acquired through DNASU Plasmid Repository (Biodesign Institute, Arizona State University, Tempe, AZ, USA) and cloned into a lentiviral backbone *pRRLSIN LacZS11*. This backbone is derived from *pRRLSIN* described by Dull et al. (1998) and was established by replacing the original GFP by LacZ-S11 fusion as described in Chapter VII. For cloning the metabolic genes, LacZ was removed and the S11 fragment was maintained for titer determination. Metabolic genes were cloned in the place of LacZ using In-Fusion® HD Cloning Kit (Clontech Laboratories, Inc., Terra Bella Avenue, CA, USA). The mock vector was obtained by re-ligating the lentiviral backbone after LacZ removal.

For lentiviral transient production the lentiviral packaging system and the transfection procedure described in Dull et al. (1998) were adopted using *pMDLg/pRRE*, *pRSV-REV*, *pMD2G* and *pRRLSIN* derived backbones harboring the different metabolic genes. *pMDLg/pRRE* and *pRSV-REV* are 3rd generation lentiviral vector packaging constructs containing HIV1 gag-pol and the second and third exons of HIV-1 REV, respectively. *pMD2G* expresses the envelope G glycoprotein of the vesicular stomatitis virus (VSV-G) under the control of a CMV promoter. The three plasmids were kindly provided by Dr. D. Trono through Addgene plasmid repository (Cambridge, MA, USA). Viral vector supernatants were clarified through 0.45 µm cellulose acetate filter, aliquoted and stored at -85°C until further use.

2.3 Cell growth and viral production studies

293 FLEX S11, transduced populations and their derived clones were analyzed for cell growth and infectious retroviral vector production using a 48+24 hours production/harvesting operation mode described in Chapter II (Rodrigues et al. 2013).

2.4 Retro and lentiviral vector titration

For LacZ based staining titration (retroviral vector production from manipulated and non-manipulated cells), infectious procedure and viral titer determination were

performed by serial dilution infection assay, as previously described in Rodrigues et al. (2009). For GFP transcomplementation titration (lentiviral vector metabolic gene stocks), Te 671 S10 target cells were seeded at 5×10^4 cells/cm² in 24-well plates 24 hour before infection. Transduction was performed by removing the cell supernatant and infecting with 0.2 mL of viral suspension using several dilutions in fresh DMEM (Gibco) with 10% (v/v) FBS and 8 µg/mL of polybrene (Sigma). Cells were incubated at 37°C overnight after which 0.5 mL of fresh medium was added. Two days after infection, cells were harvested and analyzed for GFP fluorescence by flow cytometry (CyFlow-space, Partec GmbH).

2.5 Cell transduction for metabolic gene delivery

Metabolic genes were delivered by lentiviral vector infection of 293 FLEX S11. The cells were seeded at a density of 1×10^4 cells/cm² 24 hours before infection in 6-well plates. Transduction was performed by removing the cell supernatant and infecting with 2 mL of viral suspension using the appropriate dilution to achieve multiplicities of infection (infectious particles *per cell*) of 1, 3 and 5. Dilutions were made in fresh DMEM (Gibco) with 10% (v/v) FBS (Gibco) and 8 µg/mL of polybrene (Sigma). Cells were incubated at 37°C overnight after which medium was exchanged. Two days after infection, cells were amplified to 75 cm² t-flasks and re-passaged 3-4 days after. At this point, part of the cells was frozen and the other part was seeded to assess infectious particles production of transduced populations (section 2.3). Single step cloning titration method was then performed.

2.6 Quantification of vector transgene genomic copies, RNA extraction and quantitative real-time PCR for gene expression

Quantification of CBS genomic copies was performed using genomic DNA with the primer set (F): 5' – TCATCGTGATGCCAGAGAAG – 3' and (R): 5' – TTGGGGATTTCGTTCTTCAG – 3'. Genomic DNA extraction, quantitative real-time PCR and copy number calculations were performed as described in Chapter VII (Section 2.4 of Materials and methods).

RNA extraction and quantitative real-time PCR were carried as described in Chapter VII (Section 2.5 of Materials and methods).

2.7 Single step cloning-titration procedure

Single step cloning titration method procedure was performed as described in Chapter VII. For the case of cystathionine-beta-synthase (CBS) and cystathionase (CTH) transduced cells, medium was fed with glycine, methionine and serine (Sigma) during the polybrene addition steps, to replenish their original concentration. These amino acids are used by these enzymes in glutathione biosynthesis (refer to Fig. 6) and were added given the long-term culture associated to the SSCT method. For the case in which oxidative injury was induced, *tert*-butyl hydroperoxide (TBHP, Sigma) was added at a final concentration of 5 μ M 24 hours before target cell seeding. For target cell seeding, the medium from the wells was completely removed to eliminate THBP traces and the protocol was carried as described previously (Chapter VII).

2.8 Data analysis and density distribution curves

For kernel density distribution curves, the data was treated and processed in MATLAB™ 7.10 (The MathWorks Inc., Natick, MA, 2000), using the function *ksdensity()* as described in Chapter VII. Boxplot analysis was also performed in MATLAB™ 7.10 using the function *boxplot()*.

3. Results

In this work, genes that were previously identified as potential targets to improve retrovirus production were manipulated in 293 FLEX S11 producer cells. These cells were derived from 293 FLEX 18 through recombinase mediated cassette exchange (RCME) (Coroadinha et al. 2006) to exchange the LacZ transgene to LacZ-S11 fusion (please refer to Chapter VII for cell line establishment details). The transgene exchange

was carried to support the use of the single step cloning-titration method (SSCT) for fast screening of high-titer clones.

The genes chosen to be manipulated in this work are given in Table I. Some of them were chosen based on significant differential expression between a high and a low producing cell substrate (Chapter II, Table II). Others, although not differentially expressed, presented low expression values, having been chosen in an attempt to further activate the reactions they are involved in. Others are specific to serum independence phenotype: LSS, MVK, SREBF1/2 (Chapter V). All genes belong to metabolic pathways recruited in the production of recombinant retrovirus (Chapter II, Fig. 1, Rodrigues et al. (2013)).

Table I – Gene candidates to improve retroviral vector production

Pathway	Gene																																
	GLUL	ASS1	ARG1	OAT	MTHFD2	ODC1	AZIN1	SLC29A1	PNP	RPIA	G6PD	IDH1	CTH	CBS	GSS	GSTM1	GPX7	GSR	XBP1	PDIA2	HSPA5	BCL2	HIF1AN	PDP1	PDP2	IDH2	CS	LSS	MVK	SREBF1	SREBF2		
Amino acid metabolism																																	
Co-factors metabolism																																	
Polyamines metabolism																																	
Nucleic acid metabolism																																	
Pentose phosphate pathway																																	
Glutathione metabolism																																	
Lipid metabolism																																	
Protein processing in the ER																																	
Apoptosis																																	
Energy generation																																	

Black indicates genes that have already been tested, at least by analyzing average effects on transduced populations. Grey indicates genes currently under testing. ASS1: argininosuccinate synthase; ARG1: arginase 1; AZIN1: antizyme inhibitor 1; BCL2: B-cell CLL/lymphoma; CBS: cystathionine-beta-synthase; CS: citrate synthase; CTH: cystathionase; G6PD: glucose-6-phosphate dehydrogenase; GLUL: glutamate-ammonia ligase; GPX7: glutathione peroxidase 7; GSR: glutathione reductase; GSS: glutathione synthase; GSTM1: glutathione S-transferase mu 1; HIF1AN: hypoxia inducible factor 1, alpha subunit inhibitor; HSPA5: heat shock 70kDa protein 5; IDH1: isocitrate dehydrogenase 1 (cytosolic); IDH2: isocitrate dehydrogenase 2 (mitochondrial); LSS: lanosterol synthase; MTHFD2: methylenetetrahydrofolate dehydrogenase (NADP+ dependent) 2; MVK: mevalonate kinase; OAT: ornithine aminotransferase; ODC1: ornithine decarboxylase; PDIA2: protein disulfide isomerase 2; PDP1/2: pyruvate dehydrogenase phosphatase, catalytic subunit 1/2; PNP: purine nucleoside phosphorylase; RPIA: ribose 5-phosphate isomerase A; SLC29A1: solute carrier family 29 (equilibrative nucleoside transporter), member 1; SREBF1/2: sterol regulatory element binding factor 1/2; XBP1: X-box binding protein 1.

3.1 Controls

For all the manipulations conducted in this work, genes were delivered by lentiviral vector transduction. For each of them, three multiplicities of infection (MOI) were tested: 1, 3 and 5. After 4-5 passages following transduction, cells were cloned and screened for high titers using the SSCT method. The productivity of infectious particles was also assessed for each of the populations. Before starting gene manipulation, two types of controls were analyzed: non-transduced and mock transduced cells.

293 FLEX S11 non-transduced cells were subjected to the single step cloning-titration method 6 independent times to evaluate the reproducibility of the density distribution curve (Fig. 2). These replicates include different passages and freezing batches.

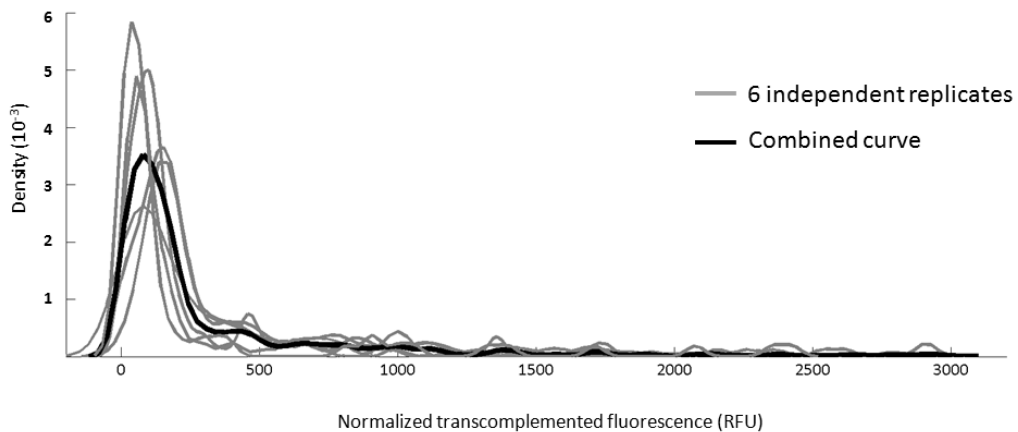


Figure 2 – Density distribution of non-transduced cells. Kernel density distribution curve of non-transduced 293 FLEX S11. Six independent replicates are shown. Each distribution comprises approximately 200 clones corresponding to 10 cloning plates, of 60 wells each, at a seeding density of 0.7 cells/well assuming 50% cloning efficiency (see Chapter VII).

The density distribution curves of 293 FLEX S11 were found to be similar, with the median around 150 RFU and extended tails up to 3000 RFU. The black curve represents the combination of these 6 replicates and was used as a representative of non-transduced 293 FLEX S11 density distribution curve from herein on.

293 FLEX S11 have additionally been transduced with the mock lentiviral vector simulating the MOIs used for gene manipulation (1, 3 and 5). The density distribution curve of mock transduced cells is shown in Figure 3, as well as specific productivity of the populations and their derived clones.

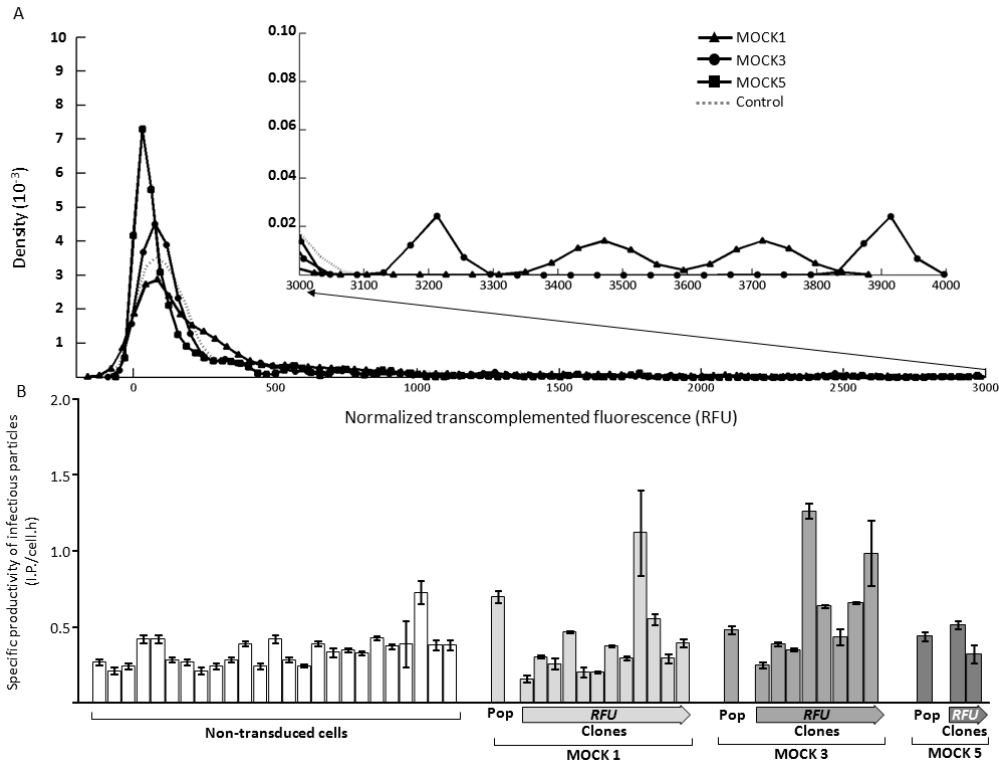


Figure 3 – Mock transduction of 293 FLEX S11. Kernel density distribution curve of mock transduced cells (A); non-transduced control is shown in dashed grey. Specific productivity of infectious retroviral particles from 293 FLEX non-transduced cells, high-fluorescence yielding clones isolated from (A) and/or their corresponding populations (B). Values are shown as average \pm standard deviation (n=3).

The major peak of mock curves fell in the same RFU region of that of non-transduced cells, with slightly lower median (110 RFU) while the tail extended beyond that of the control, particularly for mock 1 and mock 3 (Fig. 3A). Therefore, the highest fluorescence mock clones were isolated, expanded and analyzed for infectious vector titers (Fig. 3B). Although the majority of these were false positives, some of the mock clones actually presented increased productivities. The highest producer from these

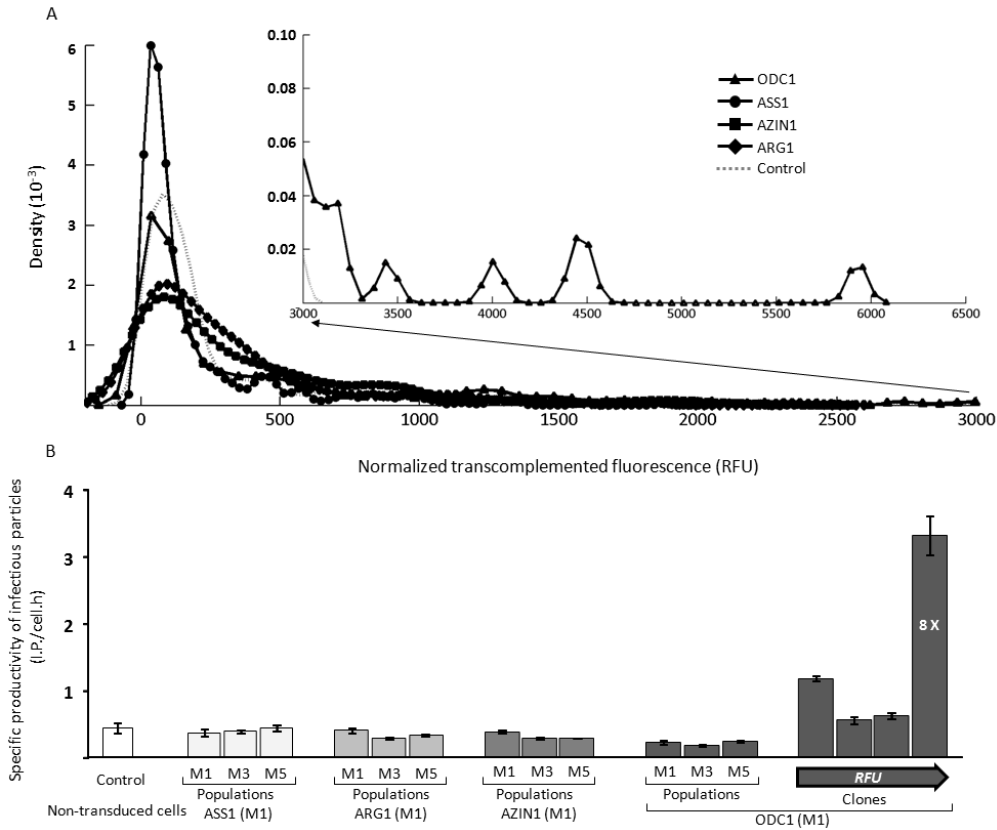


Figure 5 – Transduction with ASS1, ARG1, AZIN1 and ODC1. Kernel density distribution curves of non-transduced, ASS1, ARG1, AZIN1 and ODC1 transduced 293 FLEX S11 (A). Specific productivity of infectious particles from high-transcomplemented GFP yielding clones isolated from (A) and/or their corresponding populations (B). “M” stands for multiplicity of infection. Values are shown as average \pm standard deviation (n=3). Non-transduced control corresponds to average of 25 independent replicates (Fig 3). Clones are ordered by fluorescence signal. Only clones with fluorescence signals higher than the maximum of non-transduced cells were isolated (Fig. 2). For clones producing more than 3-fold higher than non-transduced control, the fold-increase is shown (X-fold). 3-fold was assumed as a confidence threshold for specific productivities significantly higher than MOCK transduced cells (Fig. 3). ASS1: argininosuccinate synthase 1; ARG1: arginase 1; AZIN1: antizyme inhibitor 1; ODC1: ornithine decarboxylase.

No major increases in the transduced populations were observed for any of the delivered genes (Fig. 5B). In fact, except for ASS1, all of the genes appeared to reduce average productivity (populations) when increasing MOI. Therefore, MOI 1 was chosen to be screened using the SSCT method (Fig. 5A).

For MOI 1 transduced cells, AZIN1 and ARG1 seemed to displace the major peak to higher fluorescence values than those of the control, suggesting an overall improvement in infectious particles titer. Yet, no high-producing phenotypes were

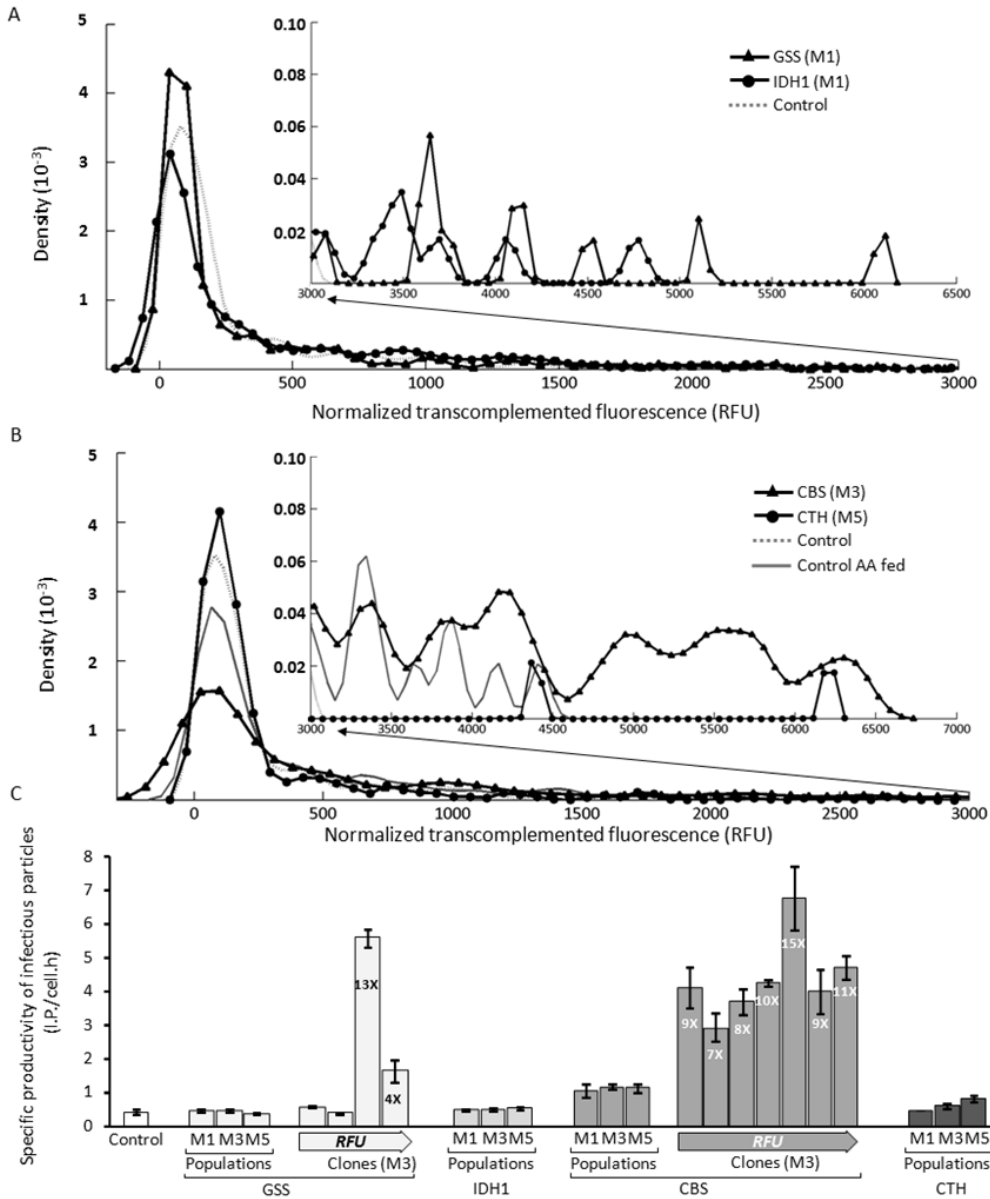


Figure 7 – Transduction with GSS, IDH1, CBS and CTH. Kernel density distribution curves of non-transduced, GSS, and IDH1 transduced 293 FLEX S11 (A). Kernel density distribution curves of non-transduced, CBS and CTH transduced 293 FLEX S11 (B). Control AA fed refers to 293 FLEX S11 non-transduced control fed with serine and methionine as described in Materials and methods for CBS and CTH during SSCT procedure. Specific productivity of infectious particles from high-transcomplemented GFP yielding clones isolated from (A and B) and/or their corresponding populations (C). “M” stands for multiplicity of infection. Values are shown as average \pm standard deviation (n=3). Non-transduced control corresponds to average of 25 independent replicates (Fig. 3). Clones are ordered by fluorescence signal. Only clones with fluorescence signals higher than the maximum of non-transduced cells were isolated (Fig. 2). For clones producing more than 3-fold higher than non-transduced control, the fold-increase is shown (X-fold). 3-fold was assumed as a confidence threshold for specific productivities significantly higher than MOCK transduced cells (Fig. 3). CBS: cystathionine-beta-synthase; CTH: cystathionase; GSS: glutathione synthase; IDH1: isocitrate dehydrogenase 1 (cytosolic).

No major differences in the transduced populations were observed for GSS or IDH1 (Fig. 7B). Therefore, the intermediated MOI 3 was chosen to be screened using the SSCT method (Fig. 7A). IDH1 presented an extended tail, 2000 RFU above the control. Yet, none of the isolated clones was found to be a high producing phenotype. One of the clones produced 2.5-fold higher, but this falls below the mock variability threshold (3-fold, Fig. 3). In GSS, the tail extended 3000 RFU above the control (Fig. 7A) and clones isolated from this range produced up to 13-fold higher (Fig. 7C). For CBS, not only the curve tail extended 3000 RFU above the control, as it presented high density in this range, denoting high amount of high producing clones (Fig. 7B). The majority of the clones isolated from this range presented significant titer improvements, up to 15-fold. For CTH clones, the behavior was more like GSS, with fewer amounts in high fluorescence ranges. These clones are currently under analysis to assess specific productivity.

3.4 Protein processing in the ER

For the manipulation of the machinery involved in protein processing in the endoplasmic reticulum (ER) four genes were considered: HSPA5, PDIA, XBP1 and GSR (Fig. 8).

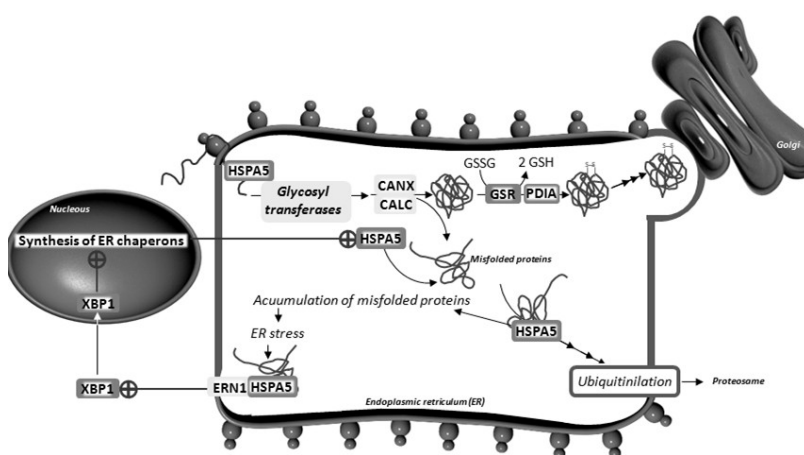


Figure 8 – Protein processing in the endoplasmic reticulum.

Schematic representation of protein processing in the endoplasmic reticulum (ER) and the targeted genes (dark grey boxes). Herein, HSPA5 and XBP1 were evaluated. For a matter of simplicity only the main metabolites are shown; thus, the reactions are not necessarily balanced. CALC: calreticulin;

CANX: calnexin; ERN1: endoplasmic reticulum to nucleus signaling 1; GSR: glutathione reductase; HSPA5: heat shock 70kDa protein 5; PDIA: protein disulfide isomerase; XBP1: X-box binding protein 1

Figure 9 shows density distribution profile of transduced cells as well as specific productivity of the populations and their derived clones.

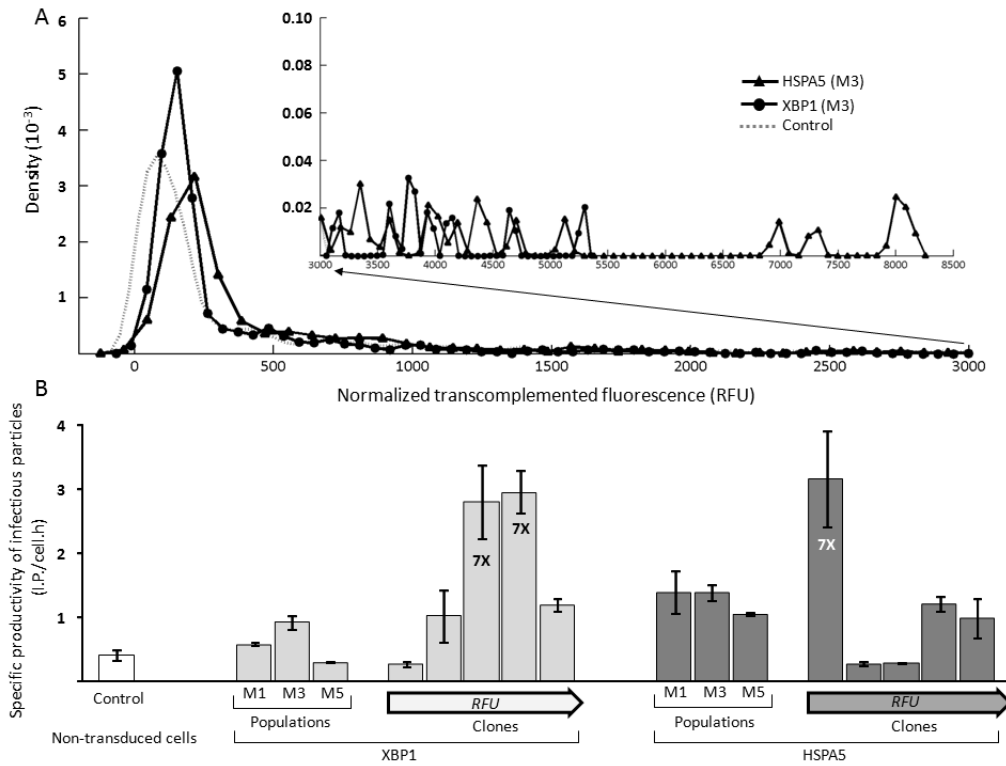


Figure 9 – Transduction with XBP1 and HSPA5. Kernel density distribution curves of non-transduced, XBP1 and HSPA5 transduced 293 FLEX S11 (A). Specific productivity of infectious particles from high-transduced GFP yielding clones isolated from (A) and/or their corresponding populations (B). “M” stands for multiplicity of infection. Values are shown as average ± standard deviation (n=3). Non-transduced control corresponds to average of 25 independent replicates (Fig. 3). Clones are ordered by fluorescence signal. Only clones with fluorescence signals higher than the maximum of non-transduced cells were isolated (Fig. 2). For clones producing more than 3-fold higher than non-transduced control, the fold-increase is shown (X-fold). 3-fold was assumed as a confidence threshold for specific productivities significantly higher than MOCK transduced cells (Fig. 3). HSPA5: heat shock 70kDa protein 5; XBP1: X-box binding protein 1.

Transduced populations readily presented increased (average) productivities, both for XBP1 and HSPA5 (Fig. 9B). The intermediated MOI 3 appeared to be that with higher improvements and was screened with the SSCT method (Fig. 9A).

HSPA5 presented an extended tail, 5000 RFU above the control and the majority of the isolated clones were high-titer phenotypes, producing up to 7-fold more. For XBP1, the extended tail did not exceeded 2500 RFU above the control but also high-

titer phenotypes, producing up to 7-fold more could be isolated. The higher fluorescence values in HSPA5 were, in part, derived from an average larger colony size (data not shown).

3.5 Apoptosis

For the manipulation of apoptosis, B-cell CLL/lymphoma 2 (BCL2) gene was over-expressed in 293 FLEX S11 using an MOI of 5. Figure 10A and C shows, respectively, the density distribution profile of transduced cells and specific productivity of their derived clones. This same population was screened using the SSCT method during the exposure to an oxidative stress environment (Fig. 10B). BCL2 transduced cells presented an extended tail, 2000 RFU above the control, although with low density (Fig. 10A). Still, all the clones isolated presented increased productivities, some of them up to 5-fold more (Fig 10C).

When exposed to an oxidative environment, both transduced and non-transduced cells presented a down-shifting of the major peak and the extended tail also fell below that of the (non-oxidative stress exposed) control. Still, BCL2 transduced cells always presented higher clone density indicating increased cell survival.

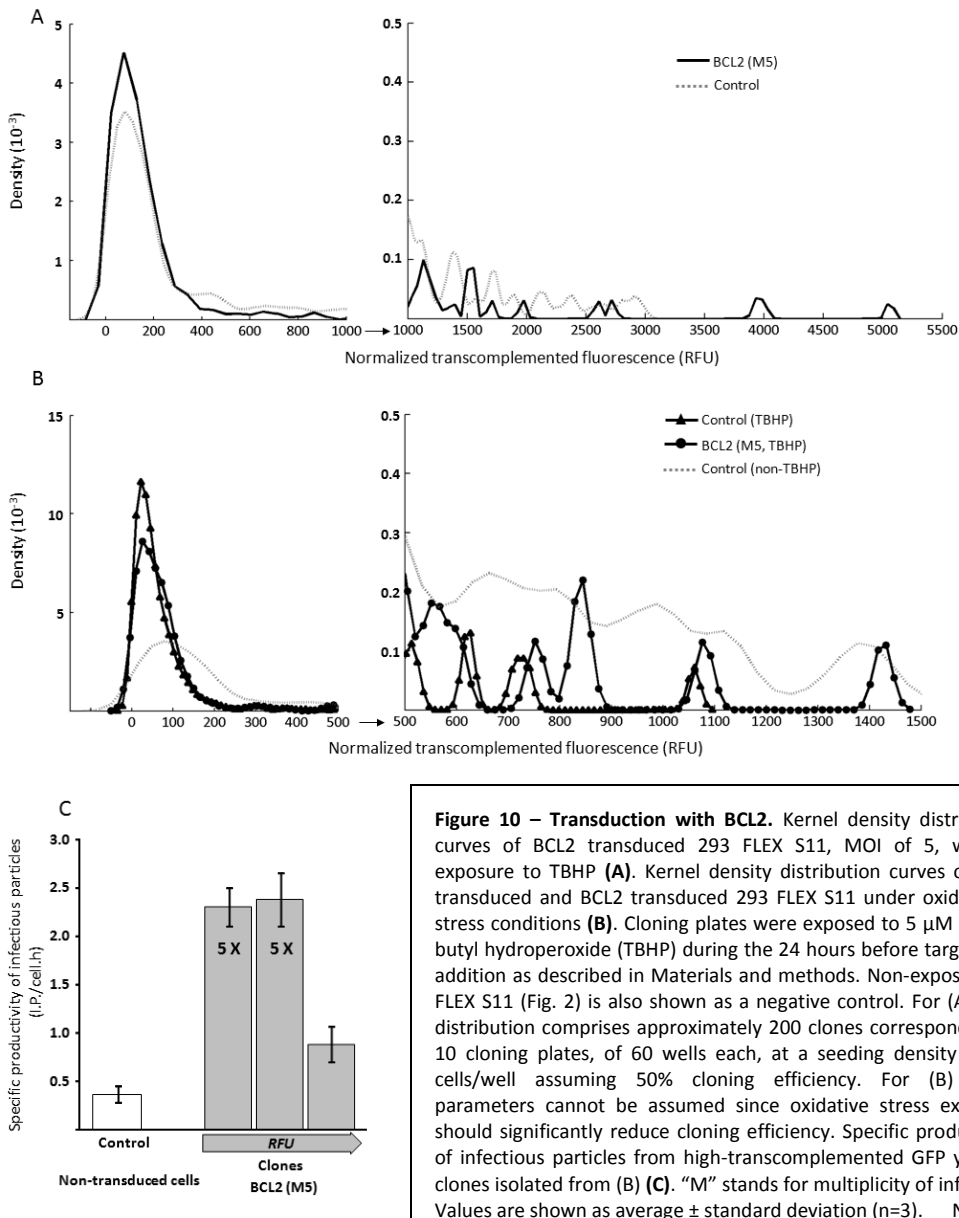


Figure 10 – Transduction with BCL2. Kernel density distribution curves of BCL2 transduced 293 FLEX S11, MOI of 5, without exposure to TBHP (A). Kernel density distribution curves of non-transduced and BCL2 transduced 293 FLEX S11 under oxidative e stress conditions (B). Cloning plates were exposed to 5 μ M of *tert*-butyl hydroperoxide (TBHP) during the 24 hours before target cells addition as described in Materials and methods. Non-exposed 293 FLEX S11 (Fig. 2) is also shown as a negative control. For (A) each distribution comprises approximately 200 clones corresponding to 10 cloning plates, of 60 wells each, at a seeding density of 0.7 cells/well assuming 50% cloning efficiency. For (B) these parameters cannot be assumed since oxidative stress exposure should significantly reduce cloning efficiency. Specific productivity of infectious particles from high-transcomplemented GFP yielding clones isolated from (B) (C). “M” stands for multiplicity of infection. Values are shown as average \pm standard deviation (n=3). Non-

transduced control corresponds to average of 25 independent replicates (Fig. 3). Clones are ordered by fluorescence signal. Only clones with fluorescence signals higher than the maximum of non-transduced cells were isolated (Fig. 2). For clones producing more than 3-fold higher than non-transduced control, the fold-increase is shown (X-fold). 3-fold was assumed as a confidence threshold for specific productivities significantly higher than MOCK transduced cells (Fig. 3). BCL2: B-cell CLL/lymphoma 2.

3.6 Energy metabolism

For the manipulation of the energy metabolism the approach of down-regulating the Warburg effect was re-assessed (Chapter VI). In our previous proof-of-concept study, specific productivities of 293 FLEX GFP could be improved, on average 20-fold, using short hairpin RNA interference against hypoxia inducible factor 1 (HIF1) and pyruvate dehydrogenase kinase (Chapter VI). However, the deleterious off-target effects of using short hairpin RNA interference limited the combination of these two down-regulations and, to a certain extent, may have skewed the real effect of HIF1 and PDK reduction in infectious virus production.

In this part of the work, we aimed at improving the energy generation metabolism by i) simulating the down-regulation of HIF1 and PDK avoiding down-regulation tools (i.e. RNA interference) and ii) increasing the expression of potentially limiting genes (Fig. 11).

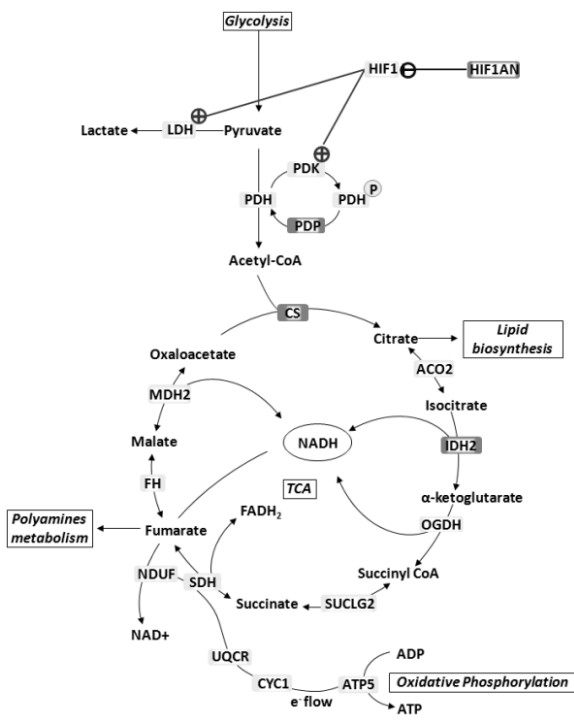


Figure 11 – Manipulation of the energy generation metabolism.

Schematic representation of the integration of energy metabolism through glycolysis, TCA and oxidative phosphorylation. It is additionally represented the Warburg effect lactogenic phenotype mediated by HIF1, which activates glycolytic enzymes, LDH and PDK. The latter inactivates PDH by phosphorylation limiting the entrance of pyruvate into the TCA (for further details please refer to Chapter VI). Manipulation targets are shown in dark grey. The over expression of HIF1AN and PDP is expected to promote identical effects to HIF1 and PDK down-regulation, respectively. CS and IDH2 over-expression is expected to push TCA towards citrate and NADH generating reactions. ACO2: aconitase 2; ATP5: ATP synthase; CS: citrate synthase; CYC1: cytochrome c-1; FH: fumarate hydratase; HIF1AN: hypoxia inducible factor 1, alpha subunit inhibitor; IDH2: isocitrate dehydrogenase 2 (mitochondrial); LDH: lactate dehydrogenase; MDH2: malate dehydrogenase 2 (mitochondrial); OGDH: oxoglutarate (alpha-ketoglutarate) dehydrogenase; PDH: pyruvate dehydrogenase complex; PDK: pyruvate dehydrogenase kinase; PDP: pyruvate dehydrogenase phosphatase; SUCLG2: succinate-CoA ligase; SDH: succinate dehydrogenase complex.

For i), the manipulation targets considered were hypoxia inducible factor 1 alpha subunit inhibitor (HIF1AN), pyruvate dehydrogenase phosphatase 1 and 2 (PDP 1 and 2); for ii), citrate synthase (CS) and isocitrate dehydrogenase 2 (mitochondrial) (IDH2) were chosen (Fig. 11). Herein, HIF1AN and IDH2 were analyzed.

Figure 7 shows density distribution profile of transduced cells as well as specific productivity of the populations and their derived clones.

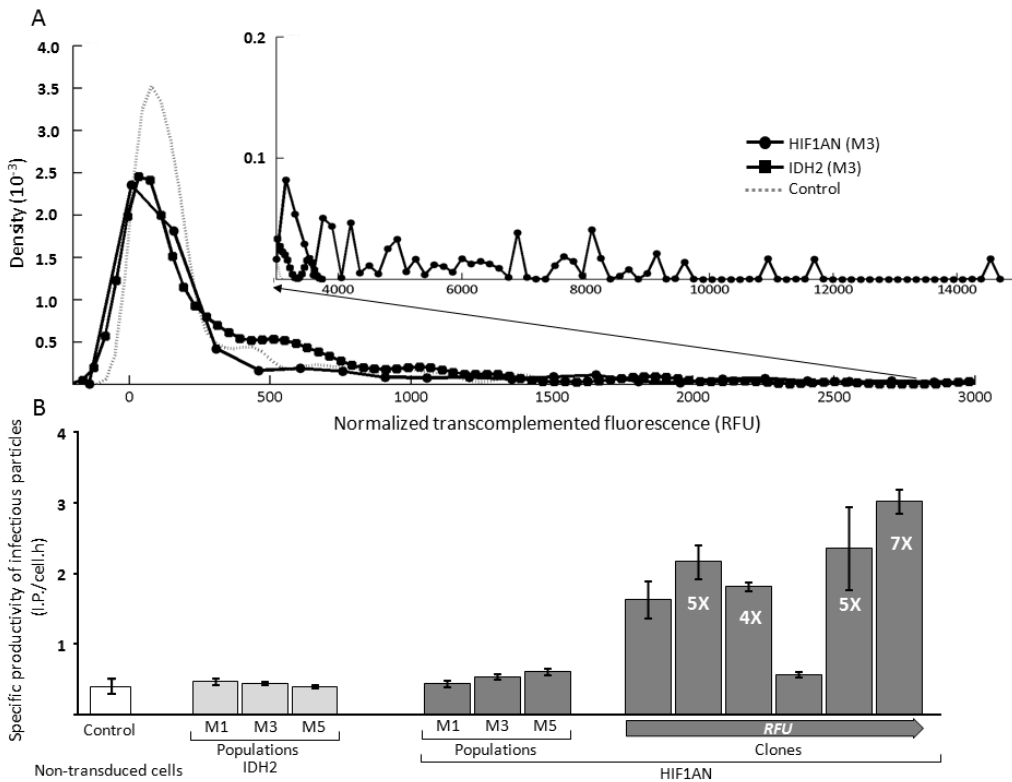


Figure 12 – Transduction with HIF1AN and IDH2. Kernel density distribution curves of non-transduced, HIF1AN and IDH2 transduced 293 FLEX S11 (A). Each distribution comprises approximately 200 clones corresponding to 10 cloning plates, of 60 wells each, at a seeding density of 0.7 cells/well assuming 50% cloning efficiency. Specific productivity of infectious particles from high-transcomplemented GFP yielding clones isolated from (A) and/or their corresponding populations (B). “M” stands for multiplicity of infection. Values are shown as average ± standard deviation (n=3). Non-transduced control corresponds to average of 25 independent replicates (Fig. 3). Clones are ordered by fluorescence signal. Only clones with fluorescence signals higher than the maximum of non-transduced cells were isolated (Fig. 2). For clones producing more than 3-fold higher than non-transduced control, the fold-increase is shown (X-fold). 3-fold was assumed as a confidence threshold for specific productivities significantly higher than MOCK transduced cells (Fig. 3). HIF1AN: hypoxia inducible factor 1, alpha subunit inhibitor; IDH2: isocitrate dehydrogenase 2 (mitochondrial).

For IDH2, no high-titer phenotypes could be isolated. However, clone density for fluorescence values above 500 RFU was considerably higher than that of the controls, suggesting average improvements (Fig. 12A). On the other hand, for HIF1AN transduced cells, the tail extended almost 11000 RFU above the control. Clones isolated from this range, were found to produce up to 7-fold higher than non-transduced cells. Still, the majority of these clones were not analyzed. Further analysis will be required.

3.7 Overall analysis and curve validation

In the above sections, each of the genetic modifications was analyzed individually. In this section, the data was gathered into boxplots to provide a global overview of all the manipulations conducted. Some of the curves were re-analyzed by conducting the SSCT method on the same population but different passages or by establishing new populations with different lentiviral vector batches (Fig. 13).

The same populations, independently analyzed, were found to yield similar distributions. Slight variations can arise, but the median and quartile distribution around the median appeared identical. For populations established with new lentiviral vector stocks, we found median and quartile distribution around the median to be shifted – to higher or lower fluorescence values – although high-producing phenotypes are still obtained.

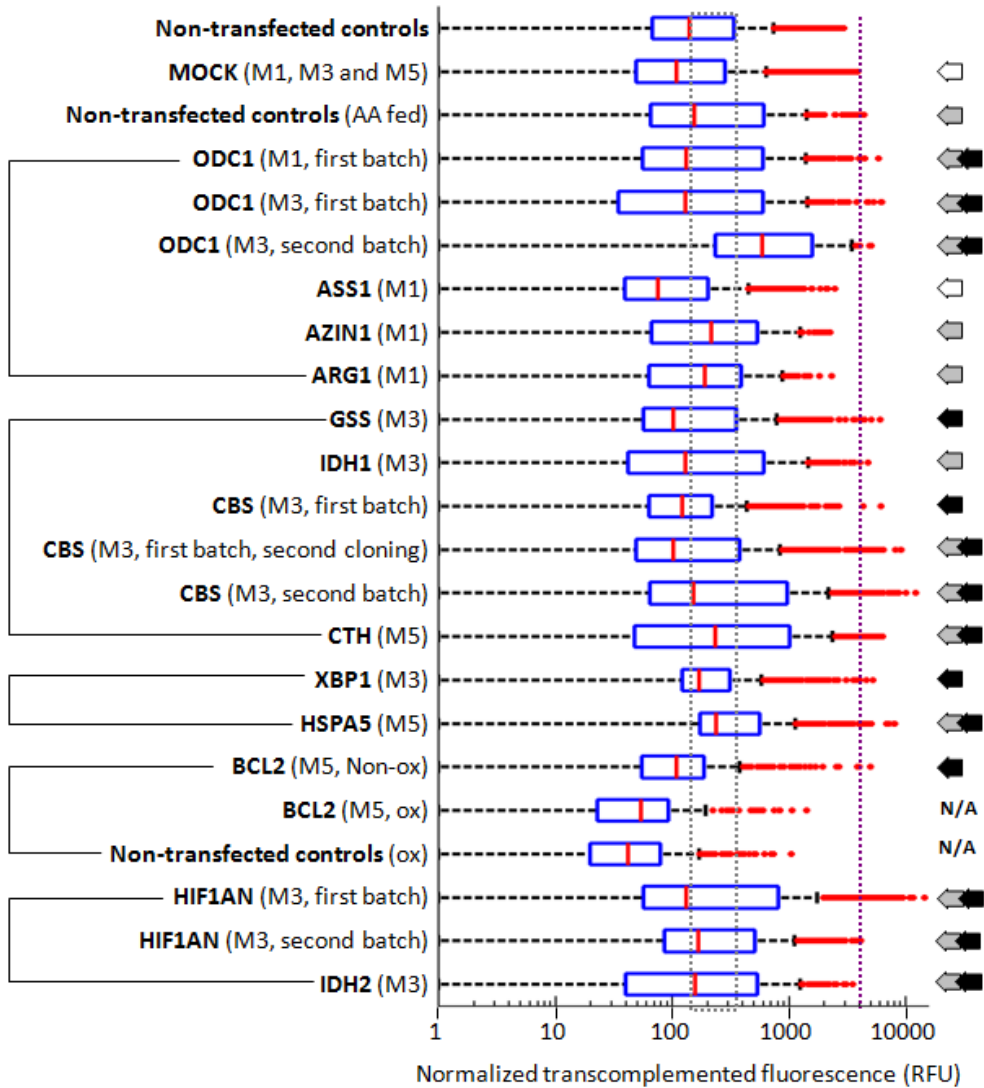
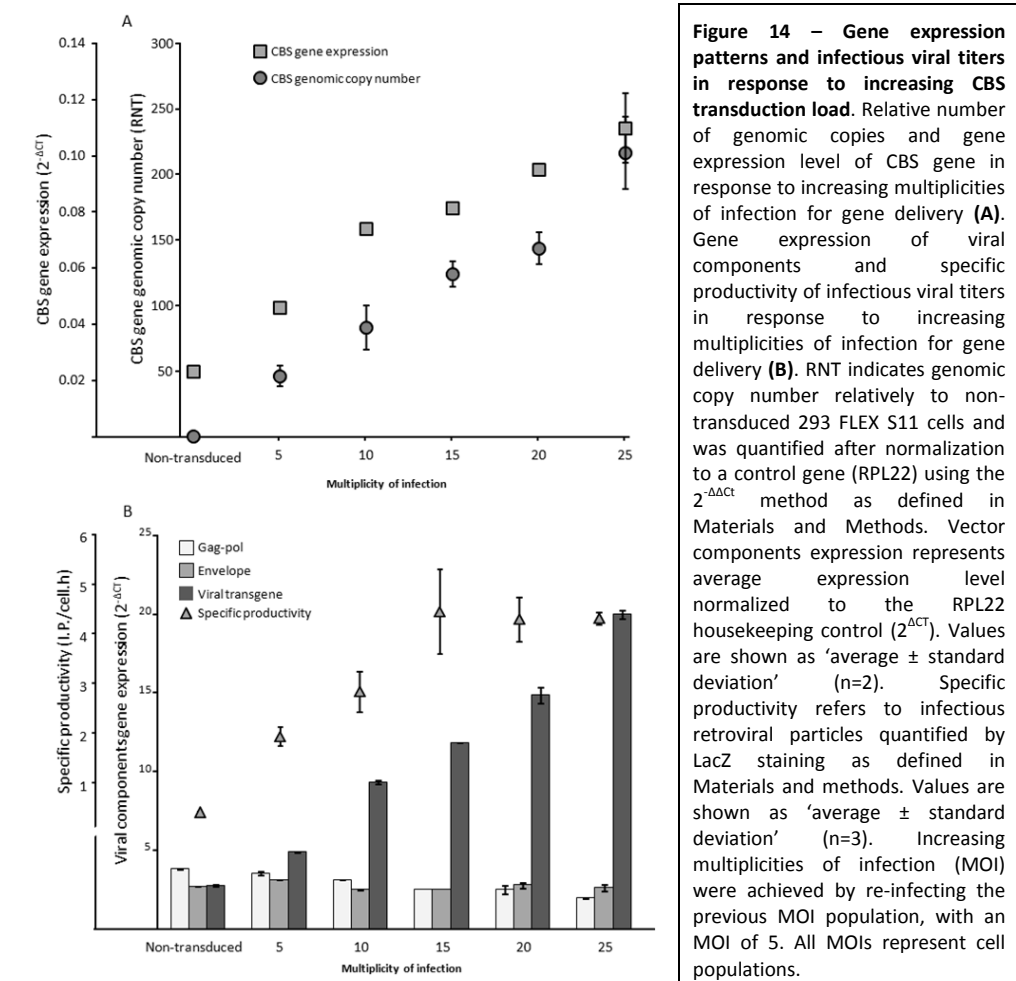


Figure 13 – Boxplot analysis of gene manipulations conducted in this work. Grey dashed box indicates the third quartile of non-transduced cells (Fig. 2). Purple dashed line indicates the threshold for high-producing phenotypes given by maximum titer increase in mock transduced controls (Fig. 3). Average improvements were considered when the third quartile of manipulated cells exceeds that of non-transduced cells, while deleterious effects were considered for the third quartile below that of non-transduced cells. For CBS, ODC1 and HIF1AN, the curves were independently re-analyzed by repeating the SSCT procedure with the same population but different passages (first batch second cloning) and/or by establishing new populations but using new lentiviral vector stocks (second batch). “M” stands for multiplicity of infection. Genes are grouped by targeted pathway. ASS1: argininosuccinate synthase 1; ARG1: arginase 1; AZIN1: antizyme inhibitor 1; BCL2: B-cell CLL/lymphoma 2; CBS: cystathionine-beta-synthase; CTH: cystathionase; GSS: glutathione synthase; HIF1AN: hypoxia inducible factor 1, alpha subunit inhibitor; HSPA5: heat shock 70kDa protein 5; IDH1: isocitrate dehydrogenase 1 (cytosolic); IDH2: isocitrate dehydrogenase 2 (mitochondrial); ODC1: ornithine decarboxylase. XBP1: X-box binding protein 1. N/A: not applicable; refers to cells exposed to oxidative stress injury (*tert*-butyl hydroperoxide, Fig. 10).

3.8 Impact of metabolic genes on viral production dynamics – a preliminary analysis with the CBS case study

The over-expression of certain genes has been showing to significantly impact infectious virus titers. Yet, as important as identifying new (and old) genes delivering high titers is the understanding on the changes promoting such improvements. In this context, CBS over-expression was studied in deeper detail in terms of number of delivered copies, how it translated into gene expression levels (mRNA) and how it modulates vector components dynamics and infectious particles titers (Fig. 14).



CBS gene copy number appeared to directly correlate with the multiplicity of infection, demonstrating effective gene delivery. Gene expression of CBS also was found to increase but for higher MOIs, tended to reach a plateau (Fig. 14A). Infectious particles titers followed an identical behavior (Fig. 14B). For viral components gene expression, gag-pol and envelope appeared as relatively unchanged, while the viral transgene presented sharp increases, directly correlated with the multiplicity of infection (Fig. 14B).

4. Discussion

During the last decade a body of evidences indicates that metabolic engineering of mammalian cells should be conducted in a multi-gene manipulation approach to potentiate the combination of favorable physiological traits (Lim et al. 2010; Seth et al. 2007; Seth et al. 2006). On the other hand, multi-gene engineering has been hampered by the lack of high-throughput power for clone screening, rendering the manipulation of more than 2-3 genes extremely difficult.

In this work, we set up the basis for multi-gene engineering of mammalian cell metabolism using, as study model, a human cell line producing recombinant retrovirus. To face the challenge of clone screening, a novel method for fast identification of high-titer clones was established by merging cell cloning and virus titration: the single step cloning-titration method (SSCT, Chapter VII). Assisted by a previous study on the metabolic networks recruited when establishing a retrovirus producer cell line (Chapter II, Rodrigues et al. (2013)), more than 30 candidates, including metabolic and regulatory genes, were chosen for manipulation (Table I). Currently, 17 of those candidates have already been evaluated. Four of these 17 genes were used to manipulate lipid metabolism in an attempt to revert serum heterotrophy in retroviral vector production (Chapter V). The remaining 13 genes were evaluated herein and their effects on infectious virus production are discussed bellow.

When analyzing non-transduced controls subject to independent SSCT rounds, we found that, although their density distribution curves was relatively similar, centered on 150 RFU, extended tails up to 3000 RFU could also be observed (Fig. 2). These tails may seem to contradict the fact that 293 FLEX S11 derives from a single clone. However, as discussed in Chapter VII, differences can arise from variations in the location of the colony in the cloning well during the SSCT procedure. Additionally, some degree of variability is inevitable: even non-transduced cells are known to present phenotypic variability despite repeated rounds of cloning (Barnes et al. 2006). These variations might be related to epigenetics (Kim et al. 2009). Apart from that, the transduction-induced variability had also to be taken into account. Indeed, some mock clones presented productivity improvements up to 3-fold, although no gene was being delivered. Yet, when comparing the boxplot distributions of non-transfected and mock-transfected controls, it become clear that these were rare and random events as no average improvements occurred for mock populations (Fig. 13). In fact, a slight reduction could be observed.

In the manipulation of polyamines metabolism the transduction with antizyme inhibitor (AZIN1) and arginase 1 (ARG1) suggested an overall improvement in infectious particles titer although no high-producing phenotypes were observed (Fig. 5A and Fig. 13). The upstream location of ARG1 in feeding polyamines biosynthesis is in line with these results since, its over-expression might not be translated into higher production if, for instance, the downstream machinery is limiting (Fig. 4). For AZIN1, however, one could expect a more evident improvement and/or high-producing phenotypes, considering it directly activates ornithine decarboxylase (ODC1), catalyzing the first step in polyamines biosynthesis (Fig. 4). When directly over-expressing ODC1, high-producing phenotypes (up to 8-fold increase) could be isolated (Fig. 5B). Moreover, a second ODC1 population transduced with MOI of 3 presented an obvious up-shifting of the second and third quartiles to higher fluorescence values indicating enhanced improvements (Fig. 14). Thus, the low MOI used to deliver polyamines biosynthesis genes (MOI of 1) may be insufficient to evaluate the full

extent of their effects. Argininosuccinate synthase (ASS1) transduction seemed to induce an overall down-regulation on infectious particles productivity. It could be hypothesized that, since ASS1 feeds citrulline – unable to be converted to ornithine given the poor expression of ornithine carbamoyltransferase (OTC, Fig. 4) – this could favor other citrulline-fed pathways eventually deleterious for virus production. From this perspective, over-expressing ornithine synthesizing enzymes (as ARG1) would be a preferable approach. The over-expression of ornithine aminotransferase (OAT), considered for future manipulation, also fits this purpose (Fig. 4). Nevertheless, ASS1's were the only transduced populations from polyamines metabolism manipulation presenting higher average productivities when increasing the MOI (Fig. 5B). Therefore, also for ASS1 higher MOIs should be evaluated by the SSCT method to better clarify the effects of its over-expression into virus production. In addition to cell growth, polyamines can bind to nucleic acids participating in their stabilization, modulate gene transcription events, play a role in membrane rigidity and present anti-oxidant properties (Wallace et al. 2003). These properties can have a beneficial effect on viral production, particularly by stabilizing viral genome leading to improved encapsidation, changing viral membrane rigidity and preventing its lipid peroxidation. They have also been reported to improve viral DNA polymerase activity (Marcus et al. 1981). Polyamines metabolism has not, up to the date, been considered in metabolic engineering approaches.

In the manipulation of glutathione metabolism, the over-expression of glutathione synthase (GSS) could be translated in titer improvements up to 13-fold (Fig. 7C), while the over-expression of isocitrate dehydrogenase 1 (IDH1) only delivered 2.5-fold. Although this does not pass the mock-set threshold (3-fold) to be considered significant, IDH1 over-expression translated into overall improvements (Fig. 13). Thereby, it is possible that this 2.5-fold increase, is effectively related to IDH1. Combining IDH1 over-expression on the top of GSS manipulation should be performed to evaluate potential cumulative effects. Still in the glutathione metabolism, cystathionine-beta-synthase (CBS) revealed to be a very potent gene to improve viral

productivity (Fig. 7B). Not only the curve tail extended above the control, as it presented high density in this range, denoting high amount of high producing clones, by opposite to more rare behavior in GSS. Indeed, the majority of the clones isolated from this range presented high titer improvements, up to 15-fold, relatively to non-transduced cells. This behavior was so impressive that CBS population, MOI 3, was reanalyzed after a few passages. Also, a second population was established using a newly produced lentiviral stock (Fig. 13). In all the cases, high concentration of high-titer phenotypes was observed. Interestingly, for the secondly transduced population, a shift to higher fluorescence values occurred, suggesting that, apart from the delivered gene, the lentiviral vector stock used to transduced the cells influences the final performance of infectious particles productivity. It is noteworthy that the manipulation of glutathione metabolism translated in the highest titer improvements from all the genes evaluated in this work. Indeed, glutathione metabolism is transversal to key pathways including glycolysis, pentose phosphate pathway and protein processing in the endoplasmic reticulum and serves important detoxification routes. All of these are likely to contribute to improved cell robustness and increased viral production. Glutathione metabolism has not, up to the date, been considered in metabolic engineering approaches.

In the manipulation of protein processing in the endoplasmic reticulum (ER), heat shock 70kDa protein 5 (HSPA5, also called HSP70) manipulated cells presented an extended tail, 5000 RFU above the control and the majority of the isolated clones were high-titer phenotypes, producing up to 7-fold more. However, considering, for instance, CBS curve, which extended 3000 RFU above the controls and contained clones producing up to 15-fold higher, 7-fold increase for a 5000 RFU extension might seem disappointing. Yet, HSPA5 colonies were considerable higher than those of non-transduced controls. Interestingly, these clones do not seem to grow faster, thus suggesting that the bigger colonies by the end of cloning procedure may result from an earlier replication beginning after the single cell is seeded on the well. HSP70 has been used for engineering mammalian cell lines producing recombinant proteins. Lasunskai

et al. (2003) reported increased cell viability, stress resistance and monoclonal antibody stability in the culture medium by over-expressing HSP70 in NS0 hybridoma cells, although with no productivity increase. Later on, Ishaque et al. (2007), achieved enhanced secretion of recombinant factor VIII and also increased resistance to apoptosis in BHK-21 cells.

Still in the manipulation of protein processing in the ER, X-box binding protein 1 (XBP1), one of the identified genes arising from the transcriptional comparison high vs. low producer was also targeted. High-titer clones, producing up to 7-fold more, could be isolated (Fig. 9B). XBP1 is known to be a key regulator in the differentiation of B cells into immunoglobulin-secreting plasma cells, activating several genes of secretory pathway, physically expanding the ER, increasing cell size, lysosome content, mitochondrial mass and function, ribosome numbers and total protein synthesis (Shaffer et al. 2004). Thus, it appears to be a general organelle biogenesis factor more than a specific tool for any single pathway. XBP1 has been previously used for engineering CHO cells (Tigges and Fussenegger 2006). The authors reported the expansion of the endoplasmic reticulum and the Golgi with an increase in the overall production capacity. Interestingly, they also reported the same manipulation not to be functional in other cell lines, including HEK 293. In fact, boxplot analysis showed a rather limited effect on overall productivity performance of transduced cells (Fig. 13). However, two high-producing phenotypes, with productivity improvements up to 7-fold were obtained, unlikely to be randomly derived from transduction-induced phenotypic variability. It should be noted that both HSPA5 and XBP1, by increasing the overall capacity of protein processing, reduce the burden of ER stress thereby increasing cellular resistance to apoptosis (Chakrabarti et al. 2011). In fact, viral replication is known to increase ER stress and unfolded protein response, potentially leading to apoptosis (Zhang and Wang 2012), substantiating the over-expression of HSPA5 and XBP1 to improve virus production.

For the direct manipulation of apoptosis, B-cell CLL/lymphoma 2 (BCL2), also identified as a potential target to improve viral productivity from the transcriptional

comparison high vs. low producer (Chapter II), was targeted. BCL2 transduced cells contained high-producing phenotypes up to 5-fold increase relatively to non-transduced cells. Additionally, we observed higher robustness to stressful conditions of BCL2 transduced cells, by inducing oxidative injury (Fig. 10B). Therefore, BCL2 over-expression not only delivered more resistant cells – as already reported for other mammalian production systems (Meents et al. 2002) – but was confirmed as a gene target to improve specific productivity of infectious virus. Anti-apoptosis metabolic engineering has, indeed, been extensively used to increase the robustness and extend the life span of cultured mammalian cells producing recombinant protein. Increased productivities are often obtained, although mainly based on volumetric productivity (for a review see Majors et al. (2007)). For the specific case of virus production, the subject requires a finer analysis, as virus replication is already accompanied by strong anti-apoptotic mechanisms as part of the viral replication strategy and many viruses carry their own BCL2 homologs (Tschopp et al. 1998). Although this is not the case of murine leukemia (retro)virus, BCL2 over-expression is one of the hallmarks of leukemia, therefore a potentially important gene in MLV replication and pathogenesis (Butturini and Gale 1990).

In the manipulation of energy metabolism we sought for improving energy generation by simulating the down-regulation of the Warburg effect, and by over-expressing the TCA cycle enzymes catalyzing the reactions downstream of acetyl-CoA entrance to stimulate enhanced TCA activity (Fig. 11). Hypoxia inducible factor 1 inhibitor (HIF1AN) was over-expressed an attempt to simulate hypoxia inducible factor 1 (HIF1) down-regulation while avoiding the deleterious effects of RNA interference. Clones producing up to 7-fold more than non-transduced cells were obtained (Fig. 12). Comparatively to the average 20-fold increase obtained with 293 FLEX GFP in Chapter VI, 7-fold may seem modest. Yet, 293 FLEX GFP produce in the range of $0.5\text{-}2 \times 10^6$ infectious particles *per* mL while 293 FLEX S11 produce one order of magnitude higher. For IDH2 transduction, no high-titer phenotypes could be isolated although the clone density for higher fluorescence values suggested average improvements (Fig. 12A).

This is thus a candidate gene to be added to HIF1AN high-titer clones to potentiate synergistic effects. The physiological implications of down-regulating the Warburg effect in retrovirus producer cells have been discussed in Chapter VI. From a more global perspective, increasing the channeling of pyruvate into TCA and improving its activity leads to enhanced energy generation with less formation of toxic by-products (e.g. lactate). For an energetically *expensive* product, such as viral particles, this should be of increased importance. Also, TCA intermediates feed important pathways, including lipid metabolism, relevant for several aspects of viral replication (Heaton and Randall 2011). Yet, it is worthy highlighting that the Warburg effect with the reduction of TCA activity in cultured mammalian cells is believed to provide a proliferative advantage based on reduced oxidative stress burden, due to low oxidative phosphorylation (Shlomi et al. 2011). Therefore, engineering strategies aiming at increasing TCA activity and energy generation at the level of oxidative phosphorylation should benefit from a combination with genes involved in reactive oxygen species scavenging, such as those of glutathione metabolism (Fig. 6).

The over-expression of certain genes showed to significantly impact infectious virus titers. However, as important as identifying genes prompting higher titer, is the understanding on the changes promoting such improvements. In this context, CBS over-expression was studied in detail in terms of number of delivered copies, how it translated into gene expression levels (mRNA) and how it modulates vector components dynamics and infectious particles titers (Fig. 14). CBS gene copy number was found to directly increase with increasing multiplicities of infection (Fig. 14A). These results demonstrated not only effective gene delivery but also no signals of transduction inhibition in cells already infected. This is of particular relevance in the follow-up of this work which shall be based on multiple lentiviral transduction of different genes. Interestingly, for multiplicity of infection 5, the number of CBS genomic copies was found to be around 50-times that of non-transduced cells (Fig. 14). Considering that genomic copy number of CBS in non-transduced cells is unlikely to be 10 – corresponding to karyotype quintuplication – these results indicate an

under-estimation of the infectious titers in metabolic gene lentiviral stocks. This under-estimation had been previously detected for S11 transcomplementation titration (Chapter VII). Gene expression of CBS (mRNA) also was found to increase but for higher MOIs, tended to reach a plateau (Fig. 14A). Indeed, although the genomic copy number could, theoretically, be increased up to the infinitum, gene expression would always be inherently limited by the transcriptional machinery – ribosomes, polymerases and nucleotides. For viral components gene expression, gag-pol and envelope appeared as relatively unchanged, while the viral transgene presented sharp increases, directly correlated with the multiplicity of infection. Interestingly, infectious viral titers correlated better with CBS gene expression – also reaching a plateau – than with viral transgene expression, which kept increasing (Fig. 14B). This last result is of particular relevance for two reasons: i) it strengthens a pattern observed for all the high titer-yielding manipulations conducted during this thesis in which high titer clones were intrinsically associated to enhanced viral transgene expression but more importantly, ii) it suggests that high viral transgene expression levels are a consequence of over-expressing the metabolic gene, rather than the cause for high titers.

For all the clones isolated during this work, an extensive characterization is further required including: i) evaluation of physical and genome-containing particles production, ii) quantification of gene expression by qRT-PCR of the delivered genes and also of the viral component genes and iii) western-blotting analysis on the protein encoded by the delivered gene. For some of the already analyzed clones, the expression of the delivered genes was found to increase between 1.5- to 3-fold, in line with the low multiplicities of infections used and the moderate strength of the promoter driving metabolic genes expression (PGK). Increased protein levels were also confirmed (for GSS and CBS clones). All of the (high-titer) analyzed clones additionally revealed substantial expression changes in viral components, most notably, on viral transgene.

From the 13 genes studied, 10 are, to the best of our knowledge, herein reported as metabolic engineering targets for the first time. Thirteen additional targets are under evaluation. After this first stage on assessing average productivity effects and screen for high-titer phenotypes for each gene, those found to deliver significant titer improvement should be combined: i) on an intra-pathway basis and ii) on an inter-pathway basis on a last stage.

The work herein described sets the basis for a pioneer multi-gene manipulation approach. It is the most extensive metabolic engineering study performed in mammalian cells, so far, further enlightening virus-host metabolic interaction.

5. Author contribution

Ana Filipa A. F. Rodrigues participated on the experimental setup and design, performed part of the experiments, analyzed the data and wrote the chapter.

6. References

- Barnes LM, Moy N, Dickson AJ. 2006. Phenotypic variation during cloning procedures: analysis of the growth behavior of clonal cell lines. *Biotechnol Bioeng* 94(3):530-7.
- Butturini A, Gale RP. 1990. Oncogenes and leukemia. *Leukemia* 4(2):138-60.
- Chakrabarti A, Chen AW, Varner JD. 2011. A review of the mammalian unfolded protein response. *Biotechnol Bioeng* 108(12):2777-93.
- Coroadinha AS, Schucht R, Gama-Norton L, Wirth D, Hauser H, Carrondo MJ. 2006. The use of recombinase mediated cassette exchange in retroviral vector producer cell lines: predictability and efficiency by transgene exchange. *J Biotechnol* 124(2):457-68.
- Dull T, Zufferey R, Kelly M, Mandel RJ, Nguyen M, Trono D, Naldini L. 1998. A third-generation lentivirus vector with a conditional packaging system. *J Virol* 72(11):8463-71.
- Edwards JS, Palsson BO. 1999. Systems properties of the *Haemophilus influenzae* Rd metabolic genotype. *J Biol Chem* 274(25):17410-6.
- Fussenegger M, Schlatter S, Datwyler D, Mazur X, Bailey JE. 1998. Controlled proliferation by multigene metabolic engineering enhances the productivity of Chinese hamster ovary cells. *Nat Biotechnol* 16(5):468-72.
- Heaton NS, Randall G. 2011. Multifaceted roles for lipids in viral infection. *Trends Microbiol* 19(7):368-75.
- Ishaque A, Thrift J, Murphy JE, Konstantinov K. 2007. Over-expression of Hsp70 in BHK-21 cells engineered to produce recombinant factor VIII promotes resistance to apoptosis and enhances secretion. *Biotechnol Bioeng* 97(1):144-55.
- Kim JK, Samaranyake M, Pradhan S. 2009. Epigenetic mechanisms in mammals. *Cell Mol Life Sci* 66(4):596-612.
- Kim TY, Sohn SB, Kim YB, Kim WJ, Lee SY. 2011. Recent advances in reconstruction and applications of genome-scale metabolic models. *Curr Opin Biotechnol* 23(4):617-23.
- Lasunskaja EB, Fridlianskaia, II, Darieva ZA, da Silva MS, Kanashiro MM, Margulis BA. 2003. Transfection of NS0 myeloma fusion partner cells with HSP70 gene results in higher hybridoma yield by improving cellular resistance to apoptosis. *Biotechnol Bioeng* 81(4):496-504.
- Lim Y, Wong NS, Lee YY, Ku SC, Wong DC, Yap MG. 2010. Engineering mammalian cells in bioprocessing - current achievements and future perspectives. *Biotechnol Appl Biochem* 55(4):175-89.
- Majors BS, Betenbaugh MJ, Chiang GG. 2007. Links between metabolism and apoptosis in mammalian cells: applications for anti-apoptosis engineering. *Metab Eng* 9(4):317-26.
- Marcus SL, Smith SW, Bacchi CJ. 1981. Polyamines stimulate DNA-directed DNA synthesis catalyzed by mammalian type C retroviral DNA polymerases. *J Biol Chem* 256(7):3460-4.

- Meents H, Enenkel B, Eppenberger HM, Werner RG, Fussenegger M. 2002. Impact of coexpression and coamplification of sICAM and antiapoptosis determinants bcl-2/bcl-x(L) on productivity, cell survival, and mitochondria number in CHO-DG44 grown in suspension and serum-free media. *Biotechnol Bioeng* 80(6):706-16.
- Palsson BØ. 2006. *Systems biology - Properties of reconstructed networks*. New York: Cambridge University Press.
- Pegg AE. 2006. Regulation of ornithine decarboxylase. *J Biol Chem* 281(21):14529-32.
- Rodrigues AF, Carmo M, Alves PM, Coroadinha AS. 2009. Retroviral vector production under serum deprivation: The role of lipids. *Biotechnol Bioeng* 104(6):1171-81.
- Rodrigues AF, Formas-Oliveiras AS, Bandeira VS, Alves PM, Hu WS, Coroadinha AS. 2013. Metabolic pathways recruited in the production of a recombinant enveloped virus: mining targets for process and cell engineering. *Metabolic Engineering* 20:131-145.
- Schucht R, Coroadinha AS, Zanta-Boussif MA, Verhoeven E, Carrondo MJ, Hauser H, Wirth D. 2006. A new generation of retroviral producer cells: predictable and stable virus production by Flp-mediated site-specific integration of retroviral vectors. *Mol Ther* 14(2):285-92.
- Seth G, Charaniya S, Wlaschin KF, Hu WS. 2007. In pursuit of a super producer-alternative paths to high producing recombinant mammalian cells. *Curr Opin Biotechnol* 18(6):557-64.
- Seth G, Hossler P, Yee JC, Hu WS. 2006. Engineering cells for cell culture bioprocessing--physiological fundamentals. *Adv Biochem Eng Biotechnol* 101:119-64.
- Shaffer AL, Shapiro-Shelef M, Iwakoshi NN, Lee AH, Qian SB, Zhao H, Yu X, Yang L, Tan BK, Rosenwald A and others. 2004. XBP1, downstream of Blimp-1, expands the secretory apparatus and other organelles, and increases protein synthesis in plasma cell differentiation. *Immunity* 21(1):81-93.
- Shlomi T, Benyamini T, Gottlieb E, Sharan R, Ruppin E. 2011. Genome-scale metabolic modeling elucidates the role of proliferative adaptation in causing the Warburg effect. *PLoS Comput Biol* 7(3):e1002018.
- Tigges M, Fussenegger M. 2006. Xbp1-based engineering of secretory capacity enhances the productivity of Chinese hamster ovary cells. *Metab Eng* 8(3):264-72.
- Tschopp J, Thome M, Hofmann K, Meink E. 1998. The fight of viruses against apoptosis. *Curr Opin Genet Dev* 8(1):82-7.
- Wallace HM, Fraser AV, Hughes A. 2003. A perspective of polyamine metabolism. *Biochem J* 376(Pt 1):1-14.
- Wand MP, Jones MC. 1995. *Kernel Smoothing* (Chapman & Hall/CRC Monographs on Statistics & Applied Probability). Boca Raton, FL, USA: Chapman and Hall/CRC.
- Zhang L, Wang A. 2012. Virus-induced ER stress and the unfolded protein response. *Front Plant Sci* 3:293.

Chapter IX

DISCUSSION AND PERSPECTIVES

Contents

1. Discussion and perspectives	245
1.1 Metabolic determinants in retroviral vector replication: transcriptomics, metabolomics and pathway analysis	246
1.2 Strategies to explore the metabolic constraints for enhanced viral titers: from data mining to gene delivery	248
1.3 Debottlenecking gene manipulation and clone screening	250
1.4 Walking the road to hyperproductivity: multi-gene manipulation and dynamic promoters.....	251
2. Author contribution	254
3. References	254

1. Discussion and perspectives

Virus based biopharmaceuticals are one of the most promising products of the 21st century medicine covering successful prophylactic, therapeutic and clinical applications. Retrovirus-derived particles occupy an important segment of this market, having found use in gene therapy (Edelstine 2013), oncolytic treatment (Dalba et al. 2007; Russell et al. 2012) and vaccination (Dalba et al. 2007; Garrone et al. 2011).

Retroviruses manufacture has always been challenging. They are characterized by low titers, high-content of non-infectious particles and short infectivity half-lives (Coroadinha et al. 2010; Merten 2004). Long-term vector production is dependent on animal blood serum supplementation, hindering the safety and standardization required in clinical-grade manufacture processes (Chan et al. 2001; Gerin et al. 1999; Merten 2004). Additionally, the physical separation of the viral genome into different expression cassettes – for safety purposes – disrupts the regulatory stoichiometry and the optimal ratios of viral components further reducing the titers and increasing the defective particles content (Bajgelman et al. 2003; Yap et al. 2000). Several strategies have been attempted to circumvent these drawbacks including engineering mutant vectors with improved stability (Vu et al. 2008), transcriptionally improving the viral cassettes (Schambach et al. 2007) and optimizing vector components stoichiometry (Carrondo et al. 2008). All of these strategies have, to some extent, focused the viral cassettes. Another line of intervention, focusing the producer cell, was initiated a few years ago. By using alternative carbon sources Coroadinha et al. (2006a and 2006b) observed marked changes in retrovirus producer cell metabolism at the level of glycolysis, TCA cycle, glutaminolysis, synthesis of fatty acids and phospholipids, with specific productivity improvements up to 5-fold. More importantly, a direct correlation between the changes in the cellular metabolic status and the viral properties – such as increased stability – was demonstrated (Coroadinha et al. 2006c).

At the same time these results encouraged our interest in exploring producer cell metabolism for enhanced titers, a new paradigm in mammalian cell engineering was

emerging. Fed by more than one decade of metabolic engineering by trial-and-error (reviewed in Seth et al. (2006)), and by the opportunities offered with the explosion of *omics* technologies in cell culture bioprocess (Griffin et al. 2007; Gupta and Lee 2007), G. Seth and colleagues envisaged an elegant concept to rationalize metabolic engineering when in the pursuit of higher productivities (Seth et al. 2007). This concept relies on the understanding that i) particular physiological/metabolic traits – in the limit, based on gene expression – confer superior attributes in what concerns productivity; ii) these attributes are, alone, insufficient to promote a hyperproducing phenotype, thereby requiring combination and iii) such phenotype might be achieved by different combinations, since there is not a unique route leading to superior productivities. Although these premises might, nowadays, seem obvious, it was on the paper of Seth et al. (2007) that they were clearly enunciated for the first time.

This PhD work aimed at improving retroviral vector production in human cell lines through gene-based metabolic optimization of the producer host. Thereby, this thesis lays on four pillars: i) understanding the metabolic constraints associated to virus replication, ii) devising theoretical and experimental strategies to explore this knowledge in promoting enhanced titers, iii) debottlenecking the experimental burden of gene manipulation and clone screening to iv) combine these strategies in one of the multiple routes to hyperproductivity. Functional genomics tools, including microarray transcriptome analysis, metabolite profiling, lipidomics, RNA interference and genetic engineering, were used and inter-crossed for knowledge generation and cell manipulation.

1.1 Metabolic determinants in retroviral vector replication: transcriptomics, metabolomics and pathway analysis

To gain further insights on the metabolic constraints associated to virus replication, large-scale transcriptome analysis was conducted, to identify potential pathways recruited when going from a non-producer to a producer cell line. As gene

manipulation was one of the final goals of this work, transcriptomics appeared as the primary surveying tool. Metabolomics, including central carbon metabolite profiling and lipidomics, functioned as a complementary approach. Indeed, although metabolomics is assumed as the layer of biological information closer to the final phenotype, metabolite profiling is associated to a high degree of uncertainty due to the inherent redundancy of the metabolic networks (Palsson 2006) and limited number of metabolites that can be accurately quantified in a biological sample (Dietmair et al. 2012; Oldiges et al. 2007).

Using pathway analysis methods, eight pathways were identified to be recruited in the retrovirus producer cells: amino acid catabolism, carbohydrate catabolism and integration of the energy metabolism, nucleotide metabolism, glutathione metabolism, pentose phosphate pathway, polyamines biosynthesis and lipid metabolism (**Chapter II**). In serum heterotrophy, lipids were identified as the key serum component associated to infectious virus titers (**Chapter III**). ¹³C-NMR lipidomics demonstrated cholesterol biosynthesis to be impaired in serum heterotroph cells (**Chapter IV**) while transcriptional profiling identified three potential bottlenecks of this pathway: mevalonate kinase (MVK), lanosterol synthase (LSS) and sterol regulatory element binding factor 2 (SREBF2) (**Chapter V.a**).

Pathway analysis methods rely on a rather simple statistic to identify *significantly enriched pathways*. Given a certain number x of differentially expressed genes, from which k are assigned to a pathway ($k < x$), from a total number of genes y comprising the dataset ($y \gg x > k$), what is the probability of, by randomly picking x genes from the total set y , exactly k will belong to that pathway? This problem can be described by a hypergeometrical distribution easily computable, the basis of pathway analysis software's, such as gene set enrichment analysis (Subramanian et al. 2005), GenMAPP (Dahlquist et al. 2002; Salomonis et al. 2007) and Ingenuity Pathway Analysis, herein used. These software's have been updated to provide other outputs than statistical significance associate to pathway enrichment, including metabolic maps, scores trying to predict pathway activation/inhibition, "leading edges" – those genes accounting for

the core enrichment signal – all linked to publications and databases where further information can be consulted. They are thus, user-friendly data analysis platforms in the daunting challenge of extracting biological information from the massive amounts of transcriptome data (reviewed in Werner (2008)). Their two main disadvantages are: i) giving a rather qualitative output – the pathway is or is not enriched – and ii) the results may be strongly biased by the databases the software uses. The latter occurs since extensively described and curated pathways are more likely to appear as significantly enriched. Also, not all pathways are equally suitable for transcriptome pathway analysis, particularly those controlled to a large extent by metabolites or protein-based events, thus less likely to appear as significantly enriched.

Because of these biases, a user-driven gene-by-gene *a posteriori* analysis is required to rationalize the biological significance of pathway analysis outputs. Therefore, in this work detailed metabolic maps were built, providing a broad and integrated overview of absolute gene expression and fold-changes for both cell lines (**Chapter II** and **Chapter V.a**). Each gene was scrutinized for the biological function and regulatory mechanisms using the BioCyc human database (Caspi et al. 2010). Additionally, before stepping forward to gene manipulation, the ability of the identified pathways to modulate viral titers was experimentally challenged by medium manipulation (**Chapter II** and **Chapter III**).

1.2 Strategies to explore the metabolic constraints for enhanced viral titers: from data mining to gene delivery

The metabolic maps and biological analysis allowed a systematized vision on actively changing genes and potentially blocked pathways. Yet, this was still a simple descriptive analysis, enclosing a potential interpretation skew: searching for actively changing genes as those to be potentially engineerable. Indeed the traditional approach in using transcriptome data to search for gene targets has mainly been based on the comparison ‘producers vs. parental’ or ‘high vs. low producers’ for clonal cells. In this work, we proposed a different approach: to mine the basis of particular

transcriptomic signatures from different cell origins. The rationale behind it is the notion that gene already *recruited* in the transition parental-to-producer or in the high producing clone, is likely to be *responsive* to that transition or phenotype. It also indicates that the cells have the intrinsic capability to express it, with no need for further over-expression. In fact, as an example, when XBP1 was chosen to be over-expressed as a metabolic engineering target in CHO cells aiming for higher protein secretion (Tigges and Fussenegger 2006), it was not because XBP1 had been noted to be up-regulated when going from parental to producer or highly expressed in high producing CHO clones. It was because *other cells* with a much higher protein secretion capacity (B-cells) relied on XBP1 to expand the overall secretion capacity (Iwakoshi et al. 2003a; Iwakoshi et al. 2003b; Shaffer et al. 2004). Taking advantage of the two different retroviral producer cell lines used for transcriptomic and metabolomic analysis and their obvious phenotypic differences in what concerned productivity and serum heterotrophy, Te Fly cells were used as a ‘positive control’, both for higher productivities and the ability to revert serum heterotrophy. For the latter case, the concept became very well illustrated: although both 293 FLEX and Te Fly up-regulated their cholesterol biosynthesis machinery in response to serum withdrawal, including the two blocking points MVK and LSS, the extension of up-regulation was substantially higher in Te Fly (**Chapter V.a**), previously found to be able to reactivate cholesterol biosynthesis (**Chapter IV**). Without this comparison term, MVK and LSS might not have been considered for manipulation in 293 FLEX. Naturally, the limitations of using α cell – in this case Te Fly – as a positive control should also be critically considered. Cellular biology is much beyond what can be rationalized using transcriptomics, proteomics and metabolomics.

Having set a list of gene candidates as potential targets to improve viral titers (or revert serum heterotrophy), it aroused the question on how the genes would be delivered. For more than 30 targets, no selectable markers existed. Additionally, traditional transfection methods limit the tuning of the number of delivered copies as, after a certain DNA amount, transfection itself becomes highly cytotoxic. Therefore,

gene delivery by lentiviral transduction was chosen as it is less invasive and allows for a better control of the number of delivered copies based on multiplicity of infection. Also, having used self-inactivating vectors (SINs) (Miyoshi et al. 1998; Zufferey et al. 1998), gene expression is driven by the internal non-lentiviral promoter, thus behaving like a plasmid-carried gene integrated by homologous recombination. From the proof-of-concept perspective and considering the final aim to be a combination of several genes, this strategy offered an effective and faster approach. For future extension of this work, however, multiple lentiviral transduction might not be the cellular engineering tool of choice. In this context, multicistronic constructions can be an option (Greber and Fussenegger 2007). Moreover, with the advances in artificial chromosomes, a not so distant future might bring the possibility of the tailored design of a mini-chromosome harboring a few dozens of genes and their regulatory machinery (Kennard 2011; Kouprina et al. 2013).

1.3 Debottlenecking gene manipulation and clone screening

After choosing a group of candidate genes and setting an experimental approach for their deliver, an additional challenge remained. The number of integrated copies, integration *loci* and the combination of downstream effects arising from gene manipulation renders an enormous clonal variability very difficult to be manually screened. This challenge was largely felt in the down-regulation of the Warburg effect (**Chapter VI**): it required several months to individually and manually screen more than eighty (shHIF1) clones. More than half of those were low-titer clones and only two were hyperproducing phenotypes (i.e.: producing one order of magnitude higher).

Inspired by a previously reported *in situ* fluorescence assay (Green and Rasko 2002) and taking advantage of transcomplementing fluorescence proteins (Cabantous et al. 2005), a novel method was conceived for fast identification of high-producing clones at the end of the cloning period. The uniqueness of the single step cloning-titration method (**Chapter VII**) relies on: i) avoiding cell expansion, cell banking and posterior growth/titration studies of the low titer clones and ii) providing a

productivity estimation on a clone-by-clone basis, which can be analyzed in terms of density distribution. Therefore it combines the power of single-cell resolution with the dynamics of cell population analysis. These two features can be explored in metabolic engineering to rapidly identify rare high producing phenotypes (single-cell resolution) and to evaluate the dynamics of the delivered gene from an average perspective (population analysis). The method also allowed the isolation of clones delivering optimal ratios of infectious to total particles: for some the highest fluorescence-yielding clones, ratios of 1 infectious *per* each 4 total particles could be obtained. These are, to the best of our knowledge, the best I.P.:T.P. ratios ever reported for retroviral vector production, being 1:100 to 1:1000 those typically obtained. This feature is intrinsic to the method layout since it evaluates the cumulative infectivity effect occurring during the relatively long-period of clone expansion. Thereby, high infectious titers clones but with equally high titers of non-infectious virus will flood the cloning well with defective interfering particles limiting the infective ones. The method main limitation is the lack of resolution in high-producing clones, hampered by some noise associated to colony location on the well. Therefore it requires 8-12 clones in the highest fluorescence ranges to be isolated to guarantee the highest producing phenotype which is not always the highest fluorescence clone. The concept behind the single step cloning-titration method can easily be translated to stable cell lines producing other types of infectious virus. For secreted recombinant protein, it should be equally suited given a few modifications.

1.4 Walking the road to hyperproductivity: multi-gene manipulation and dynamic promoters

Insightful from the theoretical point of view, the multiple routes to hyperproductivity concept (Seth et al. 2007) was, however, limited by the experimental burden of gene manipulation and heavy time-frames associated to clone screening. The single step cloning-titration method unlocked the manipulation of multiple genes by reducing the nearly one year process of clone screening to two

weeks. Starting from a group of genes identified in the first part of this thesis and leveraged by the swiftness of this method, in the latter stages of the work, the basis for an ambitious multi-gene engineering project were set. This project comprises three phases. Firstly, each of the genes is individually delivered and the derived effects analyzed. Herein, 17 out of the 31 candidates have been evaluated. In a second stage, high-titer phenotypes will be further transduced with genes found to deliver – at least – average improvements, on an intra-pathway basis. On a later stage, high-titer phenotypes from each pathway, already transduced with the pathway genes promoting improved titers, will be delivered for genes from the other pathways, in an attempt to find one of the multiple routes to hyperproductivity. At each step a thorough downstream analysis is performed on: i) average productivity improvements, ii) high-titer phenotypes, iii) the reproducibility of i) and ii) using different lentiviral vector batches, iv) dynamics of gene expression and viral titers in response to increasing metabolic gene copies, v) effects on total and genome-containing particles titers and vi) metabolic gene translation (protein). For the genes herein evaluated in the first stage, many of these parameters have been studied. Some genes delivered average improvements, others resulted in the appearance of high-titer phenotypes and a few combined both phenomena (**Chapter VIII**). For the characterization already started, the preliminary results indicate the delivered gene to contribute to an improved metabolic status accompanied with relevant changes in viral components expression – particularly the viral transgene – translated into higher content of infectious particles. These preliminary results may also change our current vision of metabolic engineering and bioproduct cassette amplification. While the accepted paradigm separates the transcriptional dynamics of the product from an improved metabolic status better coping with enhanced productivities, our results suggest a reciprocal control between the metabolic capabilities of the host and bioproduct expression, fine-tuned to deliver an enhanced producer. In this context, the dynamic behavior of the MFG-LTR promoter in the viral transgene cassette should play an important role that is worthy to investigate. In fact, 293 FLEX 18 not subjected to

RMCE, thereby with a simple MSCV-LTR, did not exhibit titer improvement in response to metabolic gene delivery with the impressive extension observed for 293 FLEX GFP (**Chapter VI**) or 293 FLEX S11 (**Chapter VIII**). Considering that the viral transgene, in all 293 FLEX cells, RCME exchanged or not, is present as a single copy integrated on *the same* unique and defined chromosomal locus, expression changes of more than 20-fold as observed in many of the manipulated clones (containing MFG-LTR), can only be explained hypothesizing a dynamic behavior of this promoter in response to the metabolic and/or transcriptional changes induced by the delivered genes. Although this hypothesis requires further investigation, extending this dynamic behavior to the other viral cassettes (gag-pol and envelope) could deliver even better production performances.

This PhD thesis contributes: i) to enlarge the technical possibilities of metabolic engineers in the demand for high-producing cells, ii) to improve the state-of-the-art of retroviral and similarly enveloped vectors (e.g.: lentivirus) manufacture for gene therapy and vaccination and iii) to deliver new insights on the metabolic dynamics modulating viral replication. It is thus, a frontier work, bridging fundamentals to applied research and touches the fields of biotechnology, bioengineering, vectorology, virology, cell and molecular biology.

2. Author contribution

Ana Filipa A. F. Rodrigues wrote the chapter.

3. References

- Bajgelman MC, Costanzi-Strauss E, Strauss BE. 2003. Exploration of critical parameters for transient retrovirus production. *J Biotechnol* 103(2):97-106.
- Cabantous S, Terwilliger TC, Waldo GS. 2005. Protein tagging and detection with engineered self-assembling fragments of green fluorescent protein. *Nat Biotechnol* 23(1):102-7.
- Carrondo MJ, Merten OW, Haury M, Alves PM, Coroadinha AS. 2008. Impact of retroviral vector components stoichiometry on packaging cell lines: effects on productivity and vector quality. *Hum Gene Ther* 19(2):199-210.
- Caspi R, Altman T, Dale JM, Dreher K, Fulcher CA, Gilham F, Kaipa P, Karthikeyan AS, Kothari A, Krummenacker M and others. 2010. The MetaCyc database of metabolic pathways and enzymes and the BioCyc collection of pathway/genome databases. *Nucleic Acids Res* 38(Database issue):D473-9.
- Chan LM, Coutelle C, Themis M. 2001. A novel human suspension culture packaging cell line for production of high-titre retroviral vectors. *Gene Ther* 8(9):697-703.
- Coroadinha AS, Alves PM, Santos SS, Cruz PE, Merten OW, Carrondo MJ. 2006a. Retrovirus producer cell line metabolism: implications on viral productivity. *Appl Microbiol Biotechnol* 72(6):1125-35.
- Coroadinha AS, Gama-Norton L, Amaral AI, Hauser H, Alves PM, Cruz PE. 2010. Production of retroviral vectors: review. *Curr Gene Ther* 10(6):456-73.
- Coroadinha AS, Ribeiro J, Roldao A, Cruz PE, Alves PM, Merten OW, Carrondo MJ. 2006b. Effect of medium sugar source on the production of retroviral vectors for gene therapy. *Biotechnol Bioeng* 94(1):24-36.
- Coroadinha AS, Silva AC, Pires E, Coelho A, Alves PM, Carrondo MJ. 2006c. Effect of osmotic pressure on the production of retroviral vectors: Enhancement in vector stability. *Biotechnol Bioeng* 94(2):322-9.
- Dahlquist KD, Salomonis N, Vranizan K, Lawlor SC, Conklin BR. 2002. GenMAPP, a new tool for viewing and analyzing microarray data on biological pathways. *Nat Genet* 31(1):19-20.
- Dalba C, Bellier B, Kasahara N, Klatzmann D. 2007. Replication-competent vectors and empty virus-like particles: new retroviral vector designs for cancer gene therapy or vaccines. *Mol Ther* 15(3):457-66.
- Dietmair S, Nielsen LK, Timmins NE. 2012. Mammalian cells as biopharmaceutical production hosts in the age of omics. *Biotechnol J* 7(1):75-89.
- Edelstine M. 2013. The Journal of Gene Medicine Clinical Trial Site.
- Garrone P, Fluckiger AC, Mangeot PE, Gauthier E, Dupeyrot-Lacas P, Mancip J, Cangialosi A, Du Chene I, LeGrand R, Mangeot I and others. 2011. A prime-boost strategy using virus-like particles pseudotyped for HCV proteins triggers broadly neutralizing antibodies in macaques. *Sci Transl Med* 3(94):94ra71.
- Gerin PA, Searle PF, Al-Rubeai M. 1999. Production of retroviral vectors for gene therapy with the human packaging cell line FLYRD18. *Biotechnol Prog* 15(5):941-8.

- Greber D, Fussenegger M. 2007. Multi-gene engineering: simultaneous expression and knockdown of six genes off a single platform. *Biotechnol Bioeng* 96(5):821-34.
- Green BJ, Rasko JE. 2002. Rapid screening for high-titer retroviral packaging cell lines using an in situ fluorescence assay. *Hum Gene Ther* 13(9):1005-13.
- Griffin TJ, Seth G, Xie H, Bandhakavi S, Hu WS. 2007. Advancing mammalian cell culture engineering using genome-scale technologies. *Trends Biotechnol* 25(9):401-8.
- Gupta P, Lee KH. 2007. Genomics and proteomics in process development: opportunities and challenges. *Trends Biotechnol* 25(7):324-30.
- Iwakoshi NN, Lee AH, Glimcher LH. 2003a. The X-box binding protein-1 transcription factor is required for plasma cell differentiation and the unfolded protein response. *Immunol Rev* 194:29-38.
- Iwakoshi NN, Lee AH, Vallabhajosyula P, Otipoby KL, Rajewsky K, Glimcher LH. 2003b. Plasma cell differentiation and the unfolded protein response intersect at the transcription factor XBP-1. *Nat Immunol* 4(4):321-9.
- Kennard ML. 2011. Engineered mammalian chromosomes in cellular protein production: future prospects. *Methods Mol Biol* 738:217-38.
- Kouprina N, Earnshaw WC, Masumoto H, Larionov V. 2013. A new generation of human artificial chromosomes for functional genomics and gene therapy. *Cell Mol Life Sci* 70(7):1135-48.
- Merten OW. 2004. State-of-the-art of the production of retroviral vectors. *J Gene Med* 6 Suppl 1:S105-24.
- Miyoshi H, Blomer U, Takahashi M, Gage FH, Verma IM. 1998. Development of a self-inactivating lentivirus vector. *J Virol* 72(10):8150-7.
- Oldiges M, Lutz S, Pflug S, Schroer K, Stein N, Wiendahl C. 2007. Metabolomics: current state and evolving methodologies and tools. *Appl Microbiol Biotechnol* 76(3):495-511.
- Palsson BØ. 2006. *Systems biology - Properties of reconstructed networks*. New York: Cambridge University Press.
- Russell SJ, Peng KW, Bell JC. 2012. Oncolytic virotherapy. *Nat Biotechnol* 30(7):658-70.
- Salomonis N, Hanspers K, Zambon AC, Vranizan K, Lawlor SC, Dahlquist KD, Doniger SW, Stuart J, Conklin BR, Pico AR. 2007. GenMAPP 2: new features and resources for pathway analysis. *BMC Bioinformatics* 8:217.
- Schambach A, Galla M, Maetzig T, Loew R, Baum C. 2007. Improving transcriptional termination of self-inactivating gamma-retroviral and lentiviral vectors. *Mol Ther* 15(6):1167-73.
- Seth G, Charaniya S, Wlaschin KF, Hu WS. 2007. In pursuit of a super producer-alternative paths to high producing recombinant mammalian cells. *Curr Opin Biotechnol* 18(6):557-64.
- Seth G, Hossler P, Yee JC, Hu WS. 2006. Engineering cells for cell culture bioprocessing--physiological fundamentals. *Adv Biochem Eng Biotechnol* 101:119-64.
- Shaffer AL, Shapiro-Shelef M, Iwakoshi NN, Lee AH, Qian SB, Zhao H, Yu X, Yang L, Tan BK, Rosenwald A and others. 2004. XBP1, downstream of Blimp-1, expands the secretory apparatus and other organelles, and increases protein synthesis in plasma cell differentiation. *Immunity* 21(1):81-93.
- Subramanian A, Tamayo P, Mootha VK, Mukherjee S, Ebert BL, Gillette MA, Paulovich A, Pomeroy SL, Golub TR, Lander ES and others. 2005. Gene set enrichment analysis: a knowledge-based approach for interpreting genome-wide expression profiles. *Proc Natl Acad Sci U S A* 102(43):15545-50.
- Tigges M, Fussenegger M. 2006. Xbp1-based engineering of secretory capacity enhances the productivity of Chinese hamster ovary cells. *Metab Eng* 8(3):264-72.
- Vu HN, Ramsey JD, Pack DW. 2008. Engineering of a stable retroviral gene delivery vector by directed evolution. *Mol Ther* 16(2):308-14.

Werner T. 2008. Bioinformatics applications for pathway analysis of microarray data. *Curr Opin Biotechnol* 19(1):50-4.

Yap MW, Kingsman SM, Kingsman AJ. 2000. Effects of stoichiometry of retroviral components on virus production. *J Gen Virol* 81(Pt 9):2195-202.

Zufferey R, Dull T, Mandel RJ, Bukovsky A, Quiroz D, Naldini L, Trono D. 1998. Self-inactivating lentivirus vector for safe and efficient in vivo gene delivery. *J Virol* 72(12):9873-80.